

Cover Page



Universiteit Leiden



The handle <http://hdl.handle.net/1887/37560> holds various files of this Leiden University dissertation.

**Author:** Karkampouna, Sofia

**Title:** Targeting TGF $\beta$  signaling pathway in fibrosis and cancer

**Issue Date:** 2016-01-28

PhD thesis

**Targeting TGF $\beta$  Signaling Pathway  
in Fibrosis and Cancer**

Sofia Karkampouna

Department of Molecular Cell Biology  
Leiden University Medical Centre

2015

Targeting TGF $\beta$  Signaling Pathway in Fibrosis and Cancer

ISBN/EAN: 978-90-824689-0-8

© 2015, Sofia Karkampouna. No part of this thesis may be reproduced or transmitted in any form, by any means, electronic or mechanical, without prior written permission of the author.

The studies were performed at the Department of Molecular Cell Biology of Leiden University Medical Centre and were supported by the Netherlands Institute for Regenerative Medicine (NIRM, grant No. FES0908).

Cover: "Gazing through the TGF $\beta$  galaxy". Concept by S.Karkampouna.  
Design by Romina Andrea Ciaffi (<http://www.ciaffi.ink>).

Artwork: Romina Andrea Ciaffi and Demetra Karkampouna.

Printed by Uitgeverij BOXpress || [proefschriftmaken.nl](http://proefschriftmaken.nl)

# **Targeting TGF $\beta$ Signaling Pathway in Fibrosis and Cancer**

**Proefschrift**

ter verkrijging van  
de graad van Doctor aan de Universiteit Leiden,  
op gezag van Rector Magnificus prof.mr. C.J.J.M. Stolker,  
volgens besluit van het College voor Promoties  
te verdedigen op donderdag 28 januari 2016  
klokke 15.00 uur

door

**Sofia Karkampouna**

geboren te Ioannina, Griekenland  
in 1986

**Promotoren**

Promotor: Prof. Dr. P. ten Dijke

Co-Promotor: Dr. M. Kruithof- de Julio

**Promotiecommissie**

Prof. Dr. C. Mummery

Prof. Dr. R. Bank (University Medical Centre Groningen)

Dr. P. Olinga (University Medical Centre Groningen)

Prof. Dr. G. Jenster (Erasmus Medical Centre)

*“Either we shall find  
what it is we are seeking  
or at least we shall free ourselves  
from the persuasion that we know  
what we do not know.*

*... the reorientation of a mind  
from a kind of twilight to true daylight  
is an ascent to reality  
or in other words, philosophy”.*

*Plato, Republic, Book VII,  
Parable of the Cave, 380 B.C*

*To the first educators,  
my parents Demetra & Thomas*



**Table of Contents**

<b>Chapter 1. Introduction</b>	<b>1</b>
1.1. Prologue	1
1.2. Outline of the thesis	2
1.3. TGF $\beta$ superfamily	3
1.4. TGF $\beta$ signaling pathway in homeostasis and disease- studies in liver, prostate and connective tissue	15
1.5. TGF $\beta$ signaling in fibrosis	17
1.6. TGF $\beta$ / BMP signaling in cancer	21
1.7. Anti-TGF $\beta$ strategies (antisense oligonucleotides/ small molecule kinase inhibitors/ ligand traps)	24
 <b>Chapter 2. TGF<math>\beta</math> signaling in liver regeneration</b>	 <b>47</b>
<i>Current Pharmaceutical Design, 2012;18(27):4103-13. Review</i>	
 <b>Chapter 3. Inhibition of TGF<math>\beta</math> type I receptor activity facilitates liver regeneration upon acute CCl<sub>4</sub> – intoxication in mice</b>	 <b>71</b>
<i>Archives of Toxicology, 2015 Jan 8. PMID: 25566828</i>	
 <b>Chapter 4. Human Dupuytren’s ex vivo culture for the study of myofibroblasts and extracellular matrix interactions</b>	 <b>99</b>
<i>Journal of Visualised Experiments, 2015 Apr 18;(98)</i>	
 <b>Chapter 5. Novel ex vivo culture method for the study of Dupuytren’s disease: effects of TGF<math>\beta</math> type I receptor modulation by antisense oligonucleotides</b>	 <b>119</b>
<i>Molecular Therapy Nucleic Acids, 2014 Jan 21;3:e142</i>	
 <b>Chapter 6. ALK1Fc suppresses tumor growth by impairing angiogenesis and affects cell proliferation of human prostate cancer cells in vivo</b>	 <b>141</b>
<i>Manuscript submitted</i>	
 <b>Chapter 7. General discussion &amp; future perspectives</b>	 <b>163</b>
 <b>Appendix I. Role of type III receptor, CRIPTO, in injury-induced liver regeneration and hepatocellular carcinoma</b>	 <b>179</b>
<i>Manuscript in preparation</i>	
 <b>Appendix II</b>	 <b>197</b>
Summary	199
Samenvatting	202
List of abbreviations	205
Curriculum vitae	210
List of publications	211
Acknowledgements	213









## **Introduction**

### **1.1. Prologue**

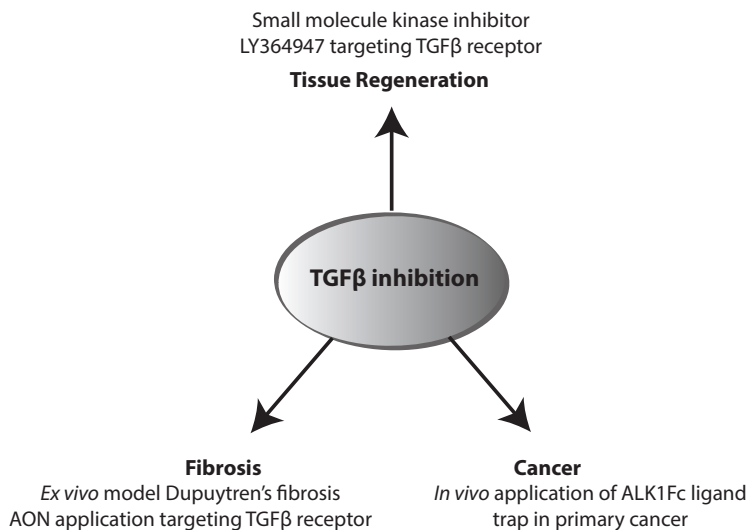
Survival of multicellular organisms requires resilience and regeneration of injured tissues due to damaging environmental or genetic factors. Virtually, all organisms from bacteria to primates have regeneration abilities at different extend (bacteria wall and flagellum regeneration<sup>1</sup>, limb regrowth in reptiles, blood, nerve and liver regeneration in mammals). Regeneration is the process of cell repair, cell replacement and renewal leading to morphogenic changes and (re) growth of damaged tissue and organs. The ultimate aim is to preserve the physiological organ functionality (homeostasis) since repetitive exposure to damaging factors eventually leads to exhaustion of the regenerative properties of cells and development of pathological conditions such as malignancies or organ fibrosis. Regenerating cells undergo cell duplication (proliferation) and phenotypic changes by gene expression modulation thus; they have increased need for DNA and protein synthesis. In order to precisely orchestrate these complex molecular processes, cells depend on mechanisms that allow communication between different parts of a single cell and among different cells. Cell communication during tissue injury occurs via signaling molecules that are being produced by injured cells (proteins, miRNAs, ions, chemical molecules). These signaling molecules cause a cascade of activation or inhibition of other molecules (signaling pathways) leading to a particular biological response in the same cell or in adjacent or further located healthy cells in different places in the body via blood circulation.

A major cell signaling pathway orchestrating homeostasis in many organ systems is the superfamily of proteins Transforming growth factor  $\beta$  (TGF $\beta$ ). Its prototype TGF $\beta$ 1 was identified over 3 decades ago. The TGF $\beta$  superfamily consists of 33 proteins encoded by the human genome, seven in *Drosophila* and four in *C.elegans*<sup>2</sup>.

Its mechanisms of signal transduction are often deregulated in human diseases; thus, it is subject of vigorous investigation in various types of cancer and fibrosis.

### 1.2. Outline of the thesis

Dysregulation of gene function of TGF $\beta$  pathway components is a common cause of human diseases such as cancer and fibrosis. The scope of the research described in this thesis is to characterize the therapeutic potential of different inhibitory strategies of TGF $\beta$  protein signaling cascade. The objective is to target and potentially “correct” the expression and function of proteins encoding TGF $\beta$  signaling components using clinically applicable compounds such as antisense oligonucleotides, small molecule inhibitors or neutralizing antibodies. We focus on inhibition of TGF $\beta$  signaling pathway in *in vivo* and *ex vivo* models of human fibrosis (Dupuytren’s, liver) and cancer (prostate, liver).



In **Chapter 1**, a general introduction on the TGF $\beta$  signaling pathway is presented and its role in normal conditions (homeostasis and tissue regeneration) as well as in pathological conditions (fibrosis, cancer) is described. An overview of different inhibitory strategies for molecular manipulation and ongoing clinical trials targeting TGF $\beta$  is provided.

In **Chapter 2**, a comprehensive review is presented about the pleiotropic role of TGF $\beta$  during liver development and regeneration with particular emphasis on regulation of epithelial cell (hepatocyte) and hepatic progenitor cell- induced regeneration. An overview of the current aspects of liver research with regards to cell replacement therapies is presented.

In **Chapter 3**, we show the *in vivo* use of a small molecule inhibitor (LY364947) targeting kinase activity of TGF $\beta$  type I receptor in a mouse model of injury-induced liver regeneration.

In **Chapter 4**, a novel *ex vivo* methodology is described for the study of human Dupuytren’s fibrosis, a primarily TGF $\beta$ -driven disease. A step-by-step protocol of the tissue *ex vivo* culture system and its applications are described. This technique is used in combination with biochemical and imaging techniques that could be applicable for the study of various types of human fibrosis.

In **Chapter 5**, the *ex vivo* culture system of human fibrotic tissue is used as a platform for TGF $\beta$  pathway deactivation using small molecule inhibitor and antisense oligonucleotides. Both strategies aim to target the activin receptor-like kinase-5 (ALK5) activity (TGF $\beta$  type I receptor) either at the protein or messenger RNA level. Specifically, the data suggest that inhibition of ALK5 activity is applicable *ex vivo* and exhibits anti-fibrotic effects evident by reduction of extracellular matrix protein deposition.

**Chapter 6** describes the use of anti-human ALK1 neutralizing antibody ACE-041 (ALK1Fc) as a tumor angiogenesis inhibitor in primary prostate cancer. This compound is currently being tested in clinical trials for solid tumor treatment. In this study, we show the *in vivo* effects of ALK1Fc in tumor burden and angiogenesis in a primary prostate cancer mouse model using orthotopic transplantation of human prostate cancer cells.

In **Chapter 7** (Discussion) the results presented in this thesis, implications deriving from this work and applicability of TGF $\beta$  targeting drugs are discussed.

In **Appendix I** we introduce preliminary data supporting a role for CRIPTO, a TGF $\beta$  superfamily type III receptor, in liver regeneration and human hepatocellular carcinoma. CRIPTO is normally expressed only during embryonic development. Our data indicate reactivation of CRIPTO in the mouse liver after toxin-induced acute injury and in human liver cancer specimens suggesting its use as a potential diagnostic biomarker for human hepatocellular carcinoma.

**Summary (Appendix II)** includes an overview of the key findings of this thesis.

### 1.3. TGF $\beta$ superfamily

The Transforming growth factors (TGFs) were firstly identified as secreted proteins from murine sarcoma virus-transformed fibroblasts; these proteins induced *in vitro* transformation to neoplastic-like phenotype as evidenced by cell division, morphological changes and anchorage-independent growth<sup>3,4</sup>. Two distinct classes of proteins were isolated, the type  $\alpha$  and type  $\beta$  with different properties and synergistic effects. In fact, the original observations suggested that TGF $\beta$  *per se* does not stimulate cell growth unless combined with other growth factors such as TGF $\alpha$  and epidermal growth factor (EGF)<sup>5</sup>. Although initially TGF $\beta$  was found present in neoplastic cells<sup>6,7</sup> further studies showed its expression in various normal human cells and tissues such as platelets<sup>8</sup>, placenta<sup>9</sup> and during embryonic development<sup>10,11</sup>. A physiological role in cell differentiation, wound healing, angiogenesis and as an inhibitor of cell growth was attributed to TGF $\beta$  in various tissues<sup>12</sup>. Despite the functional complexity of TGF $\beta$  the core signaling components and their interactions appear at first instance rather simple.

The TGF $\beta$  superfamily of ligands can be divided into subfamilies; TGF $\beta$  proteins, bone morphogenetic proteins (BMPs), the growth and differentiation factors (GDFs), ACTIVINS, MYOSTATINS, NODAL and Anti-Mullerian hormone (AMH).

The molecular skeleton of TGF $\beta$  pathway is comprised by the extracellular TGF $\beta$ -family ligands, which elicit their signals into the cell by binding to type II receptor (T $\beta$ RII), forming heterodimer complexes with type I receptor T $\beta$ RI/ACTIVIN receptor-like kinase (ALK5)<sup>13</sup>. This interaction activates the receptor's serine/threonine kinase activity to phosphorylate and activate SMAD transcription factors. Phosphorylation of receptor-activated SMADs (R-SMADs) by the activated type I receptor allows the R-SMADs to form heterodimers with partner SMAD (co-SMAD/ SMAD4) and translocate to the nucleus where, in collaboration with transcription factor complexes, they activate or inhibit the transcription of target genes<sup>14</sup> (**Fig.1**).

### 1.3.1. BMP subfamily

BMP factors were firstly identified as chondrogenic and osteogenic inducers. Further investigations revealed various roles for BMPs during embryogenesis; kidney, skin, hair, muscle, haematopoietic and neuronal development, as well as a role in iron metabolism and vascular maintenance<sup>15-17</sup>. Although BMPs typically activate BMP type I receptors and R-SMAD1, 5 and 8, they can be further classified into several subgroups, including BMP1/2/3/4 group, BMP5/6/7/8 group, growth and differentiation factor (GDF)5/6/7 group and BMP9/10 group<sup>15,18</sup>. BMP2, BMP6 and the most recently identified BMP9 are the most potent inducers of osteogenesis<sup>19</sup>. Although structurally different, other members of the BMP pathway are GDF8/MYOSTATIN and GDF9, having a role in muscle tissue and ovarian development, respectively<sup>20,21</sup>.

Signal transduction of BMP subfamily is conducted in a similar manner as the TGF $\beta$  cascade. BMP ligands use BMPRII, ACVR2A or ACVR2B type II receptors and have affinity for ALK1, ALK2, ALK3 and ALK6<sup>22</sup>. SMAD1, 5 and 8 are the BMP-specific R-SMADs that translocate to the nucleus upon activation by the type I receptor and regulate BMP target gene transcription<sup>15</sup> (**Fig.1**).

### 1.3.2. TGF $\beta$ canonical pathway

#### Level 1. Ligand synthesis and secretion

There are three types of TGF $\beta$  ligand isoforms: TGF $\beta$ 1, TGF $\beta$ 2, and TGF $\beta$ 3, all of which are highly conserved among species. Mature TGF $\beta$ 1, TGF $\beta$ 2 and TGF $\beta$ 3, which are produced after proteolytic activation from cleavage precursor proteins, share high amino acid sequence homology and functional similarity. However, it has been reported that TGF $\beta$ 2 and TGF $\beta$ 3 are biologically more active than TGF $\beta$ 1<sup>23</sup> and their tissue expression follows a distinct pattern<sup>24</sup>. Following the identification of the three isoforms<sup>25-28</sup> novel information from transgenic mouse models added to our understanding of the crucial and specific role during embryonic development for all three isoforms. Genetic deletion of TGF $\beta$ 1 in mice leads to general inflammation<sup>29</sup> and early death<sup>30</sup> due to vascular and hematopoietic abnormalities during development<sup>31</sup>. Mice lacking TGF $\beta$ 3 exhibit lung and cleft palate defects due to abnormal epithelial-to-mesenchymal transition (EMT) and die immediately after birth<sup>32</sup>. Homozygous deletion of TGF $\beta$ 2 confirmed the previously suggested role of TGF $\beta$ 2 in cardiogenesis<sup>33</sup> but also causes multiple defects (cardiac, lung, eye and skeletal tissues among others) that are not resembling the TGF $\beta$ 1 or TGF $\beta$ 3 knockout phenotype<sup>34</sup>.

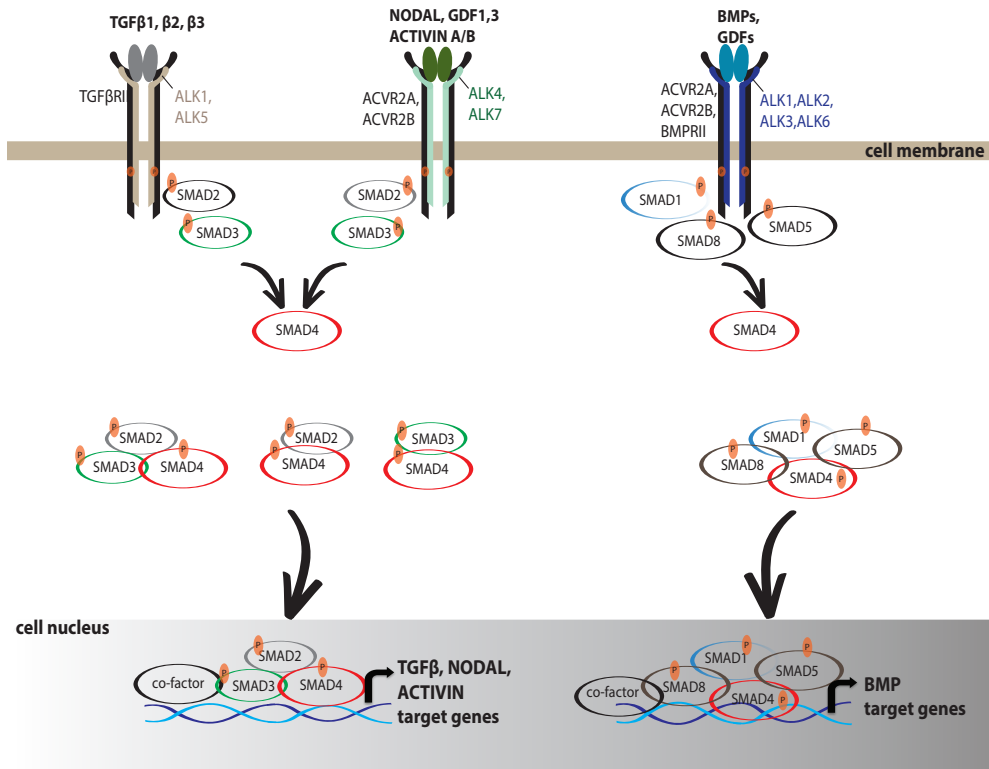


**Fig.1. Overview of TGF $\beta$  signaling pathway**

The core of the pathway is comprised by the SMAD effectors that mediate downstream signaling from extracellular ligands; TGF $\beta$ , ACTIVINS, NODAL, BMPs, GDFs. (left) TGF $\beta$  ligands bind to type II receptor TGF $\beta$ RII, which recruits and phosphorylates the type I receptor ALK5 or ALK1 (endothelial cell-specific receptor). ALK5 phosphorylates R-SMADs (SMAD2 and SMAD3) that form complexes with phosphorylated SMAD4 and translocate into the nucleus. R-SMAD/SMAD4, together with co-factor proteins, bind to gene promoter regions and induce or repress target gene transcription. (middle) NODAL, GDF1, GDF3 and ACTIVIN-A, -B bind to ACVR2A, ACVR2B and activate ALK4 or ALK7. ALK4/7 transduce their signal via SMAD2 and SMAD3 effectors, similarly to the TGF $\beta$  cascade. (right) GDFs/BMPs bind simultaneously to a combination of type II (BMPRII, ACVR2A or ACVR2B) and type I receptors (ALK1, ALK2, ALK3 or ALK6). This leads to phosphorylation of R-SMADs, SMAD1, SMAD5 and SMAD8 which couple to SMAD4 and as a complex enter the nucleus and regulate GDF/ BMP target gene expression.

TGF $\beta$  proteins are expressed as inactive pre-pro-peptides; latency is controlled by binding to the latency-associated peptide (LAP) and latent TGF $\beta$  binding protein (LTBP) and is reversed by proteolytic cleavage<sup>35</sup>. Briefly, after protein synthesis and signal peptide removal by endoplasmic reticulum proteases, the pro-TGF $\beta$  peptides assemble in inactive homodimers and are secreted in the extracellular space. The pro-TGF $\beta$  peptide is further cleaved in the secretory vesicles or in the extracellular matrix (ECM) by enzymes (convertases) into two fragments; a C-terminal immature TGF $\beta$  peptide and an N-terminal peptide (LAP). The LAP-TGF $\beta$  complex remains non-covalently attached (small latency complex, SLC) or binds further to LTBP forming the large latency complex (LLC)<sup>36</sup>. LTBP stabilizes the complex by binding to ECM components such as fibronectin, fibrillin1 and integrins<sup>37</sup>.



Mechanical stress, cell contraction, extreme pH or temperatures are some of the factors inducing disintegration of LLC by degradation of fibrous matrix (proteases e.g. plasmin, elastase, thrombin). Cleavage of LTBP by BMP1 protease and matrix metalloprotease enzymes (MMP-2) leads to release of TGFβ from the LAP complex<sup>38</sup>. Additional mechanisms of activation of latent TGFβ include integrins<sup>39</sup>, fibronectin<sup>40</sup> and the matricellular protein thrombospondin-1<sup>41</sup>. After dissociation from the LAP, the active TGFβ homodimer is then recognized by the TGFβ type I and type II receptors on recipient cells in a cell autonomous, paracrine and endocrine manner.

**Level 2. Receptor binding**

Receptors of TGFβ signaling are serine/threonine kinase receptors and are distinguished in two types (type I and type II)<sup>12</sup>. The co-receptor class (type III; β-GLYCAN, ENDOGLIN and CRIPTO) has auxiliary function. Active TGFβ ligands bind to the constitutively active TGFβ type II receptor<sup>13</sup>. The type II receptor transphosphorylates the type I ACTIVIN receptor-like kinase (ALK) thus leading to an interacting formation between a ligand homodimer and a heterotetramer of type I/ type II receptors<sup>14</sup>. Five type II receptors (TGFβRII, BMPRII, ACVR1A, ACVR1B, and seven type I receptors (ALK1-ALK7) have been identified<sup>42</sup>. Different combinations of receptor-ligand assemblies provide differential signaling specificity (**Table 1**). The predominant type I receptor of TGFβ ligands is the ALK5<sup>43</sup>, with the exception of signaling via ALK1 in endothelial cells<sup>44</sup>. The ALKs contain an extracellular domain for ligand interaction, a glycine-serine residue rich (GS) domain; site of phosphorylation by the type II receptor occurs and the serine/threonine kinase domain<sup>45-47</sup>. Levels of activated receptors determine the levels and duration of activation of downstream signal mediators<sup>48</sup>.

	Ligand	Type I receptor	Type II receptor
<b>TGFβ</b>	TGFβ1, TGFβ2, TGFβ3	TGFβRI (ALK5) ALK1	TGFβRII
<b>BMPs</b>	BMP2, 4 GDF5/6/7 BMP5/6/7/8 BMP9/10	ACVRL1 (ALK1) ACVR1 (ALK2) BMPRI1A (ALK3) BMPRI1B (ALK6)	ACVR2A ACVR2B BMPRII
<b>ACTIVINs, NODAL</b>	ACTIVIN A, AB, A Inhibin A, B NODAL GDF1/3	ACVR1B (ALK4) ACVR1C (ALK7)	ACVR2A ACVR2B
<b>AMH</b>	AMH	ACVR1 (ALK2) BMPRI1A (ALK3)	AMHR2

**Table 1. Combinations of receptor- ligand interactions of TGFβ subfamilies**

Abbreviations: ACVR2A; ACTIVIN A receptor type IIA, ACVR2B; ACTIVIN A receptor type IIB, ACVRL (ALK); ACTIVIN A receptor type II-like, AMH; anti-mullerian hormone, AMHR2; anti-mullerian hormone receptor type II, BMPRI; bone morphogenetic protein receptor, GDF; Growth and differentiation factor. TGFβRI; transforming growth factor receptor. Adapted from<sup>49</sup>.

### Level 3. SMAD protein recruitment

The intracellular canonical TGF $\beta$  pathway effectors, which mediate signal transduction from the receptors towards the nucleus, are the SMAD proteins. Nomenclature of SMAD is based on the homology with the *C. elegans* and *Drosophila* mutants SMA and MAD, respectively, in whom they were firstly identified<sup>50</sup>. Three classes of proteins are distinguished; the receptor-associated SMADs (R-SMADs; SMAD1, 2, 3, 5, 8), the inhibitory SMADs (SMAD6, 7) and the common SMADs (co-SMAD4)<sup>14</sup>. Structurally, SMAD proteins have two globular domains (MH1 and MH2) associated by a regulatory linker region<sup>2</sup>. MH1 is required for DNA binding. The MH2 domain is required for interaction with membrane receptors, nucleoporins, other SMADs and transcription factors<sup>51</sup>. The linker region is a site for protein-protein interactions (positive and negative regulators of SMADs) and is regulated by phosphorylation e.g. by cyclin-dependent kinases (CDKs)<sup>52</sup>, MAPK kinases<sup>53</sup>. Ligand binding of TGF $\beta$ 1,  $\beta$ 2, and  $\beta$ 3 to the receptors leads to recruitment and activation of the SMAD2 and SMAD3 mediators. Instead, BMP ligands lead to recruitment of SMAD1, SMAD5 and SMAD8 to BMP receptors. In either case, R-SMADs are phosphorylated by the type I receptor at the Ser-X-Ser motif of the MH2 domain (X; any aminoacid) and form a complex with other R-SMADs and subsequently with the co-activating SMAD4 mediator<sup>42</sup>. The R-SMAD/SMAD4 protein complex relocates to the nucleus, where it interacts with DNA sequences by assembling with co-activators, transcription factors (TFs) and chromatin modifiers to regulate activation and repression of certain target genes.

### Level 4. Transcriptional activity

Activated R-SMAD2 and -3 form heterodimeric or heterotrimeric complexes with SMAD4 complexes and bind to DNA in CAGA motifs namely SRE sites (SMAD-response element). BMP-related TFs (R-SMAD1, 5, and 8) bind to SRE sites but have higher affinity for GC-rich regions containing BMP-response-elements (BRE sites). An additional BMP binding site has been identified (GC-BRE) that confers cell type- specific gene transcription in endothelial versus smooth muscle cells<sup>54</sup>. However, R-SMADs DNA binding affinity is weak, thus they form complexes with other DNA binding TFs, which explains the multifunctionality of SMAD pathway<sup>42</sup>. Cell type- specific responses are determined by differential interaction with specific TFs that direct R-SMAD2 and -3 in certain binding sites; e.g. RUNX factors in hematopoietic cells, OCT4 and SOX2 in pluripotent cells, MYO-D to initiate the muscle program<sup>55</sup>. Interactions of R-SMADs with co-activators and co-repressors determine activation or inhibition of downstream target gene transcription. Identified co-activators of SMADs include adenovirus early gene1 (E1A)- binding protein (p300), CREB binding protein (CBP) and Specificity protein-1 (SP1). Co-repressor factors associating with R-SMADs are the SWItch/Sucrose Non-Fermentable (SWI/SNF) nucleosome positioning proteins, DNA demethylating complex (DNM), Forkhead Box (FOX) and elongation factor-2 (E2F) factors<sup>2</sup>. The TGF $\beta$  target genes SKI and SNON are co-repressor factors associating with phosphorylated SMADs in the nucleus in order to repress SMAD transcriptional activity<sup>56</sup>. Multiple target genes are controlled by SMAD canonical pathway and can be classified based on the activating ligand (TGF $\beta$ /ACTIVIN/NODAL or BMPs) or depending on its function on a particular cellular process (angiogenesis, ECM, immunosuppression, apoptosis). **Table 2** indicates the most common target genes activated by TGF $\beta$  and BMP pathway.

	SMAD Target genes				
	Growth arrest	Apoptosis	Angiogenesis	ECM	EMT
TGF $\beta$ /ACTIVIN-Responsive	CDKN1A (p21CIP1), CDKN1B (p27KIP1), CDKN2B (p15INK2B), CMYC,	BAD (BCL-XL), BIM,GADD45B	TSP-1	FN, COL1A1, COL1A2, DCN, PAI-1, PDGF $\beta$ , MMP2, TIMP1, CTGF, ACTA2,	SNAIL1/2, ZEB1/2, HMGA2
	Differentiation	Osteogenesis	Inflammation	Cardiogenesis	EMT/MET
BMP-Responsive	ID1, ID2, ID3, SMAD6/7, GATA3	OSTEOCALCIN, RUNX2, OSX	JUNB, IKB $\alpha$	NKX2.5	ZO-1, SNAIL1, ID2

**Table 2. Common target genes of TGF $\beta$ / BMP pathways classified in various cellular responses**

Abbreviations. ACTA2; aorta smooth muscle actin  $\alpha$  2, BAD (BCL-XL); BCL-2 associated agonist of cell death, BIM; BCL-2-like 11, CDKN1A (p21, CIP1); cyclin-dependent kinase inhibitor 1A, CDKN1B (p27KIP1); cyclin-dependent kinase inhibitor 1B, CDKN2B (p15INK2B); cyclin-dependent kinase inhibitor 2B, CMYC; v-myc avian myelocytomatosis viral oncogene homolog, COL1A1; collagen type 1  $\alpha$  1, COL1A2; collagen type 1  $\alpha$  2, CTGF; connective tissue growth factor, DCN; decorin, ECM; extracellular matrix, EMT; epithelial-to-mesenchymal transition, GADD45B; growth arrest and DNA-damage-inducible 45 beta, FN; fibronectin, GATA3; GATA binding protein 3, HMGA2; high motility group AT-hook 2 protein, ID; inhibitor of differentiation, IKB $\alpha$ ; nuclear factor of kappa light polypeptide gene enhancer in B-cells inhibitor, alpha, JUNB; jun B proto-oncogene, MET; mesenchymal-to-epithelial transition, MMP2; matrix metalloprotease 2, NKX2.5; NK 2 homeobox 5, OSX; osterix (Sp7 transcription factor), PAI-1; plasminogen activator inhibitor 1, PDGF $\beta$ ; platelet derived growth factor  $\beta$  polypeptide, RUNX2; runt related transcription factor 2, SMAD; Sma-Mad family member, SNAIL; snail zinc finger protein, TIMP1; tissue inhibitor of metalloproteinase 1, TSP-1; thrombospondin-1, ZEB; zinc finger E-box binding homeobox, ZO-1; tight junction protein 1.

### 1.3.3. Regulation of the TGF $\beta$ pathway

Multiple inhibitory mechanisms are integrated within the network of TGF $\beta$  pathway to control the timing, duration and cell context-dependent activation of the signaling cascade. Induction of TGF $\beta$  pathway simultaneously elicits negative feedback mechanisms that span throughout the cell from the extracellular space to the nucleus (reviewed in<sup>51,56-58</sup>). Understanding these mechanisms is clinically relevant for treatment of human diseases, as the intrinsic inhibition of the pathway has been mimicked with drug compounds used in clinical trials. An overview of these mechanisms is discussed in this section, starting from the cell membrane level and progressing gradually towards the cytoplasmic and nuclear level (Fig.2).

#### 1.3.3.a. Antagonists of ligands

Extracellular inhibitory mechanisms of the TGF $\beta$  signaling include the association with LAP and LTBP that keep ligands in inactive state, as discussed in section 1.3.2 (level 1), as well as additional molecules with similar function.

For example, DECORIN is a small leucine-rich proteoglycan produced by smooth muscle cells, fibroblasts and vascular endothelial cells with inhibitory role for TGF $\beta$ <sup>59</sup>. It forms a large network with matrix proteins, receptor tyrosine kinases and growth factors, in particular with components of the TGF $\beta$  pathway<sup>60</sup>. DECORIN inhibits TGF $\beta$  signaling by sequestering the ligands and preventing their binding to the type II receptor<sup>61</sup>.

Alternatively, DECORIN employs the calmodulin-dependent kinase II to phosphorylate SMAD2 at the inhibitory Ser-240 site<sup>62</sup>. This phosphorylation does not prevent nuclear translocation of SMAD2 (due to activating Ser 465/467 phosphorylation by type I receptor) but blocks interaction of SMAD2 with SMAD3 and nuclear translocation of SMAD3<sup>62</sup>.

Other antagonists of different branches of TGF $\beta$  signaling with similar function as DECORIN are NOGGIN, GREMLIN, SCLEROSTIN, CHORDIN, FOLLISTATIN, VENTROPTIN, Follistatin-related gene protein (FLRG), CERBERUS and LEFTY<sup>18,22,63</sup> that negatively regulate signal activation at the ligand level.

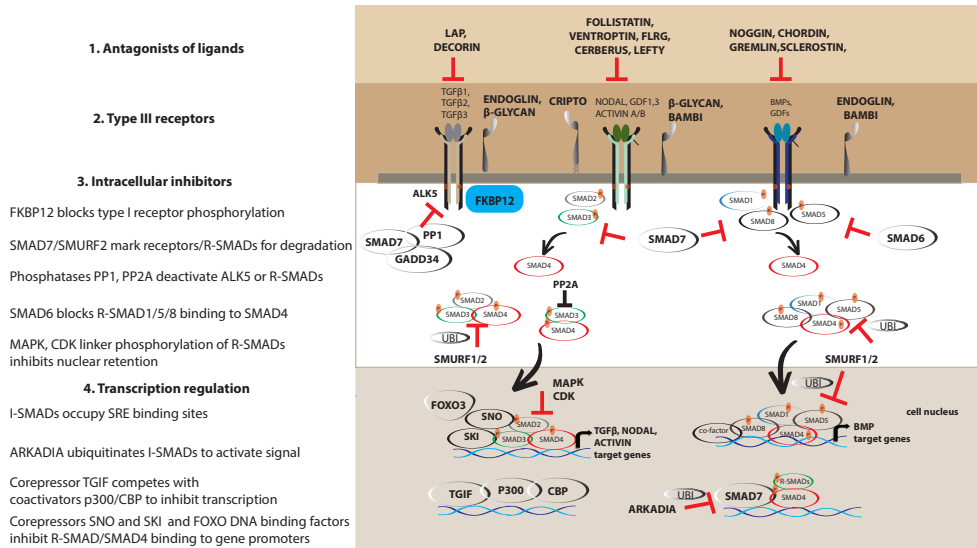


**Fig.2. Regulation of TGF $\beta$  pathway from extracellular space to nucleus**

Overview of the intrinsic TGF $\beta$  pathway mechanisms that control the duration of TGF $\beta$  signal activation at different subcellular localizations; (1) ligand antagonism in the extracellular space, (2) modulation of receptors and ligands at the membrane level by ENDOGLIN, CRIPTO,  $\beta$ -GLYCAN, pseudoreceptor bone morphogenetic protein and activin membrane-bound inhibitor BAMBI, FKBP12, (3) intracellular inhibitors I-SMADs (SMAD6 and SMAD7), E3 ligases SMURF1/2, phosphatases PP1/PP2A, MAPK and CDK kinases inhibit R-SMAD nuclear translocation via phosphorylation in the linker site of R-SMADs, (4) at the nucleus level, SMURF1/2 mark activated R-SMADs for degradation, SMAD7 and FOXO factors directly inhibit gene transcription, co-repressors TGF $\beta$ -induced factor 1 TGIF, SNO and SKI antagonize for gene promoter binding either with the co-activators p300/ CBP or R-SMAD/ SMAD4 complexes and E3 ubiquitin ligase ARKADIA marks I-SMADs for degradation to elongate signal activation.

### 1.3.3.b. Type III receptors

A third group of TGF $\beta$  receptors (type III co-receptors) modulate the interactions between the type I/II receptors and the ligands. To date, three such co-receptors have been identified;  $\beta$ -GLYCAN, ENDOGLIN (CD105) and CRIPTO (TDGF1).  $\beta$ -GLYCAN directs TGF $\beta$ 2 to the type II receptor to facilitate signal activation<sup>64</sup> and enhances ALK3 and ALK6 signaling<sup>65</sup>. ENDOGLIN plays an important role in angiogenesis along with ALK1, TGF $\beta$ , BMP9 and BMP10<sup>66,67</sup>. ENDOGLIN is present in two isoforms (S and L form) as a membranous and secreted protein<sup>68</sup> and facilitates the binding of TGF ligands to the ALK1 in endothelial cells (activation of R-SMAD1, 5, 8), therefore preventing association of TGF $\beta$  with ALK5 and activation of R-SMAD2/3<sup>69</sup>. The TGF $\beta$  ligands NODAL and GDF1/3 require association with CRIPTO co-receptor in order to bind to the ALK4, ALK5 and ALK7 and induce activation of SMAD2 and SMAD3. Paradoxically, CRIPTO can inhibit SMAD2/3 phosphorylation mediated by TGF $\beta$  by binding to TGF $\beta$  ligands and preventing their binding to receptors<sup>70,71</sup>. Multiple functions are attributed to CRIPTO that are NODAL and TGF $\beta$ -independent, such as modulation of a network of signaling pathways (e.g. NOTCH, WNT, AKT) pathways in various tissues<sup>72-74</sup> and regulation of EMT in development and cancer<sup>75</sup>. The role of CRIPTO will be extensively discussed later in this chapter.

A distinct type of co-receptors are the glycoproteins of the repulsive guidance molecules (RGM) family, which inhibit specifically the ligands of the BMP branch<sup>76-78</sup>, as opposed to other co-receptors that recognize various ligands. RGMa, RGMb (Dragon) and RGMc (hemojuvelin) particularly enhance signaling mediated by BMP2 and BMP4 or guide them to use alternative type II receptors e.g. ACVR2A instead of BMPRII<sup>79</sup>.

### 1.3.3.c. Inhibition at the cell membrane level

Assembly of type I and II heterodimers is tightly regulated by a certain type of pseudoreceptor (BMP and ACTIVIN membrane-bound inhibitors; BAMBI) that consists of an extracellular domain of high structural similarity to serine/threonine receptors<sup>80</sup>. BAMBI binds BMPs and type I/ type II receptors but lacks cytoplasmic domain, thus preventing activation of type I receptor and downstream signaling<sup>22</sup>.

TGF $\beta$  and BMPs directly induce BAMBI transcription<sup>81,82</sup> as a negative feedback mechanism to regulate the duration of signaling. To regulate the step of type II receptor-induced type I receptor transphosphorylation, the Ser/Thr residues of the type I receptor, that are phosphorylated by the type II kinase, are blocked by the inhibitor FKBP12. In the inactive state (absence of ligand), type I receptor interacts via the GS domain with the inhibitor FKBP12 at the intracellular cell membrane site<sup>83</sup>. FKBP12 prevents type I phosphorylation rather than interaction with type II receptor and is a regulatory mechanism to prevent ligand-independent receptor activation for ALK5<sup>84</sup> as well as for BMP type I receptors<sup>85</sup>. Phosphorylation in the GS domain (adjacent to FKBP12 binding site) by the type II receptor releases FKBP12 and induces conformational change that facilitates binding of downstream effectors R-SMADs<sup>84,86</sup>.

In homeostatic conditions, R-SMADs are actively retained in the cytoplasm while SMAD4 shuffles continuously from the cytoplasm to the nucleus<sup>48</sup>.

The presence of the docking complex SMAD anchor for receptor activation (SARA) in the intracellular part of cell membrane keeps SMADs in the cytoplasm to facilitate receptor interaction and phosphorylation<sup>87</sup>. SARA binds SMAD2 and blocks the nuclear import signal

located in the MH2 domain; this process is reversible upon phosphorylation of R-SMADs by the type I receptor<sup>88</sup>.

### 1.3.3.d. Post-translational modifications (PTMs) of receptors and R-SMADs

Post-translational modifications (phosphorylation, ubiquitination, sumoylation, glycosylation, fucosylation) affect protein folding and activity and as a result may increase or limit the bioavailability of the receptors and the activated R-SMADs during TGF $\beta$  response. In this paragraph an overview of the most common PTMs and their dynamic role in TGF $\beta$  pathway is discussed.

Phosphorylation promotes or inhibits kinase activity of both type I and type II receptors; the Ser/Thr kinase of TGF $\beta$ RII is constantly active due to autophosphorylation<sup>89</sup>, while Ser416 phosphorylation inhibits kinase activity<sup>90</sup>. Type I receptor exerts multiple functionalities by dual kinase activity; Ser/Thr phosphorylation as well as autophosphorylation of tyrosine (Tyr) residues. Lee et al., have demonstrated the way Tyr autophosphorylation of ALK5 activates ERK kinase which comprises a cell growth stimulus, counteracting the SMAD2/3 cytostatic pathway<sup>91</sup>. Deactivation of kinase domain and activated SMADs by dephosphorylation controls the duration and location of signal. Phosphatases are enzymes that remove the phosphate group from proteins and reverse phosphorylation, thus, switching the protein activity. There are three types of phosphatases, Ser/Thr, Tyr or of dual activity that contain catalytic and regulatory domains. Phosphatases PP1 and PP2A are established regulators of TGF $\beta$  member dephosphorylation. For instance, PP1 is recruited to dephosphorylate the type I receptor by a complex of SMAD7 and growth arrest and DNA damage protein GADD34, a regulatory subunit of PP1<sup>92</sup>. Phosphatase PP2A dephosphorylates SMAD3 but not type I receptor or SMAD2, indicating the specificity and regulatory role of these enzymes<sup>93</sup>. In addition to Ser/Thr and Tyr phosphorylation multiple other PTMs have been identified to positively or negatively regulate the function of the type I/II receptors, such as sumoylation, ubiquitination<sup>94</sup> and possibly others. Such modifications also alter protein folding, protein localization, assembly with other proteins or target a protein for degradation<sup>95</sup>. For instance, sumoylation marks on unique sumoylation site Lys389 of the ALK5 modulates the kinase activity, recruits SMAD3 and potentiates signal activation<sup>56,96,97</sup>.

Activated TGF $\beta$ /type I and type II complexes follow two intracellular routes; the clathrin-mediated endocytosis, that propagates the signal downstream, and the caveolae-associated cascade that interrupts the signal by degradation of the ligand/receptor complexes<sup>57</sup>. The degradation takes place either in lysosomes or in proteasomes; the latter requires ubiquitination by E3 ligases (ARKADIA, SMURF family)<sup>98,99</sup>.

SMURF1 and SMURF2 often bind I-SMADs, such as SMAD7<sup>100</sup>, and migrate from the nucleus to the cytoplasm to form complexes with activated receptors in the caveoli. This leads to polyubiquitination of the receptors, SMAD7 and SMURFs all of which are proteolytically degraded<sup>57,80</sup>.

ARKADIA is a RING-finger E3 ubiquitin ligase that marks SMAD7 for ubiquitin-mediated degradation thus aborting SMAD7 inhibitory function and enhancing SMAD signaling<sup>101</sup>. Inflammation-induced nuclear receptor NR4A1 is responsible for ARKADIA activation and SMAD7 degradation, a mechanism linking TGF $\beta$  hyperactivation with inflammation and tumor promoter activity<sup>102,103</sup>.

Function of ARKADIA is highly determined by sumoylation<sup>104,105</sup>. Deletion of ARKADIA in mice leads to upregulation of SMAD6, SMAD7 and SKI and it has been shown that it

ubiquitinates SMAD6 and potentiates BMP signaling<sup>106</sup>. ARKADIA has dual functions at the transcriptional level where it interacts with chromatin remodelers such as Polycomb repressive proteins but has also proven to abort methylation-induced gene silencing of TGF $\beta$  target genes<sup>107</sup>. In addition, ARKADIA ubiquitinates SKI/ SNON associated with pSMAD2/3 complexes<sup>108</sup>. Degradation of this repressory network allows the formation of new pSMAD/ DNA complexes<sup>109,110</sup>

In addition, other PTMs of R-SMADs include phosphorylation in the linker region by GSK3, MAPK kinases, or cell cycle protein CDK4 which causes ubiquitination by E3 ligases (Lys11, Lys48) and proteasomal degradation<sup>42</sup>. Sumoylation of SMAD4 (Lys 159, 113) has been reported to regulate its function in renal and breast cancer cell lines<sup>111,112</sup>. Nuclear pSMAD4 is monoubiquitinated by USP9x to disrupt activated R-SMAD/SMAD4 complexes and release SMAD4 back to the cytoplasm<sup>113</sup>.

### 1.3.3.e. Inhibitory SMADs (I-SMADs) and transcriptional repression

An intracellular negative feedback loop mechanism, directly induced by TGF $\beta$ <sup>114</sup>, as well as BMPs<sup>115</sup>, is the activation of I-SMADs, SMAD6 and SMAD7<sup>116,117</sup>. I-SMADs effectively limit or block completely the pathway by functioning in multiple subcellular localizations<sup>57,80</sup>. The intracellular circulation of I-SMADs is coupled to their function; (i) type I receptor blockers at the cell membrane<sup>117,118</sup>, (ii) antagonists of SMAD4 in the cytoplasm<sup>119,120</sup> or (iii) occupying SRE binding sites to prevent SMAD- DNA functional complexes in the nucleus<sup>121</sup>. SMAD7 is primarily found in the nucleus during absence of ligand stimulation, while presence of TGF $\beta$ 1 directly mediates the nuclear export of SMAD7 to induce inhibition of the type I receptor<sup>122</sup>. In addition, I-SMADs recruit E3 ubiquitin ligases SMURF1 and SMURF2 to direct them towards the phosphorylated type I receptors or R-SMADs for degradation<sup>2,100</sup>. SMAD7 inhibits both TGF $\beta$  and BMP signaling<sup>123,124</sup> while SMAD6 has BMP-specific action<sup>15</sup>. I-SMADs are subjected to functional restriction by other interacting proteins; e.g. BMPs activate an inhibitor of SMAD6 (associated molecule with the SH3 domain of signal transducing adaptor molecule, AMSH), which blocks SMAD6/SMAD1 complex formation and thereby SMAD1 phosphorylation is maintained<sup>125</sup>.

Ultimately, the presence of activating and repressing TFs and complexes at a given gene promoter site determines whether SMADs exert a positive or negative transcriptional activity. Co-repressors play an important role in regulating the duration of signaling and proper target gene expression. Such co-repressors SKI, SNON, TGF $\beta$ -induced factor homeobox (TGIF) that interfere with SMAD signaling by repressing transcription of TGF/BMP target genes<sup>126</sup>. In turn, expression of these co-repressor proteins is induced by SMAD signaling. Another mechanism is the recruitment of HDAC co-repressor complexes to inhibit transcription which is mediated by I-SMADs; SKI co-repressor recruits HDACs and methylase complexes to repress the expression of SMAD7<sup>127</sup>.

### 1.3.4. NODAL pathway

NODAL pathway has important functions during gastrulation, mesendoderm formation, induction of extraembryonic endoderm and left/ right asymmetry during embryonic development<sup>63,128-131</sup>. During adulthood NODAL pathway is quiescent and its reactivation is often associated with pathological situations<sup>132</sup>.

Signaling is activated upon NODAL, GDF1 or GDF3 ligand binding to ALK4 or ALK7 and

ACTIVIN type II receptors. The accessory type III receptors CRIPTO (obligatory co-receptor for NODAL, GDF1/3) and CRYPTIC bind to the activated receptor heterotetramer and mediate SMAD2 activation<sup>133</sup>. CRIPTO and CRYPTIC belong to the epidermal growth factor-like, cysteine-rich CRIPTO-FRL1-CRYPTIC (EGF-CFC) protein domain family and have a dual role both as membranous and secreted proteins after cleavage of the glucophosphatidylinositol (GPI) link<sup>134-136</sup>. CRIPTO also functions as a chaperone of immature NODAL protein, directs it to the extracellular part of cell membrane where it is being subjected to proteolytic activation by convertases (FURIN and PACE-4)<sup>137</sup>. CRIPTO interacts with NODAL and TGF $\beta$  ligands via the EGF domain and with ALK4 via the CFC domain. CRIPTO interaction with NODAL is functionally dependent on PTM O-fucosylation on Thr88 residue which is characteristic of EGF domains<sup>138</sup>.

Downstream signal transduction is primarily mediated by SMAD2/SMAD4 heterodimers, which associate with nuclear co-factors such as p53, FoxH1 to direct target gene transcription<sup>139</sup>. A role for SMAD3 during NODAL signaling remains to be further characterized<sup>140</sup>. NODAL target genes involve NODAL itself<sup>63</sup>, CRIPTO<sup>141</sup> and the negative regulators LEFTY and CERBERUS<sup>139,142</sup>. LEFTY is an extracellular direct antagonist of NODAL ligand and the ACTIVIN receptors, while CERBERUS and CERBERUS-like (DAN protein family) bind to NODAL preventing its association with the receptors. Other negative regulators of NODAL signaling include; DAPPER2 (binds type I/II receptors for lysosomal degradation)<sup>143</sup>, ECTODERMIN<sup>144</sup>, TGIF1/2 proteins (co-repressors)<sup>145</sup>, BMP3 and BMP7 (sequesters NODAL ligand)<sup>133,146</sup>. In turn, NODAL can also inhibit BMP signaling in a CRIPTO-independent manner<sup>133</sup>.

In addition, CRIPTO has autonomous signaling functions that are NODAL and SMAD-independent<sup>74</sup>. In fact, CRIPTO individually regulates a large network of signaling pathways e.g. activating p38, ERK and c-SRC/MAPK/AKT pathways<sup>130</sup>. For this alternative function CRIPTO synergizes with glucose-related protein-78 (GRP-78)<sup>70,72</sup>, GLYPICAN-1 signaling<sup>147</sup>, caveolin<sup>148</sup>, apelin<sup>149</sup>, leucine-rich protein 5 (LRP5)<sup>150</sup> or NOTCH to modulate WNT and NOTCH signal transduction<sup>75,151</sup>,

Aberrant CRIPTO pathway activity, particularly mediated via GRP78 by inhibiting TGF $\beta$  and activating and c-SRC/MAPK/AKT, is associated with human malignancies; breast, lung, prostate, ovarian, bladder, colon, liver, melanoma and glioblastoma<sup>73,152-160</sup>. Prognostic methods and strategies for *in vivo* inhibition of tumor-promoter role of CRIPTO/ GRP78 (peptides, monoclonal antibodies, tumor vaccines) are being studied preclinically<sup>161-163</sup> and in phase I clinical trials<sup>164</sup>.

### 1.3.5. Non canonical SMAD pathways

In addition to the classical SMAD pathways TGF $\beta$  receptors exert their multifunctionality by activating non-SMAD pathways such as PI3K/Akt, Ras/ MAPK kinases ERK, p38 and JNK<sup>165</sup> (**Fig.3**). Both canonical and non-canonical branches have as starting point the TGF $\beta$  receptors, however, differential activities of the receptor complex due to PTMs, ligand-independent oligomerization or binding to different interaction partners determine which subpathway will be activated<sup>56</sup>.

Cells circumvent the growth inhibition of TGF $\beta$ /SMAD signaling by using TGF $\beta$  to activate the growth stimulatory RAS/ RAF/ MEK/ ERK MAPK kinase pathway<sup>42</sup>. The MAPK kinase pathway is activated in response to mitogens such as EGF bound to receptor tyrosine kinases (RTKs)<sup>57</sup>. However, TGF $\beta$  elicits MAPK response due to the dual kinase activity of TGF $\beta$ RI and TGF $\beta$ RII to transautophosphorylate not only serine/ threonine but also tyrosine



residues (RTK function)<sup>56</sup>. Activation of RTK leads to activation of monomeric GTPase RAS, which acts as a scaffold between the RTK and RAF kinase (MAPKKK). Phosphorylation and activation cascade of downstream kinases MEK (MAPKK) and finally ERK (MAPK) propagates the signal to alter gene expression in favor of cell growth and proliferation<sup>166</sup>. ERK MAPK kinase propagates the signal via phosphorylation of target proteins in the cytoplasm (e.g. inhibition of SMADs by linker phosphorylation) and also translocates to the nucleus to activate gene regulatory proteins<sup>166,167</sup>.

Another TGF $\beta$ / non-SMAD mediated mechanism is the RTK function of TGF $\beta$  receptors, which activates the phosphoinositole-3 kinase (PI3K) pathway<sup>168</sup>. PI3K activation leads to recruitment of kinases PDK1 and Akt receptors in phosphorylated lipid docking sites where the two kinases phosphorylate each other leading to activation of Akt<sup>169</sup>. Akt phosphorylates other proteins such as cell survival complex mTOR 170 or inactivates the proapoptotic protein BAD via recruiting adaptor protein 14-3-3<sup>171,172</sup>. The net outcome is cell survival, growth and proliferation.

In addition, TGF $\beta$  regulates actin cytoskeleton formation and cell adhesion by interfering with the monomeric GTPase proteins of the RHO family (RHO, RAC and CDC42)<sup>168</sup>; TGF $\beta$ RII phosphorylates polarity protein PAR6 that together with SMURF1 marks RHO for ubiquitin-mediated degradation<sup>173</sup>. The function of RHO signaling is to maintain the epithelial tight junctions, thus, TGF $\beta$  induces a mesenchymal transformation of epithelial cells<sup>173</sup>.

Another example of non-SMAD activation by TGF $\beta$  receptor is the network of ubiquitin ligase TNF $\alpha$ -associated factor 6 (TRAF6) and TGF $\beta$ -associated kinase 1 (TAK1), key inducers of p38 and JNK MAPK pathway<sup>56</sup>. TGF $\beta$  activates TAK1 via TRAF6; TRAF6 is constitutively bound to ALK5 and upon oligodimerization due to TGF $\beta$  binding, TRAF6 molecules reach physical proximity, which facilitates their transautoubiquitination. Subsequently, TRAF6 ubiquitinates TAK1 and activates its kinase catalytic domain. TAK1 activates p38 and JNK MAPK by phosphorylation resulting in activation of transcription factors AP-1, c-JUN and c-FOS<sup>174-176</sup>. Furthermore, as TGF $\beta$  activates other non-SMAD pathways similarly members of other signaling pathways are modifying SMAD effectors<sup>2</sup>. Thus, it should be kept under consideration that crosstalk between pathways is usually bi- or multidirectional, increasing the complexity of cellular responses to extracellular stimuli.

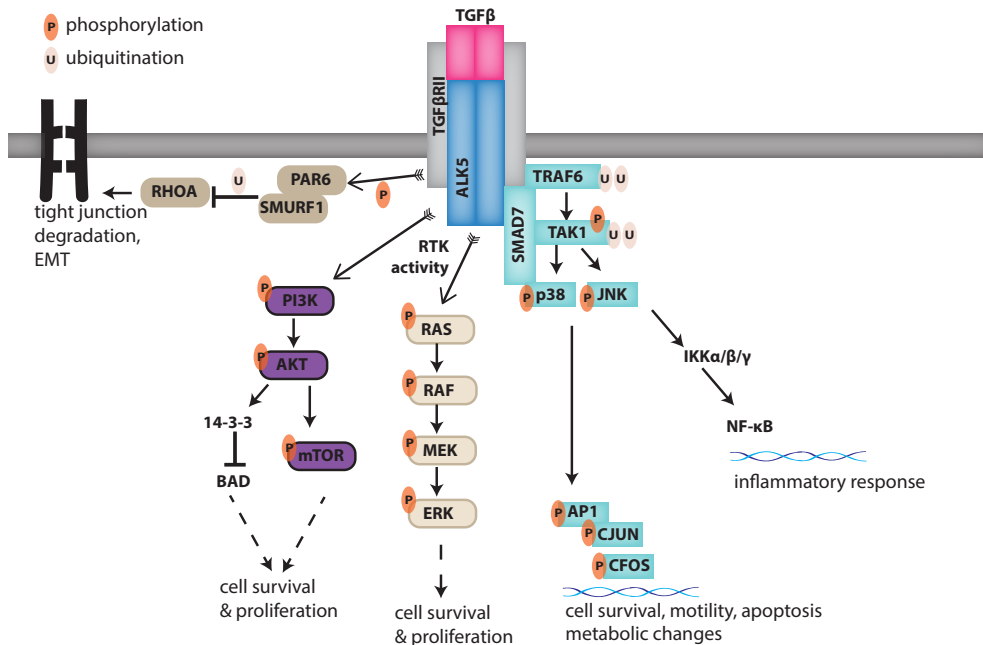


**Fig.3. TGFβ/non-SMAD pathways and their biological effects**

TGFβ receptors alter gene expression via the MAPK/ERK, TRAF6/TAK1/p38/JNK, NF-κB, PI3K/AKT/mTOR and PAR6/RHO signaling pathways that lead to multiple cellular responses.

## 1.4. TGFβ signaling pathway in homeostasis and disease- studies in liver, prostate and connective tissue

A plethora of biological processes are regulated by TGFβ cytokine in embryonic and adult tissues by means of growth arrest, cell differentiation, EMT, immune system regulation and angiogenesis. In fact, the description attributed to TGFβ as cytokine (growth factor) is a paradox since it promotes growth inhibition and halts cell proliferation (cytostasis) under nearly all physiological conditions. Transcriptomic analyses have revealed that TGFβ signaling controls the activation and repression of hundreds of genes in a single cell and leads to differential gene responses<sup>177,178</sup>. Thus, tight regulation of this pathway is crucial to guard signal specificity; the importance of growth inhibition is evident in human cancers where TGFβ-induced cytostasis is often disrupted.

The homeostatic role of TGFβ is cell type and microenvironment-dependent. In brief, anti-proliferative effects are exerted in epithelial tissues (for instance; skin, liver, breast, prostate, and lung)<sup>58</sup>. Mechanistically, TGFβ inhibits cell cycle progression via regulation of cyclin-dependent kinase inhibitors p15INK4B, p21CIP1, and p27KIP1<sup>179,180</sup>, inhibits cell cycle promoters such as the proto-oncogene C-MYC and ID proteins. Apoptosis is induced through activation of caspase protein cascade<sup>181</sup>. Non-epithelial tissues are also under growth control e.g. endothelium<sup>182,183</sup>, fibroblasts<sup>184</sup>, neuronal tissues<sup>185</sup>, cells of the immune and hematopoietic system<sup>186</sup>. In addition, TGFβ signaling orchestrates wound-healing response in most organ systems. If aberrantly regulated, it may lead to excess scar tissue formation, accumulation of collagen-producing cells and extracellular matrix (ECM) and eventually disrupt normal tissue structure and physiology.

In this thesis the homeostatic role of TGF $\beta$  is highlighted in three organ systems; liver, prostate epithelium and connective tissue (**Fig.4**).

Liver function is crucial for the homeostasis of the whole organism and is evident by the evolutionarily preserved regenerative capacity of mammalian liver. Under normal conditions, the liver is metabolically active but quiescent in terms of cell proliferation; cell division is minimal greatly due to cytostatic role of TGF $\beta$  among other factors. Overexpression of TGF $\beta$ 1 in hepatocytes (liver epithelial cells) leads to increased apoptosis, fibrosis and reduced proliferative and regenerative response<sup>187,188</sup>. Liver fibrosis is associated with genetic polymorphisms of TGF $\beta$  gene leading to increased TGF $\beta$ 1 serum levels<sup>189</sup>. The role of TGF $\beta$  in the liver is extensively discussed in Chapter 2.

Prostate tissue is divided in proximal, distal and intermediate ducts and androgen hormones are the main regulators of its physiology<sup>190</sup>. Androgens have functional convergence with TGF $\beta$ <sup>191</sup> which is expressed in a gradient form in prostate tissue. High levels of TGF $\beta$  signaling are present in the quiescent proximal region of ducts and androgen ablation reverses the proximal-distal TGF $\beta$  signaling gradient, leading to an increase in TGF $\beta$  signaling in the distal region<sup>192</sup>. Testosterone (5 $\alpha$ -dihydro) decreases the level of TGF $\beta$  receptor II (TGF $\beta$ RII) leading to suppression of the ability of TGF $\beta$  to down-regulate expression of Bcl-xL and cyclin D, activate caspase-3, and induce apoptosis<sup>193</sup>. Overexpression of dominant-negative form of TGF $\beta$  receptor type II in transgenic mice decreased apoptosis in the prostate epithelium<sup>194</sup>. Accordingly, *in vivo* injection of TGF $\beta$ 1, in the ventral prostate, increases apoptotic events<sup>195</sup>. Connective tissue is an example of a non-epithelial system that is regulated by TGF $\beta$  signaling. Connective tissue is comprised of cells and ECM, and is found in different types in the body. ECM is composed by glycoproteins, fibrous proteins and glycosaminoglycans, which are secreted by cells, mainly fibroblasts. Variations in the ECM composition determine the properties of the connective tissue (tendons, cartilage, eye cornea or if the matrix is calcified, it can form bone or teeth). Generally, connective tissue is either loose (adipose), or dense (tendons between muscles and bones), depending on the fiber arrangement. TGF $\beta$  plays an important role in the maintenance of the structural elements of ECM (collagen, elastin fibers) as well as the proliferation of fibroblasts and their transdifferentiation into myofibroblasts (MFBs). MFBs are crucial for wound healing as the main source of ECM proteins and maintain a vicious cycle of TGF $\beta$  production, responsiveness to TGF $\beta$  and ECM secretion. In fact, normal wound healing in adult animals is greatly regulated by TGF $\beta$ ; initially TGF $\beta$  is secreted by platelets, which leads to recruitment of other immune cell types (neutrophils, macrophages) and fibroblasts<sup>196</sup>. Fibroblasts initially migrate into the wound area and secrete a collagen- and cellular fibronectin-rich ECM<sup>197</sup>. In fact, fibronectin cross-talks with TGF $\beta$  signaling influencing activation of latent TGF $\beta$  in the matrix. Wound closure is achieved by ECM remodeling and angiogenesis; both processes are orchestrated by the pro-fibrotic and pro-angiogenic actions of TGF $\beta$ .

Despite the plethora of biological processes that TGF $\beta$  signaling is involved in, from a clinical point of view, aberrant TGF $\beta$  expression/ downstream activation is often associated with connective tissue disorders<sup>198</sup>. Mutations in TGF $\beta$  receptors are linked with Marfan syndrome<sup>199</sup>, Loeys-Dietz syndrome and others<sup>200</sup>.

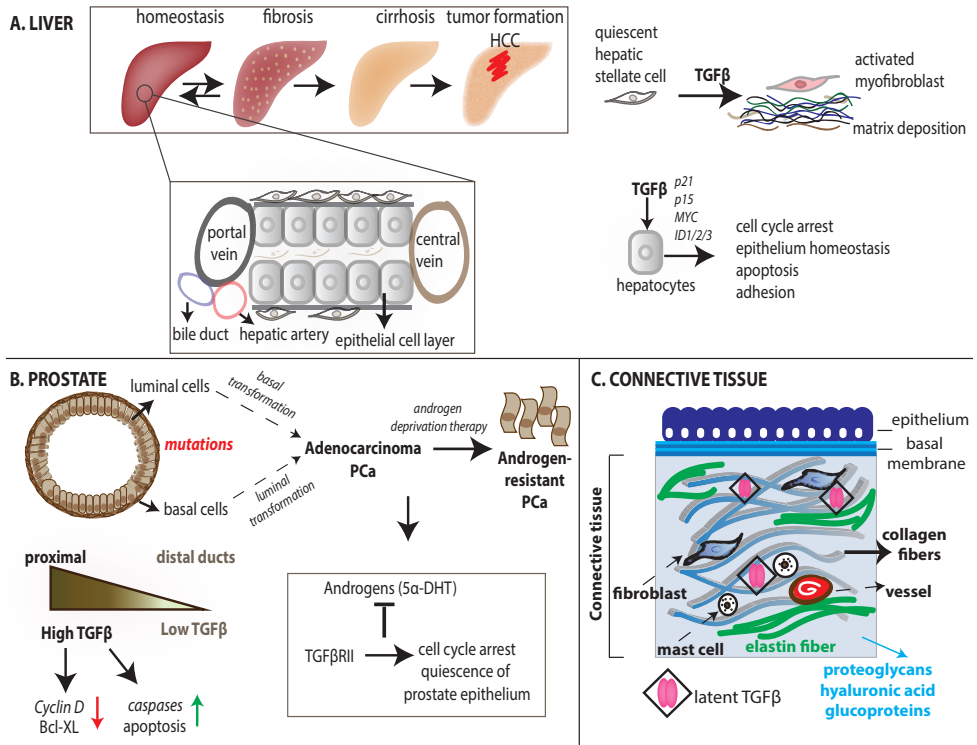


**Fig.4. Homeostasis in distinct organ systems and their regulation by TGFβ signaling**

(A). Liver disease progression from fibrosis to hepatocellular carcinoma (HCC), tissue cell types and morphology are depicted. Effects of TGFβ are summarized for the epithelial cells (hepatocytes and cholangiocytes) and the hepatic stellate cells (HSCs), precursors of myofibroblasts (MFBs) in the liver. (B). Prostate tissue morphology with proximal and distal ducts comprised by luminal and basal cells (neuroendocrine cells are not depicted here). TGFβ ligands exist in morphogenic pattern during homeostasis; highest concentration and signaling occurs in the proximal duct site (note that prostate stem cells reside in this area). Androgens promote cell proliferation by interfering with TGFβRII levels and androgen ablation therapy following prostate cancer detection leads to reversal of TGFβ distribution (distal instead of proximal). Transformed luminal cells cause adenocarcinoma development. Basal cells also contribute to prostate malignancy following a step of luminal differentiation. (C). Morphology and cell type distribution in the connective tissue underlying the epithelial barrier. Connective tissue is comprised by matrix (proteoglycans, hyaluronan, glycoproteins, elastin and collagen fibers) and a cellular component (endothelial cells, macrophages, mast cells and the most abundant, fibroblasts).

## 1.5. TGFβ signaling in fibrosis

We discussed the structural role of the matrix in connective tissues in the previous section. However, the matrix is not a static element made by cellular proteins but it mechanically and biochemically influences basic cellular processes<sup>201</sup>. Bissell *et al.*, firstly defined this phenomenon, as dynamic reciprocity between ECM, cell cytoskeleton and nuclear matrix<sup>202</sup>. This interplay of matrix and cells not only affects cell shape or motility but also actively alters signal transduction and gene expression pattern (mechanotransduction)<sup>203-205</sup>. TGFβ, a latent extracellular cytokine that regulates cellular processes by activating intracellular signaling is a key factor in the interface between cells and their ECM context<sup>206</sup>. For instance, the matrix can induce the expression of TGFβ1<sup>207</sup>. Moreover, the extracellular agonist of TGFβ ligands, DECORIN, is also a regulator of collagen maturation and assembly<sup>208</sup>. In this

section, we will discuss the implications of TGF $\beta$  in pathological fibrosis, in particular liver and Dupuytren's fibrosis (DD).

During the last decades fibrosis has accounted for up to 45% of deaths<sup>209</sup> and yet there are no approved antifibrotic therapies available. Fibrosis is a pathological state characterized by the excessive deposition of ECM proteins commonly occurring during wound healing and tissue regeneration. Excess deposition of collagen and proteoglycans is associated with reduced tissue epithelization and cell death, and eventually disrupted cell functionality and tissue architecture (**Fig.5**). Fibrosis may affect most organ systems and lead to a variety of diseases including liver cirrhosis, connective tissue fibrosis, pulmonary hypertension, systemic sclerosis and heart fibrosis representing a major medical challenge.

A complex set of genetic, immune response, epigenetic factors may lead to fibrosis by triggering constant activation of quiescent tissue fibroblasts to MFBs, the key pathogenic cells in fibrosis. The cellular and molecular phenotype of MFBs is highly dependent on TGF $\beta$  signaling pathway<sup>210,211</sup>. TGF $\beta$  stimulates ECM protein synthesis and secretion, decreases expression of proteases that cleave ECM (matrix metalloproteases, MMPs) and increases protease inhibitors (TIMPs)<sup>212</sup>. The outcome is a shift of balance towards ECM protein synthesis, secretion and deposition rather than degradation leading to scar tissue formation. TGF $\beta$  family members and target genes include ECM and cytoskeleton proteins that are often deregulated in fibrotic and other diseases, such as plasminogen activator inhibitor 1 (PAI-1)<sup>213</sup>, collagen type1 $\alpha$ 1 (COL1A1), COL1A2, COL4A2, COL5A1, COL5A2,  $\alpha$ -smooth muscle actin ( $\alpha$ -SMA, ACTA2) and fibronectin<sup>214-216</sup>.

### 1.5.1. Liver fibrosis

Liver fibrosis (cirrhosis) occurs in response to chronic liver injury due to alcohol intoxication or viral hepatitis B and C infections (HBV, HCV)<sup>217</sup>. TGF $\beta$  plays a role in all the stages of liver disease progression from inflammation, cirrhosis to cancer formation<sup>218</sup>.

Cirrhosis often is a precursor to hepatocellular carcinoma (HCC), thus, the need for effective treatment is high. Collagen-depositing MFBs accumulate around the portal and central vein of the liver lobules. The source of MFBs in the liver is mainly the pericyte population of the liver, hepatic stellate cells (HSCs), transformed epithelial cells and fibrocytes from the bone marrow. The activation of HSCs and their transdifferentiation to MFBs is controlled by the pro-fibrogenic effect of TGF $\beta$  pathway, evident by multiple studies (reviewed extensively in<sup>218-220</sup>). Fibronectin modulates this response of HSCs to TGF $\beta$  during liver injury in a way that controls the extend of fibrosis<sup>221</sup>. *In vivo* deletion of SMAD3 results in improvement of liver fibrosis in mice<sup>222</sup>.

Expression of fibrosis-related genes, such as collagens or PAI-1 in MFBs is induced by phosphorylation of SMAD2 and SMAD3 in the linker site by CDK4, p38 and JNK MAPK kinases<sup>223</sup>. In fact, the differential phosphorylation isoforms of SMAD2/3 (linker, cytoplasmic) may induce different levels of the inhibitor SMAD7<sup>223</sup>. SMAD2 and SMAD3 both are needed for induction of MMP2 and  $\alpha$ SMA expression, however, it seems that SMAD2 mostly orchestrates the TGF $\beta$ -mediated cytotaxis and maintains the epithelial phenotype while SMAD3 is indispensable for TGF $\beta$ -profibrogenic role<sup>224,225</sup>. SMAD7 blocks the fibrogenic response of HSCs in acute liver injury but not in chronic liver injury indicating that this negative feedback mechanism might be deactivated in liver fibrosis<sup>226</sup>. However, hepatocyte-specific deletion of SMAD7 in transgenic mice with chronic carbon tetrachloride (CCl<sub>4</sub>)-induced fibrosis ameliorates the fibrotic phenotype<sup>227</sup>.

TGF $\beta$  binds to both ALK1 and ALK5 in the liver, thus, a certain balance of ALK1/ ALK5 ratio is necessary to maintain the balance between protective, anti-fibrogenic action and pro-fibrogenic activity of TGF $\beta$ . TGF $\beta$ /ALK1 signaling appears to directly antagonize TGF $\beta$ /ALK5 signaling, while in other circumstances, the presence of ALK5 is an absolute requirement for efficient TGF $\beta$ /ALK1 signaling<sup>228</sup>. The role of BMPs in liver diseases is also being addressed by recent studies suggesting BMP9 as a pathological driver<sup>229</sup> and BMP7 as an anti-fibrotic factor that antagonizes TGF $\beta$  pathway<sup>230-232</sup>.

### 1.5.2. Dupuytren's fibrosis (part of this section is published in<sup>233</sup>)

Dupuytren's disease (DD) is one of the most common connective tissue disorders with a higher prevalence in Caucasians of northern Europe<sup>234</sup> and particularly in males<sup>234-236</sup>. DD is a fibroproliferative disease affecting the palmar fascia, and may lead to permanent flexion contracture of the digits<sup>237</sup> (**Fig.5**). Current treatment of DD is symptomatic; surgical removal of the fibrotic nodules and cords leads to immediate relief of the contracted digits. Injection of collagenase enzyme obtained from *Clostridium Histolyticum*, has been approved by FDA (Xiaflex, Pfizer) as alternative treatment for DD<sup>238</sup>. However, the recurrence rate of the disease using the current therapeutic approaches remains high.

Several environmental and genetic risks have been linked to DD supported by studies of familial cases, ethnicity and sex prevalence, occurrence in twins and postoperative recurrence<sup>239</sup>. However, the genetic mechanism is not fully understood and there is no evidence of a single genetic dysregulation as a cause of DD. Thus, the aetiology of DD remains unknown, although it is clear that TGF $\beta$  plays a role in the pathogenesis<sup>210,237</sup>.

High TGF $\beta$ 1, TGF $\beta$ 2 mRNA and protein levels have been associated with DD fibrosis<sup>210,215,240</sup>. TGF $\beta$ 2 shows intracellular localization within MFBs in the proliferative and involution stages of the disease<sup>241,242</sup>. In fact, transdifferentiation of quiescent fibroblasts into MFBs requires signaling by TGF $\beta$ <sup>243,244</sup>. Contractility of MFBs is increased after *in vitro* stimulation with low concentrations of exogenous TGF $\beta$ <sup>245-247</sup>. Presence of SMAD binding sites on the promoters of connective tissue growth factor (CTGF/CCN2),  $\alpha$ SMA, fibronectin and collagens, Serpine-1 (PAI-1) show that TGF $\beta$  directly controls the expression of MFBs-associated proteins<sup>248-253</sup>. The high proliferative properties of MFBs contradict the TGF $\beta$  proapoptotic and growth inhibitory role. However, it has been proven that in DD cells TGF $\beta$  induces expression of other cytokines such as platelet-derived growth factor (PDGF); in turn, PDGF activates ERK MAPK kinase pathway, induces expression of proto-oncogene c-MYC<sup>242</sup> and promotes cell proliferation. Studies on BMP signaling have not proven a link between deregulated BMP pathway members and DD pathogenesis. BMP6 has a potential antagonistic role against TGF $\beta$  as shown by reduced *in vitro* contractility and SMAD/ ERK activation in fibroblasts treated with BMP6<sup>254</sup>.

Although much work has attempted to unravel the complex mechanisms underlying fibrosis, the current state of the art in DD and generally in fibrosis research fails to meet the demanding need for treatment<sup>255</sup>. Cell culture models for studying fibrosis currently include primary cells and/or cell lines as well as the use of different culture matrices and co-culture models. It is now evident that two-dimensional (2D) cultures of fibroblasts have distinctly different properties and gene expression profile than the intact tissue<sup>256,257</sup>. This can be, in part, attributed to the *in vitro* protocols and adaptation to culture conditions. For experimental reasons, connective tissue obtained from carpal tunnel tissue operations is used for comparison to diseased DD palmar fascia, and arbitrarily considered "healthy

control” while it may be molecularly very similar to DD<sup>258</sup>. All these describe one of the biggest limitations of the field, i.e. the lack of an *in vitro/ex vivo* model that allows molecular and genetic manipulation. A recent study proposes xenograft transplantation of human DD fibroblasts in the subcutaneous layer of the skin of mice as an *in vivo* model for DD research, but yet this model poorly recapitulates the human disease.

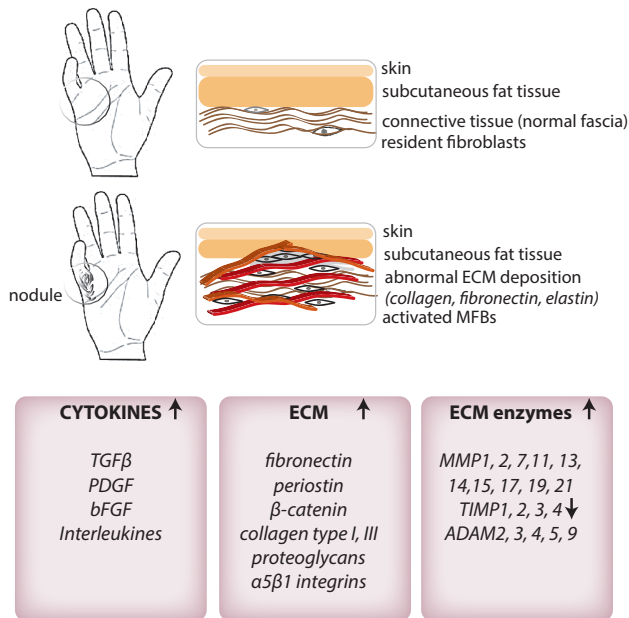


**Fig.5. Overview of the disrupted tissue architecture and the most common molecular aberrations associated with Dupuytren's fibrosis**

Fibrotic nodules consist of highly proliferative and contractile myofibroblasts (MFBs) that deposit matrix proteins. Normal matrix turnover and degradation are decreased due to molecular aberrations leading to fibrosis, tissue disfiguration and digit contracture. Adapted from <sup>237</sup>.

## 1.6. TGF $\beta$ / BMP signaling in cancer

In normal cells, growth inhibition mediated by TGF $\beta$  is usually dominant over growth stimulatory action of other factors. However, the situation is reversed in malignant situations that are characterized by hyperproliferation due to mitogens, action of mutated oncogenes and hyposensitivity to anti-proliferative action of TGF $\beta$ <sup>198,259</sup>. In normal conditions, TGF $\beta$  keeps normal epithelial tissues in a proliferation blockage, thus having tumor-suppressor role. Occurrence of oncogenic somatic mutations in epithelial cells leads to formation of primary carcinoma. Aberrant cell division without tight regulation of DNA synthesis and repair leads to additional accumulation of oncogenic mutations.

The primary carcinoma may remain spatially confined if the TGF $\beta$ -mediated cytostatic cues are intact. However, if mutations in TGF $\beta$ / BMP ligands, receptors and SMADs occur, then the cells acquire proliferative and migratory properties that facilitate cancer metastasis<sup>58</sup>.

Apart from its cytostatic role, TGF $\beta$  regulates many other biological processes that are hallmarks of cancer, such as EMT, suppression of cytotoxic T lymphocytes and angiogenesis. Thus, malignant cells hijack TGF $\beta$  to obtain phenotypic characteristics crucial for cancer progression such as mesenchymal cell shape, increased motility and invasion through basal membranes into extracellular space and blood vessels (**Fig.6**).

The tumor-promoting role of TGF $\beta$  in advanced carcinomas is mainly due to TGF $\beta$  signaling through the SMAD/1/5/8 machinery and inducing expression of ID proteins<sup>260</sup>, via non-SMAD pathways (circumventing the Ser/Thr kinase activity of TGF $\beta$  receptors or PTM regulation of linker and C-terminal SMAD phosphorylation) to activate the growth-stimulatory pathways ERK and AKT<sup>56,168,261</sup>. The essential role of TGF $\beta$  in stimulating metastasis<sup>262</sup> and the high frequency of genetic mutations in TGF $\beta$  pathway leading to cancer<sup>263</sup> highlight the necessity for TGF $\beta$ -targeting therapies.

### 1.6.1. Epithelial-to-mesenchymal transition (EMT)

Polarized cells, positioned adjacent to each other via tight junctions, comprise epithelial tissues. Epithelial cells are stably in contact with the basal membrane forming a basal-apical polarity and have epithelial-specific gene expression pattern (E-CADHERIN, ZO-1, LAMININS)<sup>264</sup>. However, epithelial cells are quite plastic under certain conditions such as tissue morphogenesis during development and wound healing<sup>49</sup>. Plasticity allows them to progressively switch on the genetic program of mesenchymal gene expression that leads to loss of epithelial phenotype and acquisition of a mesenchymal one. This cellular process of epithelial cells disintegrating from the basal membrane, losing cell-cell contacts and becoming motile is termed epithelial-to-mesenchymal transition (EMT) and is reversible (MET) (**Fig.6**). Both EMT and MET are mechanisms of cancer metastasis; cancer cells undergo EMT to extravasate from the primary tumor into blood circulation or from blood vessels into other epithelia and reverse to MET program to invade and colonize the new sites<sup>259</sup> (**Fig.6**). During EMT, epithelial proteins such as E-CADHERIN are downregulated and mesenchymal, cytoskeletal and ECM proteins are upregulated (FIBRONECTIN, VIMENTIN, NCADHERIN<sup>265</sup>). High motility group AT-hook 2 protein (HMGA2) via TGF $\beta$ /SMAD pathway regulates EMT master transcription factors SNAIL1/2, ZEB1/2 and TWIST, which repress epithelial genes and activate mesenchymal genes<sup>266-268</sup>. In addition, TGF $\beta$  signaling, via the SMAD1/5/8/



ID1 activation, is implicated in MET and promotes metastasis<sup>260,269</sup>. TGF $\beta$  promotes EMT by interfering with RHO complexes in epithelial cell junctions; this mechanism is TGF $\beta$ RI and SMAD-independent (TGFBRII/PAR6/SMURF1/RHO)<sup>173</sup>. The reverse process (MET) is regulated by BMP signaling, in particular BMP7<sup>270</sup>.

### 1.6.2. Tumor angiogenesis

Deregulation of TGF $\beta$  and BMP pathways lead to vascular defects, such as pulmonary hypertension, hereditary telangiectasia (HHT)<sup>198,271</sup>. Deletion of TGF $\beta$  ligands or ALK1 in transgenic mice results in embryonic lethality due to vasculogenesis defects<sup>272,273</sup>. Vascular homeostasis relies on endothelial cells, smooth muscle cells and pericytes<sup>274</sup>. The key angiogenesis-related members are TGF $\beta$  ligands, ENDOGLIN, ALK1 and its ligands BMP9 and BMP10, that synergize with proangiogenic factors such as vascular endothelial growth factor (VEGF), NOTCH pathway, PDGF, angiopoietins and basic fibroblast growth factor (bFGF)<sup>271,275,276</sup>.

Angiogenesis determines normal and malignant tissue growth. The requirement for new vessels is high in primary tumors as the highly metabolic and proliferative cancer cells need oxygen, nutrients, and cytokines from the blood. As the epithelial cells cluster and proliferate forming a primary carcinoma, new vessels must be formed (**Fig.6**) in order for the blood flow to reach all the cells within the tumor (angiogenic switch). However, since tumor cells cannot perform *de novo* angiogenesis they have evolved to disrupt the existing normal vasculature and recruit endothelial cells into the tumor<sup>277</sup>. TGF $\beta$  promotes tumor angiogenesis by inducing expression of MMPs that degrade the basal membrane and assist endothelial cell migration<sup>278</sup>. TGF $\beta$  induces MMP2 and MMP9 in tumor cells<sup>279</sup>. Tumor angiogenesis is also influenced by MMP14 protease that releases membranous ENDOGLIN into its secreted form<sup>280</sup>. High TGF $\beta$ -expressing prostate cancer cells induce an angiogenic response when transplanted *in vivo*<sup>281</sup> and inhibition of TGF $\beta$  activity by neutralizing antibodies decreases tumor angiogenesis<sup>282</sup>.

### 1.6.3. Prostate cancer

Prostate cancer (PCa) arises from precursor lesions, defined as prostatic intraepithelial neoplasia (PIN), gradually progresses to locally invasive disease and ultimately to metastasis. Disease progression from PIN lesions or organ-confined PCa towards metastatic PCa involves multiple genetic and epigenetic events to take place. Each stage of this disease is associated with characteristic morphological and histo-pathological alterations. Associated with the human disease are also genetic chromosomal alterations, which have led to the identification of several tumor suppressor genes (for example, TP53, CDKN1B and PTEN) and androgen related gene fusions (such as TMPRSS2-ERG) of key importance in the early stages of the disease<sup>282, 283</sup>. Furthermore, the androgen receptor (AR) is required for maintenance of the prostate epithelium during normal organogenesis as well as carcinogenesis, including hormone-independent cancer. The androgen refractory stage is the final and most aggressive stage of the cancer, characterized by bone and lymph node metastases. As in most cancer types, TGF $\beta$  has growth inhibitory effects on primary PCa, but tumor-promoting role during advanced stages and leads to metastasis formation. In addition, stromal TGF $\beta$  can activate AR signaling in absence of androgens, which might contribute to hormone-independent growth of tumor<sup>284</sup>.

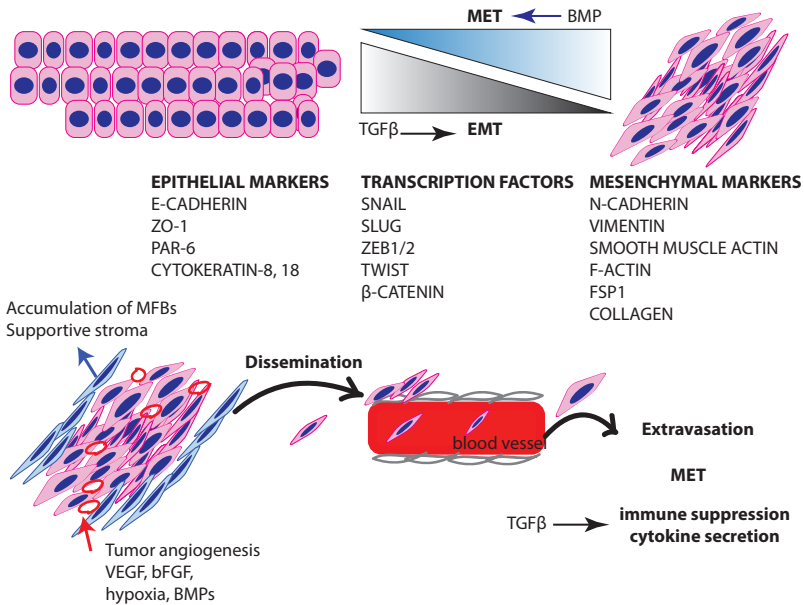


**Fig.6. Stages of cancer progression and TGFβ/BMP signaling**

Formation of primary carcinoma and phenotypic transition of epithelial cells into mesenchymal cells (EMT) are depicted. Tumor microenvironment (supportive stroma) consists of infiltrating immune cells and myfibroblasts (MFBS) derived by quiescent fibroblasts or by tumor epithelial cells via EMT. Crosstalk between the stroma and tumor cells, using cytokines and other signaling molecules, promotes acquisition of tumor vasculature (angiogenesis) which sustains tumor growth by delivery of nutrients and oxygenated blood. Tumor cells may disseminate from the primary tumor into the blood circulation, extravasate from the vessels through the perivascular and extracellular matrix and metastasize to secondary tissues (mesenchymal-to-epithelial transition, MET).

EMT and migration of PCa cells are induced by TGFβ via MAPK kinase ERK2 and c-MYC expression<sup>285</sup>. BMP ligands also play a role in PCa<sup>286</sup>, in particular BMP2, BMP4, BMP7<sup>287, 288</sup>. Cell proliferation is increased in presence of BMP2 and BMP4, however, it is not clear from the existing studies whether BMP7 is tumor promoter or suppressor in prostate<sup>289</sup>. BMP2 expressed by osteoclasts might act as chemotactic factor for PCa cells to metastasize to the bone<sup>290</sup>. BMP9, the primary ligand of ALK1 in endothelial cells, might also play a role in PCa, as in other types of cancer as we will discuss in the next section. BMP9 is expressed in prostate epithelium along with BMP receptors<sup>291</sup>.

### 1.6.4. Hepatocellular carcinoma

Liver tissue can endure chronic damage and symptoms become evident in advanced disease stage making prognosis of liver diseases difficult. Hepatocellular carcinoma (HCC), one of the most frequent forms of cancer, is usually detected at a late stage, thus the current forms of therapy are often not curative e.g. tumor resection, treatment with sorafenib or eventually liver transplantation<sup>292</sup>.

TGF $\beta$  plays a role in HCC development<sup>218,293</sup> and one of the first indications was the finding that circulating levels of TGF $\beta$ 1 in plasma from HCC patients are significantly higher than in patients with cirrhosis or viral hepatitis<sup>294</sup>. SMAD7 overexpression has tumor-suppressing role<sup>295</sup>. Liver expresses high amounts of BMP9 that are also secreted in the circulation<sup>296</sup>. HSCs and potentially also hepatocytes, express ALK1 and ENDOGLIN, the interaction partners of BMP9, under normal and pathological conditions. Apart from a role in endothelial cells and HSCs, BMP9 has been associated with HCC<sup>297</sup>.

NODAL expression is shut down after embryonic development, but it is re-expressed in adult tissues, along with its co-receptor CRIPTO during malignant conditions. NODAL and CRIPTO are involved in plasticity of tumor cells, cancer-stem cell maintenance and metastasis<sup>298,49</sup>. In the liver, stem cell renewal transcription factor NANOG is reactivated during HCC and it mediates EMT by activating NODAL/ CRIPTO and SMAD3 expression<sup>158</sup>. Moreover, the interaction partner of CRIPTO, GRP78, has been associated with liver cell stress response and HCC<sup>299-301</sup>. Thus, both the canonical and the non-canonical NODAL pathway have a contributing role in HCC.

### 1.7. Anti-TGF $\beta$ strategies (antisense oligonucleotides/ small molecule kinase inhibitors/ ligand traps)

Several components of the TGF $\beta$  pathway have been investigated for drug development; however, only a few compounds have proceeded into later stages of clinical trials<sup>302,303</sup>. TGF $\beta$  signaling is a key pathway for homeostasis and given its pleiotropic, cell-type and context-dependent role, therapeutic interventions are beneficial for a particular tissue or cell type, at a specific stage of the disease. During cancer progression, if tumor cells are insensitive to growth inhibition by TGF $\beta$ , therapeutic enhancement of signaling might be useful to constrain their proliferation if the tumor is detected at an early stage<sup>304</sup>. Nevertheless, malignant cells quickly adapt and start using TGF $\beta$  to promote their metastatic spread. Given that cancer diagnosis does not detect micrometastasis events, it is more logic to preventively inhibit rather than induce TGF $\beta$  signaling when a primary tumor is diagnosed in order to stop the lethal consequences of metastasis. Moreover, expression levels of TGF $\beta$  pathway members are often elevated during conditions such as organ fibrosis and cancer; thus, inhibitory strategies are required to block the fibroproliferative role of TGF $\beta$  in MFBs (fibrosis), cancer-associated fibroblasts (CAFs) and to suppress tumor cell metastasis.

A growing number of recent studies have tested TGF $\beta$  inhibitors as combination treatment with chemotherapeutics<sup>305</sup>, immune stimulatory agents (interleukin-2)<sup>303,306</sup> or to minimize radiotherapy-induced carcinogenesis<sup>307</sup>. In the cancer field inhibition of TGF $\beta$  type I and type II receptors has been accomplished, while in the fibrosis field most of the anti-fibrotic drugs are designed to interfere at the ligand level of pathway transduction, therefore preventing their binding to the receptors<sup>308</sup>. The most successful TGF $\beta$  inhibitory strategies (**Fig.7**) used in experimental and clinical studies (**table 3**) are the antisense oligonucleotides

AONs targeting TGF $\beta$  ligand mRNA (Antisense Pharma), the competitive peptides against ligands (ligand traps, Digna Biotech), the neutralizing antibodies and the small molecule inhibitors of receptor kinase activity.

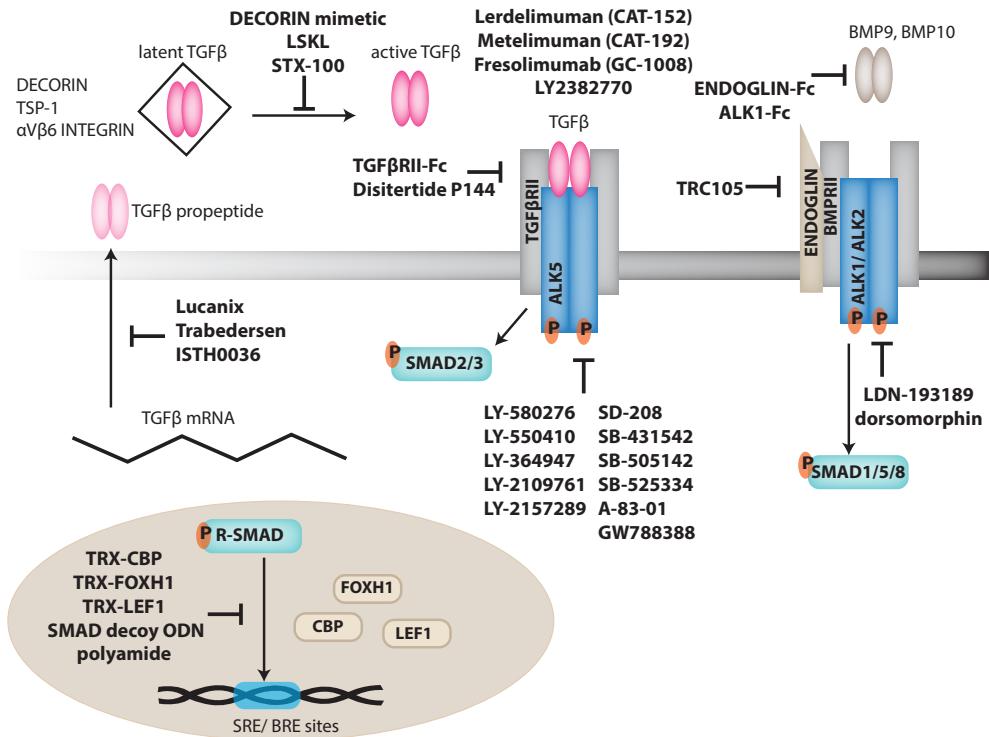


**Fig.7. Schematic overview of different inhibitory strategies targeting TGF $\beta$ /BMP signaling activation** TGF $\beta$  pathway activation can be inhibited by different compounds, which target mRNA/ protein expression or protein function and act at different subcellular compartments; (1) compounds that inhibit activation of latent TGF $\beta$  (DECORIN mimetic, THROMBOSPONDIN and  $\alpha$ v $\beta$ 6 INTEGRIN antagonists), (2) soluble type II/ III receptor ectodomain peptides that trap ligands and prevent interaction with a functional receptor, (3) neutralizing antibodies against TGF $\beta$ , BMP ligands and receptors, (4) small molecule kinase inhibitors that inhibit activity of type I or type II receptors, (5) antisense oligonucleotides interfering with mRNA translation of TGF $\beta$ 2 mRNA, oligonucleotides that bind to gene promoters mimicking SMAD binding (pyrrole-imidazole polyamide, SMAD decoy ODN), (6) thioredoxin peptide aptamers for SMAD binding to co-factors FOXH1, LEF and CBP (TRX).

### 1.7.1. Antisense oligonucleotides (AONs)

AON methodology is used to modulate gene expression in a sequence-specific way and has shown broad therapeutic applicability in many human diseases, particularly in the field of muscular dystrophies<sup>309</sup> with very promising results reported in clinical trials<sup>310,311</sup>. The use of AONs in basic and translational research aims to either “partially correct” a non-functional protein or to disrupt a protein of interest as a way to inhibit its expression or functionality. AONs can be designed to interfere at the molecular level either during messenger RNA (mRNA) splicing or mRNA translation into protein. Splicing involves the

removal of non-coding sequences (introns) and “stitching” of the remaining coding DNA (exons). Particular exon(s) encoding protein domains crucial for protein function can become excluded from the mature mRNA; specific AONs bind to sites involved in exon splicing in the exon-intron boundaries and interfere with the splice machinery. Thereby, the particular exon is not integrated as part of the mRNA<sup>312</sup>. The resulting mRNA has an intact open reading frame and is translated into a protein that lacks only the particular peptide sequence encoded by the skipped exon. The advantage of this system is that no genetic alterations are introduced, since interference occurs exclusively at the pre-mRNA splicing process. Translation-blocking AONs function by forming a complex with complementary mRNA sequence; RNA-RNA or RNA-DNA dimers are then recognized by RNase helicase (H), which leads to mRNA degradation<sup>313</sup>. Alternatively, AON binding to mRNA in the 5' untranslated region might interfere with 5' cap formation, ribosome binding and recognition of the ATG starting codon, thus hindering mRNA translation into protein<sup>314</sup>.

AON-mediated inhibition of TGF $\beta$  ligand expression has been proposed and attempted as a novel cancer therapy for various malignancies. Interference with TGF $\beta$ 1 production at the mRNA level by AON AP11014, developed by Antisense Pharma/Isana Therapeutics, significantly reduces TGF $\beta$ 1 in prostate, lung and colon cancer cell lines<sup>315</sup>. TGF $\beta$ 2 cytokine plays a key role in glioblastoma and pancreatic cancer. Trabedersen, interferes with TGF $\beta$ 2 mRNA translation and has reached the phase III of clinical trials for glioblastoma treatment<sup>316</sup>. The same company has developed TGF $\beta$ 2-targeting AONs for glaucoma treatment (phase I trials). Another antisense TGF $\beta$ 2 strategy has been developed for tumor vaccines (Lucanix, NovaRx)<sup>317,318</sup>. TGF $\beta$ 2 AON sequence is transfected into lung cancer cells, which are used as anti-tumor vaccination. The vaccine has progressed into phase III clinical trials.

A distinct type of gene therapy is the nucleic acid or peptide-based strategies that inhibit SMAD transcriptional activity at the DNA level; (1) the SMAD transcription factor- “decoy” double stranded oligonucleotides (decoy ODN) that block SMAD binding to SRE binding sites<sup>319,320</sup>, (2) pyrrole-imidazole polyamide compounds designed to bind to DNA minor groove in SRE binding sites, thus inhibiting SMADs to interact with gene promoters and other cis-regulatory elements<sup>321</sup>.

### 1.7.2. Peptides that antagonize ligand function

Ligand traps are peptides engineered to have the extracellular domain (ECD) of receptors or receptor-associated proteins, fused to stable region of an antibody (Fc of IgG). The logic is that the soluble receptor ectodomains will bind with the same affinity its ligands in the extracellular space and sequester them from binding to a functioning receptor on the cell membrane<sup>322,323</sup>. Soluble receptor type II (TGF $\beta$ RII-Fc) ligand trap was developed by Genzyme but did not progress into clinical trials<sup>324</sup>.

Similar anti-TGF $\beta$  peptide mimicking the ECD of TGF $\beta$ RIII receptor  $\beta$ -GLYCAN (Disitertide P144, Digma Biotech) is currently in phase II trials. P144 TGF $\beta$ 1-inhibitor has been specifically designed to block the interaction of TGF $\beta$ 1 with  $\beta$ -GLYCAN. It has shown significant anti-fibrotic activity when applied topically in mice receiving repeated subcutaneous injections of bleomycin, a widely accepted animal model of human scleroderma<sup>325</sup>. Anti-fibrotic effects have been reported for liver fibrosis<sup>326</sup>, myocardial fibrosis<sup>327</sup> and as combination therapy with antitumor immunotherapy<sup>328</sup>. Another compound of the same company is an antagonist based on the structure of THROMBOSPONDIN-1 (TSP-1) for the treatment of diabetic nephropathy<sup>329</sup>. The LSKL peptide binds to LAP domain of the latent complex

via the motif LSKL (Leu-Ser-Lys-Leu) and blocks TGF $\beta$  activation.  $\alpha$ v $\beta$ 6 INTEGRIN mediates release of latent TGF $\beta$  from LAP complex; anti- $\alpha$ v $\beta$ 6 INTEGRIN antibody (STX-100, Stromedix) inhibits tumor progression *in vivo* by blocking activation of latent TGF $\beta$  ligands<sup>330</sup>. A similar peptide has been developed that mimics DECORIN binding to latent TGF $\beta$ ; by blocking release of latent TGF $\beta$  the compound enhanced anti-tumor immune response in glioma<sup>331</sup>. Treatment with soluble ENDOGLIN ECD (ENDOGLIN-Fc) has beneficial outcome in inhibiting BMP9/ALK1 signaling and VEGF-mediated tumor angiogenesis and reducing tumor size in preclinical studies<sup>332</sup>. The ALK1-Fc ligand trap for BMP9 and BMP10 has anti-angiogenic<sup>333-335</sup> effects with enhanced safety profile compared to VEGF inhibitors<sup>336</sup>. Treatment with ALK1Fc indicates anti-tumorigenic response of patients with solid tumors<sup>336</sup> and is currently being tested in phase I clinical trials for recurrent ovarian and endometrial cancer (ClinicalTrials.gov identifier; NCT01720173). Peptide aptamers (TRX-CBP, TRX-FOXH1, TRX-LEF1) have been engineered to inhibit SMAD binding to their transcription factor interacting partners CBP, FOXH1, LEF1<sup>337</sup>.

### 1.7.3. Neutralizing monoclonal antibodies

Monoclonal antibodies are used for neutralization of excessive ligand or soluble receptors at the extracellular space. Due to their *in vivo* stability they can be administered less frequently however, administration is done intravenously, which remains a drawback.

Neutralizing antibodies have been developed for binding to an individual or all TGF $\beta$  ligands (pan-TGF $\beta$ ). TGF $\beta$ 1-specific neutralizing antibody LY2382770 (Eli Lilly) was tested in phase II clinical trials for kidney fibrosis and although it was safe, it proved not sufficiently effective in ameliorating disease progression (ClinicalTrials.gov identifier; NCT01113801). CAT-192 (Metelimumab) is a humanized antibody against TGF $\beta$ 1. CAT-152 (Lerdelimumab) binds TGF $\beta$ 2 (anti-scarring postoperative treatment of glaucoma)<sup>338</sup>. However, both antibodies did not show adequate efficacy and the studies did not proceed any further. A more effective neutralizing antibody is the pan-TGF $\beta$  compound Fresolimumab, which targets all three TGF $\beta$  ligands and showed promising anti-fibrotic and anti-carcinogenic potential. Single-shot treatment with Fresolimumab against glomerulosclerosis is in phase I<sup>339</sup> and is also being tested for malignant melanoma and renal cell carcinoma<sup>340</sup>. The antibody against human ENDOGLIN (TRC105) has anti-tumorigenic effects in advanced solid tumors<sup>341</sup> and is currently in phase II clinical trials for glioblastoma<sup>342</sup>. Currently, TRC105 is also tested as combination therapy with VEGF inhibitors for prostate, breast, ovarian, and liver cancer (HCC). Phase II trials of TRC105 in combination with chemotherapy agents such as bevacizumab for recurrent glioblastoma (ClinicalTrials.gov identifier; NCT01564914), or sorafenib (VEGFR, PDGFR, RAF kinase inhibitor) for HCC (ClinicalTrials.gov identifier; NCT01306058) have shown promising outcome.

### 1.7.4. Small molecule kinase inhibitors (SMIs)

SMIs is a class of receptor kinase inhibitors which bind into the ATP pocket of the kinase domain, thus, preventing ADP to ATP conversion (phosphorylation) and receptor activation. During this mode of inhibition, TGF $\beta$  ligands bind to non-functional receptors (SMI blockage of the type I or type II receptor); thereby the signal is not transmitted downstream. SMIs have the advantages that are cell permeable due to their small molecular weight (as opposed to antibodies), however, they are less specific for a particular receptor because of the high

structural similarity of the ATP pocket among kinases.

Several SMIs have been developed against TGF and BMP receptors with different selectivity for particular kinases or *in vitro* and *in vivo* performance<sup>343</sup>. A panel of frequently used SMIs (**Fig.7**) targeting the TGF $\beta$  branch (ALK4, ALK5 and ALK7) is the SB-431542, SB-505142, LY-364947 (selective for ALK5) and A-83-01. Potent BMP receptor inhibitors against ALK2, ALK3, ALK6) is the LDN-193189 and dorsomorphin (compound C).

Although several SMIs have shown promising results in *in vitro* and *in vivo* preclinical studies (SB-431542, SB-505124, GW788388, SD-208)<sup>344</sup> they did not meet the pharmacokinetic stability criteria of clinical trials<sup>303</sup>. Currently, the SMIs being tested in preclinical studies are the LY-580276<sup>345</sup>, LY-550410<sup>346,347</sup>, LY-364947<sup>348</sup> and LY-2109761<sup>349</sup> for the treatment of various types of cancer. A study for HCC treatment with sorafenib (VEGFR, PDGFR, RAF kinase inhibitor) combined with ALK5 kinase inhibitor (LY-2157299) in patients with HCC is currently in phase II of clinical trials (NCT01246986)<sup>350</sup>.

Drug	Type	Target	Disease	Stage	Refs/Identifier
Trabedersen	Antisense oligo	TGFβ2	Glioblastoma, Pancreatic cancer	Phase II	316
Belagen- pumatu cel-L (Lucanix)	Antisense oligo- mediated tumor cell vaccine	TGFβ2	Non-small-cell- lung-carcinoma	Phase III	317,318
ISTH0036	Antisense oligo	TGFβ2	Post-operative glaucoma treatment		NCT02406833
LY2382770	Neutralizing antibody	TGFβ1	Diabetic kidney fibrosis	Phase II	NCT01113801
Pirfenidone	Small molecule	TGFβ activity	Idiopathic pulmonary fibrosis	Clinic	351
P144	peptide	TGFβ1, β-GLYCAN	Skin fibrosis, Systemic sclerosis	Phase II	325
CAT-192	Neutralizing antibody	TGFβ1	Systemic sclerosis	Phase II	352
GC-1008/ Fresolimumab NCT00043706	Neutralizing antibody	TGFβ1,2,3	Melanoma, Renal fibrosis, glaucoma	Phase I	339,340, NCT01472731
STX-100/ Stromedix	Neutralizing antibody	αVβ6 INTEGRIN	Fibrosis	Phase II	NCT01371305
TRC105	Neutralizing antibody	ENDOGLIN	Glioblastoma, Liver cancer	Phase II	NCT01564914
ALK1Fc	Ligand trap	BMP9, BMP10	Endometrial cancer Ovarian cancer	Phase I	NCT01720173
LY2157299	Small molecule kinase inhibitor	ALK5	Hepatocellular carcinoma	Phase II	NCT01246986

**Table 3. Ongoing clinical trials on compounds targeting TGFβ pathway members in fibrosis and cancer**



### References

1. Kerridge, D., The effect of inhibitors on the formation of flagella by *Salmonella typhimurium*. *J Gen Microbiol*, 1960. 23: p. 519-38.
2. Massagué, J., J. Seoane, and D. Wotton, Smad transcription factors. *Genes Dev*, 2005. 19(23): p. 2783-2810.
3. Roberts, A.B., et al., Transforming growth factors: isolation of polypeptides from virally and chemically transformed cells by acid/ethanol extraction. *Proc Natl Acad Sci U S A*, 1980. 77(6): p. 3494-3498.
4. de Larco, J.E. and G.J. Todaro, Growth factors from murine sarcoma virus-transformed cells. *Proc Natl Acad Sci U S A*, 1978. 75(8): p. 4001-5.
5. Anzano, M.A., et al., Synergistic interaction of two classes of Transforming growth factors from murine sarcoma cells. *Cancer Res*, 1982. 42(11): p. 4776-4778.
6. Roberts, A.B., et al., Isolation from murine sarcoma cells of novel transforming growth factors potentiated by EGF. *Nature*, 1982. 295(5848): p. 417-9.
7. Moses, H.L., et al., Transforming growth factor production by chemically transformed cells. *Cancer Res*, 1981. 41(7): p. 2842-2848.
8. Assoian, R.K., et al., Transforming growth factor  $\beta$  in human platelets. Identification of a major storage site, purification, and characterization. *J Biol Chem*, 1983. 258(11): p. 7155-7160.
9. Frolik, C.A., et al., Purification and initial characterization of a type  $\beta$  transforming growth factor from human placenta. *Proc Natl Acad Sci U S A*, 1983. 80(12): p. 3676-3680.
10. Stromberg, K., et al., Human term placenta contains transforming growth factors. *Biochem Biophys Res Commun*, 1982. 106(2): p. 354-361.
11. Twardzik, D.R., J.E. Ranchalis, and G.J. Todaro, Mouse embryonic Transforming growth factors related to those isolated from tumor cells. *Cancer Res*, 1982. 42(2): p. 590-593.
12. Massague, J., et al., Affinity labeling of a transforming growth factor receptor that does not interact with epidermal growth factor. *Proc Natl Acad Sci U S A*, 1982. 79(22): p. 6822-6826.
13. ten Dijke, P., K. Miyazono, and C.H. Heldin, Signaling via hetero-oligomeric complexes of type I and type II serine/threonine kinase receptors. *Curr Opin Cell Biol*, 1996. 8(2): p. 139-45.
14. Heldin, C.-H., K. Miyazono, and P. ten Dijke, TGF $\beta$  signaling from cell membrane to nucleus through SMAD proteins. *Nature*, 1997. 390(6659): p. 465-471.
15. Miyazono, K., Y. Kamiya, and M. Morikawa, Bone morphogenetic protein receptors and signal transduction. *J Biochem*, 2010. 147(1): p. 35-51.
16. Steinbicker, A.U., et al., Perturbation of hepcidin expression by BMP type I receptor deletion induces iron overload in mice. *Blood*, 2011. 118(15): p. 4224-4230.
17. Cai, J., et al., BMP signaling in vascular diseases. *FEBS Lett*, 2012. 586(14): p. 1993-2002.
18. Canalis, E., A.N. Economides, and E. Gazzerro, Bone morphogenetic proteins, their antagonists, and the skeleton. *Endocr Rev*, 2003. 24(2): p. 218-235.
19. Yang, J., et al., Bone morphogenetic proteins: Relationship between molecular structure and their osteogenic activity. *Food Sci Hum Welln*, 2014. 3(3-4): p. 127-135.
20. Kawabata, M., T. Imamura, and K. Miyazono, Signal transduction by bone morphogenetic proteins. *Cytokine Growth Factor Rev*, 1998. 9(1): p. 49-61.
21. Elkasrawy, M.N. and M.W. Hamrick, Myostatin (GDF-8) as a key factor linking muscle mass and skeletal form. *J Musculoskelet Neuronal Interact*, 2010. 10(1): p. 56-63.
22. Bragdon, B., et al., Bone morphogenetic proteins: A critical review. *Cell Signal*, 2011. 23(4): p. 609-620.
23. Graycar, J.L., et al., Human transforming growth factor- $\beta$  3: recombinant expression, purification, and biological activities in comparison with transforming growth factors- $\beta$  1 and - $\beta$  2. *Mol Endocrinol*, 1989. 3(12): p. 1977-86.
24. Millan, F.A., et al., Embryonic gene expression patterns of TGF $\beta$ 1,  $\beta$ 2 and  $\beta$ 3 suggest different

- developmental functions in vivo. *Development*, 1991. 111(1): p. 131-143.
25. ten Dijke, P., et al., Identification of another member of the transforming growth factor type  $\beta$  gene family. *Proc Natl Acad Sci U S A*, 1988. 85(13): p. 4715-4719.
  26. Derynck, R., et al., Human transforming growth factor- $\beta$  complementary DNA sequence and expression in normal and transformed cells. *Nature*, 1985. 316(6030): p. 701-5.
  27. Derynck, R., et al., A new type of transforming growth factor- $\beta$ , TGF- $\beta$ 3. *EMBO J*, 1988. 7(12): p. 3737-3743.
  28. Madisen, L., et al., Transforming growth factor- $\beta$  2: cDNA cloning and sequence analysis. *DNA*, 1988. 7(1): p. 1-8.
  29. Shull, M.M., et al., Targeted disruption of the mouse transforming growth factor- $\beta$ 1 gene results in multifocal inflammatory disease. *Nature*, 1992. 359(6397): p. 693-699.
  30. Kulkarni, A.B., et al., Transforming growth factor  $\beta$  1 null mutation in mice causes excessive inflammatory response and early death. *Proc Natl Acad Sci U S A*, 1993. 90(2): p. 770-774.
  31. Dickson, M.C., et al., Defective haematopoiesis and vasculogenesis in transforming growth factor- $\beta$  1 knock out mice. *Development*, 1995. 121(6): p. 1845-1854.
  32. Kaartinen, V., et al., Abnormal lung development and cleft palate in mice lacking TGF $\beta$ 3 indicates defects of epithelial-mesenchymal interaction. *Nat Genet*, 1995. 11(4): p. 415-421.
  33. Dickson, M.C., et al., RNA and protein localisations of TGF $\beta$  2 in the early mouse embryo suggest an involvement in cardiac development. *Development*, 1993. 117(2): p. 625-639.
  34. Sanford, L.P., et al., TGF $\beta$ 2 knockout mice have multiple developmental defects that are non-overlapping with other TGF $\beta$  knockout phenotypes. *Development*, 1997. 124(13): p. 2659-2670.
  35. Miyazono, K., et al., Latent high molecular weight complex of transforming growth factor  $\beta$  1. Purification from human platelets and structural characterization. *J Biol Chem*, 1988. 263(13): p. 6407-6415.
  36. ten Dijke, P. and H.M. Arthur, Extracellular control of TGF $\beta$  signaling in vascular development and disease. *Nat Rev Mol Cell Biol*, 2007. 8(11): p. 857-869.
  37. Munger, J.S. and D. Sheppard, Cross talk among TGF- $\beta$  signaling pathways, integrins, and the extracellular matrix. *Cold Spring Harb Perspect Biol*, 2011. 3(11): p. a005017.
  38. Pappano, W.N., et al., Use of Bmp1/Tll1 doubly homozygous null mice and proteomics to identify and validate in vivo substrates of Bone morphogenetic protein 1/Tolloid-like metalloproteinases. *Mol Cell Biol*, 2003. 23(13): p. 4428-4438.
  39. Sheppard, D., Integrin-mediated activation of latent transforming growth factor  $\beta$ . *Cancer Metastasis Rev*, 2005. 24(3): p. 395-402.
  40. Fontana, L., et al., Fibronectin is required for integrin  $\alpha$ v $\beta$ 6-mediated activation of latent TGF- $\beta$  complexes containing LTBP-1. *FASEB J*, 2005. 19(13): p. 1798-1808.
  41. Crawford, S.E., et al., Thrombospondin-1 is a major activator of TGF- $\beta$ 1 in vivo. *Cell*, 1998. 93(7): p. 1159-1170.
  42. Massague, J., TGF $\beta$  signaling in context. *Nat Rev Mol Cell Biol*, 2012. 13(10): p. 616-630.
  43. Franzén, P., et al., Cloning of a TGF $\beta$  type I receptor that forms a heteromeric complex with the TGF $\beta$  type II receptor. *Cell*, 1993. 75(4): p. 681-692.
  44. Lux, A., L. Attisano, and D.A. Marchuk, Assignment of Transforming growth factor  $\beta$ 1 and  $\beta$ 3 and a third new ligand to the type I receptor ALK-1. *J Biol Chem*, 1999. 274(15): p. 9984-9992.
  45. ten Dijke, P., et al., Activin receptor-like kinases: a novel subclass of cell-surface receptors with predicted serine/threonine kinase activity. *Oncogene*, 1993. 8(10): p. 2879-87.
  46. ten Dijke, P., et al., Characterization of type I receptors for transforming growth factor- $\beta$  and activin. *Science*, 1994. 264(5155): p. 101-4.
  47. Vellucci, V.F. and M. Reiss, Cloning and genomic organization of the human Transforming growth

- factor- $\beta$  type I receptor gene. *Genomics*, 1997. 46(2): p. 278-283.
48. Inman, G.J., F.J. Nicolás, and C.S. Hill, Nucleocytoplasmic shuttling of Smads 2, 3, and 4 permits sensing of TGF- $\beta$  receptor activity. *Mol Cell*, 2002. 10(2): p. 283-294.
49. Wakefield, L.M. and C.S. Hill, Beyond TGF $\beta$ : roles of other TGF $\beta$  superfamily members in cancer. *Nat Rev Cancer*, 2013. 13(5): p. 328-341.
50. Schmierer, B. and C.S. Hill, TGF $\beta$ -SMAD signal transduction: molecular specificity and functional flexibility. *Nat Rev Mol Cell Biol*, 2007. 8(12): p. 970-982.
51. Wrana, J.L., Crossing Smads. *Sci STKE*, 2000. 2000(23): p. re1.
52. Alarcón, C., et al., Nuclear CDKs drive Smad transcriptional activation and turnover in BMP and TGF $\beta$  pathways. *Cell*, 2009. 139(4): p. 757-769.
53. Sapkota, G., et al., Balancing BMP signaling through integrated inputs into the Smad1 linker. *Mol Cell*, 2007. 25(3): p. 441-454.
54. Morikawa, M., et al., ChIP-seq reveals cell type-specific binding patterns of BMP-specific Smads and a novel binding motif. *Nucleic Acids Res*, 2011. 39(20): p. 8712-8727.
55. Mullen, A.C., et al., Master transcription factors determine cell-type-specific responses to TGF- $\beta$  signaling. *Cell*, 2011. 147(3): p. 565-576.
56. Heldin, C.-H., M. Landström, and A. Moustakas, Mechanism of TGF- $\beta$  signaling to growth arrest, apoptosis, and epithelial-mesenchymal transition. *Curr Opin Cell Biol*, 2009. 21(2): p. 166-176.
57. Itoh, S. and P. ten Dijke, Negative regulation of TGF- $\beta$  receptor/Smad signal transduction. *Curr Opin Cell Biol*, 2007. 19(2): p. 176-184.
58. Massagué, J., S.W. Blain, and R.S. Lo, TGF $\beta$  Signaling in growth control, cancer, and heritable disorders. *Cell*, 2000. 103(2): p. 295-309.
59. Iozzo, R.V. and L. Schaefer, Proteoglycans in health and disease: Novel regulatory signaling mechanisms evoked by the small leucine-rich proteoglycans. *FEBS J*, 2010. 277(19): p. 3864-3875.
60. Neill, T., L. Schaefer, and R.V. Iozzo, Decorin: A guardian from the matrix. *Am J Pathol*, 2012. 181(2): p. 380-387.
61. Yamaguchi, Y., D.M. Mann, and E. Ruoslahti, Negative regulation of transforming growth factor- $\beta$  by the proteoglycan decorin. *Nature*, 1990. 346(6281): p. 281-284.
62. Abdel-Wahab, N., et al., Decorin suppresses transforming growth factor- $\beta$ -induced expression of plasminogen activator inhibitor-1 in human mesangial cells through a mechanism that involves Ca<sup>2+</sup>-dependent phosphorylation of Smad2 at serine-240. *Biochem J*, 2002. 362(Pt 3): p. 643-649.
63. Schier, A.F. and M.M. Shen, Nodal signaling in vertebrate development. *Nature*, 2000. 403(6768): p. 385-389.
64. López-Casillas, F., J.L. Wrana, and J. Massagué, Betaglycan presents ligand to the TGF $\beta$  signaling receptor. *Cell*, 1993. 73(7): p. 1435-1444.
65. Lee, N.Y., et al., The Transforming growth factor- $\beta$  type III receptor mediates distinct subcellular trafficking and downstream signaling of Activin-like kinase (ALK)3 and ALK6 receptors. *Mol Biol Cell*, 2009. 20(20): p. 4362-4370.
66. Blanco, F.J., et al., Interaction and functional interplay between endoglin and ALK-1, two components of the endothelial transforming growth factor- $\beta$  receptor complex. *J Cell Physiol*, 2005. 204(2): p. 574-584.
67. Gougos, A. and M. Letarte, Primary structure of endoglin, an RGD-containing glycoprotein of human endothelial cells. *J Biol Chem*, 1990. 265(15): p. 8361-4.
68. Bellón, T., et al., Identification and expression of two forms of the human transforming growth factor- $\beta$ -binding protein endoglin with distinct cytoplasmic regions. *Eur J Immunol*, 1993. 23(9): p. 2340-2345.
69. Lebrin, F., et al., Endoglin promotes endothelial cell proliferation and TGF- $\beta$ /ALK1 signal transduction.

- EMBO J, 2004. 23(20): p. 4018-4028.
70. Shani, G., et al., GRP78 and Cripto form a complex at the cell surface and collaborate to inhibit Transforming growth factor  $\beta$  signaling and enhance cell growth. *Mol Cell Biol*, 2008. 28(2): p. 666-677.
  71. Gray, P.C., et al., Cripto binds Transforming growth factor  $\beta$  (TGF- $\beta$ ) and inhibits TGF- $\beta$  signaling. *Mol Cell Biol*, 2006. 26(24): p. 9268-9278.
  72. Gray, P.C. and W. Vale, Cripto/GRP78 modulation of the TGF- $\beta$  pathway in development and oncogenesis. *FEBS Lett*, 2012. 586(14): p. 1836-1845.
  73. Spike, Benjamin T., et al., CRIPTO/GRP78 signaling maintains fetal and adult mammary stem cells ex vivo. *Stem Cell Reports*, 2014. 2(4): p. 427-439.
  74. Nagaoka, T., et al., An evolving web of signaling networks regulated by Cripto-1. *Growth Factors*, 2012. 30(1): p. 13-21.
  75. Klauzinska, M., et al., The multifaceted role of the embryonic gene Cripto-1 in cancer, stem cells and epithelial-mesenchymal transition. *Semin Cancer Biol*, 2014. 29(0): p. 51-58.
  76. Healey, E.G., et al., Repulsive guidance molecule is a structural bridge between neogenin and bone morphogenetic protein. *Nat Struct Mol Biol*, 2015. 22(6): p. 458-465.
  77. Samad, T.A., et al., DRAGON, a Bone morphogenetic protein co-receptor. *J Biol Chem*, 2005. 280(14): p. 14122-14129.
  78. Babitt, J.L., et al., Repulsive guidance molecule (RGMa), a DRAGON homologue, is a Bone morphogenetic protein co-receptor. *J Biol Chem*, 2005. 280(33): p. 29820-29827.
  79. Xia, Y., et al., Repulsive guidance molecule RGMa alters utilization of Bone morphogenetic protein (BMP) type II receptors by BMP2 and BMP4. *J Biol Chem*, 2007. 282(25): p. 18129-18140.
  80. Miyazono, K., Positive and negative regulation of TGF- $\beta$  signaling. *J Cell Sci*, 2000. 113(7): p. 1101-1109.
  81. Sekiya, T., et al., Transcriptional regulation of the TGF- $\beta$  pseudoreceptor BAMBI by TGF- $\beta$  signaling. *Biochem Biophys Res Commun*, 2004. 320(3): p. 680-684.
  82. Karaulanov, E., W. Knöchel, and C. Niehrs, Transcriptional regulation of BMP4 synexpression in transgenic *Xenopus*. *EMBO J*, 2004. 23(4): p. 844-856.
  83. Okadome, T., et al., Characterization of the interaction of FKBP12 with the transforming growth factor- $\beta$  type I receptor in vivo. *J Biol Chem*, 1996. 271(36): p. 21687-90.
  84. Chen, Y.G., F. Liu, and J. Massague, Mechanism of TGF $\beta$  receptor inhibition by FKBP12. *EMBO J*, 1997. 16(13): p. 3866-3876.
  85. Spiekerkoetter, E., et al., FK506 activates BMPR2, rescues endothelial dysfunction, and reverses pulmonary hypertension. *J Clin Invest*, 2013. 123(8): p. 3600-3613.
  86. Wang, T., et al., The immunophilin FKBP12 functions as a common inhibitor of the TGF $\beta$  family type I receptors. *Cell*, 1996. 86(3): p. 435-444.
  87. Tsukazaki, T., et al., SARA, a FYVE domain protein that recruits Smad2 to the TGF $\beta$  receptor. *Cell*, 1998. 95(6): p. 779-791.
  88. Xu, L., Y.-G. Chen, and J. Massague, The nuclear import function of Smad2 is masked by SARA and unmasked by TGF $\beta$ -dependent phosphorylation. *Nat Cell Biol*, 2000. 2(8): p. 559-562.
  89. Lin, H.Y., et al., Expression cloning of the TGF- $\beta$  type II receptor, a functional transmembrane serine/threonine kinase. *Cell*, 1992. 68(4): p. 775-785.
  90. Luo, K. and H.F. Lodish, Positive and negative regulation of type II TGF $\beta$  receptor signal transduction by autophosphorylation on multiple serine residues. *EMBO J*, 1997. 16(8): p. 1970-1981.
  91. Lee, M.K., et al., TGF- $\beta$  activates Erk MAP kinase signaling through direct phosphorylation of ShcA. *EMBO J*, 2007. 26(17): p. 3957-3967.
  92. Shi, W., et al., GADD34-PP1c recruited by Smad7 dephosphorylates TGF $\beta$  type I receptor. *J Cell Biol*,

2004. 164(2): p. 291-300.
93. Heikkinen, P.T., et al., Hypoxia-activated Smad3-specific dephosphorylation by PP2A. *J Biol Chem*, 2010. 285(6): p. 3740-3749.
94. Geiss-Friedlander, R. and F. Melchior, Concepts in sumoylation: a decade on. *Nat Rev Mol Cell Biol*, 2007. 8(12): p. 947-956.
95. Dikic, I., S. Wakatsuki, and K.J. Walters, Ubiquitin-binding domains from structures to functions. *Nat Rev Mol Cell Biol*, 2009. 10(10): p. 659-671.
96. Cashman, R., et al., SENP5 mediates breast cancer invasion via a TGF $\beta$ RI SUMOylation cascade. *Oncotarget*, 2014. 5(4).
97. Kang, J.S., et al., The type I TGF- $\beta$  receptor is covalently modified and regulated by sumoylation. *Nat Cell Biol*, 2008. 10(6): p. 654-664.
98. Kavsak, P., et al., Smad7 binds to Smurf2 to form an E3 ubiquitin ligase that targets the TGF $\beta$  receptor for degradation. *Mol Cell*, 2000. 6(6): p. 1365-1375.
99. Ebisawa, T., et al., Smurf1 interacts with Transforming growth factor- $\beta$  type I receptor through Smad7 and induces receptor degradation. *J Biol Chem*, 2001. 276(16): p. 12477-12480.
100. Cao, Y. and L. Zhang, A Smurf1 tale: function and regulation of an ubiquitin ligase in multiple cellular networks. *Cell Mol Life Sci*, 2013. 70(13): p. 2305-2317.
101. Liu, W., et al., Axin is a scaffold protein in TGF- $\beta$  signaling that promotes degradation of Smad7 by Arkadia. *EMBO J*, 2006. 25(8): p. 1646-58.
102. Zhou, F., et al., Nuclear receptor NR4A1 promotes breast cancer invasion and metastasis by activating TGF- $\beta$  signaling. *Nat Commun*, 2014. 5.
103. Sharma, V., et al., Enhancement of TGF- $\beta$  signaling responses by the E3 ubiquitin ligase Arkadia provides tumor suppression in colorectal cancer. *Cancer Res*, 2011. 71(20): p. 6438-49.
104. Sun, H. and T. Hunter, PolySUMO-binding proteins identified through a string search. *J Biol Chem*, 2012.
105. Erker, Y., et al., Arkadia, a novel SUMO-targeted ubiquitin ligase involved in PML degradation. *Mol Cell Biol*, 2013. 33(11): p. 2163-2177.
106. Tsubakihara, Y., et al., Arkadia enhances BMP signaling through ubiquitylation and degradation of Smad6. *J Biochem*, 2015.
107. Sun, H., Y. Liu, and T. Hunter, Multiple Arkadia/RNF111 structures coordinate its Polycomb body association and transcriptional control. *Mol Cell Biol*, 2014. 34(16): p. 2981-2995.
108. Nagano, Y., et al., Arkadia induces degradation of SnoN and c-Ski to enhance Transforming growth factor- $\beta$  signaling. *J Biol Chem*, 2007. 282(28): p. 20492-20501.
109. Levy, L., et al., Arkadia activates Smad3/Smad4-dependent transcription by triggering signal-induced SnoN degradation. *Mol Cell Biol*, 2007. 27(17): p. 6068-6083.
110. Mavrakis, K.J., et al., Arkadia enhances Nodal/TGF- $\beta$  signaling by coupling phospho-Smad2/3 activity and turnover. *PLoS Biol*, 2007. 5(3): p. e67.
111. Lee, P.S.W., et al., Sumoylation of Smad4, the common Smad mediator of Transforming growth factor- $\beta$  family signaling. *J Biol Chem*, 2003. 278(30): p. 27853-27863.
112. Zhou, X., et al., High glucose induces sumoylation of Smad4 via SUMO2/3 in mesangial cells. *Biomed Res Int*, 2014. 2014: p. 782625.
113. Dupont, S., et al., FAM/USP9x, a deubiquitinating enzyme essential for TGF $\beta$  signaling, controls Smad4 monoubiquitination. *Cell*, 2009. 136(1): p. 123-135.
114. Maeda, S., et al., Endogenous TGF- $\beta$  signaling suppresses maturation of osteoblastic mesenchymal cells. *EMBO J*, 2004. 23(3): p. 552-563.
115. Ishida, W., et al., Smad6 is a Smad1/5-induced Smad inhibitor: Characterization of Bone morphogenetic protein-responsive element in the mouse Smad6 promoter *J Biol Chem*, 2000. 275(9): p. 6075-6079.

116. Afrakhte, M., et al., Induction of inhibitory Smad6 and Smad7 mRNA by TGF $\beta$  family members. *Biochem Biophys Res Commun*, 1998. 249(2): p. 505-511.
117. Nakao, A., et al., Identification of Smad7, a TGF $\beta$ -inducible antagonist of TGF- $\beta$  signaling. *Nature*, 1997. 389(6651): p. 631-635.
118. Goto, K., et al., Selective inhibitory effects of Smad6 on Bone morphogenetic protein type I receptors. *J Biol Chem*, 2007. 282(28): p. 20603-20611.
119. Hata, A., et al., Smad6 inhibits BMP/Smad1 signaling by specifically competing with the Smad4 tumor suppressor. *Genes Dev*, 1998. 12(2): p. 186-197.
120. Morén, A., et al., Degradation of the tumor suppressor Smad4 by WW and HECT domain ubiquitin ligases. *J Biol Chem*, 2005. 280(23): p. 22115-22123.
121. Zhang, S., et al., Smad7 antagonizes Transforming growth factor  $\beta$  signaling in the nucleus by interfering with functional Smad-DNA complex formation. *Mol Cell Biol*, 2007. 27(12): p. 4488-4499.
122. Itoh, S., et al., Transforming growth factor  $\beta$ 1 induces nuclear export of inhibitory Smad7. *J Biol Chem*, 1998. 273(44): p. 29195-29201.
123. Valdimarsdottir, G., et al., Smad7 and protein phosphatase 1 $\alpha$  are critical determinants in the duration of TGF- $\beta$ /ALK1 signaling in endothelial cells. *BMC Cell Biol*, 2006. 7: p. 16-16.
124. Ishisaki, A., et al., Differential inhibition of Smad6 and Smad7 on bone morphogenetic protein- and activin-mediated growth arrest and apoptosis in B cells. *J Biol Chem.*, 1999. 274(19): p. 13637-13642.
125. Itoh, F., et al., Promoting bone morphogenetic protein signaling through negative regulation of inhibitory Smads. *EMBO J*, 2001. 20(15): p. 4132-4142.
126. Yang, J., et al., Downregulation of Smad transcriptional corepressors SnoN and Ski in the fibrotic kidney: An amplification mechanism for TGF- $\beta$ 1 signaling. *J Am Soc Nephrol*, 2003. 14(12): p. 3167-3177.
127. Tabata, T., et al., Ski co-repressor complexes maintain the basal repressed state of the TGF- $\beta$  target gene, SMAD7, via HDAC3 and PRMT5. *Genes Cells*, 2009. 14(1): p. 17-28.
128. Zhou, X., et al., Nodal is a novel TGF- $\beta$ -like gene expressed in the mouse node during gastrulation. *Nature*, 1993. 361(6412): p. 543-547.
129. Shen, M.M., Nodal signaling: developmental roles and regulation. *Development*, 2007. 134(6): p. 1023-1034.
130. Kruihof-de Julio, M., et al., Regulation of extra-embryonic endoderm stem cell differentiation by Nodal and Cripto signaling. *Development*, 2011. 138(18): p. 3885-3895.
131. Sarkar, P., et al., Activin/Nodal signaling switches the terminal fate of human embryonic stem cell-derived trophoblasts. *J Biol Chem*, 2015. 290(14): p. 8834-8848.
132. Bianco, C., et al., Role of Cripto-1 in stem cell maintenance and malignant progression. *Am J Pathol*, 2010. 177(2): p. 532-540.
133. Yeo, C.-Y. and M. Whitman, Nodal signals to Smads through Cripto-dependent and Cripto-independent mechanisms. *Mol Cell*, 2001. 7(5): p. 949-957.
134. Rosa, F.M., Cripto, a multifunctional partner in signaling: molecular forms and activities. *Sci Signal*, 2002. 2002(158): p. pe47-pe47.
135. Yan, Y.-T., et al., Dual roles of Cripto as a ligand and coreceptor in the Nodal signaling pathway. *Mol Cell Biol*, 2002. 22(13): p. 4439-4449.
136. Chen, C., et al., The Vg1-related protein Gdf3 acts in a Nodal signaling pathway in the pre-gastrulation mouse embryo. *Development*, 2006. 133(2): p. 319-329.
137. Blanchet, M.-H., et al., Cripto localizes Nodal at the limiting membrane of early endosomes. *Sci Signal*, 2008. 1(45): p. ra13.
138. Schiffer, S.G., et al., Fucosylation of Cripto is required for its ability to facilitate Nodal signaling. *J Biol Chem*, 2001.

139. Schier, A.F., Nodal Morphogens. *Cold Spring Harb Perspect Biol*, 2009. 1(5): p. a003459.
140. Cruz, C.D., et al., Expression of Nodal, Cripto, SMAD3, phosphorylated SMAD3, and SMAD4 in the proliferative endometrium of women with endometriosis. *Reprod Sci*, 2015. 22(5): p. 527-533.
141. Loying, P., et al., Autoregulation and heterogeneity in expression of human Cripto-1. *PLoS One*, 2015. 10(2): p. e0116748.
142. Schier, A.F., NODAL signaling in vertebrate development *Annu Rev Cell Dev Biol*, 2003. 19(1): p. 589-621.
143. Su, Y., et al., The evolutionally conserved activity of Dapper2 in antagonizing TGF- $\beta$  signaling. *FASEB J*, 2007. 21(3): p. 682-690.
144. Dupont, S., et al., Germ-layer specification and control of cell growth by ectodermin, a Smad4 ubiquitin ligase. *Cell*, 2005. 121(1): p. 87-99.
145. Powers, S.E., et al., Tgif1 and Tgif2 regulate Nodal signaling and are required for gastrulation. *Development*, 2010. 137(2): p. 249-259.
146. Cai, W., et al., Coordinate Nodal and BMP inhibition directs Baf60c-dependent cardiomyocyte commitment. *Genes Dev*, 2013. 27(21): p. 2332-2344.
147. Bianco, C., et al., A Nodal- and ALK4-independent signaling pathway activated by Cripto-1 through Glypican-1 and c-Src. *Cancer Res*, 2003. 63(6): p. 1192-1197.
148. Bianco, C., et al., Regulation of Cripto-1 signaling and biological activity by Caveolin-1 in mammary epithelial cells. *Am J Pathol*, 2008. 172(2): p. 345-357.
149. D'Aniello, C., et al., G Protein-coupled receptor APJ and its ligand apelin act downstream of Cripto to specify embryonic stem cells toward the cardiac lineage through extracellular signal-regulated kinase/p70S6 kinase Signaling Pathway. *Circ Res*, 2009. 105(3): p. 231-238.
150. Nagaoka, T., et al., Cripto-1 enhances the canonical Wnt/ $\beta$ -catenin signaling pathway by binding to LRP5 and LRP6 co-receptors. *Cell Signal*, 2013. 25(1): p. 178-189.
151. Watanabe, K., et al., Enhancement of Notch receptor maturation and signaling sensitivity by Cripto-1. *J Cell Biol*, 2009. 187(3): p. 343-353.
152. Xu, C.-H., et al., Elevated expression of Cripto-1 correlates with poor prognosis in non-small cell lung cancer. *Tumour Biol*, 2014. 35(9): p. 8673-8678.
153. Cocciaferro, L., et al., Profiling cancer stem cells in androgen-responsive and refractory human prostate tumor cell lines. *Ann NY Acad Sci*, 2009. 1155(1): p. 257-262.
154. Terry, S., et al., CRIPTO overexpression promotes mesenchymal differentiation in prostate carcinoma cells through parallel regulation of AKT and FGFR activities. *Oncotarget*, 2015. 6(14): p. 11994-2008.
155. D'Antonio, A., et al., Transforming growth factor alpha, amphiregulin and cripto-1 are frequently expressed in advanced human ovarian carcinomas. *Int J Oncol*, 2002. 21(5): p. 941-8.
156. Fujii, K., et al., Expression of CRIPTO in human gall bladder lesions *J Pathol.*, 1996. 180(2): p. 166-168.
157. Giorgio, E., et al., Cripto haploinsufficiency affects in vivo colon tumor development. *Int J Oncol*, 2014. 45(1): p. 31-40.
158. Sun, C., et al., NANOG promotes liver cancer cell invasion by inducing epithelial-mesenchymal transition through NODAL/SMAD3 signaling pathway. *Int J Biochem Cell Biol*, 2013. 45(6): p. 1099-1108.
159. Strizzi, L., et al., The significance of a Cripto-1-positive subpopulation of human melanoma cells exhibiting stem cell-like characteristics. *Cell Cycle*, 2013. 12(9): p. 1450-1456.
160. Tysnes, B.B., et al., Age-dependent association between protein expression of the embryonic stem cell marker Cripto-1 and survival of glioblastoma patients. *Transl Oncol*, 2013. 6(6): p. 732-741.
161. Sato, M., et al., GRP78 signaling hub: A receptor for targeted tumor therapy. *Adv Genet*, 2010. Volume 69: p. 97-114.
162. Adkins, H.B., et al., Antibody blockade of the Cripto CFC domain suppresses tumor cell growth in vivo.

- J Clin Invest, 2003. 112(4): p. 575-587.
163. Bianco, C. and D.S. Salomon, Targeting the embryonic gene Cripto-1 in cancer and beyond. *Expert Opin Ther Pat*, 2010. 20(12): p. 1739-1749.
164. Bianco, C. and D.S. Salomon, Human Cripto-1 as a target for a cancer vaccine: WO2008040759. *Expert Opin Ther Pat*, 2009. 19(2): p. 141-144.
165. Derynck, R. and Y.E. Zhang, Smad-dependent and Smad-independent pathways in TGF- $\beta$  family signaling. *Nature*, 2003. 425(6958): p. 577-584.
166. Hackel, P.O., et al., Epidermal growth factor receptors: critical mediators of multiple receptor pathways. *Curr Opin Cell Biol*, 1999. 11(2): p. 184-189.
167. Chen, R.H., C. Sarnecki, and J. Blenis, Nuclear localization and regulation of ERK- and RSK-encoded protein kinases. *Mol Cell Biol*, 1992. 12(3): p. 915-927.
168. Mu, Y., S. Gudey, and M. Landström, Non-Smad signaling pathways. *Cell Tissue Res*, 2012. 347(1): p. 11-20.
169. Yi, J.Y., I. Shin, and C.L. Arteaga, Type I Transforming growth factor  $\beta$  receptor binds to and activates phosphatidylinositol 3-kinase. *J Biol Chem*, 2005. 280(11): p. 10870-10876.
170. Lamouille, S. and R. Derynck, Emergence of the phosphoinositide 3-kinase-Akt-mammalian target of rapamycin axis in Transforming growth factor- $\beta$ -induced epithelial-mesenchymal transition. *Cells Tissues Organs*, 2010. 193(1-2): p. 8-22.
171. Zhang, L., et al., USP4 is regulated by AKT phosphorylation and directly deubiquitylates TGF- $\beta$  type I receptor. *Nat Cell Biol*, 2012. 14(7): p. 717-726.
172. Zhang, X., et al., Akt, FoxO and regulation of apoptosis. *Biochim Biophys Acta*, 2011. 1813(11): p. 1978-1986.
173. Ozdamar, B., et al., Regulation of the polarity protein Par6 by TGF $\beta$  receptors controls epithelial cell plasticity. *Science*, 2005. 307(5715): p. 1603-1609.
174. Yamaguchi, K., et al., Identification of a member of the MAPKKK family as a potential mediator of TGF- $\beta$  signal transduction. *Science*, 1995. 270(5244): p. 2008-11.
175. Yamashita, M., et al., TRAF6 mediates Smad-independent activation of JNK and p38 by TGF- $\beta$ . *Mol Cell*, 2008. 31(6): p. 918-924.
176. Sorrentino, A., et al., The type I TGF- $\beta$  receptor engages TRAF6 to activate TAK1 in a receptor kinase-independent manner. *Nat Cell Biol*, 2008. 10(10): p. 1199-1207.
177. Zavadil, J., et al., Genetic programs of epithelial cell plasticity directed by transforming growth factor- $\beta$ . *Proc Natl Acad Sci U S A*, 2001. 98(12): p. 6686-6691.
178. Kang, Y., C.-R. Chen, and J. Massagué, A self-enabling TGF $\beta$  response coupled to stress signaling: Smad engages stress response factor ATF3 for Id1 repression in epithelial cells. *Mol Cell*, 2003. 11(4): p. 915-926.
179. Reynisdóttir, I., et al., Kip/Cip and Ink4 Cdk inhibitors cooperate to induce cell cycle arrest in response to TGF- $\beta$ . *Genes Dev*, 1995. 9(15): p. 1831-1845.
180. Hannon, G.J. and D. Beach, p15INK4B is a potential effector of TGF- $\beta$ -induced cell cycle arrest. *Nature*, 1994. 371(6494): p. 257-261.
181. Oberhammer, F.A., et al., Induction of apoptosis in cultured hepatocytes and in regressing liver by transforming growth factor  $\beta$  1. *Proc Natl Acad Sci U S A*, 1992. 89(12): p. 5408-5412.
182. Pardali, K. and A. Moustakas, Actions of TGF- $\beta$  as tumor suppressor and pro-metastatic factor in human cancer. *Biochim Biophys Acta*, 2007. 1775(1): p. 21-62.
183. Takehara, K., E.C. LeRoy, and G.R. Grotendorst, TGF- $\beta$  inhibition of endothelial cell proliferation: Alteration of EGF binding and EGF-induced growth-regulatory (competence) gene expression. *Cell*, 1987. 49(3): p. 415-422.
184. Leask, A. and D.J. Abraham, TGF- $\beta$  signaling and the fibrotic response. *FASEB J*, 2004. 18(7): p. 816-827.



185. Böttner, M., K. Kriegelstein, and K. Unsicker, The Transforming growth factor- $\beta$ s. *J Neurochem*, 2000. 75(6): p. 2227-2240.
186. Blank, U. and S. Karlsson, TGF $\beta$  signaling in the control of hematopoietic stem cells. *Blood*, 2015. 125(23): p. 3542-50.
187. Karkampouna, S. and M. Kruithof-de Julio, Fibrosis: a novel approach for an old problem. *Receptors Clin Investig*, 2014. 1(5).
188. Sanderson, N., et al., Hepatic expression of mature transforming growth factor  $\beta$  1 in transgenic mice results in multiple tissue lesions. *Proc Natl Acad Sci U S A*, 1995. 92(7): p. 2572-2576.
189. Böttinger, E.P., et al., The recombinant proregion of transforming growth factor  $\beta$ 1 (latency-associated peptide) inhibits active transforming growth factor  $\beta$ 1 in transgenic mice. *Proc Natl Acad Sci U S A*, 1996. 93(12): p. 5877-5882.
190. Gewaltig, J., et al., Association of polymorphisms of the transforming growth factor- $\beta$ 1 gene with the rate of progression of HCV-induced liver fibrosis. *Clin Chim Acta*, 2002. 316(1-2): p. 83-94.
191. Goto, K., et al., Proximal prostatic stem cells are programmed to regenerate a proximal-distal ductal axis. *Stem Cells*, 2006. 24(8): p. 1859-1868.
192. Kang, H.Y., et al., From transforming growth factor- $\beta$  signaling to androgen action: Identification of Smad3 as an androgen receptor coregulator in prostate cancer cells. *Proc Natl Acad Sci U S A*, 2001. 98(6): p. 3018-3023.
193. Salm, S.N., et al., TGF- $\beta$  maintains dormancy of prostatic stem cells in the proximal region of ducts. *J Cell Biol*, 2005. 170(1): p. 81-90.
194. Song, K., et al., Androgenic control of Transforming growth factor- $\beta$  signaling in prostate epithelial cells through transcriptional suppression of Transforming growth factor- $\beta$  receptor II. *Cancer Res*, 2008. 68(19): p. 8173-8182.
195. Kundu, S.D., et al., Absence of proximal duct apoptosis in the ventral prostate of transgenic mice carrying the C3(1)-TGF- $\beta$  type II dominant negative receptor. *Prostate*, 2000. 43(2): p. 118-124.
196. Martikainen, P., N. Kyprianou, and J.T. Isaacs, Effect of transforming growth factor- $\beta$  1 on proliferation and death of rat prostatic cells. *Endocrinology*, 1990. 127(6): p. 2963-8.
197. Walraven, M., et al., Altered TGF- $\beta$  signaling in fetal fibroblasts: What is known about the underlying mechanisms? *Wound Repair Regen*, 2014. 22(1): p. 3-13.
198. Tomasek, J.J., et al., Myofibroblasts and mechano-regulation of connective tissue remodelling. *Nat Rev Mol Cell Biol*, 2002. 3(5): p. 349-363.
199. Akhurst, R.J., TGF $\beta$  signaling in health and disease. *Nat Genet*, 2004. 36(8): p. 790-792.
200. Mizuguchi, T., et al., Heterozygous TGF $\beta$ R2 mutations in Marfan syndrome. *Nat Genet*, 2004. 36(8): p. 855-860.
201. Akutsu, K., et al., Phenotypic heterogeneity of Marfan-like connective tissue disorders associated with mutations in the TGF $\beta$  receptor genes. *Circ J*, 2007. 71(8): p. 1305-1309.
202. Schultz, G.S., et al., Dynamic reciprocity in the wound microenvironment. *Wound Repair Regen*, 2011. 19(2): p. 134-148.
203. Bissell, M.J., H.G. Hall, and G. Parry, How does the extracellular matrix direct gene expression? *J Theor Biol*, 1982. 99(1): p. 31-68.
204. Bornstein, P. and E.H. Sage, Matricellular proteins: extracellular modulators of cell function. *Curr Opin Cell Biol*, 2002. 14(5): p. 608-616.
205. Vogel, V. and M. Sheetz, Local force and geometry sensing regulate cell functions. *Nat Rev Mol Cell Biol*, 2006. 7(4): p. 265-275.
206. Xu, R., A. Boudreau, and M. Bissell, Tissue architecture and function: dynamic reciprocity via extra- and intra-cellular matrices. *Cancer Metastasis Rev*, 2009. 28(1-2): p. 167-176.
207. Maeda, T., et al., Conversion of mechanical force into TGF- $\beta$ -mediated biochemical signals. *Curr Biol*,

2011. 21(11): p. 933-941.
208. Streuli, C.H., et al., Extracellular matrix regulates expression of the TGF- $\beta$ 1 gene. *J Cell Biol*, 1993. 120(1): p. 253-260.
209. Weber, I.T., R.W. Harrison, and R.V. Iozzo, Model structure of decorin and implications for collagen fibrillogenesis. *J Biol Chem*, 1996. 271(50): p. 31767-70.
210. Wynn, T.A., Cellular and molecular mechanisms of fibrosis. *J Pathol*, 2008. 214(2): p. 199-210.
211. Kloen, P., et al., Transforming growth factor- $\beta$ : possible roles in Dupuytren's contracture. *J Hand Surg Am*, 1995. 20(1): p. 101-108.
212. Rehman, S., et al., Molecular phenotypic descriptors of Dupuytren's disease defined using Informatics analysis of the transcriptome. *J Hand Surg Am*, 2008. 33(3): p. 359-372.
213. Border, W.A. and N.A. Noble, Transforming growth factor  $\beta$  in tissue fibrosis. *N Engl J Med*, 1994. 331(19): p. 1286-92.
214. Westerhausen, D.R., Jr., W.E. Hopkins, and J.J. Billadello, Multiple transforming growth factor- $\beta$ -inducible elements regulate expression of the plasminogen activator inhibitor type-1 gene in Hep G2 cells. *J Biol Chem*, 1991. 266(2): p. 1092-100.
215. Shih, B., S. Watson, and A. Bayat, Whole genome and global expression profiling of Dupuytren's disease: systematic review of current findings and future perspectives. *Ann Rheum Dis*, 2012. 71(9): p. 1440-1447.
216. Kraljevic Pavelic, S., et al., An integrated proteomics approach for studying the molecular pathogenesis of Dupuytren's disease. *J Pathol*, 2009. 217(4): p. 524-533.
217. Ignatz, R.A. and J. Massague, Transforming growth factor- $\beta$  stimulates the expression of fibronectin and collagen and their incorporation into the extracellular matrix. *J Biol Chem*, 1986. 261(9): p. 4337-45.
218. Su, T.H., J.H. Kao, and C.J. Liu, Molecular mechanism and treatment of viral hepatitis-related liver fibrosis. *Int J Mol Sci*, 2014. 15(6): p. 10578-604.
219. Dooley, S. and P. ten Dijke, TGF- $\beta$  in progression of liver disease. *Cell Tissue Res*, 2012. 347(1): p. 245-56.
220. Meindl-Beinker, N.M. and S. Dooley, Transforming growth factor- $\beta$  and hepatocyte transdifferentiation in liver fibrogenesis. *J Gastroenterol Hepatol*, 2008. 23 Suppl 1: p. S122-7.
221. Gabbiani, G., The myofibroblast in wound healing and fibrocontractive diseases. *J Pathol*, 2003. 200(4): p. 500-503.
222. Kawelke, N., et al., Fibronectin protects from excessive liver fibrosis by modulating the availability of and responsiveness of stellate cells to active TGF- $\beta$ . *PLoS One*, 2011. 6(11): p. e28181.
223. Jeong, D.H., et al., Smad3 deficiency ameliorates hepatic fibrogenesis through the expression of senescence marker protein-30, an antioxidant-related protein. *Int J Mol Sci*, 2013. 14(12): p. 23700-23710.
224. Furukawa, F., et al., p38 MAPK mediates fibrogenic signal through Smad3 phosphorylation in rat myofibroblasts. *Hepatology*, 2003. 38(4): p. 879-89.
225. Phanish, Mysore K., et al., The differential role of Smad2 and Smad3 in the regulation of pro-fibrotic TGF $\beta$ 1 responses in human proximal-tubule epithelial cells. *Biochem J*, 2006. 393(Pt 2): p. 601-607.
226. Ju, W., et al., Deletion of Smad2 in mouse liver reveals novel functions in hepatocyte growth and differentiation. *Mol Cell Biol*, 2006. 26(2): p. 654-667.
227. Tahashi, Y., et al., Differential regulation of TGF- $\beta$  signal in hepatic stellate cells between acute and chronic rat liver injury. *Hepatology*, 2002. 35(1): p. 49-61.
228. Dooley, S., et al., Hepatocyte-specific Smad7 expression attenuates TGF- $\beta$ -mediated fibrogenesis and protects against liver damage. *Gastroenterology*, 2008. 135(2): p. 642-59.
229. Goumans, M.J., et al., Balancing the activation state of the endothelium via two distinct TGF- $\beta$  type I receptors. *EMBO J*, 2002. 21(7): p. 1743-53.

230. Herrera, B., S. Dooley, and K. Breitkopf-Heinlein, Potential roles of bone morphogenetic protein (BMP)-9 in human liver diseases. *Int J Mol Sci*, 2014. 15(4): p. 5199-220.
231. Zhong, L., et al., The anti-fibrotic effect of bone morphogenetic protein-7(BMP-7) on liver fibrosis. *Int J Med Sci*, 2013. 10(4): p. 441-50.
232. Wang, L.P., et al., BMP-7 attenuates liver fibrosis via regulation of epidermal growth factor receptor. *Int J Clin Exp Pathol*, 2014. 7(7): p. 3537-47.
233. Kinoshita, K., et al., Adenovirus-mediated expression of BMP-7 suppresses the development of liver fibrosis in rats. *Gut*, 2007. 56(5): p. 706-14.
234. Flatt, A.E., The Vikings and Baron Dupuytren's disease. *Proc (Bayl Univ Med Cent)*, 2001. 14(4): p. 378-84.
235. Gudmundsson, K.G., T. Jónsson, and R. Arngrímsson, Guillaume Dupuytren and finger contractures. *Lancet*, 2003. 362(9378): p. 165-168.
236. McFarlane, R.M., On the origin and spread of Dupuytren's disease. *J Hand Surg Am*, 2002. 27(3): p. 385-390.
237. Shih, B. and A. Bayat, Scientific understanding and clinical management of Dupuytren disease. *Nat Rev Rheumatol*, 2010. 6(12): p. 715-726.
238. Witthaut, J., et al., Efficacy and safety of Collagenase Clostridium Histolyticum injection for Dupuytren contracture: short-term results from 2 open-label studies. *J Hand Surg Am*, 2013. 38(1): p. 2-11.
239. Hindocha, S., et al., Dupuytren's diathesis revisited: evaluation of prognostic indicators for risk of disease recurrence. *J Hand Surg Am*, 2006. 31(10): p. 1626-1634.
240. Kloen, P., et al., Transforming growth factor- $\beta$ : Possible roles in Dupuytren's contracture. *J Hand Surg Am*, 1995. 20(1): p. 101-108.
241. Badalamente, M.A., et al., The role of transforming growth factor  $\beta$  in Dupuytren's disease. *J Hand Surg Am*, 1996. 21(2): p. 210-215.
242. Kraljevic Pavelic, S., et al., An integrated proteomics approach for studying the molecular pathogenesis of Dupuytren's disease. *J Pathol*, 2009. 217(4): p. 524-533.
243. Zhang, A.Y., et al., Gene expression analysis of Dupuytren's disease: the role of TGF- $\beta$ 2. *J Hand Surg Eur Vol*, 2008. 33(6): p. 783-790.
244. Krause, C., P. Kloen, and P. ten Dijke, Elevated transforming growth factor  $\beta$  and mitogen-activated protein kinase pathways mediate fibrotic traits of Dupuytren's disease fibroblasts. *Fibrogenesis Tissue Repair*, 2011. 4(1): p. 14.
245. Hinz, B., et al., The myofibroblast: one function, multiple origins. *Am J Pathol*, 2007. 170(6): p. 1807-1816.
246. Vaughan, M.B., E.W. Howard, and J.J. Tomasek, Transforming growth factor- $\beta$ 1 promotes the morphological and functional differentiation of the myofibroblast. *Exp Cell Res*, 2000. 257(1): p. 180-9.
247. Wong, M. and V. Mudera, Feedback inhibition of high TGF- $\beta$ 1 concentrations on myofibroblast induction and contraction by Dupuytren's fibroblasts. *J Hand Surg Br*, 2006. 31(5): p. 473-83.
248. Bisson, M.A., et al., Transforming growth factor- $\beta$ 1 stimulation enhances Dupuytren's fibroblast contraction in response to uniaxial mechanical load within a 3-dimensional collagen gel. *J Hand Surg Am*, 2009. 34(6): p. 1102-10.
249. Tse, R., et al., Enhanced Dupuytren's disease fibroblast populated collagen lattice contraction is independent of endogenous active TGF- $\beta$ 2. *BMC Musculoskelet Disord*, 2004. 5(1): p. 41.
250. Vindevoghel, L., et al., SMAD3/4-dependent transcriptional activation of the human type VII collagen gene (COL7A1) promoter by transforming growth factor  $\beta$ . *Proc Natl Acad Sci U S A*, 1998. 95(25): p. 14769-74.
251. Deckers, M., et al., The tumor suppressor Smad4 is required for transforming growth factor  $\beta$ -induced epithelial to mesenchymal transition and bone metastasis of breast cancer cells. *Cancer Res*, 2006.

- 66(4): p. 2202-9.
252. Leask, A., Potential therapeutic targets for cardiac fibrosis: TGF $\beta$ , angiotensin, endothelin, CCN2, and PDGF, partners in fibroblast activation. *Circ Res*, 2010. 106(11): p. 1675-80.
253. Desmouliere, A., et al., Transforming growth factor- $\beta$  1 induces alpha-smooth muscle actin expression in granulation tissue myofibroblasts and in quiescent and growing cultured fibroblasts. *J Cell Biol*, 1993. 122(1): p. 103-11.
254. Wynn, T.A. and T.R. Ramalingam, Mechanisms of fibrosis: therapeutic translation for fibrotic disease. *Nat Med*, 2012. 18(7): p. 1028-40.
255. Taura, K., et al., Hepatocytes do not undergo epithelial-mesenchymal transition in liver fibrosis in mice. *Hepatology*, 2010. 51(3): p. 1027-36.
256. Mosakhani, N., et al., Unique microRNA profile in Dupuytren's contracture supports deregulation of  $\beta$ -catenin pathway. *Mod Pathol*, 2010. 23(11): p. 1544-52.
257. Satish, L., et al., Fibroblasts from phenotypically normal palmar fascia exhibit molecular profiles highly similar to fibroblasts from active disease in Dupuytren's Contracture. *BMC Med Genomics*, 2012. 5: p. 15.
258. Massagué, J., TGF $\beta$  in Cancer. *Cell*, 2008. 134(2): p. 215-230.
259. Liu, I.M., et al., TGF $\beta$ -stimulated Smad1/5 phosphorylation requires the ALK5 L45 loop and mediates the pro-migratory TGF $\beta$  switch. *EMBO J*, 2009. 28(2): p. 88-98.
260. Massague, J., Integration of Smad and MAPK pathways: a link and a linker revisited. *Genes Dev*, 2003. 17(24): p. 2993-7.
261. Oft, M., R.J. Akhurst, and A. Balmain, Metastasis is driven by sequential elevation of H-ras and Smad2 levels. *Nat Cell Biol*, 2002. 4(7): p. 487-94.
262. Levy, L. and C.S. Hill, Alterations in components of the TGF- $\beta$  superfamily signaling pathways in human cancer. *Cytokine Growth Factor Rev*, 2006. 17(1-2): p. 41-58.
263. Thiery, J.P., Epithelial-mesenchymal transitions in development and pathologies. *Curr Opin Cell Biol*, 2003. 15(6): p. 740-6.
264. Kalluri, R. and R.A. Weinberg, The basics of epithelial-mesenchymal transition. *J Clin Invest*, 2009. 119(6): p. 1420-1428.
265. Thuaux, S., et al., Transforming growth factor- $\beta$  employs HMGA2 to elicit epithelial-mesenchymal transition. *J Cell Biol*, 2006. 174(2): p. 175-183.
266. Yang, J., et al., Twist, a master regulator of morphogenesis, plays an essential role in tumor metastasis. *Cell*, 2004. 117(7): p. 927-39.
267. Batlle, E., et al., The transcription factor Snail is a repressor of E-cadherin gene expression in epithelial tumour cells. *Nat Cell Biol*, 2000. 2(2): p. 84-89.
268. Stankic, M., et al., TGF $\beta$ -Id1 signaling opposes Twist1 and promotes metastatic colonization via a mesenchymal-to-epithelial transition. *Cell Rep*, 2013. 5(5): p. 1228-1242.
269. Buijs, J., et al., TGF- $\beta$  and BMP7 interactions in tumour progression and bone metastasis. *Clin Exp Metastasis*, 2007. 24(8): p. 609-617.
270. Pardali, E., M.-J. Goumans, and P. ten Dijke, Signaling by members of the TGF- $\beta$  family in vascular morphogenesis and disease. *Trends Cell Biol*, 2010. 20(9): p. 556-567.
271. ten Dijke, P. and H.M. Arthur, Extracellular control of TGF $\beta$  signaling in vascular development and disease. *Nat Rev Mol Cell Biol*, 2007. 8(11): p. 857-69.
272. Urness, L.D., L.K. Sorensen, and D.Y. Li, Arteriovenous malformations in mice lacking activin receptor-like kinase-1. *Nat Genet*, 2000. 26(3): p. 328-31.
273. Armulik, A., A. Abramsson, and C. Betsholtz, Endothelial/pericyte interactions. *Circ Res*, 2005. 97(6): p. 512-523.
274. Liu, Z., et al., ENDOGLIN is dispensable for vasculogenesis, but required for vascular endothelial

- growth factor-induced angiogenesis. *PLoS One*, 2014. 9(1): p. e86273.
275. Risau, W., Mechanisms of angiogenesis. *Nature*, 1997. 386(6626): p. 671-674.
276. Siegel, P.M. and J. Massague, Cytostatic and apoptotic actions of TGF- $\beta$  in homeostasis and cancer. *Nat Rev Cancer*, 2003. 3(11): p. 807-21.
277. Adams, R.H. and K. Alitalo, Molecular regulation of angiogenesis and lymphangiogenesis. *Nat Rev Mol Cell Biol*, 2007. 8(6): p. 464-478.
278. Kim, E.S., M.S. Kim, and A. Moon, TGF- $\beta$ -induced upregulation of MMP-2 and MMP-9 depends on p38 MAPK, but not ERK signaling in MCF10A human breast epithelial cells. *Int J Oncol*, 2004. 25(5): p. 1375-82.
279. Hawinkels, L.J., et al., Matrix metalloproteinase-14 (MT1-MMP)-mediated endoglin shedding inhibits tumor angiogenesis. *Cancer Res*, 2010. 70(10): p. 4141-50.
280. Stearns, M.E., et al., Role of Interleukin 10 and Transforming growth factor  $\beta$ 1 in the angiogenesis and metastasis of human prostate primary tumor lines from orthotopic implants in severe combined immunodeficiency mice. *Clin Cancer Res*, 1999. 5(3): p. 711-720.
281. Tuxhorn, J.A., et al., Inhibition of Transforming growth factor- $\beta$  activity decreases angiogenesis in a human prostate cancer-reactive stroma xenograft model. *Cancer Res*, 2002. 62(21): p. 6021-6025.
282. Barlow, L.J. and M.M. Shen, SnapShot: Prostate cancer. *Cancer Cell*, 2013. 24(3): p. 400 e1.
283. Baca, S.C., et al., Punctuated evolution of prostate cancer genomes. *Cell*, 2013. 153(3): p. 666-677.
284. Yang, F., et al., Stromal TGF- $\beta$  signaling induces AR activation in prostate cancer. *Oncotarget*, 2014. 5(21): p. 10854-10869.
285. Amatangelo, M.D., et al., c-Myc expression and MEK1-induced Erk2 nuclear localization are required for TGF $\beta$  induced epithelial-mesenchymal transition and invasion in prostate cancer. *Carcinogenesis*, 2012. 33(10): p. 1965-1975.
286. Nishimori, H., et al., Prostate cancer cells and bone stromal cells mutually interact with each other through Bone morphogenetic protein-mediated signals. *J Biol Chem*, 2012. 287(24): p. 20037-20046.
287. Yang, S., et al., A novel Bone morphogenetic protein signaling in heterotypic cell interactions in prostate cancer. *Cancer Res*, 2008. 68(1): p. 198-205.
288. Lee, Y.-C., et al., BMP4 promotes prostate tumor growth in bone through osteogenesis. *Cancer Res*, 2011. 71(15): p. 5194-5203.
289. Morrissey, C., et al., Bone morphogenetic protein 7 is expressed in prostate cancer metastases and its effects on prostate tumor cells depend on cell phenotype and the tumor microenvironment. *Neoplasia*, 2010. 12(2): p. 192-205.
290. Lai, T.-H., et al., Osteoblasts-derived BMP-2 enhances the motility of prostate cancer cells via activation of integrins. *Prostate*, 2008. 68(12): p. 1341-1353.
291. Ye, L., H. Kynaston, and W.G. Jiang, Bone morphogenetic protein-9 induces apoptosis in prostate cancer cells, the role of prostate apoptosis response-4. *Mol Cancer Res*, 2008. 6(10): p. 1594-1606.
292. Llovet, J.M., et al., Advances in targeted therapies for hepatocellular carcinoma in the genomic era. *Nat Rev Clin Oncol*, 2015.
293. Majumdar, A., et al., Hepatic stem cells and transforming growth factor  $\beta$  in hepatocellular carcinoma. *Nat Rev Gastroenterol Hepatol*, 2012. 9(9): p. 530-538.
294. Shirai, Y., et al., Plasma transforming growth factor- $\beta$  1 in patients with hepatocellular carcinoma. Comparison with chronic liver diseases. *Cancer*, 1994. 73(9): p. 2275-9.
295. Wang, J., et al., Inhibitory role of Smad7 in hepatocarcinogenesis in mice and in vitro. *J Pathol*, 2013. 230(4): p. 441-452.
296. Wiercinska, E., et al., Id1 is a critical mediator in TGF- $\beta$ -induced transdifferentiation of rat hepatic stellate cells. *Hepatology*, 2006. 43(5): p. 1032-41.
297. Herrera, B., et al., BMP9 is a proliferative and survival factor for human hepatocellular carcinoma cells.

- PLoS One, 2013. 8(7): p. e69535.
298. Lonardo, E., et al., Nodal/Activin signaling drives self-renewal and tumorigenicity of pancreatic cancer stem cells and provides a target for combined drug therapy. *Cell Stem Cell*, 2011. 9(5): p. 433-46.
299. Ji, C., et al., Liver-specific loss of GRP78 perturbs the global unfolded protein response and exacerbates a spectrum of acute and chronic liver diseases. *Hepatology*, 2011. 54(1): p. 229-239.
300. Kuo, T.-C., et al., A unique P-glycoprotein interacting agent displays anticancer activity against hepatocellular carcinoma through inhibition of GRP78 and mTOR pathways. *Biochem Pharmacol*, 2011. 81(9): p. 1136-1144.
301. Chen, W.-T., et al., GRP78 as a regulator of liver steatosis and cancer progression mediated by loss of the tumor suppressor PTEN. *Oncogene*, 2014. 33(42): p. 4997-5005.
302. Connolly, E.C., J. Freimuth, and R.J. Akhurst, Complexities of TGF $\beta$  targeted cancer therapy. *Int J Biol Sci*, 2012. 8(7): p. 964-978.
303. Akhurst, R.J. and A. Hata, Targeting the TGF $\beta$  signaling pathway in disease. *Nat Rev Drug Discov*, 2012. 11(10): p. 790-811.
304. Derynck, R., R.J. Akhurst, and A. Balmain, TGF- $\beta$  signaling in tumor suppression and cancer progression. *Nat Genet*, 2001. 29(2): p. 117-29.
305. Bhola, N.E., et al., TGF $\beta$  inhibition enhances chemotherapy action against triple-negative breast cancer. *J Clin Invest*, 2013. 123(3): p. 1348-1358.
306. Park, J., et al., Combination delivery of TGF- $\beta$  inhibitor and IL-2 by nanoscale liposomal polymeric gels enhances tumour immunotherapy. *Nat Mater*, 2012. 11(10): p. 895-905.
307. Biswas, S., et al., Inhibition of TGF- $\beta$  with neutralizing antibodies prevents radiation-induced acceleration of metastatic cancer progression. *J Clin Invest*, 2007. 117(5): p. 1305-1313.
308. Katz, L.H., et al., Targeting TGF- $\beta$  signaling in cancer. *Expert Opin Ther Targets*, 2013. 17(7): p. 743-760.
309. Aartsma-Rus, A., et al., Targeted exon skipping as a potential gene correction therapy for Duchenne muscular dystrophy. *Neuromuscul Disord*, 2002. 12(1): p. 71-77.
310. Goemans, N.M., et al., Systemic administration of PRO051 in Duchenne's muscular dystrophy. *N Engl J Med*, 2011. 364(16): p. 1513-1522.
311. Cirak, S., et al., Exon skipping and dystrophin restoration in patients with Duchenne muscular dystrophy after systemic phosphorodiamidate morpholino oligomer treatment: an open-label, phase 2, dose-escalation study. *Lancet*, 2011. 378(9791): p. 595-605.
312. Aartsma-Rus, A., et al., Guidelines for antisense oligonucleotide design and insight into splice-modulating mechanisms. *Mol Ther*, 2008. 17(3): p. 548-553.
313. Kole, R., T. Williams, and L. Cohen, RNA modulation, repair and remodeling by splice switching oligonucleotides. *Acta Biochim Pol*, 2004. 51(2): p. 373-8.
314. Chan, J.H.P., S. Lim, and W.S.F. Wong, Antisense oligonucleotides: from design to therapeutic application. *Clin Exp Pharmacol Physiol*, 2006. 33(5-6): p. 533-540.
315. Saunier E.F., A.R.J., TGF $\beta$  inhibition for cancer therapy. *Curr Cancer Drug Targets*, 2006.
316. Bogdahn, U., et al., Targeted therapy for high-grade glioma with the TGF- $\beta$ 2 inhibitor trabedersen: results of a randomized and controlled phase IIb study. *Neuro Oncol*, 2011. 13(1): p. 132-142.
317. Nemunaitis, J., et al., Phase II trial of Belagenpumatucel-L, a TGF- $\beta$ 2 antisense gene modified allogeneic tumor vaccine in advanced non small cell lung cancer (NSCLC) patients. *Cancer Gene Ther*, 2009. 16(8): p. 620-624.
318. Nemunaitis, J., et al., Phase II study of belagenpumatucel-L, a Transforming growth factor  $\beta$ 2 antisense gene-modified allogeneic tumor cell vaccine in non-small-cell lung cancer. *J Clin Oncol*, 2006. 24(29): p. 4721-4730.
319. An, H.J., et al., Effects of Smad decoy ODN on shear stress-induced atherosclerotic ApoE $^{-/-}$  mouse. *Int J Clin Exp Pathol*, 2015. 8(4): p. 3971-8.

320. Boros, D.L., et al., A novel nonsteroidal antifibrotic oligo decoy containing the TGF- $\beta$  element found in the COL1A1 gene which regulates murine schistosomiasis liver fibrosis. *J Cell Physiol*, 2005. 204(2): p. 370-4.
321. Matsuda, H., et al., Development of gene silencing pyrrole-imidazole polyamide targeting the TGF- $\beta$ 1 promoter for treatment of progressive renal diseases. *J Am Soc Nephrol*, 2006. 17(2): p. 422-32.
322. George, J., et al., In vivo inhibition of rat stellate cell activation by soluble transforming growth factor  $\beta$  type II receptor: A potential new therapy for hepatic fibrosis. *Proc Natl Acad Sci U S A*, 1999. 96(22): p. 12719-12724.
323. Qi, Z., et al., Blockade of type  $\beta$  transforming growth factor signaling prevents liver fibrosis and dysfunction in the rat. *Proc Natl Acad Sci U S A*, 1999. 96(5): p. 2345-2349.
324. Muraoka, R.S., et al., Blockade of TGF- $\beta$  inhibits mammary tumor cell viability, migration, and metastases. *J Clin Invest*, 2002. 109(12): p. 1551-9.
325. Santiago, B., et al., Topical application of a peptide inhibitor of Transforming growth factor- $\beta$ 1 ameliorates bleomycin-induced skin fibrosis. *J Investig Dermatol*, 2005. 125(3): p. 450-455.
326. Ezquerro, I.J., et al., A synthetic peptide from transforming growth factor  $\beta$  type III receptor inhibits liver fibrogenesis in rats with carbon tetrachloride liver injury. *Cytokine*, 2003. 22(1-2): p. 12-20.
327. Hermida, N., et al., A synthetic peptide from transforming growth factor- $\beta$ 1 type III receptor prevents myocardial fibrosis in spontaneously hypertensive rats. *Cardiovasc Res*, 2009. 81(3): p. 601-9.
328. Llopiz, D., et al., Peptide inhibitors of transforming growth factor- $\beta$  enhance the efficacy of antitumor immunotherapy. *Int J Cancer*, 2009. 125(11): p. 2614-23.
329. Lu, A., et al., Blockade of TSP1-dependent TGF $\beta$  activity reduces renal injury and proteinuria in a murine model of diabetic nephropathy. *Am J Pathol*, 2011. 178(6): p. 2573-86.
330. Van Aarsen, L.A., et al., Antibody-mediated blockade of integrin  $\alpha$  v  $\beta$  6 inhibits tumor progression in vivo by a transforming growth factor- $\beta$ -regulated mechanism. *Cancer Res*, 2008. 68(2): p. 561-70.
331. Stander, M., et al., Decorin gene transfer-mediated suppression of TGF- $\beta$  synthesis abrogates experimental malignant glioma growth in vivo. *Gene Ther*, 1998. 5(9): p. 1187-94.
332. Castonguay, R., et al., Soluble endoglin specifically binds bone morphogenetic proteins 9 and 10 via its orphan domain, inhibits blood vessel formation, and suppresses tumor growth. *J Biol Chem*, 2011. 286(34): p. 30034-46.
333. Kerr, G., et al., A small molecule targeting ALK1 prevents Notch cooperativity and inhibits functional angiogenesis. *Angiogenesis*, 2015. 18(2): p. 209-17.
334. Mitchell, D., et al., ALK1-Fc inhibits multiple mediators of angiogenesis and suppresses tumor growth. *Mol Cancer Ther*, 2010. 9(2): p. 379-88.
335. Cunha, S.I., et al., Genetic and pharmacological targeting of activin receptor-like kinase 1 impairs tumor growth and angiogenesis. *J Exp Med*, 2010. 207(1): p. 85-100.
336. Bendell, J.C., et al., Safety, pharmacokinetics, pharmacodynamics, and antitumor activity of dalantercept, an activin receptor-like kinase-1 ligand trap, in patients with advanced cancer. *Clin Cancer Res*, 2014. 20(2): p. 480-9.
337. Cui, Q., et al., Selective inhibition of TGF- $\beta$  responsive genes by Smad-interacting peptide aptamers from FoxH1, Lef1 and CBP. *Oncogene*, 2005. 24(24): p. 3864-74.
338. Mead, A.L., et al., Evaluation of anti-TGF- $\beta$ 2 antibody as a new postoperative anti-scarring agent in glaucoma surgery. *Invest Ophthalmol Vis Sci*, 2003. 44(8): p. 3394-3401.
339. Trachtman, H., et al., A phase 1, single-dose study of fresolimumab, an anti-TGF- $\beta$  antibody, in treatment-resistant primary focal segmental glomerulosclerosis. *Kidney Int*, 2011. 79(11): p. 1236-1243.
340. Morris, J.C., et al., Phase I study of GC1008 (Fresolimumab): a human anti-Transforming growth factor- $\beta$  (TGF $\beta$ ) monoclonal antibody in patients with advanced malignant melanoma or renal cell

- carcinoma. PLoS One, 2014. 9(3): p. e90353.
341. Seon, B.K., et al., Long-lasting complete inhibition of human solid tumors in SCID mice by targeting endothelial cells of tumor vasculature with antihuman endoglin immunotoxin. *Clin Cancer Res*, 1997. 3(7): p. 1031-44.
342. Rosen, L.S., et al., A phase I first-in-human study of TRC105 (anti-endoglin antibody) in patients with advanced cancer. *Clin Cancer Res*, 2012. 18(17): p. 4820-9.
343. Vogt, J., R. Traynor, and G.P. Sapkota, The specificities of small molecule inhibitors of the TGF $\beta$  and BMP pathways. *Cell Signal*, 2011. 23(11): p. 1831-1842.
344. Hawinkels, L.J.A.C. and P. ten Dijke, Exploring anti-TGF- $\beta$  therapies in cancer and fibrosis. *Growth Factors*, 2011. 29(4): p. 140-152.
345. Yingling, J.M., K.L. Blanchard, and J.S. Sawyer, Development of TGF- $\beta$  signaling inhibitors for cancer therapy. *Nat Rev Drug Discov*, 2004. 3(12): p. 1011-1022.
346. Scott Sawyer, J., et al., Synthesis and activity of new aryl- and heteroaryl-substituted 5,6-dihydro-4H-pyrrolo[1,2-b]pyrazole inhibitors of the transforming growth factor- $\beta$  type I receptor kinase domain. *Bioorg Med Chem Lett*, 2004. 14(13): p. 3581-3584.
347. Flavell, R.A., et al., The polarization of immune cells in the tumour environment by TGF $\beta$ . *Nat Rev Immunol*, 2010. 10(8): p. 554-567.
348. Kano, M.R., et al., Improvement of cancer-targeting therapy, using nanocarriers for intractable solid tumors by inhibition of TGF- $\beta$  signaling. *Proc Natl Acad Sci U S A*, 2007. 104(9): p. 3460-3465.
349. Korpai, M., et al., Imaging transforming growth factor- $\beta$  signaling dynamics and therapeutic response in breast cancer bone metastasis. *Nat Med*, 2009. 15(8): p. 960-966.
350. Gueorguieva, I., et al., Defining a therapeutic window for the novel TGF- $\beta$  inhibitor LY2157299 monohydrate based on a pharmacokinetic/pharmacodynamic model. *Br J Clin Pharmacol*, 2014. 77(5): p. 796-807.
351. Noble, P.W., et al., Pirfenidone in patients with idiopathic pulmonary fibrosis (CAPACITY): two randomised trials. *Lancet*, 2011. 377(9779): p. 1760-1769.
352. Denton, C.P., et al., Recombinant human anti-transforming growth factor  $\beta$ 1 antibody therapy in systemic sclerosis: A multicenter, randomized, placebo-controlled phase I/II trial of CAT-192. *Arthritis Rheum*, 2007. 56(1): p. 323-333.







## Chapter 2

# TGF $\beta$ signaling in liver regeneration

**Sofia Karkampouna<sup>1,\*</sup>, Peter ten Dijke<sup>1</sup>,  
Steven Dooley<sup>2</sup>, Marianna Kruithof-de Julio<sup>1,\*</sup>**

<sup>1</sup>Department of Molecular and Cell Biology, Centre of Biomedical Genetics,  
Leiden University Medical Center, Leiden, The Netherlands

<sup>2</sup>Molecular Hepatology - Alcohol Associated Diseases II Medical Clinic Medical  
Faculty Mannheim, Heidelberg University, Mannheim, Germany

\* Corresponding author

***Current Pharmaceutical Design, 2012;18(27):4103-13. Review***



## **Abstract**

Adult organ regeneration occurs in many systems, such as in liver, skin, intestine and heart, indicating that postnatal life is not a static or quiescent state but a dynamic and complex process. The liver is a spectacular organ, exhibiting high regenerative capacity crucial for homeostasis and tissue repair: injuries induced mechanically or chemically, can be completely restored. Regeneration involves extensive cell division, inflammation and extracellular matrix remodeling processes. At the molecular level, one of the key mediators of regeneration response is the secreted cytokine transforming growth factor-β (TGFβ). TGFβ is a profibrogenic and anti-proliferative protein with pleiotropic functions depending on the cellular context. In this review, we discuss the role of TGFβ in the development of the liver and in adult liver regeneration, with particular emphasis on its role in regulation of hepatocyte regeneration and hepatic progenitor cell-induced regeneration. Finally, we give an overview of the current direction of liver research towards cell replacement therapies.

## **Keywords**

Liver- regeneration- TGFβ- hepatocytes- hepatic progenitor cells

## **Abbreviations**

PH	partial hepatectomy
TGFβ	transforming growth factor β
TGFβR	transforming growth factor β receptor
HSCs	hepatic stellate cells
ECs	endothelial cells
BECs	biliary epithelial cells
MFBS	myofibroblasts
HPCs	hepatic progenitor cells
BMPs	bone morphogenetic proteins
FGFs	fibroblast growth factor
SMAD	Drosophila mothers against decapentaplegic
AFP	α-fetoprotein
Hnf	hepatocyte nuclear factor
Foxa	Forkhead box A
HGF	hepatocyte growth factor
EGF	epidermal growth factor
EMT	epithelial to mesenchymal transition
miRNA	micro ribonucleic acid molecule
DDPIV	dipetidyl dipeptidase IV
EpCam	epithelial cell adhesion molecule
CTGF	connective tissue growth factor
PAI-1	plasminogen activator inhibitor-1
OV-6	oval cell protein-6
Trop-2	tumor-associated calcium signal transducer 2
HCC	hepatocellular carcinoma
CCl <sub>4</sub>	carbon tetrachloride
iPSCs	induced pluripotent stem cells
iNs	induced neuronal cells
αSMA	alpha-smooth muscle actin

### 1. Introduction

In the adult organism, the liver has a prominent role in maintaining homeostasis under both normal and pathogenic conditions. Cholesterol and glucose metabolism, lipoprotein, bile acid and serum protein synthesis and secretion are complex functions performed in the liver<sup>1,2</sup>. Dysregulation of these vital functions not only impairs the organ function itself but also affects all other organ systems; this may explain the phenomenal regenerative capacity of the liver throughout adult life. Following 60-70% partial hepatectomy (PH)<sup>3,4</sup> the remaining intact part of the liver can compensate for the tissue loss by restoring the initial size and mass, while maintaining full liver functionality. Interestingly, hepatic progenitor cells (HPCs) are not required for this regeneration process; however, if liver function is impaired HPCs take over the regeneration capability<sup>5,6</sup>. PH is a standardized strategy to study regeneration of the entire organ within a time frame of 5-7 days in rodents<sup>7</sup>, in humans it is employed to enhance organ repair<sup>8</sup>.

A unique feature of liver regeneration is that it does not depend on a single stem cell population as in other tissues such as blood, intestine, and skin<sup>9,10</sup>. All liver cell types are involved through rounds of mitosis and apoptosis: hepatocytes, stellate cells (HSCs), endothelial cells (ECs), biliary epithelial cells (BECs or cholangiocytes) and macrophages (Kupffer cells). Hepatic cells are organized in symmetric structures, liver lobules, which contain a central vein, in the centre of each lobule, and six surrounding portal triads (portal vein, hepatic artery and bile duct). From early response, through *de novo* synthesis of transcription factors to termination of proliferation and size adjustment, each step is tightly regulated. Cell-cell and cell-extracellular matrix interactions are crucial for the liver architecture. After injury, the hepatocytes, the main functional liver cell type, become apoptotic and release signals that stimulate cell proliferation of the remaining hepatocytes. Cell proliferation follows a consistent pattern, starting from the portal triads of the liver lobule and proceeding towards the central vein. Hepatocytes maintain high contact with sinusoidal cells during regeneration, a process named hepatocyte-sinusoid alignment<sup>11</sup>, ECs and BECs start proliferating, stellate cells progress from a quiescent to an activated state, differentiating to myofibroblasts (MFBs). MFBs contribute to the final stages of liver regeneration as they are responsible for extracellular matrix protein synthesis such as collagen, fibronectin, laminin, integrins<sup>12</sup> and matrix protein remodeling. Only after chronic liver damage, when the hepatocyte proliferation is exhausted, the hepatic progenitor cells, also referred as HPCs in the mouse, become activated and can differentiate into both hepatic and cholangiocytic lineages.

Despite the high regenerative capacity of adult liver, compared to other organs, liver abnormalities such as cirrhosis and liver cancer still occur with high incidence. Epidemiologic data indicate that hepatocellular carcinoma is the fifth most prevalent type of cancer and the second cause of cancer death worldwide<sup>13</sup>. The puzzle of the molecular mechanisms controlling liver regeneration has only begun to assemble and our current understanding is that several signaling pathways are involved and act dependently to each other. One of the main orchestrators of the injury-induced response in the liver is transforming growth factor  $\beta$  (TGF $\beta$ ) signaling pathway and in this review, we will discuss the recent advances regarding the function of TGF $\beta$  during regeneration and how this knowledge can be used in cell replacement therapies. Bone morphogenetic proteins (BMPs), also members of the TGF $\beta$  family, while important players in liver regeneration, will not be discussed and we refer instead to other reviews<sup>14,15</sup>. Moreover, fibrosis and hepatocellular carcinoma will not be

addressed in this review<sup>16</sup>. Finally, the role of other signaling pathways, such as Fibroblast Growth Factor (FGF) and Wingless/Integrated (Wnt) will be addressed by others in this edition.

## **2. Liver architecture and function**

### **2.1. Hepatic development**

During embryonic development, the formation of definitive endoderm at gastrulation is the first step towards hepatogenesis. Endoderm germ layer forms a primitive gut tube consisting of three subdomains, the foregut, midgut and hindgut and gives rise to liver, pancreas, lungs and thyroid tissue<sup>17</sup>. The first hepatic formation, called the hepatic diverticulum, can be distinguished, around 9 dpc, adjacent to the developing cardiac tissue. Fetal hepatic progenitor cells or hepatoblasts, that will generate the main functional liver cell types, hepatocytes and BECs, delaminate from the epithelium at 9.5 dpc and migrate to the septum transversum mesenchyme (STM) to form the liver bud. During 10-15 dpc, the liver bud undergoes growth and eventually becomes the main site for fetal hematopoiesis until bone marrow takes over just before birth<sup>18</sup>.

The embryonic liver originates from the ventral foregut<sup>19</sup>; however, liver tissue is in fact a mosaic of both endoderm and mesoderm-derived cell types. Epithelial cells (hepatocytes and BECs) derive from endoderm, while hepatic mesenchymal cells such as HSCs, Kupffer cells and blood vessels, have mesodermal origin<sup>20</sup>. Interactions among these two embryonic layers activate molecular pathways that are important for proper patterning of the liver. Initially, inhibition of mesodermal Wnt and FGF4 signaling in the foregut enables liver and pancreas induction, whereas active mesodermal Wnt signaling in the posterior gut suppresses these tissue fates<sup>21</sup>. Retinoic acid signaling, produced from paraxial mesoderm cells, assists in the anterior-posterior positioning of liver and pancreas<sup>22</sup>. In the ventral foregut, FGF signals from cardiac mesoderm and BMP signals from septum transversum mesenchymal cells induce the liver program<sup>23,24</sup>. Mesodermal-derived BMPs affect the levels of the endoderm specific gene *Gata4*, therewith blocking pancreatic and inducing liver specification, which is one of the key processes where TGF $\beta$ /BMP is required during hepatogenesis<sup>24</sup>.

### **2.2. Role of TGF $\beta$ during liver development**

TGF $\beta$  ligands (TGF $\beta$ 1, TGF $\beta$ 2 and TGF $\beta$ 3) bind and activate TGF $\beta$  type I and type II Ser/Thr kinase receptors. Upon stimulation with TGF $\beta$ , the type II receptor phosphorylates the type I receptor which phosphorylates receptor-regulated SMADs (R-SMADs). The TGF $\beta$  pathway specific R-Smads, Smad2 and Smad3 subsequently form heteromeric complexes with the common co-SMAD or Smad4. These heteromeric complexes then accumulate in the nucleus, where they participate in transcriptional regulation of gene expression<sup>25,26</sup>. Inhibitory Smad7 antagonizes the activation of R-Smads<sup>27</sup>.

TGF $\beta$  is part of a large superfamily of proteins that includes, TGF $\beta$ s, activins, nodal and BMPs. Activins and nodal, like TGF $\beta$ , signal via R-Smad2 and Smad3, whereas BMPs signal via R-Smad1, R-Smad5 and R-Smad8<sup>25</sup>.

TGF $\beta$ /Nodal signals are present in the embryo already at onset of gastrulation, inducing endoderm formation<sup>17,28</sup> and their disruption leads to abnormalities in all endoderm-derived organs. Regarding the liver, TGF $\beta$  ligands are expressed in the bud mesenchyme<sup>29</sup>. Embryos with double heterozygous mutations in Smad2 and Smad3 nuclear effectors of TGF $\beta$

downstream signaling, have impaired liver organogenesis due to defective endodermal competence<sup>30</sup>. Proper dosage of Smad2 and Smad3 in the embryo is necessary for activation of Forkhead family member Foxa2 (Hnf-3) and Homeobox class protein (Hex) expression, two genes required for hepatic development<sup>37</sup>. Foxa2 is expressed early in development and regulates activation of hepatocytic gene expression program, including that of Hex and  $\alpha$ -fetoprotein (AFP)<sup>37,32</sup>. In detail, Foxa2 binds to p53/Smad binding element sequences (SBE) of the AFP gene<sup>33,34</sup> and the related Foxa1 transcription factor also interacts with TGF $\beta$ -activated Smad2/Smad4 complexes to facilitate chromatin access and subsequent DNA binding and gene regulation<sup>35</sup>, suggesting the possibility of Smad proteins to cooperate with other transcription factors towards activation of AFP during development. AFP protein has a crucial developmental function and is expressed in fetal and neonatal mouse hepatoblasts but is silenced in adult hepatic progenitor cells or mature hepatocytes<sup>36</sup>.

However, reactivation can occur in HPCs of adult regenerating rat liver following liver damage<sup>37</sup>. Also, in human hepatocellular carcinoma, postnatal silence of AFP is activated and facilitates re-entry into the cell cycle of differentiated hepatocytes<sup>34</sup>. Interestingly, once these cells are stimulated with TGF $\beta$ 1, endogenous AFP protein expression is diminished<sup>34</sup>. TGF $\beta$  directly participates in the regulation of postnatal AFP repression and disrupting its signaling pathway leads to reactivation of AFP. Therefore, TGF $\beta$  signaling via Smad proteins is important not only for activation of developmentally important genes, such as AFP, but also for repression of these genes after birth.

From another developmental aspect, studies on liver and pancreas organogenesis showed that progenitors of each lineage emerge from neighboring parts of the ventral foregut endoderm<sup>38</sup>. TGF $\beta$ /BMP and FGF signaling act in parallel and dynamic ways to restrict specification of hepatic and pancreatic progenitors<sup>39</sup>. Moreover, the TGF $\beta$  pathway plays an important role in hepatoblast specification<sup>40,41</sup>. Differentiation of bi-potential hepatoblasts to either hepatocytes or BECs fate follows a very distinct, spatial pattern. Hepatoblasts of liver parenchyma give rise to hepatocytes, while hepatoblasts located in the mesenchyme next to the portal vein, differentiate into BECs<sup>30,40</sup>. In particular, high activin/TGF $\beta$  signaling near the portal vein is needed for differentiation of BECs. On the contrary, activin/TGF $\beta$  must be suppressed in liver parenchyma by combined action of Hnf6/OC-1 and OC-2 transcription factors in order to permit hepatocyte generation<sup>40,42</sup>. Thus, TGF $\beta$  is involved in multiple aspects of hepatogenesis, such as hepatic competence of endoderm and lineage specification of bipotential hepatoblasts and keeps hepatic gene expression tightly regulated.

### 3. Liver regeneration

Liver regeneration is a perfectly orchestrated process, able to restore liver architecture and mass within a very short period in rodents and human. Organ re-growth occurs in mammals and reptiles and usually recapitulates mechanisms of embryonic development<sup>43</sup>. Liver regeneration does not rely on an embryonic-like multipotential cell population, but mainly depends on the regenerative capacity of fully differentiated cells such as hepatocytes, HSCs and BECs. In the adult liver, mature hepatocytes are normally quiescent but they rapidly start proliferating after tissue damage. Their ability to reactivate telomerase activity prevents accumulation of mutations during cell divisions<sup>44</sup>. The combined action of all liver cell types is sufficient to reconstitute liver mass loss after liver damage induced by different causes such as viral infections, metabolic problems and 70% hepatectomy<sup>8</sup>.

Adult liver regeneration and hepatogenesis are quite distinct processes, with differential

requirements regarding molecular signals, expression status and properties of the involved cell types. Although, regeneration is considered a postnatally-restricted process, recent studies<sup>43,45-48</sup> discuss the potential capacity of embryonic liver for regeneration, in terms of cell proliferation and organ size growth as a response to injury or developmental defects. Such a paradigm was addressed in chimeric embryos generated with Hex null cells. The Hex gene is required for the formation of liver bud epithelium and thus, Hex chimeric embryos have disrupted integrity of the epithelium. Hex-null cells cannot form pseudostratified epithelium and were excluded from the epithelium by wild-type cells, which respond by increasing their proliferative rate in order to allow regrowth of the liver bud<sup>47</sup>. Therefore, hepatic endoderm cells can undergo compensatory growth to maintain the appropriate size of the developing liver bud, which indicates liver regeneration occurrence in the embryo. Another study has provided evidence of regrowth of developing liver following partial destruction of hepatic progenitor cells right after their emergence. Such elimination of progenitors was expected to lead to a smaller organ as it was observed with pancreas<sup>43</sup>. In contrast, by birth the liver had expanded up to the normal size, comparable to that of wild type animals. In addition, rat embryos that have undergone in utero partial hepatectomy have the potential to restore liver organ size within two days<sup>48</sup>. It is remarkable that not only adult liver has regenerative capacity but also embryonic liver can compensate for progenitor cell and growth factor deficiency, even at the crucial stages of embryogenesis.

### 3.1. Molecular mechanisms controlling liver regeneration- implication of TGF $\beta$ signaling

The liver regenerative response is mediated by many signals. The main growth factors involved are hepatocyte growth factor (HGF), epidermal growth factor (EGF), interleukin-6 (IL-6) and TGF $\beta$ <sup>49</sup>. TGF $\beta$  ligands play a controversial key role in adult liver regeneration. A summary of the genetic models of TGF $\beta$  family members and the liver developmental or pathologic phenotype can be found in **Table 1**. In early stages of regeneration, the hepatocytes must proliferate, therefore the inhibitory proliferation signals exerted from TGF $\beta$  are not needed, however, a few hours after liver damage, TGF $\beta$  is expressed in both liver and serum<sup>50</sup>, suggesting a central role for regeneration. TGF $\beta$  is also required at the end of this process for induction of EMT, inflammation, restoration of the original tissue architecture and cell-cell interactions<sup>51,52</sup>. The implication of TGF $\beta$  signaling in liver regeneration has been studied using different approaches, depending on the type of liver damage and cell type response (**Table 2**).

There is equilibrium among hepatic growth factors and mitoinhibition by TGF $\beta$  signaling. During regeneration initiation, cells must immediately divide in response to injury, thus, there is requirement for growth factors such as HGF and EGF. At this time point, TGF $\beta$  is upregulated, but the synchronous activation of HGF causes urokinase activation dependent removal of TGF $\beta$ . Urokinase protease degrades extracellular matrix proteins, in particular decorin, an inhibitory TGF $\beta$  binding protein<sup>53</sup>. TGF $\beta$  is, therefore, released from the liver matrix into the blood stream to allow cell proliferation and growth induction by HGF<sup>8,54</sup>, firstly removed from the portal area and progressively from the central area<sup>55</sup>, allowing hepatocyte proliferation<sup>56</sup>.

A required signal for termination of cell proliferation is the shift of expression balance from HGF towards TGF $\beta$ -like factors. The purpose is to allow transfer of TGF $\beta$  back to the liver parenchyma to block further hepatocyte proliferation and restore cell-cell interactions and



extracellular matrix integrity<sup>57</sup>. The signals regulating inhibition of HGF and influx of TGF $\beta$  from circulation into the liver parenchyma are mainly unknown, but it is likely that a direct reciprocal antagonism between HGF and TGF $\beta$  components exists. In lung fibroblasts, TGF $\beta$  directly downregulates the expression of HGF<sup>58</sup>, which could also be the case in the liver. Molecular antagonism among HGF and TGF $\beta$  signals converges at the level of common miRNAs; HGF inhibits the fibrogenic action of TGF $\beta$ -induced myofibroblast transition and epithelial to mesenchymal transition (EMT) by upregulating miRNA-29. TGF $\beta$  itself aborts HGF inhibition by directly downregulating miRNA-29<sup>59</sup>. Other miRNAs have also been identified as regulators of TGF $\beta$ 1/Smad3 activation during termination of regeneration<sup>60</sup>. The pro-fibrogenic and inflammatory action of TGF $\beta$  and its importance for regeneration termination has been extensively reviewed<sup>8</sup>. In this review we will highlight the role of TGF $\beta$  signaling in regeneration of both hepatocytes and hepatic stem/progenitor cells.

### 3.2. Regulation of hepatocyte regeneration by TGF $\beta$ signaling

TGF $\beta$ -like factors, particularly TGF $\beta$ 1, are produced at high levels in regenerating liver<sup>50</sup> by nonparenchymal cells, such as HSCs, and act in a paracrine way exerting its antiproliferative effects by inducing apoptosis of mature hepatocytes (**Fig. 1A**)<sup>61</sup> via Smad and p38/ mitogen-activated protein kinase (MAPK) dependent mechanisms<sup>62</sup>. Functional roles of Smad2 and Smad3 in normal and regenerating adult liver was addressed by hepatocyte-specific inactivation of either or both Smads, which indicated that Smad3 is required for TGF $\beta$ -induced apoptosis, whereas Smad2 is dispensable<sup>63</sup>. Administration of TGF $\beta$ 1 and TGF $\beta$ 2 *in vivo* after PH causes a reduction of the fraction of hepatocytes that progress from G1 to the DNA synthesis phase during regeneration<sup>64</sup>. This inhibitory effect is transient and reversible, causing a delay but not complete abolishment of regeneration. Enhanced proliferation of hepatocytes, observed in presence of dominant negative TGF $\beta$  receptor mutants<sup>65</sup> and hepatocyte specific conditional deletion of TGF $\beta$ RII<sup>57</sup>, supports the hypothesis that TGF $\beta$ 1 sustains quiescent hepatocytes in a differentiated state. Apoptosis induced by TGF $\beta$  is necessary as a growth stop signal for termination of regeneration process, but apoptosis must be circumvented at the early phase of regeneration, since hepatocytes must rapidly start proliferating at approximately 12-16 hours after injury<sup>66</sup>. Interestingly, during that stage, hepatocytes were described resistant to mitoinhibition of TGF $\beta$  either by downregulation of TGF $\beta$  receptors, TGF $\alpha$ , norepinephrine protective action<sup>67</sup> or upregulation of transcriptional repressors<sup>68</sup>. Apoptotic signals induced by TGF $\beta$  in hepatocytes require reactive oxygen species (ROS) production mediated by NADPH oxidase NOX4<sup>69</sup>. Anti-apoptotic signals such as phosphatidylinositol-3-phosphate kinase or the MAPK/extracellular signal-regulated kinase (ERK) pathways inhibit TGF $\beta$ -induced NOX4 expression<sup>70</sup>. Such or similar mechanisms would secure normal liver regeneration even in case of TGF $\beta$  overrepresentation<sup>71</sup>. Disruption of TGF $\beta$  signaling by conditional knockout of TGF $\beta$ RII affects hepatocyte proliferation<sup>57</sup>, but not termination of regeneration<sup>72</sup>. Downstream molecules Smad2 and Smad3 may operate even when TGF $\beta$  signaling is eliminated, due to stimulation from Activin A. Only combined inhibition of TGF $\beta$  and Activin A results in high proliferation of hepatocytes and delay of termination, implicating Activin A as a TGF $\beta$  equivalent regulator of regeneration<sup>72</sup>. Although it seems that presence of other signals (e.g. Activin A) will compensate for TGF $\beta$  ablation at the termination stage of liver regeneration, it should not be concluded that TGF $\beta$  signaling is not required.

A remarkable aspect of liver regeneration is the transdifferentiation capacity of differentiated

hepatic cells into other cell types. Transdifferentiation may occur among hepatocytes and BECs. Failure of BEC regeneration, due to bile duct damage, induces hepatocyte transdifferentiation into bipotential progenitors which give rise to BECs facilitating their regeneration<sup>73,74</sup>. Gradual loss of hepatocyte-specific and acquisition of BEC-specific transcription factors<sup>54</sup> has been proposed as a mechanism for hepatocyte-to-BEC transdifferentiation. In the opposite direction, when hepatocytes are incapable of proliferation, BECs transdifferentiate into hepatocytes via an intermediate progenitor stage, by altering their molecular signature. Therefore, mature BECs and hepatocytes, both of which are embryonically derived from multipotent hepatoblasts, represent facultative stem cells for each other after cell damage<sup>75-77</sup>. This provides a paradigm of adult, fully differentiated cells, which retain and activate stem cell properties exclusively to replenish the needs of the adult organism. Indeed, the liver has evolved a unique regenerative capacity to guard its complex and vital functions and has fully capability to regenerate within. Studies on hepatocyte transdifferentiation towards BEC lineages suggest TGF $\beta$ 1 signaling to participate in this process<sup>54</sup>. Cell tracking was performed in dipetidyl dipeptidase IV (DDPIV) chimeric rats that carry a DPPIV-positive population of hepatocytes transplanted from donor DPPIV positive rats. Hepatocytes and BECs of the recipient DPPIV negative rats do not express DPPIV. Following BEC injury by BEC-specific toxin administration and bile duct ligation, ~20% of the BEC population turned DPPIV-positive, indicating that they are derived from transdifferentiated DPPIV-positive hepatocytes<sup>54</sup>. An induction of TGF $\beta$ 1 was observed in the hepatocytes at the area surrounding the repairing biliary ductules, resembling its expression pattern during development where high TGF $\beta$ 1 signaling is also observed near the portal vein and is considered responsible for differentiation of hepatoblasts into biliary cells<sup>54</sup>. Thus, appearance of BEC clusters positive for the hepatocyte marker DPPIV provides strong evidence that BECs are derived from hepatocytes and that the apparent induction of TGF $\beta$ 1 at the damaged portal area may be crucial for switching between hepatocyte, bipotential progenitor and BEC gene expression programs. However, the transdifferentiation concept of hepatocyte-to-BEC conversion was recently disputed by Malato et al.<sup>78</sup> The authors used an *in situ* hepatocyte fate-tracing model. They assessed that all newly formed hepatocytes are derived from preexisting hepatocytes, that bile duct proliferation is necessary for the emergence of liver progenitor cell-derived hepatocytes and could not find evidence for hepatocyte-derived biliary epithelial cells or liver progenitor cells (double labeled EYFP and CK19 where not detected in this system, indicating that EYFP positive hepatocytes are not converted into BECs). TGF $\beta$ 1 signaling may promote another transdifferentiation event, the conversion of fetal hepatocytes into a putative liver progenitor population, at least *in vitro*<sup>79</sup>. Fetal hepatocytes can circumvent growth inhibition and apoptosis by TGF $\beta$ 1 if cultured in serum containing media. TGF $\beta$ -treated cells display a mesenchymal phenotype with loss of liver specific transcription factors (Hnf1 $\alpha$ , Hnf4 $\alpha$ , and Hnf6) and downregulation of gene expression signatures characteristic of differentiated hepatocytes, such as albumin and AFP. These cells are considered dedifferentiated cells, with induction of stem cell marker expression<sup>79</sup>, according to the authors representing a population of liver progenitors derived from hepatocytes under stimulation with TGF $\beta$ 1. They further propose that such progenitors, *in vitro* retain differentiation potential back to hepatocytic cell fate, and could be used as a tool for isolation of such cells, although the molecular mechanisms behind this process remain unclear. Similar spontaneous hepatocyte mesenchymal transdifferentiation events that were enhanced with TGF $\beta$  have been reported for mouse hepatocytes that were cultured as monolayer. In an EMT-like process, hepatocyte features like albumin and transferrin

expression were lost with culture duration, whereas vimentin and collagen expression were established<sup>80-84</sup>. In this setting, TGF $\beta$  drives a so called late signature, including direct Smad target genes, like connective tissue growth factor (CTGF), plasminogen activator inhibitor -1 (PAI-1), Snail<sup>80,85</sup>, which has been associated with poor prognosis for HCC patients<sup>86</sup>. If, however, such scenario as described for cultured hepatocytes similarly occurs *in vivo* remains to be proven.

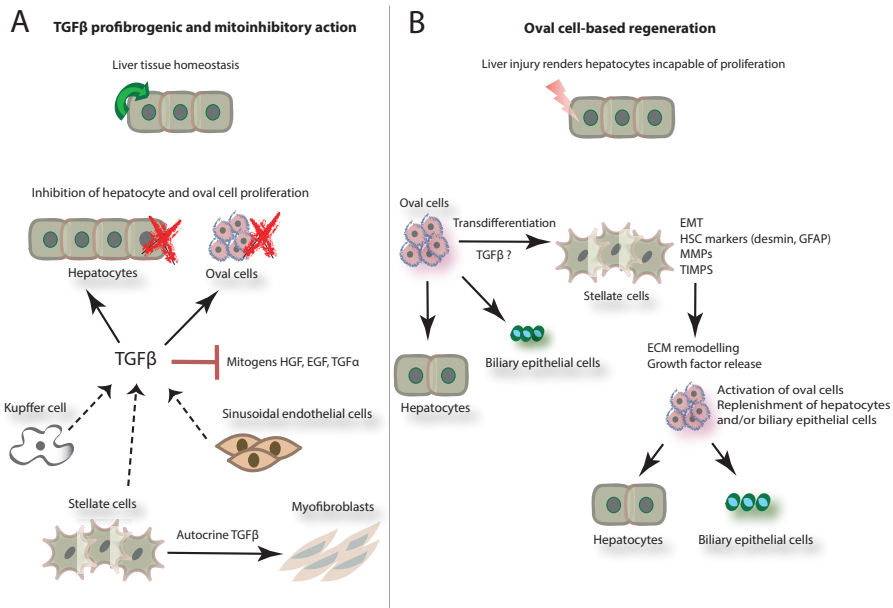


**Fig.1. TGF $\beta$  profibrogenic and mitoinhibitory action in (A) quiescent state and (B) after liver injury induction** (A). Stellate cells (HSCs) produce TGF $\beta$  ligands, which in an autocrine manner promote transdifferentiation of HSCs into MFBs and in paracrine way acts upon hepatocytes and biliary cells (not indicated here). Other cell types also produce and secrete TGF $\beta$ , such as Kupffer cells and sinusoidal ECs. The anti-proliferative role of TGF $\beta$  on hepatocytes and HPCs is mediated by antagonism with HGF, EGF, TGF $\alpha$  mitogens. (B). HPC/oval cell-based regeneration for replenishment of non-replicative hepatocytes after extensive liver injury. TGF $\beta$  signals keep HPCs in quiescent state; however, there is evidence that TGF $\beta$  assists regeneration by promoting transdifferentiation of a subset of HPCs into HSCs. The production and remodeling of ECM by HSCs causes release of growth factors, which activate remnant HPCs to proliferate and differentiate into hepatocytic and BEC lineages.

### 3.3. Regulation of oval cell response by TGF $\beta$ signaling

Hepatocyte proliferation is the first key regenerative response; however, after extended and chronic liver damage replicative senescence leads to problematic cell regeneration<sup>87</sup>. Hepatocytes incapable of proliferating, such as in prolonged hepatitis infections, cirrhosis, non-alcoholic and alcoholic fatty liver diseases<sup>16</sup>, are replenished by hepatic progenitor cells (HPCs), which are not present in normal adult liver nor required for normal cell turnover<sup>78</sup>. HPCs or oval cells are believed to be bipotent epithelial cells that give rise to hepatocytes and BECs similarly to hepatoblasts. Such cells have been identified in the adult mouse and rat liver and there is debate concerning their identity, whether they comprise hepatic stem cells or transit amplifying cells<sup>78,88</sup>.

Following liver injury, HPCs emerge around the portal vein and the canals of Hering, they express both hepatic (albumin, transferrin) and BEC specific markers (CK19 and EpCam) and also unique markers such as OV-6 and Trop2<sup>89</sup>. A population of Sox9-positive liver progenitors has been identified around the bile duct area during the regenerative process and is able to differentiate into hepatocytes in response to different types of hepatic injuries<sup>77</sup>, however it is not clear whether these Sox9-expressing progenitors comprise HPCs or precursors of HPCs. Further, cells expressing Oct3/4 stem cell markers have also been identified exclusively in the periportal tract during liver regeneration<sup>90</sup>.

Spatial specification of adult stem or progenitor cells in the periportal area of the liver lobules and the canals of Hering suggest the existence of a stem cell niche or morphogenic signals that allow stem cell activation<sup>91,92</sup>. In regenerating liver, upon hepatic damage due to acetaminophen (APAP) administration, label retaining assays show the *in vivo* existence of four epithelial stem cell niches, that is the proximal biliary tree, intralobular bile ducts, periductal mononuclear cells and peribiliary hepatocytes<sup>91</sup>. It is conceivable to hypothesize that the liver regenerative capability is mediated by host stem/progenitor, located in intra-hepatic niches that respond to microenvironment signals and contribute to the efficiency and flexibility of liver regeneration. Regarding TGF $\beta$ 1 and its potential regulation of HPCs activation, it is essential to have insight on whether the spatial expression pattern of TGF $\beta$  and its downstream effectors coincide around the stem cell niches.

Indeed, TGF $\beta$ 1 is expressed in rat HSCs surrounding HPCs, which migrate from the site of emergence, the periportal area, towards the pericentral part while differentiating into ductile or hepatic cells<sup>93</sup>. To study the effect of TGF $\beta$ 1 on HPCs, Park et al., used a model of PH combined with hepatocyte ablation by administration of acetylaminofluorene (2-AAF-PH). A scenario was suggested as following; hepatocyte damage promotes HPC generation and HSC activation. HSCs secrete TGF $\beta$ 1 which acts in a paracrine way to induce apoptosis of HPCs thus inhibiting their activation<sup>93</sup>.

The stem cell compartment of human liver, as identified by expression of stem cell markers Oct4 and Stat3, also expresses the TGF $\beta$  members TGF $\beta$ RII and ELF<sup>94</sup>. Heterozygous Smad3-adaptor protein  $\beta$ 2-spectrin ( $\beta$ 2SP)/ELF deficient mice have an expanded population of Oct3/4 positive progenitor cells residing in the periportal region, which highlights the inhibitory role of TGF $\beta$  on proliferation of progenitor cells<sup>90</sup>. Surprisingly, given the negative effect of TGF $\beta$  on HPC activation, disruption of TGF $\beta$  signaling, particularly of  $\beta$ 2SP, does not enhance regeneration but instead causes a significant delay in regenerating human liver and in mice after PH<sup>95</sup>. Another aspect that highlights the role of TGF $\beta$  in liver regeneration is the increasing spatial expression of TGF $\beta$ RI<sup>55</sup> and  $\beta$ 2SP from periportal to central areas, which is in line with the wave of proliferating cells. Undoubtedly, TGF $\beta$  is important for tuning liver regeneration but there is a dichotomy of the TGF $\beta$  effects on differentiation, emergence of stem/progenitor cells, apoptosis, cell proliferation, which is depending on the cell type and stage of damage or disease. For instance, TGF $\beta$  ligands affect the regeneration process by stimulating apoptosis of both hepatocytes and HPCs<sup>76</sup> although both cell types may exhibit a differential response and sensitivity to TGF $\beta$ 1, which is dependent on the cell physiological stage. Thus, in hepatocellular carcinoma, HPCs emerge and are highly proliferative in presence of the "growth inhibitor" TGF $\beta$ 1. Interestingly, HPCs respond to TGF $\beta$ 1, as seen by nuclear localization of phosphorylated Smad2, however they are insensitive to its mitoinhibitory actions (Ki67 staining), as compared to hepatocytes<sup>96</sup>. The difference in sensitivity between hepatocytes and hepatic progenitor cells in such settings has been attributed to the absence of inhibitory Smad6 in hepatocytes<sup>96</sup>. Thus, inhibition of hepatocyte

proliferation and the regenerative response mediated by TGF $\beta$  is circumvented by hepatic progenitor cell activation, thus providing a rescue mechanism to safeguard liver repair. This further indicates, that apoptosis and growth control exerted by TGF $\beta$ 1 signaling on hepatic progenitor cells is only one aspect, since TGF $\beta$ 1 may promote transdifferentiation or differentiation of hepatic progenitor cells into other lineages, e.g. towards the HSC lineage<sup>97</sup>. In presence of TGF $\beta$ 1, hepatic progenitor cells not only upregulate ECM genes, such as collagen, matrix metalloproteases (MMPs) or tissue inhibitor of metalloprotease (TIMPs), but also induce expression of HSC markers such as desmin and glial fibrillary acidin protein (GFAP). Such conversion of epithelial hepatic progenitor cells to mesenchymal HSCs results from an EMT process that is at least partially orchestrated by TGF $\beta$  signaling<sup>97</sup>. Activation of HSCs is highly correlated with the hepatic progenitor cell response during injury, e.g. upon induction in the 2-AAF/PH model, when hepatocyte function is compromised. HSC activation requires TGF $\beta$  and the generated myofibroblasts can be detected around the portal vein area and in the proximity of hepatic progenitor cells. Stellate cells excrete MMPs and TIMPs, which by ECM remodeling cause release of bound growth factors that act on HPCs and, e.g., enhance their proliferation<sup>98</sup>. Selective inhibition of HSC activation causes diminished HPC activation (OV-6 and AFP positive) in the periportal area and thus, severely interferes with the regenerative response<sup>99</sup>. Hepatic rat stem cell lines when exposed to TGF $\beta$  increase the expression of differentiation markers such as albumin and tyrosine aminotransferase<sup>100</sup>, suggesting TGF $\beta$  as a signal required for differentiation of hepatocytes from HPCs.

In summary, TGF $\beta$  has a direct negative effect on proliferation of hepatocytes and HPCs (**Fig.1B**). During regeneration, these cells lose sensitivity to the TGF $\beta$  cytostatic program and continue to divide in presence of TGF $\beta$ . The action of TGF $\beta$  in liver regeneration should not be reduced to its proapoptotic and growth inhibitory signal, as it is usually done. The contribution of TGF $\beta$  signaling in regeneration could be exerted by activating HSCs, which in turn promote HPC activation, directing them towards hepatocyte differentiation. Thus, TGF $\beta$  has pleiotropic functions depending on the cell type and the physiological situation of the organ. Therefore, the molecular mechanism of TGF $\beta$  action should be studied in detail in such context. Further knowledge on the supporting role of TGF $\beta$  during regeneration and dissecting its interplay with other signaling pathways such as HGF and EGF can provide insight on improved possibilities for manipulation of cell regeneration processes for therapeutic applications.

## 4. Hepatocyte reprogramming and liver regeneration- New prospective

With liver transplantation being the only therapy and the reduced availability of liver donors, research has shifted focus on cell replacement therapies<sup>101</sup>. Regarding the liver, this is particularly promising because of the powerful regenerative characteristics of differentiated liver cells such as hepatocytes. In this respect, we do not need to rely on a limited number of stem or progenitor cells but can use a source of hepatocytes, the main functional cell types, as a therapy. A barrier to this approach, however, is the incapability of hepatocytes to be maintained or expanded *in vitro*.

Several studies have managed to generate hepatic-like cells by different approaches, from embryonic stem cells, induced pluripotent stem cells or even from pluripotent germ cells<sup>102-106</sup>. Homogeneous populations of functional hepatic-like cells have been derived from human ES cells via a process mimicking endoderm development and hepatic specification<sup>107</sup>. Fetal liver stem/progenitor cells when transplanted into adult rat liver, display efficient differentiation into mature hepatocytes and high repopulating capabilities<sup>108</sup>. Cell lineage reprogramming of somatic cells into induced pluripotent stem cells (iPS cells) by modulation of transcription factor dosage is a promising therapeutic approach for liver diseases. Recently, direct reprogramming of mouse fibroblasts to hepatocytes (iHeps) by overexpression of two transcription factors in different combinations, Hnf4a together with Foxa1, Foxa2 or Foxa3<sup>109</sup> or by transduction of Hnf1a, Gata4, Foxa3 and inactivation of p19Arf has been achieved<sup>110</sup>. Personalized medicine with a patient-specific hepatocyte source would limit the risk of organ rejection and eliminate the need of an external source of hepatocytes. However, *in vivo* functionality and stability of the properties of these cells have to be further validated before any clinical translation. Another recent study to address the importance of generating “self” hepatocytes for transplantation purpose has been carried out by Liu et al.<sup>111</sup>. The authors derived iPS cells from different cell types, which retained similar epigenetic signatures. As proof of principal for retention of hepatic functionality of these differentiated cells, the authors intravenously infused mice after liver damage. Remarkably, the cells integrate in the regenerating liver with an efficiency of 8 to 15%, which is comparable to that of hepatocytes (11%)<sup>37</sup>. These encouraging observations point in the direction of “self”-derived hepatic like cells as clinically applicable in liver regeneration.

Finally, hepatic generation by non-hepatic cell types has also been accomplished from human mesenchymal cells<sup>112</sup> or by cell fusion with bone marrow derived cells<sup>113</sup>.

An exceptional paradigm of the plasticity of hepatocytes is their potential to transdifferentiate into neurons (iN) after ectopic expression of neuronal transcription factors (Ascl1, Brn2, Myt1l)<sup>114</sup>. Interestingly, genes inducing iPS phenotype such as REST, Oct3/ 4, cMyc and Nanog are expressed in cultured primary hepatocytes and control cell proliferation and apoptosis *in vitro*, but may also control liver regeneration *in vivo*<sup>115</sup>. Another therapeutic option—relative to cell transplantation—would be to stimulate hepatic progenitor cells as a resident source, thus, avoiding the drawbacks of limited graft survival, restricted homing to the site of injury and host immune rejection. So, the hepatic progenitor cell population supported from the environment could possibly be induced to proliferate and transdifferentiate into major hepatocyte/ BDC by exogenous stimulation of stemness factor expression, to provide a resident cell based therapy, as previously successfully described for cardiomyocytes in adult heart injury<sup>116</sup>.

The remarkable cell plasticity and regenerative ability of hepatocytes shows that they are an excellent tool for cell based therapies for liver diseases (**Fig.2**), however, efforts should also focus on the therapeutic use of hepatic progenitor cells as they have even higher proliferative potential than hepatocytes and are less susceptible to inhibition by TGF $\beta$  signals. Further knowledge of the intrinsic signals controlling liver regeneration is needed, to provide a way to manipulate these signals and stimulate *in vivo* regeneration.

**Plasticity of hepatocytes & Implications for liver engineering**

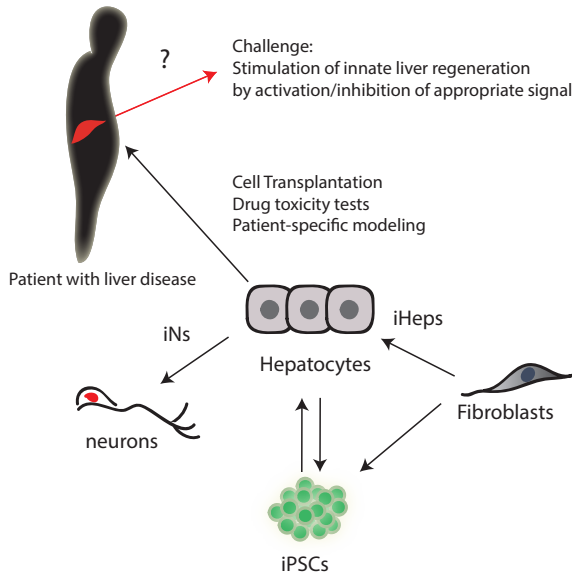


**Fig.2. Model of therapeutic approaches for liver diseases**

Scheme of recent advances and possibilities in the field of induced hepatocytes (iHeps) and pluripotent stem cells (iPSCs). Hepatocytes are highly regenerative and plastic cells, which can be derived from iPSCs and ES cells, and in turn can give rise to iPSCs and directly transdifferentiate into neuronal-like cells (iNs). Human induced hepatocytes could be utilized for patient-specific disease modelling, drug toxicity trials and cell transplantation. Such studies would contribute to our understanding of the molecular mechanisms that control normal and aberrant liver regeneration. Activation or inhibition of the key signals can be manipulated in a therapeutic way in order to stimulate regeneration *in vivo*. Such approach could be applied to the treatment of several liver diseases, such as fibrosis, cirrhosis, hepatocellular carcinoma, as well as for regeneration of other tissues.

TGFβ component	Transgenic model	Phenotype	Organism/ Stage	Reference
TGFβ1	<i>Alb;Tgfβ1</i> (hepatocyte-specific overexpression)	Liver fibrosis, decreased hepatocyte mitogenic response after PHx	Mouse, adult	71,117
TGFβ2, β3	<i>Tgfβ2<sup>-/-</sup>;Tgfβ3<sup>-/-</sup></i> <i>Tgfβ2<sup>-/-</sup>;Tgfβ3<sup>+/-</sup></i>	Early embryonic lethality, liver malformations	Mouse, embryonic	118
TGFβR-II	<i>Alb-Cre;TgfβrII<sup>fl/fl</sup></i> (TgfβrII-KO)	Increased hepatocyte proliferation in regenerating liver and increased liver mass: body weight ratio	Mouse, adult	57
TGFβR-III	<i>TGFβR-III<sup>-/-</sup></i>	Early embryonic lethality, liver defects	Mouse, embryonic	119
Activin βC, βE	<i>Actβc<sup>-/-</sup>; ActβE<sup>-/-</sup></i>	No obvious defect in liver development, normal regeneration	Mouse, embryonic and adult	120
Elf/ β2-spectrin	<i>elf<sup>-/-</sup></i>	Midgestational death due to hypoplastic liver	Mouse, embryonic	121
	<i>elf<sup>-/-</sup></i>	Spontaneous development of HCC	Mouse, adult	122
	<i>elf<sup>-/-</sup></i>	Delayed hepatocyte proliferation followed by activation of progenitors cells	Mouse, adult	95
Smad2	<i>Smad2<sup>-/-</sup></i>	Lethal, gastrulation defects	Mouse, embryonic	123
	<i>Alb-Cre;Smad2<sup>fl/fl</sup></i> (Smad2-KO)	Increased hepatocyte proliferation after CCl <sub>4</sub> injection and EMT transition	Mouse, adult	63
Smad3	<i>Smad3<sup>-/-</sup></i>	Viable, postnatal immunity defects at first few months	Mouse, embryonic and adult	124,125
	<i>Smad<sup>lox8/lox8</sup></i> (Smad3 KO)	Blockage of TGFβ-induced EMT and apoptosis	Mouse, adult	63
Smad2, Smad3	<i>Smad2<sup>-/-</sup>;Smad3<sup>-/-</sup></i>	Lethal, lack of mesoderm, gastrulation defects	Mouse, embryo	126
	<i>Alb-Cre;Smad2<sup>fl/fl</sup> Smad<sup>lox8/lox8</sup></i> (Smad2, 3 double KO)	High susceptibility to toxic liver injury	Mouse, adult	63
	<i>Smad2<sup>+/-</sup>;Smad3<sup>+/-</sup></i>	Defects in definitive endoderm and liver development	Mouse, embryonic	30,31
Smad4	<i>Alb-Cr;Smad4<sup>fl/fl</sup></i>	Iron overload in liver and other organs and premature death	Mouse, adult	127,128
Smad7	<i>Smad7<sup>-/-</sup></i>	Promotes TGFβ fibrogenic action via CTGF upregulation	Mouse, adult	85

**Table 1. Representative list of available animal models of TGFβ signaling components selected with regards to defective liver developmental, functional or regenerative phenotype**

Alb; albumin, cre: cre recombinase, KO; knock out, EMT; epithelial-to-mesenchymal transition, CTGF; connective tissue growth factor, f/f; homozygous floxed (loxP containing) gene locus, CCl<sub>4</sub>; carbon tetrachloride, +/-; heterozygous mutant, -/-; homozygous mutant.



Regeneration model	Species	TGFβ component	Functional implication	Reference
Transplantation	Human	β2-spectrin	HPC/Oval cell response	90
Partial hepatectomy (PH)	Mouse	TGFβR-II	Hepatocyte proliferation	57
	Mouse	TGFβ1, LAP	Neutralisation of TGFβ1 mitoinhibitory activity upon hepatocytes	117
	Mouse	SnoN, Ski inhibitors	Activation status of Smad complexes, hepatocyte resistance to TGFβ mitoinhibition	68
	Rat	TGFβ1	Inhibition of TGFβ1 by neutralizing antibody, hepatocyte mitosis, liver regeneration	129
	Rat	TGFβ1, TGFβ2	Inhibition of early proliferation response	64
Carbon tetrachloride (CCl <sub>4</sub> )	Mouse	Endoglin	Activation of HSCs, fibrogenesis	130
	Mouse	SnoN, Ski inhibitors	Activation status of Smad complexes, hepatocyte resistance to TGFβ mitoinhibition	68
	Mouse	TGFβ1	Activation and transdifferentiation of HSCs, collagen and αSMA expression in HSCs	131,132
	Mouse	Smad3	Smad3 induces collagen expression but is dispensable for HSC activation	132
Bile ligation	Mouse	Endoglin	Activation of HSCs, fibrogenesis	130
Choline-deficient, ethionine-supplemented diet (CDE)	Mouse	Smad2	Proliferation and sensitivity of HPCs to TGFβ1	96
Partial liver irradiation	Rat	TGFβ1	Stimulation of intrinsic regeneration by irradiation and TGFβ1 expression pattern	133
Dimethylnitrosamine (DMN)	Rat	TGFβR	Anti-TGFβR molecular intervention and regulation of transcription factors important regeneration	65

**Table 2. Liver regeneration models reported to have elucidated functions on TGFβ family members**

Different liver injury/ regeneration models are indicated, which have provided insight into the functional implementation of TGFβ ligands, receptors, R-Smads in the liver or in combination with therapeutic interventions such as neutralizing antibodies or small molecule inhibitors against TGFβ molecules.

## Acknowledgements

The authors would like to thank Marie-Jose Goumans for critically reviewing the manuscript and to apologize to all whose work could not be cited due to space limitations. Our research on TGFβ signaling in liver regeneration is supported by Netherlands Institute for Regenerative Medicine (NIRM) and Centre of Biomedical Genetics.

**References**

1. Chiang, J.Y.L., Bile acids and nuclear receptors. *Am J Physiol Gastrointest Liver Physiol*, 2003. 284(3): p. G349-G356.
2. Wagner, M., G. Zollner, and M. Trauner, Nuclear receptors in liver disease. *Hepatology*, 2011. 53(3): p. 1023-1034.
3. Taub, R., Liver regeneration: from myth to mechanism. *Nat Rev Mol Cell Biol*, 2004. 5(10): p. 836-847.
4. Michalopoulos, G.K., Liver regeneration: Alternative epithelial pathways. *Int J Biochem Cell Biol*, 2011. 43(2): p. 173-179.
5. Fausto, N., Liver regeneration and repair: hepatocytes, progenitor cells, and stem cells. *Hepatology*, 2004. 39(6): p. 1477-1487.
6. Duncan, A.W., C. Dorrell, and M. Grompe, Stem cells and liver regeneration. *Gastroenterology*, 2009. 137(2): p. 466-481.
7. Fausto, N., J.S. Campbell, and K.J. Riehle, Liver regeneration. *Hepatology*, 2006. 43(S1): p. S45-S53.
8. Michalopoulos, G.K., Liver regeneration. *J Cell Physiol*, 2007. 213(2): p. 286-300.
9. Staal, F.J.T., et al., Stem cell self-renewal: lessons from bone marrow, gut and iPS toward clinical applications. *Leukemia*, 2011. 25(7): p. 1095-1102.
10. Barker, N., S. Bartfeld, and H. Clevers, Tissue-resident adult stem cell populations of rapidly self-renewing organs. *Cell Stem Cell*, 2010. 7(6): p. 656-670.
11. Hoehme, S., et al., Prediction and validation of cell alignment along microvessels as order principle to restore tissue architecture in liver regeneration. *Proc Natl Acad Sci USA*, 2010. 107(23): p. 10371-10376.
12. Ozaki, I., et al., Regulation of TGF- $\beta$ 1-induced proapoptotic signaling by growth factor receptors and extracellular matrix receptor integrins in the liver. *Front Physiol*, 2011. 2.
13. Jemal, A., et al., Global cancer statistics. *CA Cancer J Clin*, 2011. 61(2): p. 69-90.
14. Nakatsuka, R., et al., Transient expression of Bone morphogenetic protein-2 in acute liver injury by carbon tetrachloride. *J Biochem*, 2007. 141(1): p. 113-119.
15. Sugimoto, H., et al., BMP-7 functions as a novel hormone to facilitate liver regeneration. *FASEB J*, 2007. 21(1): p. 256-264.
16. Dooley, S. and P. ten Dijke, TGF- $\beta$  in progression of liver disease. *Cell Tissue Res*, 2012. 347(1): p. 245-256.
17. Zorn, A.M. and J.M. Wells, Molecular basis of vertebrate endoderm development. *Int Rev Cytol*, 2007. 259: p. 49-111.
18. Dzierzak, E. and N.A. Speck, Of lineage and legacy: the development of mammalian hematopoietic stem cells. *Nat Immunol*, 2008. 9(2): p. 129-136.
19. Tremblay, K.D. and K.S. Zaret, Distinct populations of endoderm cells converge to generate the embryonic liver bud and ventral foregut tissues. *Dev Biol*, 2005. 280(1): p. 87-99.
20. Zaret, K.S., Genetic programming of liver and pancreas progenitors: lessons for stem-cell differentiation. *Nat Rev Genet*, 2008. 9(5): p. 329-340.
21. McLin, V.A., S.A. Rankin, and A.M. Zorn, Repression of Wnt/ $\beta$ -catenin signaling in the anterior endoderm is essential for liver and pancreas development. *Development*, 2007. 134(12): p. 2207-2217.
22. Zaret, K.S. and M. Grompe, Generation and regeneration of cells of the liver and pancreas. *Science*, 2008. 322(5907): p. 1490-1494.
23. Calmont, A., et al., An FGF response pathway that mediates hepatic gene induction in embryonic endoderm cells. *Dev Cell*, 2006. 11(3): p. 339-348.
24. Rossi, J.M., et al., Distinct mesodermal signals, including BMPs from the septum transversum

- mesenchyme, are required in combination for hepatogenesis from the endoderm. *Genes Dev*, 2001. 15(15): p. 1998-2009.
25. Shi, Y. and J. Massagué, Mechanisms of TGF- $\beta$  signaling from cell membrane to the nucleus. *Cell*, 2003. 113(6): p. 685-700.
26. ten Dijke, P., K. Miyazono, and C.H. Heldin, Signaling inputs converge on nuclear effectors in TGF- $\beta$  signaling. *Trends Biochem Sci*, 2000. 25(2): p. 64-70.
27. Itoh, S. and P. ten Dijke, Negative regulation of TGF- $\beta$  receptor/Smad signal transduction. *Curr Opin Cell Biol*, 2007. 19(2): p. 176-184.
28. Zhou, X., et al., Nodal is a novel TGF- $\beta$ -like gene expressed in the mouse node during gastrulation. *Nature*, 1993. 361(6412): p. 543-547.
29. Pelton, R.W., et al., Immunohistochemical localization of TGF $\beta$  1, TGF $\beta$  2, and TGF $\beta$  3 in the mouse embryo: expression patterns suggest multiple roles during embryonic development. *J Cell Biol*, 1991. 115(4): p. 1091-1105.
30. Weinstein, M., et al., Smad proteins and hepatocyte growth factor control parallel regulatory pathways that converge on  $\beta$ 1-integrin to promote normal liver development. *Mol Cell Biol*, 2001. 21(15): p. 5122-5131.
31. Liu, Y., et al., Smad2 and Smad3 coordinately regulate craniofacial and endodermal development. *Dev Biol*, 2004. 270(2): p. 411-426.
32. Mohn, D., et al., Mouse Mix gene is activated early during differentiation of ES and F9 stem cells and induces endoderm in frog embryos. *Dev Dyn*, 2003. 226(3): p. 446-459.
33. Lee, K.C., A.J. Crowe, and M.C. Barton, p53-mediated repression of alpha-fetoprotein gene expression by specific DNA binding. *Mol Cell Biol*, 1999. 19(2): p. 1279-1288.
34. Wilkinson, D.S., et al., A direct intersection between p53 and Transforming growth factor  $\beta$  pathways targets chromatin modification and transcription repression of the  $\alpha$ -fetoprotein gene. *Mol Cell Biol*, 2005. 25(3): p. 1200-1212.
35. Taube, J.H., et al., Foxa1 functions as a pioneer transcription factor at transposable elements to activate Afp during differentiation of embryonic stem cells. *J Biol Chem*, 2010. 285(21): p. 16135-16144.
36. Schmelzer, E., E. Wauthier, and L.M. Reid, The phenotypes of pluripotent human hepatic progenitors. *Stem Cells*, 2006. 24(8): p. 1852-1858.
37. Jelnes, P., et al., Remarkable heterogeneity displayed by oval cells in rat and mouse models of stem cell-mediated liver regeneration. *Hepatology*, 2007. 45(6): p. 1462-1470.
38. Deutsch, G., et al., A bipotential precursor population for pancreas and liver within the embryonic endoderm. *Development*, 2001. 128(6): p. 871-881.
39. Wandzioch, E. and K.S. Zaret, Dynamic signaling network for the specification of embryonic pancreas and liver progenitors. *Science*, 2009. 324(5935): p. 1707-1710.
40. Clotman, F., et al., Control of liver cell fate decision by a gradient of TGF $\beta$  signaling modulated by Onecut transcription factors. *Genes Dev*, 2005. 19(16): p. 1849-1854.
41. Clotman, F. and F.P. Lemaigre, Control of hepatic differentiation by Activin/TGF $\beta$  signaling. *Cell Cycle*, 2006. 5(2): p. 168-171.
42. Plumb-Rudewicz, N., et al., Transcription factor HNF-6/OC-1 inhibits the stimulation of the HNF-3 $\alpha$ /Foxa1 gene by TGF- $\beta$  in mouse liver. *Hepatology*, 2004. 40(6): p. 1266-1274.
43. Stanger, B.Z., A.J. Tanaka, and D.A. Melton, Organ size is limited by the number of embryonic progenitor cells in the pancreas but not the liver. *Nature*, 2007. 445(7130): p. 886-891.
44. Sirma, H., et al., The promoter of human telomerase reverse transcriptase is activated during liver regeneration and hepatocyte proliferation. *Gastroenterology*, 2011. 141(1): p. 326-337.e3.
45. Michalopoulos, G.K. and M.C. DeFrances, Liver regeneration. *Science*, 1997. 276(5309): p. 60-66.
46. Bort, R., et al., Hex homeobox gene-dependent tissue positioning is required for organogenesis of the

- ventral pancreas. *Development*, 2004. 131(4): p. 797-806.
47. Bort, R., et al., Hex homeobox gene controls the transition of the endoderm to a pseudostratified, cell emergent epithelium for liver bud development. *Dev Biol*, 2006. 290(1): p. 44-56.
  48. Elchaninov, A. and G. Bolshakova, Reparative regeneration of rat fetal liver after partial hepatectomy. *Bull Exp Biol Med*, 2011. 150(3): p. 383-386.
  49. Böhm, F., et al., Regulation of liver regeneration by growth factors and cytokines. *EMBO Mol Med*, 2010. 2(8): p. 294-305.
  50. Braun, L., et al., Transforming growth factor  $\beta$  mRNA increases during liver regeneration: a possible paracrine mechanism of growth regulation. *Proc Natl Acad Sci USA*, 1988. 85(5): p. 1539-1543.
  51. Margadant, C. and A. Sonnenberg, Integrin-TGF- $\beta$  crosstalk in fibrosis, cancer and wound healing. *EMBO Rep*, 2010. 11(2): p. 97-105.
  52. Streuli, C.H., et al., Extracellular matrix regulates expression of the TGF- $\beta$  1 gene. *J Cell Biol*, 1993. 120(1): p. 253-260.
  53. Mars, W.M., et al., Immediate early detection of urokinase receptor after partial hepatectomy and its implications for initiation of liver regeneration. *Hepatology*, 1995. 21(6): p. 1695-1701.
  54. Limaye, P., et al., Expression of hepatocytic- and biliary-specific transcription factors in regenerating bile ducts during hepatocyte-to-biliary epithelial cell transdifferentiation. *Comp Hepatol*, 2010. 9(1): p. 9.
  55. Jirtle, R.L., B.I. Carr, and C.D. Scott, Modulation of insulin-like growth factor-II/mannose 6-phosphate receptors and transforming growth factor- $\beta$  1 during liver regeneration. *J Biol Chem*, 1991. 266(33): p. 22444-50.
  56. Sakamoto, T., et al., Mitosis and apoptosis in the liver of interleukin-6-deficient mice after partial hepatectomy. *Hepatology*, 1999. 29(2): p. 403-411.
  57. Romero-Gallo, J., et al., Inactivation of TGF- $\beta$  signaling in hepatocytes results in an increased proliferative response after partial hepatectomy. *Oncogene*, 2005. 24(18): p. 3028-3041.
  58. Harrison, P., L. Bradley, and A. Bomford, Mechanism of regulation of HGF/SF gene expression in fibroblasts by TGF- $\beta$ 1. *Biochem Biophys Res Commun*, 2000. 271(1): p. 203-211.
  59. Kwiecinski, M., et al., Hepatocyte growth factor (HGF) inhibits collagen I and IV synthesis in hepatic stellate cells by miRNA-29 induction. *PLoS One*, 2011. 6(9): p. e24568.
  60. Yuan, B., et al., Down-regulation of miR-23b may contribute to activation of the TGF- $\beta$ 1/Smad3 signaling pathway during the termination stage of liver regeneration. *FEBS Lett*, 2011. 585(6): p. 927-934.
  61. Oberhammer, F.A., et al., Induction of apoptosis in cultured hepatocytes and in regressing liver by transforming growth factor  $\beta$  1. *Proc Natl Acad Sci USA*, 1992. 89(12): p. 5408-5412.
  62. Yoo, J., et al., Transforming growth factor- $\beta$ -induced apoptosis is mediated by Smad-dependent expression of GADD45b through p38 activation. *J Biol Chem*, 2003. 278(44): p. 43001-43007.
  63. Ju, W., et al., Deletion of Smad2 in mouse liver reveals novel functions in hepatocyte growth and differentiation. *Mol Cell Biol*, 2006. 26(2): p. 654-667.
  64. Russell, W.E., et al., Type  $\beta$  transforming growth factor reversibly inhibits the early proliferative response to partial hepatectomy in the rat. *Proc Natl Acad Sci USA*, 1988. 85(14): p. 5126-5130.
  65. Nakamura, T., et al., Suppression of transforming growth factor- $\beta$  results in upregulation of transcription of regeneration factors after chronic liver injury. *J Hepatol*. 2004. 41(6): p. 974-982.
  66. Weglarz, T.C. and E.P. Sandgren, Timing of hepatocyte entry into DNA synthesis after partial hepatectomy is cell autonomous. *Proc Natl Acad Sci USA*, 2000. 97(23): p. 12595-12600.
  67. Houck, K.A. and G.K. Michalopoulos, Altered responses of regenerating hepatocytes to norepinephrine and transforming growth factor type  $\beta$ . *J Cell Physiol*, 1989. 141(3): p. 503-509.
  68. Maci as-Silva, M., et al., Up-regulated transcriptional repressors SnoN and Ski bind Smad proteins

- to antagonize Transforming growth factor- $\beta$  signals during liver regeneration. *J Biol Chem*, 2002. 277(32): p. 28483-28490.
69. Carmona-Cuenca, I., et al., Upregulation of the NADPH oxidase NOX4 by TGF- $\beta$  in hepatocytes is required for its pro-apoptotic activity. *J Hepatol*, 2008. 49(6): p. 965-976.
70. Caja, L., et al., Overactivation of the MEK/ERK pathway in liver tumor cells confers resistance to TGF- $\beta$ -induced cell death through impairing up-regulation of the NADPH oxidase NOX4. *Cancer Res*, 2009. 69(19): p. 7595-7602.
71. Sanderson, N., et al., Hepatic expression of mature transforming growth factor  $\beta$  1 in transgenic mice results in multiple tissue lesions. *Proc Natl Acad Sci USA*, 1995. 92(7): p. 2572-2576.
72. Oe, S., et al., Intact signaling by transforming growth factor  $\beta$  is not required for termination of liver regeneration in mice. *Hepatology*, 2004. 40(5): p. 1098-1105.
73. Fukuda, K., et al., The origin of biliary ductular cells that appear in the spleen after transplantation of hepatocytes. *Cell Transplant*, 2004. 13(1): p. 27-33.
74. Michalopoulos, G.K., L. Barua, and W.C. Bowen, Transdifferentiation of rat hepatocytes into biliary cells after bile duct ligation and toxic biliary injury. *Hepatology*, 2005. 41(3): p. 535-544.
75. Crosby, H.A., et al., Immunolocalization of OV-6, a putative progenitor cell marker in human fetal and diseased pediatric liver. *Hepatology*, 1998. 28(4): p. 980-985.
76. Isfort, R.J., et al., The combination of epidermal growth factor and transforming growth factor- $\beta$  induces novel phenotypic changes in mouse liver stem cell lines. *J Cell Sci*, 1997. 110(24): p. 3117-3129.
77. Furuyama, K., et al., Continuous cell supply from a Sox9-expressing progenitor zone in adult liver, exocrine pancreas and intestine. *Nat Genet*, 2011. 43(1): p. 34-41.
78. Malato, Y., et al., Fate tracing of mature hepatocytes in mouse liver homeostasis and regeneration. *J Clin Invest*, 2011. 121(12): p. 4850-4860.
79. del Castillo, G., et al., Isolation and characterization of a putative liver progenitor population after treatment of fetal rat hepatocytes with TGF- $\beta$ . *J Cell Physiol*, 2008. 215(3): p. 846-855.
80. Dooley, S., et al., Hepatocyte-specific Smad7 expression attenuates TGF- $\beta$ -mediated fibrogenesis and protects against liver damage. *Gastroenterology*, 2008. 135(2): p. 642-659.e46.
81. Zeisberg, M., et al., Fibroblasts derive from hepatocytes in liver fibrosis via epithelial to mesenchymal transition. *J Biol Chem*, 2007. 282(32): p. 23337-23347.
82. Kaimori, A., et al., Transforming growth factor- $\beta$ 1 induces an epithelial-to-mesenchymal transition state in mouse hepatocytes in vitro. *J Biol Chem*, 2007. 282(30): p. 22089-22101.
83. Godoy, P., et al., Extracellular matrix modulates sensitivity of hepatocytes to fibroblastoid dedifferentiation and transforming growth factor  $\beta$ -induced apoptosis. *Hepatology*, 2009. 49(6): p. 2031-2043.
84. Zellmer, S., et al., Transcription factors ETF, E2F, and SP-1 are involved in cytokine-independent proliferation of murine hepatocytes. *Hepatology*, 2010. 52(6): p. 2127-2136.
85. Weng, H.L., et al., Profibrogenic transforming growth factor- $\beta$ /activin receptor-like kinase 5 signaling via connective tissue growth factor expression in hepatocytes. *Hepatology*, 2007. 46(4): p. 1257-1270.
86. Coulouarn, C., V.M. Factor, and S.S. Thorgeirsson, Transforming growth factor- $\beta$  gene expression signature in mouse hepatocytes predicts clinical outcome in human cancer. *Hepatology*, 2008. 47(6): p. 2059-2067.
87. Liu, L., et al., The microenvironment in hepatocyte regeneration and function in rats with advanced cirrhosis. *Hepatology*, 2011.
88. Fausto, N. and J.S. Campbell, The role of hepatocytes and oval cells in liver regeneration and repopulation. *Mech Dev*, 2003. 120(1): p. 117-130.
89. Okabe, M., et al., Potential hepatic stem cells reside in EpCAM+ cells of normal and injured mouse

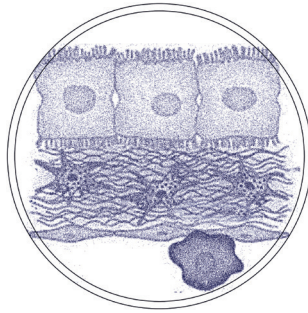
- liver. *Development*, 2009. 136(11): p. 1951-1960.
90. Thenappan, A., et al., Role of transforming growth factor  $\beta$  signaling and expansion of progenitor cells in regenerating liver. *Hepatology*, 2010. 51(4): p. 1373-1382.
  91. Kuwahara, R., et al., The hepatic stem cell niche: identification by label-retaining cell assay. *Hepatology*, 2008. 47(6): p. 1994-2002.
  92. Cardinale, V., et al., Multipotent stem/progenitor cells in human biliary tree give rise to hepatocytes, cholangiocytes, and pancreatic islets. *Hepatology*, 2011. 54(6): p. 2159-2172.
  93. Park, D.Y. and K.S. Suh, Transforming growth factor- $\beta$ 1 protein, proliferation and apoptosis of oval cells in acetylaminofluorene-induced rat liver regeneration. *J Korean Med Sci*, 1999. 14(5): p. 531-538.
  94. Kitisin, K., et al., Disruption of transforming growth factor- $\beta$  signaling through  $\beta$ -spectrin ELF leads to hepatocellular cancer through cyclin D1 activation. *Oncogene*, 2007. 26(50): p. 7103-7110.
  95. Thenappan, A., et al., Loss of transforming growth factor  $\beta$  adaptor protein  $\beta$ -2 spectrin leads to delayed liver regeneration in mice. *Hepatology*, 2011. 53(5): p. 1641-1650.
  96. Nguyen, L.N., et al., Transforming growth factor- $\beta$  differentially regulates oval cell and hepatocyte proliferation. *Hepatology*, 2007. 45(1): p. 31-41.
  97. Wang, P., et al., Expression of extracellular matrix genes in cultured hepatic oval cells: an origin of hepatic stellate cells through transforming growth factor  $\beta$ ? *Liver Int*, 2009. 29(4): p. 575-584.
  98. Lowes, K.N., et al., Oval cell-mediated liver regeneration: Role of cytokines and growth factors. *J Gastroenterol Hepatol.*, 2003. 18(1): p. 4-12.
  99. Pintilie, D.G., et al., Hepatic stellate cells involvement in progenitor-mediated liver regeneration. *Lab Invest*, 2010. 90(8): p. 1199-1208.
  100. Hirata, M., et al., Establishment and characterization of hepatic stem-like cell lines from normal adult rat liver. *J Biochem.*, 2009. 145(1): p. 51-58.
  101. Riehle, K.J., et al., New concepts in liver regeneration. *J Gastroenterol Hepatol.*, 2011. 26: p. 203-212.
  102. Shiraki, N., et al., Efficient differentiation of embryonic stem cells into hepatic cells in vitro using a feeder-free basement membrane substratum. *PLoS One*, 2011. 6(8): p. e24228.
  103. Kawabata, K., M. Inamura, and H. Mizuguchi, Efficient hepatic differentiation from human iPS cells by gene transfer liver stem cells. *Methods Mol Biol*, 2012. p. 115-124.
  104. Song, Z., et al., Efficient generation of hepatocyte-like cells from human induced pluripotent stem cells. *Cell Res*, 2009. 19(11): p. 1233-1242.
  105. Gai, H., et al., Generation of murine hepatic lineage cells from induced pluripotent stem cells. *Differentiation*, 2010. 79(3): p. 171-181.
  106. Fagoonee, S., Generation of functional hepatocytes from mouse germ line cell-derived pluripotent stem cells in vitro. *Stem Cells Dev*, 2010. 19(8): p. 1183-1194.
  107. Touboul, T., et al., Generation of functional hepatocytes from human embryonic stem cells under chemically defined conditions that recapitulate liver development. *Hepatology*, 2010. 51(5): p. 1754-1765.
  108. Oertel, M., et al., Cell competition leads to a high level of normal liver reconstitution by transplanted fetal liver stem/progenitor cells. *Gastroenterology*, 2006. 130(2): p. 507-520.
  109. Sekiya, S. and A. Suzuki, Direct conversion of mouse fibroblasts to hepatocyte-like cells by defined factors. *Nature*, 2011. 475(7356): p. 390-393.
  110. Huang, P., et al., Induction of functional hepatocyte-like cells from mouse fibroblasts by defined factors. *Nature*, 2011. 475(7356): p. 386-389.
  111. Liu, H., et al., Generation of endoderm-derived human induced pluripotent stem cells from primary hepatocytes. *Hepatology*, 2010. 51(5): p. 1810-1819.
  112. Lee, K.-D., et al., In vitro hepatic differentiation of human mesenchymal stem cells. *Hepatology*, 2004. 40(6): p. 1275-1284.

113. Vassilopoulos, G., P.R. Wang, and D.W. Russell, Transplanted bone marrow regenerates liver by cell fusion. *Nature*, 2003. 422(6934): p. 901-904.
114. Marro, S., et al., Direct lineage conversion of terminally differentiated hepatocytes to functional neurons. *Cell Stem Cell*, 2011. 9(4): p. 374-382.
115. Bhave, V.S., et al., Genes inducing iPS phenotype play a role in hepatocyte survival and proliferation in vitro and liver regeneration in vivo. *Hepatology*, 2011. 54(4): p. 1360-1370.
116. Smart, N., et al., De novo cardiomyocytes from within the activated adult heart after injury. *Nature*, 2011. 474(7353): p. 640-644.
117. Böttinger, E.P., et al., The recombinant proregion of transforming growth factor  $\beta$ 1 (latency-associated peptide) inhibits active transforming growth factor  $\beta$ 1 in transgenic mice. *Proc Natl Acad Sci USA*, 1996. 93(12): p. 5877-5882.
118. Dünker, N. and K. Kriegelstein, *Tgf $\beta$ 2*-/*Tgf $\beta$ 3*-/- double knockout mice display severe midline fusion defects and early embryonic lethality. *Anat Embryol (Berl)*, 2002. 206(1): p. 73-83.
119. Stenvers, K.L., et al., Heart and liver defects and reduced Transforming growth factor  $\beta$ 2 sensitivity in Transforming growth factor  $\beta$  type III receptor-deficient embryos. *Mol Cell Biol*, 2003. 23(12): p. 4371-4385.
120. Lau, A.L., et al., Activin  $\beta$ C and  $\beta$ E genes are not essential for mouse liver growth, differentiation and regeneration. *Mol Cell Biol*, 2000. 20(16): p. 6127-6137.
121. Tang, Y., et al., Disruption of transforming growth factor- $\beta$  signaling in ELF  $\beta$ -spectrin-deficient mice. *Science*, 2003. 299(5606): p. 574-7.
122. Tang, Y., et al., Progenitor/stem cells give rise to liver cancer due to aberrant TGF- $\beta$  and IL-6 signaling. *Proc Natl Acad Sci USA*, 2008. 105(7): p. 2445-2450.
123. Nomura, M. and E. Li, Smad2 role in mesoderm formation, left-right patterning and craniofacial development. *Nature*, 1998. 393(6687): p. 786-790.
124. Datto, M.B., et al., Targeted disruption of Smad3 reveals an essential role in Transforming growth factor  $\beta$ -mediated signal transduction. *Mol Cell Biol*, 1999. 19(4): p. 2495-2504.
125. Yang, X., et al., Targeted disruption of SMAD3 results in impaired mucosal immunity and diminished T cell responsiveness to TGF- $\beta$ . *EMBO J*, 1999. 18(5): p. 1280-1291.
126. Dunn, N.R., et al., Combinatorial activities of Smad2 and Smad3 regulate mesoderm formation and patterning in the mouse embryo. *Development*, 2004. 131(8): p. 1717-1728.
127. Wang, R.H., et al., A role of SMAD4 in iron metabolism through the positive regulation of hepcidin expression. *Cell Metab*, 2005. 2(6): p. 399-409.
128. Yang, X., et al., Generation of Smad4/Dpc4 conditional knockout mice. *Genesis*, 2002. 32(2): p. 80-81.
129. Deneme, M.A., et al., Single dose of anti-Transforming growth factor- $\beta$ 1 monoclonal antibody enhances liver regeneration after partial hepatectomy in biliary-obstructed rats. *J Surg Res*, 2006. 136(2): p. 280-287.
130. Meurer, S.K., et al., Expression and functional analysis of endoglin in isolated liver cells and its involvement in fibrogenic Smad signaling. *Cell Signal*, 2011. 23(4): p. 683-699.
131. Hellerbrand, C., et al., The role of TGF $\beta$ 1 in initiating hepatic stellate cell activation in vivo. *J Hepatol*, 1999. 30(1): p. 77-87.
132. Kulkarni, A.B., et al., Transforming growth factor  $\beta$  1 null mutation in mice causes excessive inflammatory response and early death. *Proc Natl Acad Sci USA*, 1993. 90(2): p. 770-774.
133. Zhao, J.D., et al., Hepatocyte regeneration after partial liver irradiation in rats. *Exp Toxicol Pathol*, 2009. 61(5): p. 511-518.









## Chapter 3

# Inhibition of TGF $\beta$ type I receptor activity facilitates liver regeneration upon acute CCl<sub>4</sub> – intoxication in mice

**Sofia Karkampouna<sup>1</sup>, Marie-José Goumans<sup>1</sup>, Peter ten Dijke<sup>1</sup>, Steven Dooley<sup>2</sup> and Marianna Kruithof-de Julio<sup>1,3,\*</sup>**

<sup>1</sup>Department of Molecular and Cell Biology, Centre of Biomedical Genetics, Leiden University Medical Center, Leiden, The Netherlands

<sup>2</sup>Molecular Hepatology - Alcohol Associated Diseases II Medical Clinic Medical Faculty Mannheim, Heidelberg University, Mannheim, Germany

<sup>3</sup>Department of Dermatology, Leiden University Medical Center, Leiden, The Netherlands

\* Corresponding author

***Archives of Toxicology, 2015 Jan 8. PMID: 25566828***



### Abstract

Liver exhibits a remarkable maintenance of functional homeostasis in presence of a variety of damaging toxic factors. Tissue regeneration involves cell replenishment and extracellular matrix remodeling. Key regulator of homeostasis is the transforming growth factor-β (TGFβ) cytokine. To understand the role of TGFβ during liver regeneration, we used the single-dose carbon tetrachloride (CCl<sub>4</sub>) treatment in mice as a model of acute liver damage. We combined this with *in vivo* inhibition of the TGFβ pathway by a small molecule inhibitor; LY364947, which targets the TGFβ type I receptor kinase (ALK5) in hepatocytes but not in activated stellate cells. Co-administration of LY364947 inhibitor and CCl<sub>4</sub> toxic agent resulted in enhanced liver regeneration; cell proliferation (measured by PCNA, phosphorylated histone 3, p21) levels were increased in CCl<sub>4</sub>+LY364947 versus CCl<sub>4</sub>-treated mice. Recovery of CCl<sub>4</sub>-metabolizing enzyme CYP2E1 expression in hepatocytes is enhanced seven days after CCl<sub>4</sub> intoxication in the mice that received also the TGFβ inhibitor. In summary, a small molecule inhibitor that blocks ALK5 downstream signaling and halts the cytostatic role of TGFβ pathway results in increased cell regeneration and improved liver function during acute liver damage. Thus, *in vivo* ALK5 modulation offers insight into the role of TGFβ, not only in matrix remodeling and fibrosis, but also in cell regeneration.

### Keywords

Acute-Hepatotoxicity- CCl<sub>4</sub>- Regeneration- ALK5- LY364947- TGFβ- Smad

### Introduction

Liver tissue has high regenerative capacity in response to damaging stimuli such as virus infections, chemicals, and alcohol intoxication<sup>1,2</sup>. Liver regeneration involves replenishment of dead epithelial and mesenchymal cells by proliferation and restoration of normal tissue architecture by fibrous scar formation<sup>3</sup>. Chronic organ damage leads to exhaustion of the cell pool and fibrosis, excess accumulation of extracellular matrix proteins (ECM) and eventually to clinical complications such as acute liver failure<sup>4</sup>. Thus, there is a need for better understanding of the mechanisms regulating innate tissue regeneration.

Application of the hepatotoxin carbon tetrachloride (CCl<sub>4</sub>) is an established experimental animal model for liver regeneration since single administration of CCl<sub>4</sub> *in vivo* leads to acute and reversible liver damage<sup>5</sup>. Liver regeneration occurs within 7-8 days without affecting any other organ system. Only a specific subset of hepatocytes, located around the central veins, appears to be damaged due to unique expression of CCl<sub>4</sub>-metabolising enzyme Cytochrome 450 (Cyp2E1)<sup>3,6</sup>. In turn, cytokines and stress signals derived from hepatocytes induce the activation of hepatic stellate cells (HSCs) into myofibroblasts (MFBs). The αSMA expressing MFBs<sup>7</sup> appear in clusters around the central vein and assist tissue repair by scar ECM formation. Simultaneously, quiescent HSCs located in the space of Disse become activated by cytokines released from damaged hepatocytes, and concentrate in the central vein area, e.g. due to migration and/or proliferation.

Transforming growth factor-β (TGFβ) signaling plays an important role in maintenance of liver homeostasis, terminal differentiation and apoptosis of hepatocytes<sup>8</sup>. Under liver damage conditions, TGFβ1 is up regulated and regulates parenchymal, inflammatory cells and HSCs<sup>6,9,10</sup>. Although many cells in the liver may produce TGFβ1, Kupffer cells and recruited

macrophages are the major source of TGF $\beta$ . TGF $\beta$ 1 is critical for activation of HSCs into MFBs, stimulates ECM production and inhibits ECM degradation<sup>17</sup>. Activated HSCs, and to lesser extent, sinusoidal endothelial cells (ECs), also contribute to increased TGF $\beta$  production<sup>4</sup>. However, TGF $\beta$  in the liver has additional actions, such as immunomodulatory properties and its cytostatic effects on epithelial cells (hepatocytes)<sup>12</sup>. The regenerative capacity of the liver is characterised by hepatocyte proliferation but also by increased TGF- $\beta$ 1 expression<sup>13</sup>. The level of DNA synthesis is maximal during the first 48 hours after CCl<sub>4</sub> intoxication, coinciding with the TGF $\beta$  increase in the liver<sup>6,14</sup>. Thus, hepatocytes proliferate despite the presence of an antiproliferative stimulus; however, the exact mechanism of this process is unclear. Administration of TGF $\beta$  *in vivo* after partial hepatectomy reduces the number of hepatocytes that progress from G1 to the DNA synthesis phase<sup>15</sup>. It has been proposed that during early response after liver injury, hepatocytes become transiently resistant to TGF $\beta$  either by down regulation of TGF $\beta$  receptors<sup>14</sup> and TGF $\alpha$  protective action<sup>15</sup> or by up regulation of transcriptional repressors<sup>16</sup>. Levels of T $\beta$ RI and T $\beta$ RII mRNA expression in rat hepatocytes decreased from 12 to 48 hours and returned to normal by 72 hours after CCl<sub>4</sub> administration, while T $\beta$ RI and T $\beta$ RII mRNA were expressed constantly in non-parenchymal cells<sup>14</sup>. Thus, the function of TGF $\beta$  is cell-type specific and its role on liver regeneration remains largely unknown.

TGF $\beta$  is synthesized and stored in the ECM as a latent complex with its prodomain, LAP (latency-associated peptide). Latent TGF $\beta$  is considered to be a molecular sensor that responds to specific signals by releasing active TGF $\beta$ <sup>17</sup>. These signals are often perturbations of the ECM that are associated with angiogenesis, wound repair, inflammation and, perhaps, cell growth<sup>18</sup>. Changes in the cell's environment are relayed to the sensor by a number of different molecules, including proteases, integrins and thrombospondin<sup>19</sup>. TGF $\beta$  functions by binding to cell surface receptors. Binding of free TGF $\beta$  ligands to its type II receptor causes the activation of the type I receptor, ALK5 and the assembly of a protein complex which further phosphorylates and activates the R-Smads, Smad2 and Smad3. Subsequent signal transduction occurs when the active Smad2 and Smad3 transcription factors form complexes with Smad4, and translocate from the cytoplasm to the nucleus<sup>20</sup> to induce TGF $\beta$  target gene expression.

Several studies have investigated the therapeutic potential of inhibition of TGF $\beta$  in lung, kidney and liver diseases and a number of compounds have reached the phase of clinical trials<sup>21</sup>. Smad3-deficient mice develop reduced dermal<sup>22</sup>, renal<sup>23</sup> and liver fibrosis<sup>24</sup>. However, the complexity of the TGF $\beta$  pathway, its involvement in a plethora of cellular processes and cell type specific effects impede the design of therapies in the context of liver diseases. For instance, loss of TGF $\beta$  signaling in fibroblasts causes intraepithelial neoplasia, suggesting that TGF $\beta$  controls the activity of fibroblasts as well as the oncogenic potential of neighbouring epithelial cells<sup>25</sup>. Experimental regeneration models such as partial hepatectomy indicate a role for TGF $\beta$  only at late stage of wound healing, mainly for restoration of ECM and new vessel formation<sup>7</sup>. The pleiotropic effects of TGF $\beta$  upon different cell types (hepatocytes and HSCs) and the time of action during liver damaging conditions remain yet unclear.

To study the mechanisms behind liver regeneration in regards to TGF $\beta$  signaling, in a time-dependent manner, we have selected the CCl<sub>4</sub>-induced acute liver damage model. A single dose of CCl<sub>4</sub> leads to reversible centrilobular necrosis and steatosis<sup>26</sup>, while prolonged administration leads to liver fibrosis, cirrhosis, and hepatocellular carcinoma. CCl<sub>4</sub> impairs hepatocytes directly by altering the permeability of plasma, lysosomal, and mitochondrial membranes<sup>27</sup>. We investigated the effects of *in vivo* inhibition of the TGF $\beta$  receptor by the

small molecule inhibitor LY364947 (LY) during CCl<sub>4</sub>-induced acute liver injury in order to delineate its function on hepatocytes and HSCs. LY is an ATP-competitive, cell permeable inhibitor, selective for TGFβ type I Activin receptor-like kinases (ALK4, 5 and 7)<sup>28</sup>. In this study we show that, regarding *in vivo* TGFβ inhibition, the LY compound seems to be effective in epithelial cells, particularly centrizonal hepatocytes, and enhances their proliferation and regeneration in CCl<sub>4</sub>- acute injury model.

## **Materials and Methods**

### **Acute liver damage model and administration of small molecule inhibitors**

Animal protocols were in full compliance with the guidelines for animal care and were approved by the Leiden University Medical Center Animal Care Committee. Acute liver injury was induced in 5-6 weeks old male C57Bl6 mice weighing 20 - 25 g by intraperitoneally injecting a single dose of 1 ml/kg body weight CCl<sub>4</sub> (mixed 1:1 with mineral oil), and mice were sacrificed after days 1, 2, 3, and 7 (n=2 per time point). LY364947 (5 mg/kg, Axon Medchem) was intraperitoneally injected 1 hour prior to CCl<sub>4</sub> shot on day 0. Every 24 hours since the first injection, the compound was administered (day 0- day 3). From day 3 to day 7 mice did not receive any compounds and were sacrificed after days 1, 2, 3, and 7 (n=3 mice per group and per time point). Control group received DMSO (1mg/kg mixed with PBS), LY364947 (5 mg/kg) received 4 injections every 24 hours. During day 3 to day 7, mice did not receive LY364947 and were sacrificed after days 1, 2, 3, and 7 (n=2 mice per group and per time point). From the liver tissues collected, one lobule was used for histology preparation, one lobule for RNA isolation and one lobule for protein isolation per individual mouse.

More information on Supplementary Materials and Methods.

## **Results**

### **Phenotypic changes in acute CCl<sub>4</sub>-induced liver damage model**

Induction of liver damage was performed by single injection of hepatotoxic agent CCl<sub>4</sub> in 5-6 week old male C57Bl6 mice. At several time points after vehicle control or CCl<sub>4</sub> injection (day 1, day 2, day 3, day 7) mice were sacrificed and liver tissue was collected. Upon liver damage, hepatocytes located around the central vein area metabolize CCl<sub>4</sub> and undergo functional and phenotypic changes, such as loss of hepatocyte marker HNF4α (**Fig.1A**). Dormant HSCs are distinguished by desmin expression and lack of αSMA staining, the latter being up regulated only upon activation of HSCs (**Fig.1A**). Highest expression of αSMA is reached during day 3 (**Fig.1A**) after single CCl<sub>4</sub> injection. Increased collagen staining in the CCl<sub>4</sub>-injected livers (**Fig.1A**) represents the cell population of activated HSCs, which produce ECM proteins such as collagen type I and fibronectin. During mouse liver homeostasis, TGFβ is active, as nuclear phosphorylated Smad2 (pSmad2) protein is seen in hepatocytes of normal liver (**Fig.1B**) at various time points after injection with vehicle compound (day1, day2, day3, day7). Upon tissue damage active TGFβ ligands are released leading to activation of profibrotic gene expression and wound healing response in the activated HSCs. We have observed that pSmad2 nuclear localization follows a specific spatiotemporal pattern in the hepatocytes during the early time points after acute injury. Immunostainings for HNF4α,

pSmad2 and  $\alpha$ SMA (**Fig.1A-B**) indicate that damaged hepatocytes adjacent to the central vein area transiently down regulate expression of HNF4 $\alpha$  (**Fig.1A**) and pSmad2 (**Fig.1B**), almost immediately upon tissue damage. In turn,  $\alpha$ SMA+ HSCs accumulate in the central vein between day 2- day 3 and activate pSmad2 (**Fig.1B**). This effect is transient, since pSmad2 expression is restored in the regenerated hepatocytes after seven days (**Fig.1B**). The distribution of HSCs at seven days after CCl<sub>4</sub> shot is similar to the control liver tissue (**Fig.1B**).

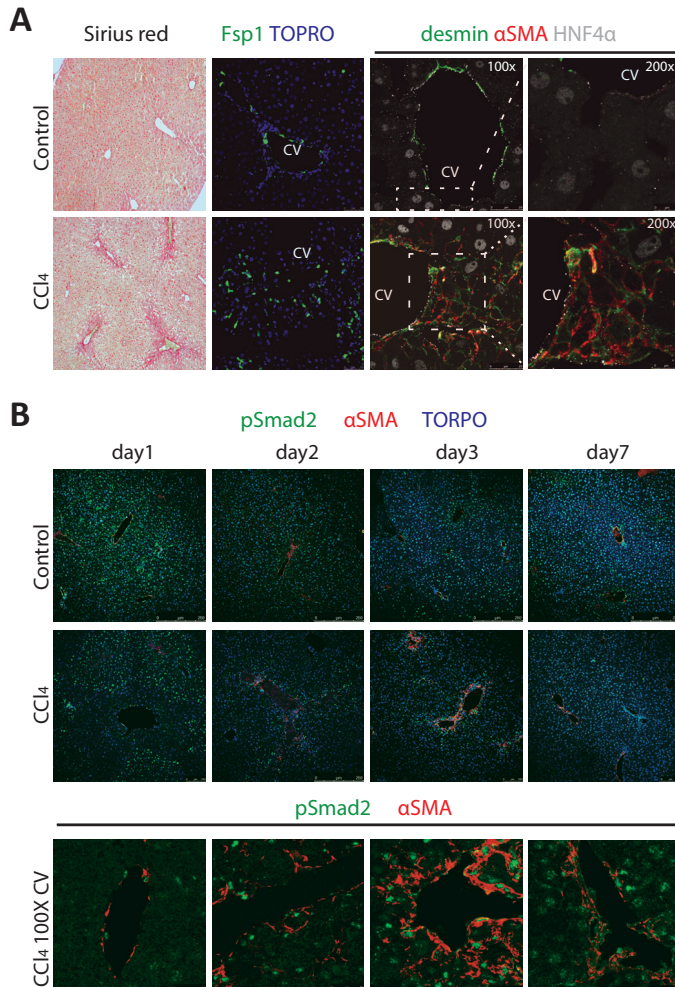


**Fig.1. Acute CCl<sub>4</sub>-induced liver damage model**

(A). From left to right: Picosirius red staining for visualization of collagen fibers in liver tissues of control and CCl<sub>4</sub>-treated mice (magnification: 10x). Immunofluorescence staining indicates protein expression of Kupffer cell marker; Fsp1 (magnification: 40x, scale bars=50 $\mu$ m). HSC markers; desmin (green) and  $\alpha$ SMA (red), hepatocyte-specific marker HNF4 $\alpha$  (grey) in control and CCl<sub>4</sub>-injected liver tissues (magnification: 100x, scale bars=250  $\mu$ m). The marked area is shown at higher magnification (200x), scale bars= 10  $\mu$ m. Nuclei (blue) were visualized by TOPRO-3 nuclear dye. Damaged central vein area is distinguished by expression of  $\alpha$ SMA-positive HSCs (red) and loss of hepatocyte marker HNF4 $\alpha$  (grey). Time point: day 3 (72 hours after CCl<sub>4</sub>). (B). Time course of pSmad2 (green) and  $\alpha$ SMA (red) co-localisation by immunofluorescence during acute liver damage. Representative images of liver tissues from vehicle and CCl<sub>4</sub>- injected mice are shown (magnification: 20x. Scale bars=100, 250  $\mu$ m). Bottom panel: image of higher magnification of the central vein (CV) (CCl<sub>4</sub>, 100x CV). Scale bars= 25  $\mu$ m. Time course (1, 2, 3, 7 days).

**Effects of ALK5 inhibitor (LY) on TGFβ signaling and hepatic apoptosis *in vivo***

In order to interfere *in vivo* with TGFβ signaling activation we have used the small molecule inhibitor (LY364947), which selectively blocks kinase activity of ALK5. The LY compound was injected one hour prior to CCl<sub>4</sub> administration, in order to inhibit the TGFβ pathway shortly before the induction of cellular damage (**Fig.2A**). Administration of the compound was performed every 24 hours for 4 days (day 0- day 3) in mice that also received a single shot of CCl<sub>4</sub> or vehicle control at day 0 (**Fig.2A**). Mice injected with vehicle substance or LY compound have normal liver morphology (**Fig.S1**). Early response (24 hours) to tissue damage involves transient loss of nuclear phosphorylated Smads (pSmad2) specifically in damaged hepatocytes of the central vein area (**Fig.2B**). To further test this observation, pSmad2 protein levels were measured in whole liver homogenates in control (vehicle), CCl<sub>4</sub> and CCl<sub>4</sub>+LY-treated mice (**Fig.S2**). In addition, reduced pSmad2 immunofluorescence staining is observed in livers that were treated only with LY (**Fig.S1**), suggesting that the LY inhibitor can attenuate the activation of ALK5/Smad2 pathway in hepatocytes. Time course of pSmad2 immunofluorescence in the damaged (CCl<sub>4</sub>) liver tissues, indicates further inhibition of pSmad2 signal after treatment with the inhibitor (**Fig.2B**). However, co-labeling of αSMA and pSmad2 (**Fig.2B; Fig.S3**) shows that HSCs still have active pSmad2 and may not be efficiently targeted by LY inhibitor when administered systemically. Hepatic mRNA expression of p21, enriched in hepatocyte population and TGFβ target gene, is down regulated after LY administration (**Fig.2C**); however expression of Collagen type I (Col1A1), that is enriched in the HSC population, is not effectively inhibited but even induced by the LY (**Fig.2D**). In addition, inhibitory role of LY on mRNA expression of Plasminogen activator type 1 (Pai-1) in whole liver extracts, is observed only at 48 hours after CCl<sub>4</sub> intoxication (**Fig.2E**). Since, hepatotoxicity mediated by CCl<sub>4</sub> causes centrilobular cell death in hepatocytes and TGFβ *per se* has a proapoptotic role on hepatocytes; we determined the occurrence of apoptosis. Two methods were used; terminal deoxynucleotidyl transferase dUTP nick end labeling (TUNEL) and activation of cleaved caspase 3, which occurs in apoptotic cells either by exogenous (death ligand) or endogenous (mitochondrial) pathways<sup>29</sup>. TUNEL positivity indicates cell death; however, it cannot distinguish necrosis from apoptosis events. TUNEL activity was observed earlier (24 hrs after CCl<sub>4</sub>) (**Fig.3**) than cleaved caspase 3 positivity (peak at 48 hours after CCl<sub>4</sub>, **Fig.S4**). TUNEL positive cells were quantified in all the mice of each group throughout the time course (day 1- day 3) of regeneration (**Fig.3B**). Only at the earliest time point (1 day after CCl<sub>4</sub>/ CCl<sub>4</sub>+LY), there is significant TUNEL activity (**Fig.3A**), compared to the positive control. CCl<sub>4</sub>+LY group has decreased number of dead cells compared to CCl<sub>4</sub> group at day 1 (**Fig.3B**). Activation of pro apoptotic protein caspase 3 in hepatocytes as detected by immunofluorescence has slightly different pattern (**Fig.S4A-B**) than TUNEL activity. It remains uncertain whether cleaved caspase 3 is expressed only by hepatocytes or HSCs in the damaged central vein area as indicated by αSMA+ HSCs (**Fig. S4B**). Quantification of cleaved caspase 3 positive areas during day 1– day 3 after damage induction shows a similar or slightly increased trend (non-significant at day 1, day 2) of caspase 3 activity in the LY-treated group, compared to CCl<sub>4</sub> (**Fig.S4C**).



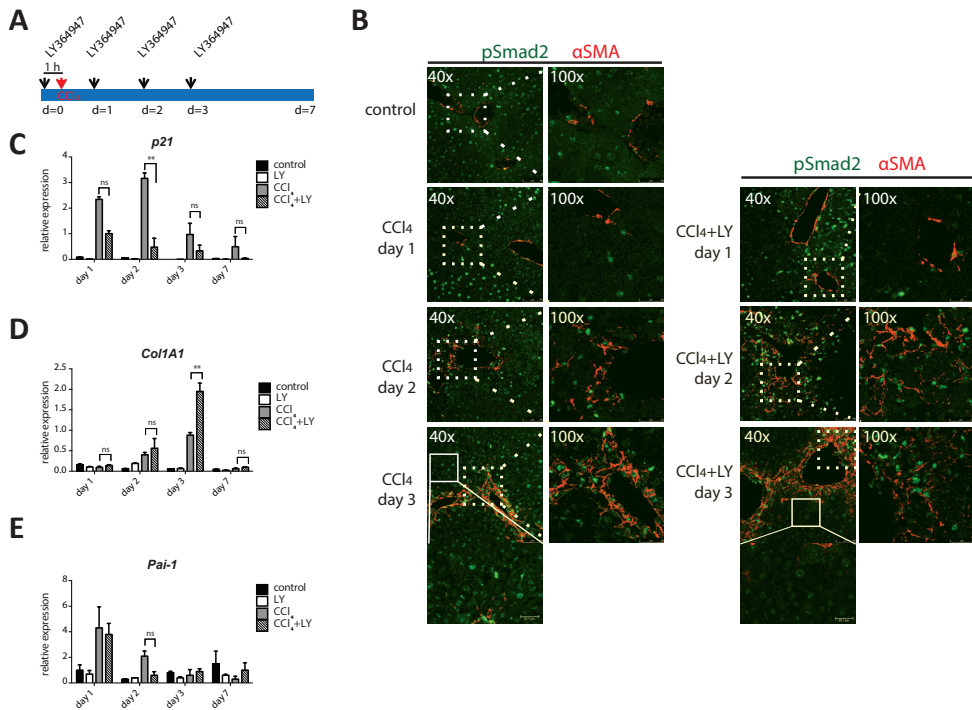


**Fig.2. Dynamics of hepatic pSmad2 expression in the central vein area after LY364947 administration**

(A). Scheme of experimental plan. Induction of acute liver damage by single shot of hepatotoxic agent  $\text{CCl}_4$  took place at day 0. ALK5 inhibitor LY364947 (LY) was administered every 24 hours (d0-d3). d; day. (B). Time course of pSmad2 (green) and  $\alpha\text{SMA}$  (red) expression by immunofluorescence during acute liver damage. Representative images of liver tissues from vehicle control,  $\text{CCl}_4$ , and  $\text{CCl}_4$ +LY injected mice. Images are shown at magnification 40x (scale bars= 50  $\mu\text{m}$ ). The marked area (dashed line) is shown at higher magnification (100x), scale bars= 25  $\mu\text{m}$ . The non-dashed marked area is shown at higher magnification, scale bars= 22.7  $\mu\text{m}$ . Time course (1, 2, 3, 7 days). (C). QPCR analysis of mRNA levels of *p21*, (D). *Col1A1*, (E). *Pai-1*; direct target genes of TGF $\beta$  pathway. Treatment groups: Control (n=2), LY (n=2),  $\text{CCl}_4$  (n=2),  $\text{CCl}_4$ +LY (n=3). Error bars indicate S.E.M. Relative expression values were normalized to *Gapdh* expression. Time point: 48 hours after  $\text{CCl}_4$ . LY; LY364947. \*\*Statistically significant,  $p < 0.01$ . ns; non-significant difference.

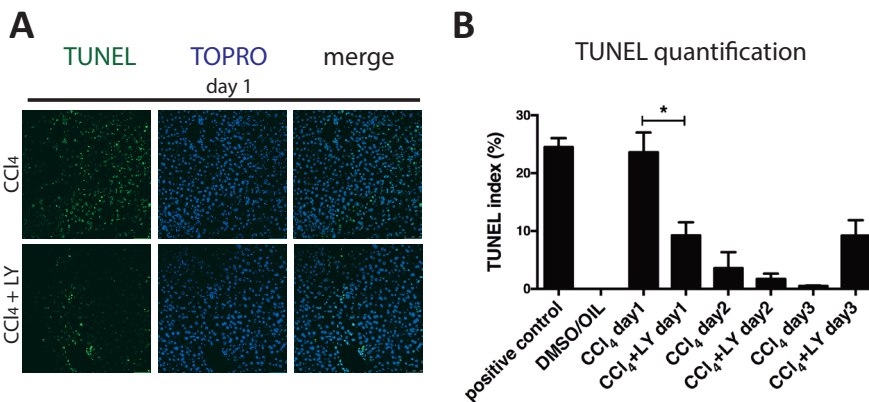


### Fig.3. Effects of LY364947 on apoptosis in CCl<sub>4</sub>-induced regeneration in mice

(A). The presence of TUNEL positive cells was determined by immunofluorescence at 24 hours after CCl<sub>4</sub> +/- LY. Representative images are shown per condition. Nuclei were visualized with TOPRO-3 (blue). Scale bars= 50 $\mu$ m. (B). Quantification of TUNEL immunofluorescence during day 1– day 3. Values are expressed as mean percentage of positive cells measured in multiple areas of liver sections from 2 mice/ CCl<sub>4</sub> group and 3 mice/ CCl<sub>4</sub>+ LY group. Error bars represent  $\pm$  SEM. DNase I-treated sections were used as positive control for DNA fragmentation and TUNEL activity. \*Statistically significant,  $p < 0.05$ . LY; LY364947

### Effect of CCl<sub>4</sub> and LY administration on expression of pericentral hepatocyte markers

Cytochrome 450 enzyme CYP2E1 and Glutamine synthetase (GS) are expressed exclusively in a subpopulation of hepatocytes of the mouse liver, specifically located around the central veins (pericentral hepatocytes). CYP2E1-expressing hepatocytes are affected by CCl<sub>4</sub> because CYP2E1 converts it into a highly reactive radical (CCl<sub>3</sub>OO) which causes severe oxidative stress and might lead to apoptosis. Upon CCl<sub>4</sub>, *Cyp2e1* (Fig.4A) and *Gs* mRNA levels (Fig.4B) are decreased, indicating either cell death of this subset of hepatocytes or temporary switching off of gene transcription. In fact, inhibition of Cyp450 enzyme activity may limit cell death and tissue damage. At seven days after CCl<sub>4</sub> intoxication, mRNA levels of *Cyp2e1* (Fig.4A) and *Gs* begin to recover (Fig.4B); however, they do not reach the levels of the control groups (Fig.4A-B). Recovery of the damaged hepatocytes seems improved in the LY treated group; mRNA expression levels of *Cyp2e1* (Fig.4A) and *Gs* (Fig.4B) resemble the normal levels by day 7, in contrast to CCl<sub>4</sub> d7 group. In view of these data, we assessed the CCl<sub>4</sub>-induced toxicity and recovery of CYP2E1+ hepatocytes by immunofluorescence in the damaged area *in situ*. Dynamics in protein expression of CYP2E1 (Fig.4C) follow similar pattern as the mRNA expression after CCl<sub>4</sub> (Fig.4A), indeed confirming that normalisation of zonation in the CV area by day 7 (Fig.4C) is improved after LY inhibitor. Despite cell death events induced by CCl<sub>4</sub> (Fig.3; Fig.S4), it is noteworthy that Cyp2E1 positive cells remain in the damaged area throughout the acute phase of injury (Fig.4C). Cells expressing  $\alpha$ SMA, such as HSCs and smooth muscle cells, seem to intermingle with Cyp2E1+ hepatocytes (Fig.4C).

### Inhibition of TGF $\beta$ *in vivo* enhances hepatocyte regeneration

Cell proliferation is a mechanism for replenishment of hepatocytes as well as expansion of repair cells such as HSCs. We determined the expression of distinct proliferation markers (PH3 and PCNA) in CCl<sub>4</sub>-induced liver damage (Fig.5). Histone 3 becomes phosphorylated only upon entry of the cell into mitosis; therefore phospho-histone 3 (PH3) expression is a marker of cell division (Fig.5A). Proliferating nuclear antigen (PCNA) is induced during duplication of DNA (S phase) prior to mitosis and also during DNA repair. Proliferation of hepatocytes is rare in the normal liver as they are quiescent cells (Fig.5S), however, upon injury they can re-enter cell cycle (Fig.5A-C). Quantification of PH3 indicates higher proliferation in presence of the LY inhibitor (Fig.5B). PH3 positive cells are mainly  $\alpha$ SMA positive HSCs upon CCl<sub>4</sub> (Fig.5A), however, proliferating  $\alpha$ SMA-negative cells were also observed in the CCl<sub>4</sub>+LY liver tissues (Fig.5A), which are likely dividing parenchymal cells. Overview images of the same liver area were acquired with lower magnification for comparison (Fig.S6). S phase marker PCNA is increased in the CCl<sub>4</sub>+LY group compared to the CCl<sub>4</sub> group in HSCs and hepatocytes around the central vein area, adjacent to necrotic cells which express cleaved caspase 3 protein (Fig.5C). Proliferating cells that are distant from the central veins are

morphologically hepatocytes (Fig.5C). Quantification of overall number of PCNA positive cells as measured by immunofluorescence in the whole liver tissue showed increased trend of proliferation in the CCl<sub>4</sub>+LY group, particularly at day 2 and day 3 (Fig.5D). Western blotting analysis in whole liver extracts also confirmed that LY-treated samples had higher PCNA expression (Fig.5E). Administration of LY seems to inhibit the total levels (whole liver) of cyclin-dependent kinase inhibitor p21 (Fig.5E) which halts cell cycle progression in G1 phase and is regulated directly by TGFβ<sup>13,14</sup>.

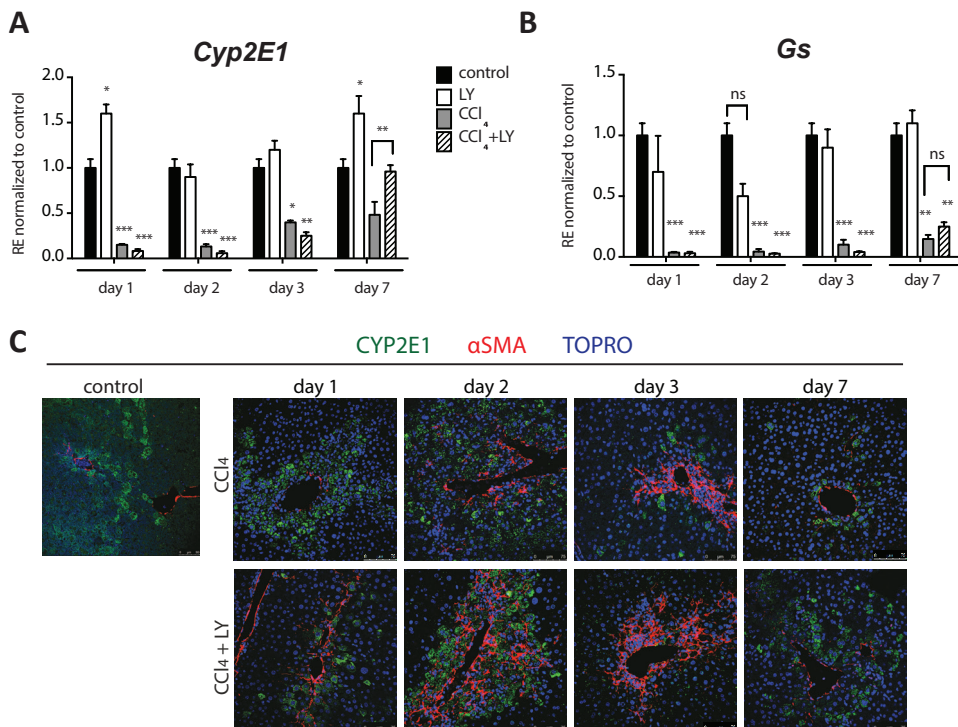


**Fig.4. Hepatic CYP2E1 expression of central hepatocytes is sustained in the damaged area during acute liver injury**

Analysis of central hepatocyte-specific transcripts by QPCR in whole liver cDNA preparations. (A). *cytochrome 450 2E1 (CYP2E1*, pericentral hepatocytes), (B). *glutamine synthetase (Gs*, pericentral hepatocytes). Treatment groups: Control (n=2), LY (n=2), CCl<sub>4</sub> (n=2), CCl<sub>4</sub>+LY (n=3). Error bars indicate S.E.M. Expression values were normalized to *Gapdh* expression and to the control sample (vehicle DMSO/oil). Time point; d1: day 1 after treatment, d2: day 2 after treatment, d3: day 3 after treatment, d7: day 7 after treatment. \*Statistically significant, p<0.05, \*\*Statistically significant, p<0.01, \*\*\* Statistically significant, p<0.001 versus control, ns; non-significant difference. (C). Immunofluorescence staining of central hepatocytes (CYP2E1, green), activated HSCs and vascular smooth muscle cells (αSMA, red) in the central vein area. Nuclei are visualized with TOPRO-3 (blue). Time points: day 1, day 2, day 3 and day 7 after CCl<sub>4</sub> or CCl<sub>4</sub>+LY. LY; LY364947. Magnification: 40x. Scale bars= 75μm.

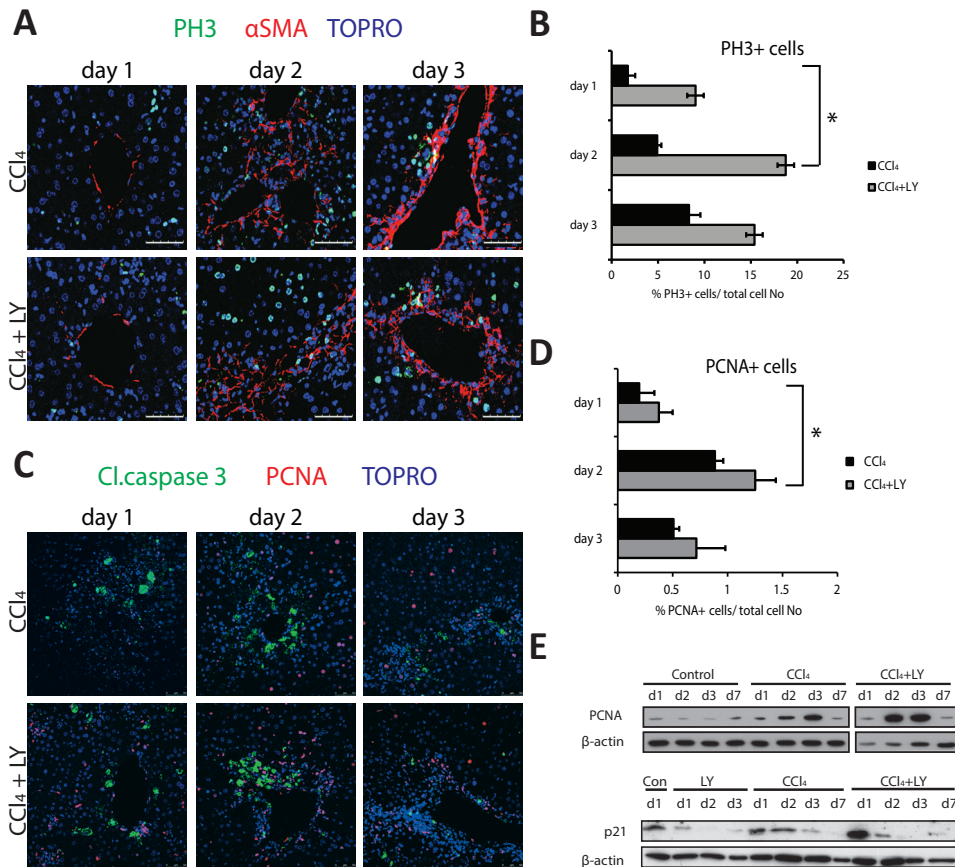


**Fig.5. Increased cell proliferation after LY364947 administration in CCl<sub>4</sub>-induced regeneration in mice** (A). Mitotic events after CCl<sub>4</sub> and in combination with LY, as determined by immunofluorescence for phosphorylated histone protein 3 (PH3, green) in the damaged central vein area (αSMA, red). A representative image is shown per condition. Nuclei are visualized with TOPRO-3 (blue). Scale bars: 100µm. (B). Quantification of PH3 positive cells during day 1- day 3, expressed as mean percentage of positive cells from 2 animals/ CCl<sub>4</sub> group and 3 mice/ CCl<sub>4</sub>+LY group. Error bars represent ± SEM. (C). Co-labeling of apoptotic and proliferating cells in the damaged central vein area; activation of proapoptotic protein caspase 3 in hepatocytes, as detected by immunofluorescence (cl.caspase 3, green) and DNA synthesis marker PCNA (red) after CCl<sub>4</sub>+/-LY administration. Scale bars: 50µm. (D). Quantification of PCNA positive cells as mentioned previously. (E). Protein expression of PCNA and p21 as measured by immunoblotting in whole liver tissue extracts. Treatment groups: Control (DMSO-oil), CCl<sub>4</sub>, CCl<sub>4</sub>+LY. Time course: day 1 (d1), day 2 (d2), day 3 (d3), day 7 (d7) after CCl<sub>4</sub> injection and small molecule inhibitor administration (day 0- day 3). β- actin was used as protein loading control. LY; LY364947. \*Statistical significance, p<0.05.

### In vivo interference of TGFβ pathway by LY does not inhibit activation of HSCs in the acute liver damage model

To assess beneficial or adverse effects of LY on wound healing response, we have performed extensive histological analyses. Induction of αSMA is a reliable marker of liver MFBs (activated HSCs), as well as MFBs resident in other tissues and vascular smooth muscle cells. To distinguish HSC-enriched genes we measured the expression of αSMA and *Ctgf* which are enriched in HSCs. αSMA (Fig.S7A) and *Ctgf* (Fig.S7B) mRNA levels show a decreasing

trend of expression in the CCl<sub>4</sub>+LY compared to the CCl<sub>4</sub> group. In the control groups, αSMA expression was only present in the smooth muscle cells lining portal and central veins (**Fig.S1**). Mice administered with CCl<sub>4</sub> toxin show signs of wound healing response during the first 48 and 72 hours (day 2, 3), with up regulation of αSMA protein, as observed by immunofluorescence (**Fig.S8A**) and by western blot analysis (**Fig.S8C**). Tissue restoration after CCl<sub>4</sub>-induced damage takes place by day 7, when αSMA protein expression is decreased back to basal levels (**Fig.S8A**). However, expression of αSMA protein as measured by western immunoblotting in whole liver protein samples (**Fig.S8C**) is similar or slightly higher in livers of the CCl<sub>4</sub>+LY group over the CCl<sub>4</sub> group. Quantification of positive staining in individual mice per group reflects a trend for higher induction of αSMA protein in the CCl<sub>4</sub>+LY group (**Fig.S8B**); therefore, HSC activation might not be affected by the LY treatment.

### ***In vitro effects of LY on TGFβ signaling***

The differential *in vivo* responses of HSCs and hepatocytes to the LY were furthermore examined using established *in vitro* mouse cell lines. Mouse HSCs and AML12 (hepatocytes) cells were stimulated with TGFβ or with TGFβ+LY and the expression of TGFβ downstream targets was tested by QPCR and western blotting. As control, non-treated cells and TGFβ-stimulated cells were used. TGFβ stimulation of HSCs up regulates mRNA expression of αSMA compared to non-stimulated HSCs (**Fig.S9**). TGFβ inhibition in HSCs is time- and dose-dependent; at high doses LY (5 uM LY, 10uM LY) abrogates the effect of TGFβ stimulation on αSMA (**Fig.S9**). However, at lower dose (1uM) LY seems to induce, rather than inhibit, the TGFβ-mediated effect on αSMA expression, particularly at later (20 hrs TGFβ+1uM LY) time points (**Fig.S9**). We measured the expression of direct target genes *Pai-1* and *Ctgf* on HSCs and hepatocytes; cell type- specific differences are observed during early induction by TGFβ (after 1 hour) (**Fig.S10**). LY treatment might be more efficient in inhibiting *Pai-1* expression in AML12 hepatocytes (**Fig.S10C**) rather than in HSCs (**Fig.S10A**). Similarly, *Ctgf* expression is efficiently down regulated in the AML12 cells as early as 1 hour (**Fig.S10D**) while *Ctgf* levels in HSCs remain high at 1 hour in presence of LY inhibitor (**Fig.S10B**). Furthermore, phosphorylation of Smad2 (**Fig.S11A-B**) and Smad3 (**Fig.S11D-E**) was analysed in a dose- dependent way after TGFβ stimulation (1 hour) and inhibition with LY (1uM, 5uM, 10uM). HSCs (**Fig.S11A, D**) and AML12 cells (**Fig.S11B, E**) *in vitro* respond to addition of exogenous TGFβ by induction of downstream pSmad2 and pSmad3. Quantification of protein bands using densitometry was done in three independent experiments, and showed that decrease of phosphorylated Smad2 (**Fig.S11C**) and Smad3 (**Fig.S11F**) levels is analogous to the concentration of LY, with 10uM dose being the most effective for both HSCs and AML12 cell types.

## **Discussion**

Acute liver failure is a severe condition of extensive hepatocyte necrosis and improper wound healing response, which occurs by exposure to intoxicants such as acetaminophen, thioacetamide, chloroform and CCl<sub>4</sub>. TGFβ is an inhibitory factor of liver regeneration by causing cytostatic response on hepatocytes and profibrotic effects on HSCs. Taking into account the deregulated levels of TGFβ in many fibrotic and malignant diseases we have investigated the impact of short term inhibition of TGFβ pathway on CCl<sub>4</sub>-induced acute damage and liver regeneration *in vivo*.

In this study we assessed the distinct roles of TGFβ in cell death and regeneration of different cell types upon acute liver damage in mice. CCl<sub>4</sub>-induced toxification occurs mainly in the central vein area, probably due to the low oxygen pressure and high cytochrome 450 enzyme levels<sup>3</sup>. Chemicals that induce cytochromes that metabolize CCl<sub>4</sub> or delay tissue regeneration when co-administered with CCl<sub>4</sub> will potentiate its toxicity, while appropriate CYP450 inhibitors will limit its toxicity<sup>6</sup>. Upon CCl<sub>4</sub>, TGFβ canonical pathway is activated and target genes *p21*, *Col1A1*, *Pai-1*, *αSMA* and *Ctgf* are induced. However, histology of the liver tissues showed a local inhibition of pSmad2 early upon tissue injury, exclusively in the centrilobular hepatocytes but not in the activated HSCs. This particular cell response may play a role in reentering of quiescent hepatocytes into the cell cycle and perhaps, initiation of the regenerative response. This observation is in line with previous studies<sup>12,14</sup> describing transient desensitization of hepatocytes to TGFβ-mediated growth arrest. Inhibition of ALK5 kinase activity by LY appears to have a potential stimulatory effect on hepatocyte proliferation during liver regeneration. Hepatocyte proliferation rate, indicative of the replacement of damaged cells by newly formed cells, was measured by PCNA immunostaining and western blotting. Proliferation is stimulated by LY co-administration with CCl<sub>4</sub> as suggested by the increased PCNA levels as well as higher levels of the mitosis marker phosphorylated histone<sup>3</sup>. Mitotic events are very few after CCl<sub>4</sub> intoxication, although this S phase marker expression is induced. A possible explanation for this difference is that hepatocytes are frequently binuclear cells since they progress through the DNA duplication phase but do not undergo cell division<sup>30</sup>. Higher proliferation rate after LY treatment is observed as early as 24 hours after injury, which may suggest that this compound leads to faster activation of innate repair and regeneration responses. Similar to our data, suppression of TGFβ induces transcription of regeneration factors (HGF, IL-6) in dimethylnitrosamine-induced chronic liver injury in rats<sup>18</sup>. Enhanced proliferation of hepatocytes, observed in the presence of dominant negative TGFβ receptor mutants<sup>18</sup> and hepatocyte specific conditional deletion of TGFβRII<sup>31</sup> supports the hypothesis that TGFβ sustains quiescent hepatocytes in a differentiated state. Cell death of a subset of hepatocytes occurs immediately due to CCl<sub>4</sub> toxicity; however, there is clearly a subpopulation of Cyp2E1 hepatocytes that remain in the central vein zone at 24 hours after CCl<sub>4</sub>. The location of these cells adjacent to the central vein may suggest that the damaged cells have the capacity to survive and to sustain their initial location and hepatocyte specific gene expression. This observation is in line with *Cyp2E1* mRNA presence in centrilobular hepatocytes as shown by *in situ* hybridisation in regenerating mouse liver<sup>32</sup>. *Cyp2E1* zonal expression is normalized to the basal levels by day 7 in the LY-treated group, indicative of better recovery of the damaged area. LY may also possibly limit the damage or necrosis as suggested by the lower levels of TUNEL activity at 24 hours after CCl<sub>4</sub> intoxication. However, cleaved caspase 3 levels are similar in CCl<sub>4</sub> and CCl<sub>4</sub>+LY and peak at a later time point than TUNEL activity; the different pattern of terminal deoxynucleotidyl transferase

(TdT) and Caspase 3 expression suggests the presence of two different cell populations and functional processes. TUNEL positive cells, which are evident at early time points, possibly represent the cells undergoing necrosis due to the toxin, while activated Caspase 3 marks cells undergoing apoptosis.

One consideration regarding HSCs is their activated MFB characteristics, such as  $\alpha$ SMA and COL1A1 expression, which are sustained by autocrine TGF $\beta$  signaling, however, due to the terminally differentiated phenotype, HSCs might not act in response to exogenously provided TGF $\beta$  stimulation<sup>33</sup>. Furthermore, other studies have shown that ALK4, ALK5 and ALK7 receptors can be targeted by SB-431542 kinase inhibitor, which blocks TGF $\beta$ -induced nuclear translocations of Smad3 and Col1A1 levels in renal epithelial carcinoma, HaCat, NIH 3T3 and C2C12 cells<sup>28,34,35</sup>. Molecular ALK5 inhibition has been shown by the use of LY364947 compound<sup>30,36,37</sup> or by other inhibitors, e.g. GW6604<sup>38</sup>, GW788388<sup>39</sup>. Selectivity of the inhibitors is dose-dependent and inhibition of TGF $\beta$  receptor kinase activity may not inhibit non-Smad signaling response which may lead to adverse effects<sup>40</sup>.

The *in vivo* co-administration of LY364947 in CCl<sub>4</sub>-mediated liver injury potentially seems to decrease the mRNA expression of direct target genes, however since whole liver (hepatic) extracts have been used in this study, the cell type-specific enrichment of target genes cannot be determined. Ctgf, p21 are expressed by parenchymal and non-parenchymal cell types<sup>41-43</sup>. Genes that are typically expressed in HSCs, such as Col1A1 and  $\alpha$ SMA, have similar mRNA and protein levels in CCl<sub>4</sub> and CCl<sub>4</sub>+LY-injected mice. Expression of *Pai-1* is not significantly different in CCl<sub>4</sub>+LY-injected mice compared to CCl<sub>4</sub>. In the model of acute hepatic injury used in this study, either HSC cell population is not sensitive to ALK5 receptor inhibition<sup>33</sup> after injury response is initiated or TGF $\beta$  inhibition is compensated by other signaling pathways (e.g. PDGF 1, p38 MAPK<sup>34</sup>). In fact,  $\alpha$ SMA is directly regulated by TGF $\beta$  and canonical Smad signaling<sup>12,15,16</sup>. Id1 target gene of BMP signaling, which is also induced by TGF $\beta$ 1/ ALK1/Smad1 branch, is important for activation of HSCs and actin polymerization<sup>44</sup>. Thus, TGF $\beta$  inhibition alone might not be sufficient to abrogate HSC proliferation and/ or accumulation of these cells. Enhanced fibrogenesis is beneficial for the regenerative response; however, if it becomes uncontrollable it may eventually lead to fibrosis. Thus, HSCs may require cell-specific targeting or longer treatment with ALK5 inhibitor in order to invert their fibrogenic properties in fibrosis studies<sup>36,45</sup>. The study of van Beuge *et al.*, 2013 showed that administration of LY without cell-specific delivery is less effective in decreasing the levels of fibronectin or collagen, similarly to our data. Other *in vivo* studies have provided evidence on the efficiency of the LY inhibitor in interstitial heart fibrosis<sup>46</sup> and in lymphangiogenesis in a chronic peritonitis mouse model<sup>47</sup>. In cancer studies, combined administration of LY and Imatinib prolongs the survival of mice with chronic myeloid leukemia<sup>48</sup>. Nevertheless, specific targeting of a TGF $\beta$  inhibitor in any disease setting is definitely advantageous over systemic administration in order to prevent on target responses that might be disadvantageous due to the differential role of TGF $\beta$  depending on the cell type/ gene expression context. An interesting hypothesis that might emerge from the analysis of our data that requires further investigation is that the damaged hepatocytes survive and remain functional under acute toxin injury condition. Thus, cell damage might not *de facto* lead to cell death and massive hepatocyte necrosis and should be carefully characterised in the different experimental models of hepatic injury. *In vivo* TGF $\beta$  inhibition by systemic administration of the LY appears to enhance hepatocyte proliferation and regeneration of the liver, thus it could be therapeutically beneficial to explore cell type-specific targeting depending on the liver disease context e.g. hepatocyte

or HSC-specific delivery for hepatocellular carcinoma or fibrosis, respectively.

## **Acknowledgements**

This study was supported by Netherlands Organization for Scientific Research (NWO-MW), Netherlands Institute for Regenerative Medicine (NIRM). This work was also supported in part by Marie Curie Initial Training Network (ITN) IT-Liver grant. We thank our colleagues, Dr. Boudewijn Kruithof and Prof. B. van de Water for valuable advice and discussion and Dr. David Scholten for the Col-GFP HSC cell line.

## **Conflict of interest**

The authors declare no conflict of interest

## **Supplementary figures**

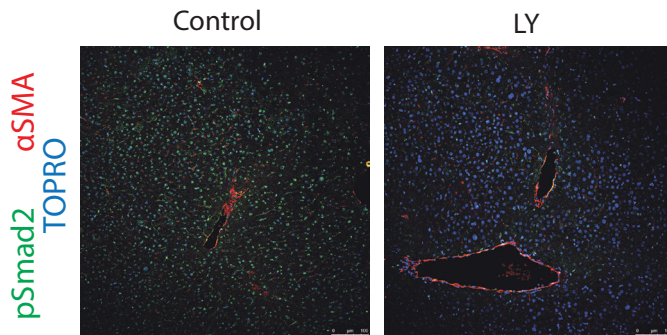


**Fig.S1. LY364947 efficiently blocks Smad2 phosphorylation in normal liver**

Staining for phosphorylated Smad2 (pSmad2, green) and alpha smooth muscle actin (αSMA, red) in control (DMSO-oil) and LY groups. LY; LY364947. 24 hours post injections. Nuclei were visualised by TOPRO-3 (blue). Magnification 20x. Scale bars= 100 μm.

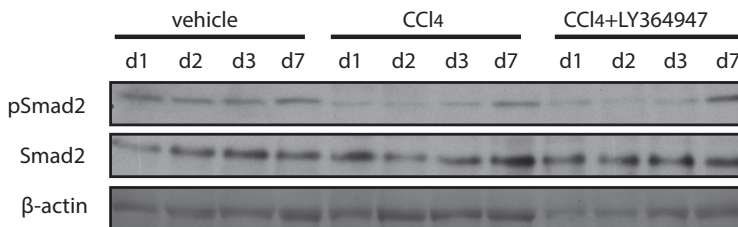


**Fig.S2. Phosphorylated and total Smad2 protein levels in whole liver homogenates**

Protein expression of pSmad2 and total Smad2 was measured by western immunoblotting in whole liver tissue extracts. Total Smad2 was detected using an antibody that recognizes the total Smad2 and Smad3 proteins. Treatment groups: vehicle (DMSO-oil), CCl<sub>4</sub>, CCl<sub>4</sub>+LY364947. Time course: day 1 (d1), day 2 (d2), day 3 (d3), day 7 (d7) after CCl<sub>4</sub> injection and small molecule inhibitor administration (day 0- day 3). β- actin was used as protein loading control.



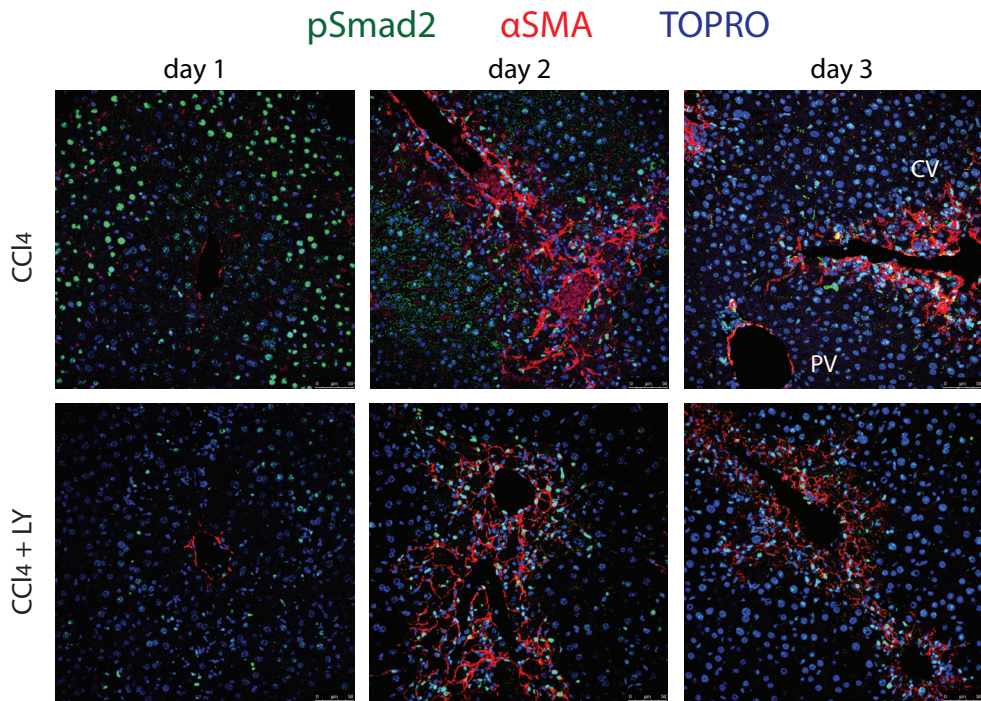


**Fig.S3. LY364947 efficiently blocks Smad2 phosphorylation in hepatocytes but not in αSMA- positive HSCs**  
 Time course (day1, day2, day3) of Smad2 phosphorylation by immunofluorescence staining (green) in liver tissues from animals that received CCl<sub>4</sub>, CCl<sub>4</sub>+LY. αSMA staining (red) marks activated HSCs (liver MFBs) as well as vascular smooth muscle cells. Nuclei were visualized by TOPRO-3 (blue). Representative images are shown per treatment group and time point. Magnification 40x, Scale bars= 50 μm. LY; LY364947.

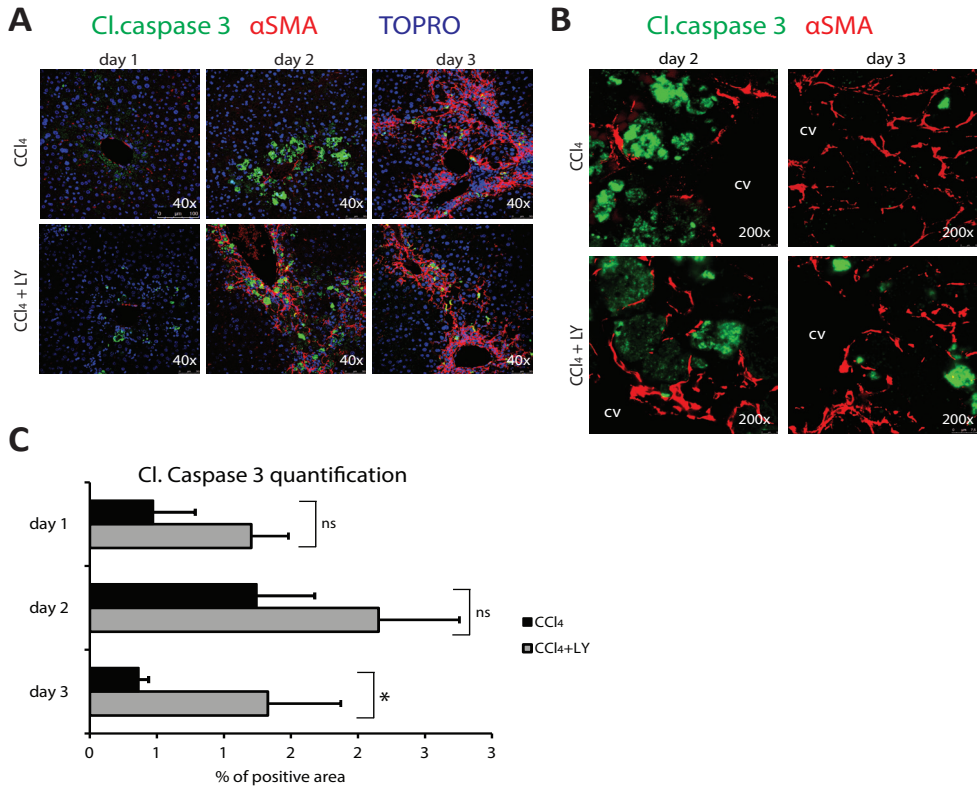


**Fig.S4. Apoptosis marker cleaved caspase 3 expression**

(A). Activation of proapoptotic protein caspase 3 in hepatocytes as detected by immunofluorescence (cleaved (Cl) Caspase 3, green) after CCl<sub>4</sub>+/- LY364947 administration in the damaged central vein area as indicated by αSMA+ HSCs (red). Nuclei were visualised by TOPRO-3 (blue). Magnification 40x. Scale bars= 50µm. (B). Cleaved caspase 3 (red) and αSMA (red) immunofluorescence of sections at higher magnification (200x) on day 2 and day 3 after CCl<sub>4</sub>-induced injury. cv; central vein Scale bars= 5 µm. (C). Quantification of cleaved caspase 3 positive area during day 1– day 3 after damage induction. Different fields of view in stained sections for every individual mouse were imaged and quantified. Graph indicates the mean percentage of positive stained area from 2 mice/ CCl<sub>4</sub> group and 3 mice/ CCl<sub>4</sub>+LY group. Error bars represent ± SEM. \*Statistical difference (P<0.05). ns; non-significant difference. LY; LY364947.

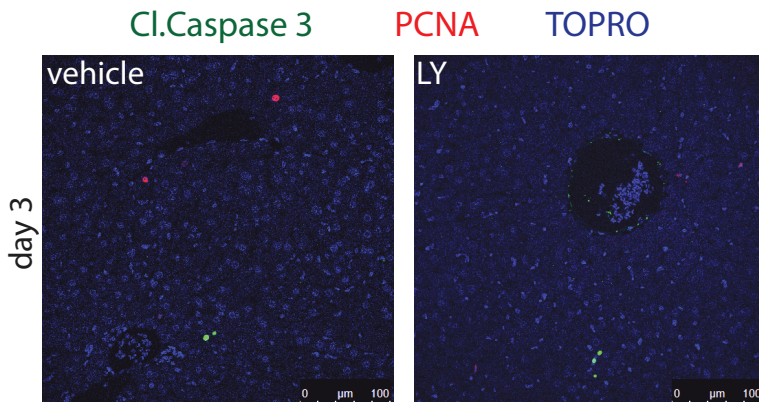


**Fig.S5. PCNA and cleaved caspase 3 levels in quiescent control liver tissues**

Time point; after 3 days of vehicle (left) or LY (right) administration. LY; LY364947. Cleaved (Cl) caspase 3; marker of apoptosis (green), PCNA; marker of proliferation (red). Nuclei were visualized with TOPRO-3 (blue). Scale bars= 100μm.

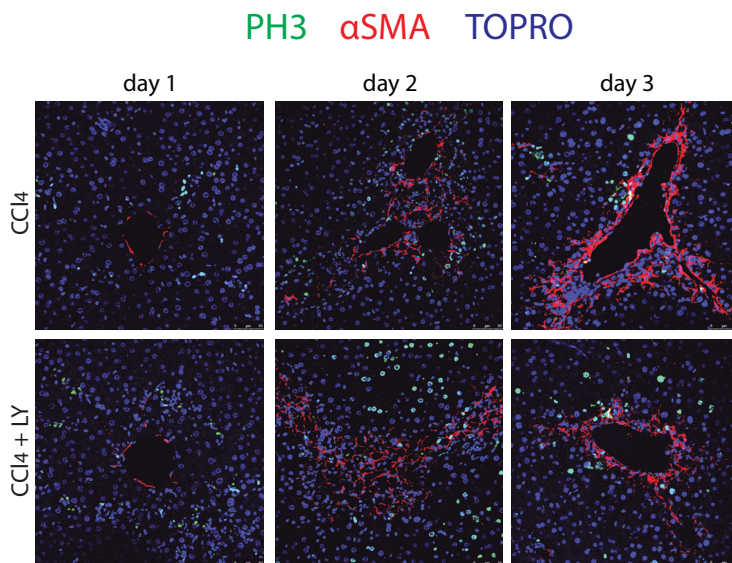


**Fig.S6. PH3 immunofluorescence**

Mitotic events after CCl<sub>4</sub> or in combination with LY364947 (LY), as determined by immunofluorescence for phosphorylated histone protein 3 (PH3, green) in the damaged central vein area (αSMA+ HSCs and smooth muscle cells, red). A representative overview image is shown per condition. Nuclei were visualized with TOPRO-3 (blue). Magnification 40x. Scale bars = 50μm.

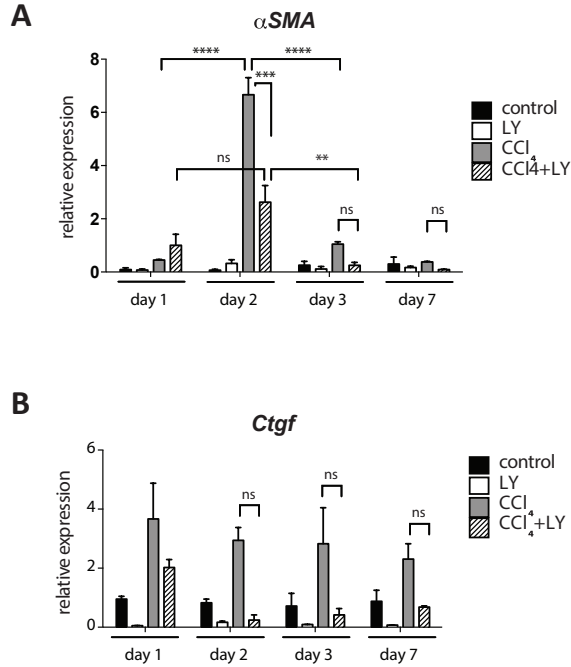


**Fig.S7. Hepatic  $\alpha$ SMA and *Ctgf* mRNA levels after CCl<sub>4</sub> administration in presence or absence of LY364947 inhibitor**

(A). mRNA levels of  $\alpha$ SMA and (B). mRNA levels of *Ctgf* as measured by QPCR. Treatment groups: Control (n=2), LY (n=2), CCl<sub>4</sub> (n=2), CCl<sub>4</sub>+LY (n=3). LY; LY364947. Error bars indicate S.E.M. Relative expression values were normalized to *Gapdh* expression. Time points: day 1- day 2- day 3- day 7 after CCl<sub>4</sub>. \*\*Statistically significant, p<0.01, \*\*\*\*Statistically significant, p<0.0001, ns; non-significant difference.

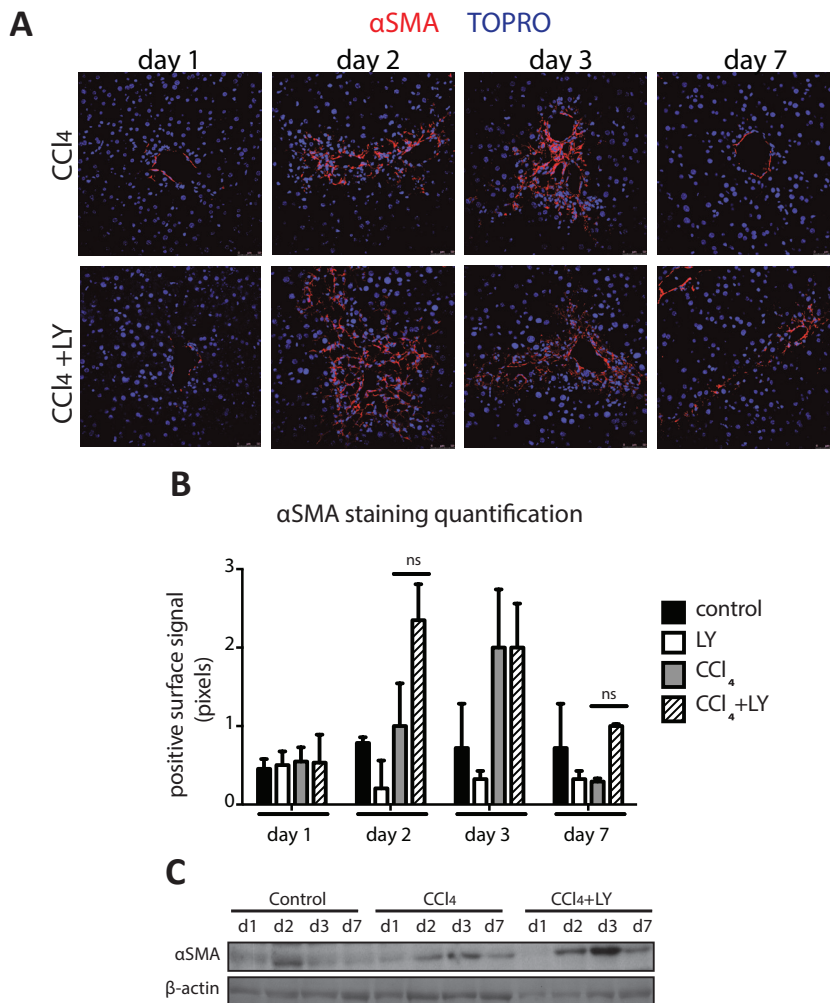


**Fig.S8. *In vivo* inhibition of TGFβ receptor kinase activity in acute liver damage model by small molecule inhibitor LY364947**

(A). Immunofluorescence staining of αSMA+ HSCs in CCl<sub>4</sub> and CCl<sub>4</sub>+LY treated liver tissues. Representative images are shown per each time point; day 1, day 2, day 3 and day 7 after single CCl<sub>4</sub> dose. Nuclei were visualized by TOPRO-3 (blue). Magnification 40x. Scale bars= 50 μm. (B). Quantification of αSMA immunofluorescence in liver tissues. Error bars represent S.E.M. Time points: day 1, day 2, day 3, day 7 after CCl<sub>4</sub> shot. Treatment groups: control (n=2 per time point), LY (n=2), CCl<sub>4</sub> (n=2) and CCl<sub>4</sub>+LY (n=3). ns; non-significant difference. (C). Protein expression of αSMA measured by western immunoblotting from whole liver tissue extracts. β- actin was used as protein loading control. Time points and treatment groups as described previously. LY; LY364947.

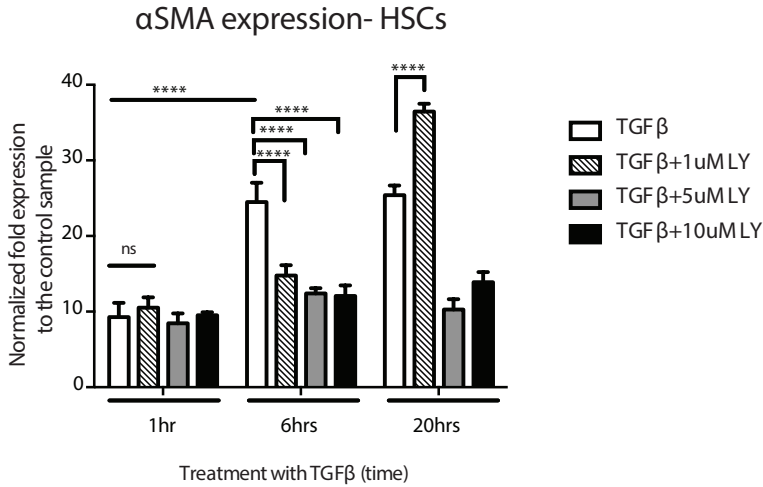


**Fig.S9. High dose of LY364947 treatment is required to inhibit αSMA expression in HSCs *in vitro***  
 Quantitative PCR analysis of αSMA expression in HSCs. Cells were pretreated with increasing concentrations of LY364947 (LY 1uM, 5uM, 10uM) for 1 hour and stimulated with TGFβ3 (5ng/ml) for 1, 6 and 20 hours. Expression was normalized to the values of the control cDNA from non-stimulated cells. \*\*\*\*Statistically significant, p<0.0001 versus TGFβ. ns; non-significant difference.

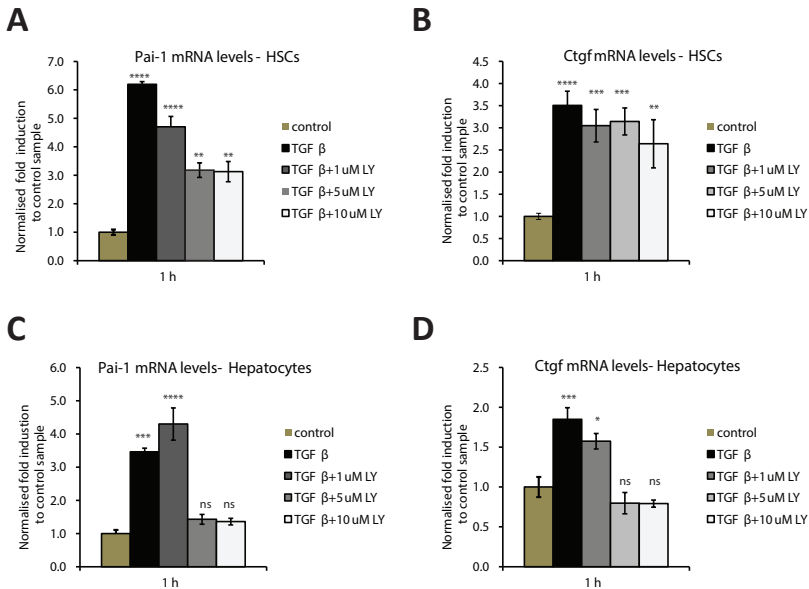


**Fig.S10. *In vitro* effects of LY364947 on TGFβ target genes in HSCs and hepatocyte AML12 cell line**  
 (A). *Pai-1* mRNA expression and (B). *Ctgf* mRNA expression in mouse HSCs. HSCs were pretreated with increasing concentrations of LY364947 (LY 1uM, 5uM, 10uM) and stimulated with TGFβ3 (5ng/ml) for 1 hour. Fold induction ( $\Delta\Delta Ct$ ) was normalized to the control sample (non-stimulated cells) and *Gapdh* expression values. (C). *Pai-1* mRNA and (D). *Ctgf* mRNA expression in mouse AML12 hepatocytes. Cells were pretreated with increasing concentrations of LY364947 (LY 1uM, 5uM, 10uM) and stimulated with TGFβ3 (5ng/ml) for 1 hour. Fold induction ( $\Delta\Delta Ct$ ) was normalized to the control sample (non-stimulated cells) and *Gapdh* expression values. \*Statistically significant, p<0.05, \*\*Statistically significant, p<0.01, \*\*\*Statistically significant, p<0.001, \*\*\*\*Statistically significant, p<0.0001 versus control sample. ns; non-significant difference.

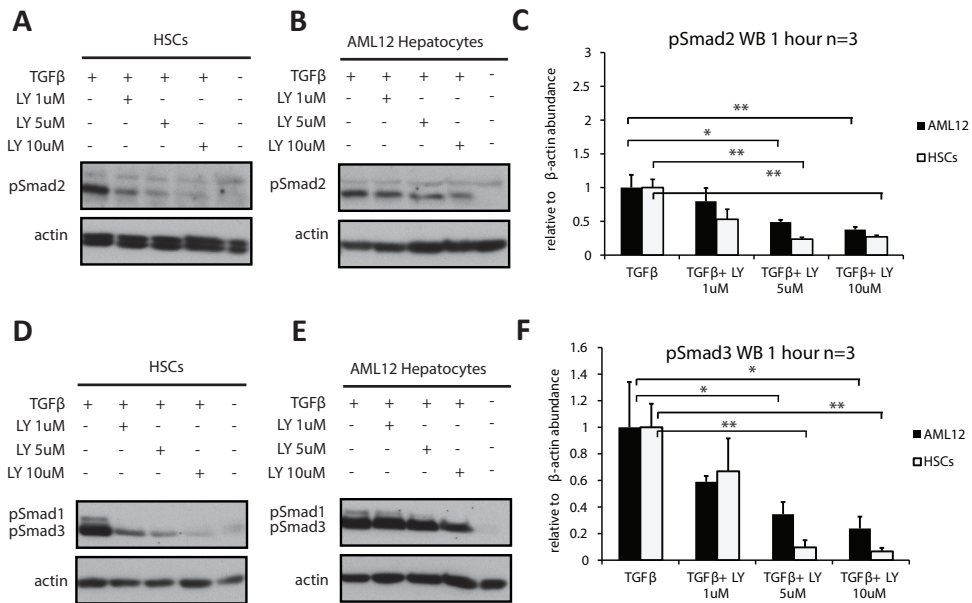


**Fig.S11. *In vitro* effects of LY364947 on Smad2, Smad3 phosphorylation in HSCs and AML12 cell lines**  
 Cells were pretreated with increasing concentrations of LY364947 (LY 1 uM, 5uM, 10uM) for 1 hour and stimulated with TGFβ3 (5ng/ml) for 1 hour (n=3). Loading control; β-actin. (A). pSmad2 in HSCs (1h time point), (B). pSmad2 in AML12 hepatocytes (1h time point), (C). Quantification of western blotting pSmad2 signal by densitometry (n=3). Relative abundance over β-actin, (D). pSmad1, pSmad3 in mouse HSCs, (E). pSmad1, pSmad3 in mouse AML12 hepatocytes, (F). Quantification of western blotting pSmad1, 3 signal by densitometry (n=3). Relative abundance over β-actin. \*Statistically significant,  $p < 0.05$ , \*\*Statistically significant,  $p < 0.01$  versus TGFβ.

## Supplementary Materials and Methods

### Immunofluorescence

Liver tissues were fixed in 4% paraformaldehyde solution overnight, washed in PBS and processed for paraffin embedding. For every mouse, one of the liver lobules was embedded in a paraffin block and multiple serial sections (0.6 μm) were prepared. For antigen retrieval, sections were boiled 10- 30 min in antigen unmasking solution (Vector Labs) and were incubated in 3% H<sub>2</sub>O<sub>2</sub> for endogenous peroxidases sequestering. Sections were blocked with 1% bovine serum albumin (BSA)- PBS-0.1% v/v Tween 20) and incubated with primary antibodies diluted in the blocking solution, overnight at 4°C or room temperature. Primary antibodies and dilutions used are as follows: anti-αSMA 1:500 (Sigma), anti-phospho-Smad2 1:1000 (Cell Signaling), anti-Cyp2e1 1:500 (Biorbyt), anti-Fsp1 1:1000 (Millipore), anti-desmin 1:500 (Santa Cruz), anti-HNF4α 1:100 (Santa Cruz), anti-PCNA 1:10.000 (Sigma), anti-phospho Histone3 1:1000 (Millipore), anti-cleaved caspase 3 1:1000 (Cell Signaling). Sections were then incubated with secondary antibodies labeled with Alexa Fluor 488, 555, or 647 (Invitrogen/Molecular Probes, 1:250 in PBS-0.1% Tween 20). Detection of pSmad2 and Cyp2e1 was enhanced using tyramide amplification (Invitrogen/Molecular Probes) by incubation of slides with horseradish peroxidase (HRP)-conjugated secondary antibody (1:100 dilution) (Invitrogen/Molecular Probes), followed by incubation with tyramide-4 88 for 10 minutes. All sections were counterstained with TOPRO-3 (Invitrogen/Molecular Probes) at 1:1000 dilution in PBS-0.1% Tween20 for nuclei visualization, and mounted with Prolong G mounting medium (Invitrogen/Molecular Probes), which contains DAPI. Every immunofluorescence staining experiment was performed multiple times using different sections from the same lobule from every mouse.

### RNA isolation, RT-PCR and Quantitative PCR

During liver tissue collection, one of the liver lobules of each individual mouse was snapfrozen in liquid nitrogen and stored at -80°C for RNA analyses. One liver part per mouse (100 μm) was homogenized using an UltraTurrax homogenizer (T25 basic, IKA) in TRIpure reagent (Roche) and directly processed for total RNA isolation according to the TRIpure RNA extraction protocol. Total RNA (0.5 μg) was used for first strand cDNA synthesis using RevertAid H Minus first strand cDNA synthesis kit (Fermentas). For quantitative PCR (Q-PCR) ten-fold diluted cDNA was amplified in a CFX Real Time Detection system (Bio-rad) using SYBR Green Supermix reagent (Bio-rad). Expression levels were normalized to housekeeping gene (Gapdh).

Primer sequences:

αSMA: *for*-ACTGGGACGACATGGAAAAG, *rev*- CATCTCCAGAGTCCAGCACA

Pai: *for*-GCCAACAAGAGCCAATCACA, *rev*-AGGCAAGCAAGGGCTGAAG

Cyp2e1: *for*- GGACATTCCTGTGTTCCAG, *rev*- CTTAGGGAAAACCTCCGCAC

Ctgf: *for*- CAGACTGGAGAAGCAGAGCC, *rev*- GCTTGGCGATTTTAGGTGC

Gs: *for*- CTCCTGACCTGTTACCCAT, *rev*- TTGCTTGATGCCTTTGTTC

Gapdh: *for*-AACTTTGGCATTGTGGAAGG, *rev*-ACACATTGGGGGTAGGAACA

p21: *for*- CGGTGTCAGAGTCTAGGGGA, *rev*- ATCACCAGGATTGGACATGG



### Western immunoblotting

During liver tissue collection, one of the liver lobules of each individual mouse was snapfrozen in liquid nitrogen and stored at -80°C for protein analyses. One liver part per mouse (100 µm) was homogenized in tissue lysis buffer (30 mM Tris pH 7.4, 150 mM NaCl, 0.5% Triton-X 100, 10 mM NaF, 1 mM Na<sub>3</sub>VO<sub>4</sub>, 10 mM EDTA pH=8.0, 1% SDS, plus complete protease inhibitors, Roche) using an Ultra Turrax homogenizer (T25 basic, IKA). Following a centrifugation step (15 min, 4000 rpm, 4°C) to remove debris, the protein extract can be collected (supernatant) and further diluted 5-fold with lysis buffer. Whole protein extract by DC protein assay (Biorad) using BSA serial dilutions in tissue lysis buffer. A total of 20 µg was diluted in 4x Laemmli buffer, separated by SDS-PAGE and transferred to nitrocellulose membranes. The following primary antibodies were used anti-αSMA 1:1000 (Abcam), anti-phospho-Smad1 1:1.000 (Cell Signaling), anti-phospho-Smad2 1:1.000 (Cell Signaling), anti-Smad2/3 1:1000 (BD Biosciences), anti-PCNA 1:5000 (Sigma), anti-p21 (Santa Cruz), GAPDH 1:10.000 (Millipore), actin 1:10.000 (Sigma). Appropriate secondary antibodies were used and detected by chemiluminescence (Biorad).

### Statistical analysis

Statistical analysis was performed using GraphPad Prism 5.0 software (San Diego, CA) and two-way ANOVA test. Data is presented as mean±SEM. Significant differences are indicated with asterisks (\* p< 0.05, \*\* p<0.01, \*\*\* p<0.001, \*\*\*\*p<0.0001). For quantitative PCR analysis experiments were repeated at least three times as technical replicates for every sample (different cDNA preparations using the RNA of one liver lobule per mouse) and the average value was calculated. The mean values obtained from individual animals for every group (n=2-3) were used for ANOVA statistical analysis. For quantifications of immunofluorescence signal; for every stained section (representing one mouse liver sample) multiple fields of view were imaged and quantified (see section Microscopy and Image analysis). The average of these values was calculated for every mouse sample. Statistical analyses were performed on the values of all the mouse samples per treatment group (n=2-3 in total).

### Cell lines

Activated HSCs (Collagen1alpha1-GFP HSC cell line, David Scholten) and AML12 mouse hepatocytes were used. Cells were serum starved, pretreated with ALK5 inhibitor LY364947 (5µg/ml) for 2 hours and stimulated with TGFβ3 (5ng/ml) for 1, 6 or 20 hours.

### Microscopy and Image analysis

Confocal microscopy of labelled specimens was performed on a Leica TC-SP5 microscope with a 40X 1.4 NA oil-immersion objective Z series were collected and reassembled in Image J software ([rsbweb.nih.gov/ij](http://rsbweb.nih.gov/ij)). Mean area fraction fluorescence was calculated in Image J software using threshold to select the root boundary and measuring the percentage of positive surface inside the intensity defined by the threshold. For quantifications of immunofluorescence signal, staining experiments were performed on all the samples simultaneously to reduce technical variation (each treatment group contains one sample from each mouse, n=2-3 in total). Experiments were repeated three times (three sections

per sample were analysed) and stained specimens in a given experiment were imaged using identical microscopic exposure and recording settings.

### **References**

1. Serini, G. and G. Gabbiani, Mechanisms of myofibroblast activity and phenotypic modulation. *Exp Cell Res*, 1999. 250(2): p. 273-283.
2. Fausto, N., Liver regeneration and repair: Hepatocytes, progenitor cells, and stem cells. *Hepatology*, 2004. 39(6): p. 1477-1487.
3. Wong, F.W.Y., W.Y. Chan, and S.S.T. Lee, Resistance to carbon tetrachloride-induced hepatotoxicity in mice which lack CYP2E1 expression. *Toxicol Appl Pharmacol*, 1998. 153(1): p. 109-118.
4. Dooley, S. and P. ten Dijke, TGF- $\beta$  in progression of liver disease. *Cell Tissue Res*, 2012. 347(1): p. 245-256.
5. Michalopoulos, G.K., Liver regeneration. *J Cell Physiol*, 2007. 213(2): p. 286-300.
6. Weber, L.W.D., M. Boll, and A. Stampfl, Hepatotoxicity and mechanism of action of haloalkanes: carbon tetrachloride as a toxicological model. *Crit Rev Toxicol*, 2003. 33(2): p. 105-136.
7. Wells, R.G., The role of matrix stiffness in hepatic stellate cell activation and liver fibrosis. *J Clin Gastroenterol*, 2005. 39(4 Suppl 2): p. S158-61.
8. Böhm, F., et al., Regulation of liver regeneration by growth factors and cytokines. *EMBO Mol Med*, 2010. 2(8): p. 294-305.
9. Braun, L., et al., Transforming growth factor  $\beta$  mRNA increases during liver regeneration: a possible paracrine mechanism of growth regulation. *Proc Natl Acad Sci U S A*, 1988. 85(5): p. 1539-1543.
10. Leask, A., Potential therapeutic targets for cardiac fibrosis: TGF- $\beta$ , angiotensin, endothelin, CCN2, and PDGF, partners in fibroblast activation. *Circ Res*, 2010. 106(11): p. 1675-1680.
11. Border, W.A. and N.A. Noble, Transforming growth factor  $\beta$  in tissue fibrosis. *N Engl J Med*, 1994. 331(19): p. 1286-1292.
12. Gu, L., et al., Effect of TGF- $\beta$ /Smad signaling pathway on lung myofibroblast differentiation. *Acta Pharmacol Sin*, 2007. 28(3): p. 382-391.
13. Li, C., L. Suardet, and J.B. Little, Potential role of WAF1/Cip1/p21 as a mediator of TGF- $\beta$  cytotoxic effect. *J Biol Chem*, 1995. 270(10): p. 4971-4974.
14. Gong, J., et al., Transforming growth factor  $\beta$ 1 increases the stability of p21/WAF1/CIP1 protein and inhibits CDK2 kinase activity in human colon carcinoma FET cells. *Cancer Res*, 2003. 63(12): p. 3340-3346.
15. Hautmann, M.B., C.S. Madsen, and G.K. Owens, A Transforming growth factor  $\beta$  (TGF $\beta$ ) control element drives TGF $\beta$ -induced stimulation of smooth muscle  $\alpha$ -actin gene expression in concert with two CArG elements. *J Biol Chem*, 1997. 272(16): p. 10948-10956.
16. Roy, S.G., Y. Nozaki, and S.H. Phan, Regulation of  $\alpha$ -smooth muscle actin gene expression in myofibroblast differentiation from rat lung fibroblasts. *Int J Biochem Cell Biol*, 2001. 33(7): p. 723-734.
17. Heldin, C.H., K. Miyazono, and P. ten Dijke, TGF- $\beta$  signaling from cell membrane to nucleus through SMAD proteins. *Nature*, 1997. 390(6659): p. 465-471.
18. Heldin, C.H., M. Landström, and A. Moustakas, Mechanism of TGF- $\beta$  signaling to growth arrest, apoptosis, and epithelial-mesenchymal transition. *Curr Opin Cell Biol*, 2009. 21(2): p. 166-176.
19. Annes, J.P., J.S. Munger, and D.B. Rifkin, Making sense of latent TGF $\beta$  activation. *J Cell Sci*, 2003. 116(2): p. 217-224.
20. Massagué, J., J. Seoane, and D. Wotton, Smad transcription factors. *Genes Dev*, 2005. 19(23): p. 2783-2810.
21. Yingling, J.M., K.L. Blanchard, and J.S. Sawyer, Development of TGF- $\beta$  signaling inhibitors for cancer therapy. *Nat Rev Drug Discov*, 2004. 3(12): p. 1011-1022.
22. Flanders, K.C., et al., Mice lacking Smad3 are protected against cutaneous injury induced by ionizing radiation. *Am J Pathol*, 2002. 160(3): p. 1057-1068.
23. Sato, M., et al., Targeted disruption of TGF- $\beta$ 1/Smad3 signaling protects against renal tubulointerstitial fibrosis induced by unilateral ureteral obstruction. *J Clin Invest*, 2003. 112(10): p. 1486-1494.
24. Jeong, D.H., et al., Smad3 deficiency ameliorates hepatic fibrogenesis through the expression of senescence marker protein-30, an antioxidant-related protein. *Int J Mol Sci*, 2013. 14(12): p. 23700-10.
25. Bhowmick, N.A., et al., TGF- $\beta$  Signaling in fibroblasts modulates the oncogenic potential of adjacent epithelia. *Science*, 2004. 303(5659): p. 848-851.
26. Pierce, R.A., et al., Increased procollagen mRNA levels in carbon tetrachloride-induced liver fibrosis in rats. *J Biol Chem*, 1987. 262(4): p. 1652-8.

27. Cai, Y., et al, Apoptosis initiated by carbon tetrachloride in mitochondria of rat primary cultured hepatocytes. *Acta Pharmacol Sin*, 2005. 26(8): p. 969-975.
28. Vogt, J., R. Traynor, and G.P. Sapkota, The specificities of small molecule inhibitors of the TGF- $\beta$  and BMP pathways. *Cell Signal*, 2011. 23(11): p. 1831-1842.
29. Ghavami, S., et al., Apoptosis and cancer: mutations within caspase genes. *J Med Genet*, 2009. 46(8): p. 497-510.
30. Guidotti, J.E., et al., Liver cell polyploidization: a pivotal role for binuclear hepatocytes. *J Biol Chem*, 2003. 278(21): p. 19095-19101.
31. Romero-Gallo, J., et al., Inactivation of TGF- $\beta$  signaling in hepatocytes results in an increased proliferative response after partial hepatectomy. *Oncogene*, 2005. 24(18): p. 3028-3041.
32. Ghafoory, S., et al., Zonation of nitrogen and glucose metabolism gene expression upon acute liver damage in mouse. *PLoS One*, 2013. 8(10): p. e78262.
33. Tahashi, Y., et al., Differential regulation of TGF- $\beta$  signal in hepatic stellate cells between acute and chronic rat liver injury. *Hepatology*, 2002. 35(1): p. 49-61.
34. Laping, N.J., et al., Inhibition of Transforming growth factor (TGF)- $\beta$ 1-induced extracellular matrix with a novel inhibitor of the TGF- $\beta$  type I receptor kinase activity: SB-431542. *Mol Pharmacol*, 2002. 62(1): p. 58-64.
35. Inman, G.J., et al., SB-431542 is a potent and specific inhibitor of Transforming growth factor- $\beta$  superfamily type I activin receptor-like kinase (ALK) receptors ALK4, ALK5, and ALK7. *Mol Pharmacol*, 2002. 62(1): p. 65-74.
36. van Beuge, M.M., et al., Enhanced effectivity of an ALK5-inhibitor after cell-specific delivery to hepatic stellate cells in mice with liver injury. *PLoS One*, 2013. 8(2): p. e56442.
37. Yoshioka, N., et al., Small molecule inhibitor of type I transforming growth factor- $\beta$  receptor kinase ameliorates the inhibitory milieu in injured brain and promotes regeneration of nigrostriatal dopaminergic axons. *J Neurosci Res*, 2011. 89(3): p. 381-393.
38. de Gouville, A.C., et al., Inhibition of TGF- $\beta$  signaling by an ALK5 inhibitor protects rats from dimethylnitrosamine-induced liver fibrosis. *Br J Pharmacol*, 2005. 145(2): p. 166-177.
39. Petersen, M., et al., Oral administration of GW788388, an inhibitor of TGF- $\beta$  type I and II receptor kinases, decreases renal fibrosis. *Kidney Int*, 2007. 73(6): p. 705-715.
40. Sorrentino, A., et al., The type I TGF- $\beta$  receptor engages TRAF6 to activate TAK1 in a receptor kinase-independent manner. *Nat Cell Biol*, 2008. 10(10): p. 1199-1207.
41. Kodama, T., et al., Increases in p53 expression induce CTGF synthesis by mouse and human hepatocytes and result in liver fibrosis in mice. *J Clin Invest*, 2011. 121(8): p. 3343-3356.
42. Manapov, F., P. Muller, and J. Rychly, Translocation of p21Cip1/WAF1 from the nucleus to the cytoplasm correlates with pancreatic myofibroblast to fibroblast cell conversion. *Gut*, 2005. 54(6): p. 814-822.
43. Marhenke, S., et al., p21 promotes sustained liver regeneration and hepatocarcinogenesis in chronic cholestatic liver injury. *Gut*, 2014. 63(9): p. 1501-1512.
44. Wiercinska, E., et al., Id1 is a critical mediator in TGF- $\beta$ -induced transdifferentiation of rat hepatic stellate cells. *Hepatology*, 2006. 43(5): p. 1032-1041.
45. Sato, Y., et al., Resolution of liver cirrhosis using vitamin A-coupled liposomes to deliver siRNA against a collagen-specific chaperone. *Nat Biotech*, 2008. 26(4): p. 431-442.
46. Chu, W., et al., Arsenic-induced interstitial myocardial fibrosis reveals a new insight into drug-induced long QT syndrome. *Cardiovasc Res*, 2012. 96(1): p. 90-98.
47. Oka, M., et al., Inhibition of endogenous TGF- $\beta$  signaling enhances lymphangiogenesis. *Blood*, 2008. 111(9): p. 4571-9.
48. Naka, K., et al., TGF- $\beta$ -FOXO signaling maintains leukaemia-initiating cells in chronic myeloid leukaemia. *Nature*, 2010. 463(7281): p. 676-680.







## Chapter 4

# Human Dupuytren's *ex vivo* culture for the study of myofibroblasts and extracellular matrix interactions

**Sofia Karkampouna<sup>1</sup>, Peter Kloen<sup>2</sup>, Miryam C. Obdeijn<sup>3</sup>, Scott M. Riester<sup>4</sup>,  
Andre J. van Wijnen<sup>4,5</sup>, Marianna Kruithof-de Julio<sup>1,6,\*</sup>**

<sup>1</sup>Department of Molecular Cell Biology, Leiden University Medical Centre,  
Leiden, The Netherlands

<sup>2</sup>Department of Orthopedic Surgery, Academic Medical Centre,  
Amsterdam, The Netherlands

<sup>3</sup>Department of Plastic, Reconstructive and Hand Surgery,  
Academic Medical Centre, Amsterdam, The Netherlands

<sup>4</sup>Department of Orthopedic Surgery, Mayo Clinic,

<sup>5</sup>Department of Biochemistry and Molecular Biology, Mayo Clinic,

<sup>6</sup>Department of Dermatology, Leiden University Medical Centre

\* Corresponding author

***Journal of Visualised Experiments, 2015 Apr 18;(98)***



## Abstract

Organ fibrosis or “scarring” is known to account for a high death toll due to the extensive amount of disorders and organs affected (from cirrhosis to cardiovascular diseases). There is no effective treatment and the *in vitro* tools available do not mimic the *in vivo* situation rendering the progress of the out of control wound healing process still enigmatic. To date, 2D and 3D cultures of fibroblasts derived from DD patients are the main experimental models available. Primary cell cultures have many limitations; the fibroblasts derived from DD are altered by the culture conditions, lack cellular context and interactions, which are crucial for the development of fibrosis and weakly represent the derived tissue. Real-time PCR analysis of fibroblasts derived from control and DD samples show that little difference is detectable. 3D cultures of fibroblasts include addition of extracellular matrix that alters the native conditions of these cells. As a way to characterize the fibrotic, proliferative properties of these resection specimens we have developed a 3D culture system, using intact human resections of the nodule part of the cord. The system is based on transwell plates with an attached nitrocellulose membrane that allows contact of the tissue with the medium but not with the plastic, thus, preventing the alteration of the tissue. No collagen gel or other extracellular matrix protein substrate is required. The tissue resection specimens maintain their viability and proliferative properties for 7 days. This is the first “organ” culture system that allows human resection specimens from DD patients to be grown *ex vivo* and functionally tested, recapitulating the *in vivo* situation.

## Introduction

Dupuytren’s disease (DD), a benign fibroproliferative disease causes permanent flexion of the fingers due to the formation of nodules and cords in the palm of the hand. Although the disease spread is particularly high among Caucasians of Northern Europe, the underlying genetic etiology of the disease remains unknown<sup>1</sup>. The main characteristic of DD is the excess production of extracellular matrix (ECM) proteins (e.g. collagen), which form a tough fibrous tissue occupying the space between the tendons and skin of the palm of the hand and fingers, permanently disrupting the fine movements of the hand<sup>2-3</sup>. The recurrence of the disease suggests underlying genetic alterations as a cause of fibrosis<sup>1,4</sup>. An effective treatment could be to target directly the uncontrollable fibrotic mechanisms at the cellular and molecular level.

Our recent work on fibrosis has led us to the development of a novel 3D culture system that allows short-term culture of human fibrotic tissue with the potential of drug testing. This system has helped to overcome the limiting approach of 2D fibroblast cultures and to define a role for the partial down regulation, achieved by exon skipping, of TGF $\beta$  pathway activation in mediating fibrosis<sup>5</sup>.

We have developed a method to culture *ex vivo* human resection specimens from DD patients to study the interaction between myofibroblasts and the surrounding ECM<sup>5,6</sup>. The study of DD connective tissue fibrosis as well as other fibrotic diseases relies on histopathological analysis of the excised surgical specimens, isolation of fibroblasts from the tissue and establishment of primary cultures or cell sorting procedures. These approaches are quite static since they do not permit exogenous manipulation of the disease properties or therapeutic intervention by the experimenter. In addition, primary cell cultures tend to



adapt to the culture conditions and their gene expression properties differ essentially from the *in vivo* situation upon every passage, even during early passages (among passage 3 and 6)<sup>7-8</sup>. We have managed to maintain the waste surgical material in *ex vivo* culture conditions for a time period that allows study of the patient-specific characteristics and screening of anti-fibrotic or anti-inflammatory drug compounds.

The system is based on a nitrocellulose membrane that permits contact of the tissue with the medium but not with the plastic, thus, preventing the alteration of the tissue upon attachment, as previously observed when culturing DD fibroblasts as well as other cell types<sup>9</sup>. No collagen gel or other ECM protein substrate is required, since the DD tissue itself produces large amounts of these proteins. This is advantageous for the maintenance of native ECM microenvironment and turnover since matrix substrates are important regulators of tissue architecture and function<sup>10-11</sup>. For instance, ECM proteins such as fibronectin, laminin and collagen, may influence front-rear polarity of fibroblasts as similarly shown for apical-basal polarity in epithelial cells<sup>12-13</sup>. Polarized cells have asymmetrical distribution of extracellular molecules which determines cell migration and gene expression, e.g.  $\alpha 1\beta 1$  integrin accessibility on the membrane affects cell adhesion to type I collagen<sup>14</sup>. Since a primary goal of this 3D model was to preserve the native microenvironment, no artificial ECM matrix substrate was used. In brief: resection specimens are equally cut in a sterile environment and placed on nitrocellular membranes. If treatment administrated via injection is required the tissues are injected after they have been placed on the membrane. If treatment does not require to be administrated via injection then the compound is added to the culture media (Dulbecco's Modified Eagle's Medium (DMEM), with 1% fetal calf serum (FCS), 1% penicillin-streptomycin (P/S)). The cultures are maintained for a maximum of ten days after which the tissue is fixed in 4% paraformaldehyde (PFA), processed through 30% sucrose solution, embedded in O.C.T. compound and stored at -80°C, as previously described<sup>5</sup>.

## Protocol

This protocol follows the LUMC and AMC guidelines of human research ethics committee.

### I. Surgical procedure and tissue collection

Note: Although various techniques for surgical excision of Dupuytren's contracture exist, the current gold standard is the partial fasciectomy<sup>15</sup>.

Most patients are treated in the day-surgery clinic.

1. Perform surgery under general or regional anesthesia according to patient's and anaesthesiologist's preferences and to patient's co-morbidities. These considerations are beyond the scope of this paper. Prior to incision, touch the skin with a sharp object to verify that anesthesia is satisfactory. Use a tourniquet to facilitate surgical visualization in a bloodless field.
2. After sterile prepping and draping, mark out the anticipated incision with a pen. Incise the skin with a scalpel under loupe magnification either longitudinally or using zigzag incisions in order to prevent additional contractures as well as to allow for sufficient exposure.

3. Using scissor dissection, free the skin and subcutaneous layer from the underlying contracted fascia palmaris. Identify and protect the neurovascular bundle of the finger because the diseased cord can displace it toward the midline. Once the fibrotic tissue (nodule and/or cord) is outlined, excise it sharply and regionally (subtotal) using a scalpel. Perform meticulous hemostasis under tourniquet control at the end of the procedure to prevent hematoma formation.
4. To close the skin, use additional Z-plasties to obtain partial lengthening of the skin.
5. For these studies use only the nodule part of the fibrotic cord, the most active and cellular part of the disease. Have the surgeon perform macroscopic identification. The isolated nodules in the palm of the hand are often precursors of a cord but are hardly ever resected, as they usually do not cause symptoms. The ones we resected were the nodules that were part of a cord of the contracted finger. Identify these nodules by the hard thick part of the cords in the handpalm (**Fig.1A**).
6. Once the surgeon removes the tissue, immediately transfer it using sterile forceps to a 50 ml tube containing DMEM medium supplemented with 10% FCS and 1% (P/S). Keep the tissue for a maximum of 2 hrs in this medium on a box of wet ice (4°C) (e.g. transportation of the tissue from the operation room to the cell culture facility).
7. Keep the samples on wet ice (4°C) while preparing for the next step. Preparation of the materials and cell culture chamber requires 10-20 min.

## **II. Preparation of instruments, culture medium and culture inserts**

Note: All procedures are performed at room temperature (RT) unless specifically stated.

1. Prepare 500 ml of DMEM supplemented with 10% FCS and 1% (P/S) and filter sterilize. Prewarm the medium at 37°C.
2. Autoclave forceps, a pair of curved-bladed Mayo scissors (150-170 mm in length) and a pair of Metzenbaum scissors and store in a sterile container.
3. Under laminar flow, open a sterile 12-well culture plate. Place a culture insert (0.45 µm pore size, 12 mm diameter) in each well of the 12-well plate (**Fig.1B**, lower panel).
4. Fill the 12-well plate with 600 µl of prewarmed (37°C) culture media by pipetting on the well and not directly on the membrane of the insert. Place the plate into the incubator (37°C, 5% CO<sub>2</sub>) (**Fig.1B**, upper panel)
  1. Alternatively, use a 24- well plate and add 300 µl of medium per well. The volume of medium per well is optimal when a meniscus layer is formed between the liquid and the lower part of the membrane insert. Note: the medium at the bottom of the well diffuses through the nitrocellulose membrane forming the meniscus layer as depicted in schemes of **Fig.1B** (lower panel).

### III. Tissue preparation and *ex vivo* tissue culture setup

Note: All procedures are performed at RT unless specifically stated.

1. Transfer the nodule part of the cord from the 50 ml tube on a 100 mm Petri dish and add 10 ml of prewarmed (37°C) medium. Ensure that the tissue is in contact with the liquid during the entire procedure.
  1. Remove the perinodular fat layer using the Metzenbaum scissors. Discard the fat tissue. With the use of forceps and the curved-bladed scissors, cut transversally the tissue into smaller pieces (maximum thickness 200 µm).
2. Transfer the 12- well plate from the incubator into the laminar hood. Check that the membrane of the insert has turned transparent (wet) and therefore is in contact with the medium.
3. Using forceps carefully lift a tissue part by touching the outer layer (do not apply tension on the tissue). Place one tissue part onto the membrane of the cell culture insert so that the tissue remains in the air-medium interphase. Culture a maximum of two tissue parts on the same insert/ well.
4. Ensure that the tissue is placed flat on the membrane, in longitudinal contact with the medium such that the tissue neither floats off the membrane nor is fully covered by medium. Avoid air bubbles.

Note: At this stage, it is possible to add growth factors or inhibitors of interest to the media; for instance, test compounds (A, B, C, D, E) in replicates and/or in concentration curve. Include at least 2 control (untreated) pieces of tissue under normal growth conditions to ensure that the experiment has been set up properly. Incubate tissues for 3-7 days in a tissue culture incubator.

5. Infect the tissue with either lentiviral or adenoviral construct if overexpression or knock down experiments of a gene-of-interest need to be performed (**Fig. 2**). Transfer a tissue part from the 12- well plate into a 35 mm dish using forceps.
  1. Use a maximum volume of 10 µl of high titer virus.
  2. Perform the injection under a dissection microscope with an insulin syringe loaded with 50 µl PBS containing 10 µl of the selected virus. Place the needle perpendicular to the center of the tissue.
  3. Slowly inject the content of the syringe. Do not retract the needle directly. When puncturing the tissue, do not let the needle go through the other side but maintain the needle within the tissue itself (around the center of the tissue).
  4. Transfer the tissue back into the 12- well plate, close the culture plate and place it into the incubator (37°C, 5% CO<sub>2</sub>).

**Table 1. Buffer solutions**

PBS (phosphate-buffered saline)	8.00 g NaCl (0.137 M) 0.20 g KCl (2.7 mM) 0.20 g $\text{KH}_2\text{PO}_4$ (1.1 mM) 0.10 g $\text{MgCl}_2 \cdot 6\text{H}_2\text{O}$ (0.5 mM) 2.16 g $\text{Na}_2\text{HPO}_4 \cdot 7\text{H}_2\text{O}$ (8.1 mM) 0.10 g anhydrous $\text{CaCl}_2$ (0.9 mM) $\text{H}_2\text{O}$ to 1 L
4% paraformaldehyde / PBS	Dissolve 4 g of paraformaldehyde in a flask containing 100 ml Phosphate Buffered Saline (PBS) in the fume hood, cover the flask. Place the flask on a heating-stirring block and gently stir the solution. Monitor the temperature so that it reaches a maximum of 65°C. Avoid over-heating. Once the paraformaldehyde has dissolved and the solution appears clear, switch off the heat but leave to stir. Do not handle for safety reasons. Allow cooling. When cooled, aliquot the solution and store long term in -20°C freezer or in a 4°C refrigerator for maximum a week.
BSA (bovine serum albumin), 10% (w/v)	Dissolve 10 g BSA in 100 ml $\text{H}_2\text{O}$ . Filter sterilize using a low-protein binding 0.22- $\mu\text{m}$ filter. Store at 4°C.
DMSO/Methanol (20%) permeabilization solution	Mix Dimethyl Sulfoxide with Methanol (1:4 analogies, total volume 100 ml).

## Chapter 4

### Materials

Name	Company	Catalog Number	Comments
Dulbecco's Modified Eagle's Medium	Invitrogen	11965-084	
fetal calf serum (FCS)	Gibco		high glucose, heat inactivated
penicillin-streptomycin	Invitrogen	15070-063	
Cell culture inserts	Millicell	PIHA01250	0.45 $\mu\text{m}$ pore size, 12 mm diameter
anti- $\alpha$ smooth muscle actin	Sigma	A2547	
anti-collagen type I	Southern Biotech	1310-08	
anti-collagen type III	Southern Biotech	1330-01	
Alexa Fluor555 Donkey Anti-Mouse IgG (H+L)	Invitrogen	A-31570	
Alexa Fluor 488 Donkey Anti-Goat IgG (H+L) Antibody	Invitrogen	A-11055	
TOPRO-3	Invitrogen	T3605	
methylsalicylate	Sigma	M6752	
paraformaldehyde	Sigma	P6148	
Tissue Tek OCT	Sakura	25608-930	
Microscope glass coverslips	Menzel-Glaser	BB024060A1	24 x 60 mm
Microscope SuperFrost slides	Menzel-Glaser	AA00000102E	76 x 26 mm
VECTASHIELD HardSet Mounting Medium	Vector laboratories	H-1400	
Leica TCS SP5 II confocal microscope	Leica Microsystems		Argon-488, 514 nm and HeNe-633 nm laser lines
Zeiss 710 NLO upright confocal microscope	Jena, Germany		Equipped with femtosecond Spectra - Physics Deep See MP laser (Santa Clara, United States) using a Plan-Apochromat 20X/1.0 NA water-immersion objective.

#### **IV. Whole-mount immunofluorescence staining and 3D reconstruction**

Note: All procedures are performed at RT unless specifically stated. The protocol for whole mount immunostaining and imaging described below is an adaptation from previously reported methods used for other tissues<sup>16-19</sup>.

Buffers and materials are described in **Table 1** and **Materials** list.

1. Transfer tissues from the culture plate to 2 ml microcentrifuge tubes containing PBS. Wash 2x for 5 min in PBS solution on a rotating platform. Fix tissues in 4% buffered PFA (1.5 ml solution per tissue in 2 ml microcentrifuge tubes), overnight at 4°C on a rotating platform.
2. Remove PFA and wash 3x in PBS for 5 min each.
3. Dehydrate tissues by immersion in a 25% methanol solution for 2 hr at RT on a rotating platform. Increase the methanol percentage gradually (50%, 75%, 100%) with the tissues immersed at each solution for 2 hrs at RT on a rotating platform.
4. Transfer tissues in DMSO/methanol solution (permeabilization step) for 3 weeks at 4°C, as described previously<sup>18</sup>.  
Note: At this stage, tissues can be stored long term in 100% methanol at -20°C.
5. Proceed with staining procedure<sup>16, 17</sup>; gradually rehydrate tissues (75%-50%-25%-0% methanol series). Perform each rehydration step for 2 hrs at RT or overnight at 4°C, under constant agitation.
6. Incubate samples with primary antibodies in PBS containing 1% bovine serum albumin (BSA) and 20% DMSO overnight at 4°C. Use antibodies at the following ratios using the commercial stocks in PBS: anti- $\alpha$  smooth muscle actin (1:500, mouse), anti-collagen type I (1:500, goat), anti-collagen type III (1:500, goat).
7. Wash extensively in PBS for 48 hrs at 4°C (change PBS solution 3 to 4 times).
8. Dilute appropriate secondary antibodies (Alexa 555 anti-mouse, Alexa 488 anti-goat) at 1:250 dilution in PBS containing 1% (BSA) and 20% DMSO. Incubate overnight at 4°C.
9. Wash extensively in PBS for 48 hrs at 4°C and incubate with nuclear counterstain, TO-PRO-3 diluted in PBS (1:500) was used at the final washing step.  
Note: TO-PRO-3 is a far-red emitting DNA dye (with a He-Ne 633 nm laser line) and is combined for simultaneous imaging with other channels; in this case collagen type I / collagen type III (488 nm),  $\alpha$  smooth muscle actin (555 nm), TO-PRO-3 (647 nm).
10. Transfer the tissues to a methanol series (25%-50%-75%) to slowly dehydrate the tissue; perform each dehydration step for 2 hrs at RT or overnight at 4°C under constant agitation.

1. Transfer tissues in polypropylene tubes. Clear tissues in methylsalicylate (handle under chemical hood)<sup>18</sup> or as an alternative use BABB solution<sup>19</sup>. Incubate the tissues at RT, under constant agitation, until they become transparent. Mount between a slide and a coverslip sealed with hard set mounting medium (**Fig.1C**, upper panel).
11. Image samples on an inverted confocal microscope equipped with high numerical aperture (NA) 63X and/or 100X oil immersion objectives (**Fig.1C**).
  1. Clean the lens with cleaning solution provided by the microscope manufacturer.
  2. Apply one drop of the oil on the objective lens. Place the slide with the specimen on the microscope stage and focus on the sample.
12. Set the configurations on the microscope for simultaneous imaging of three-channel fluorescence with laser lines 488 nm, 514 nm and 633 nm.
13. Acquire single XY images or multiple focal plane images (Z stack) (**Fig.3A**). Use increased width of Z stack for performing 3D reconstruction. To obtain a high-resolution image use low scanning speed, number of average scans ( $\geq 3$ ) and acquire 16-bit images of 1.024 x 1.024 pixel resolution.
14. Analyze the Z stack acquired images: first rename and save image file (xyz). Using the software program of the confocal microscope, configure a maximum intensity projection of the Z stack images into a 3D reconstructed image.
  1. Select the xyz file, in the "Process Tools", click under "Visualisation" and "3D Projection". Enter "Maximum" in the method of projection (or "Average" if the fluorescent signal is saturated). For a single projection do not change the X, Y, and Z planes, and apply the projection tool (**Fig.3B**, r1).
15. Use the Z stack images to create a 3D projection with animation (confocal software) for viewing purposes. Select the xyz file, in the Process Tools, click under "Visualisation" and "3D Projection".
  1. Click on "Create Movie". Enter the Start Rotation angle in degrees (e.g., 0° as starting point of the movie, Y axis) and click on "Set Start". Enter the End Rotation angle in degrees (Y axis) as end point of the movie (e.g. 180° or 360° for a complete rotation) and click on "Set End".
  2. Select "Maximum" as a method of projection (or "Average" if the fluorescent signal is saturated). Enter the "Number of Frames" for the rotation of the 3D reconstruction (e.g. 20 rotations or higher to reduce the speed of rotation). Click on "Apply". Export the movie as visual file (e.g. "avi") (**Supplementary Movie 1**) or export as "tiff" file which creates an image file for each rotation angle (**Fig.3B**; rotation r4, r10, r18).

## V. Combined second harmonic generation (collagen) and two-photon excited fluorescence (elastin) imaging on ex vivo tissue during culture

Note: All procedures are performed at RT unless specifically stated.

1. Remove transwell plates from incubator and place a single (unfixed) tissue part in a 35 mm cell culture plate containing 500  $\mu$ l of medium.
2. Position the tissue so that the long axis is flat on the plate. Keep tissue wet at all times however, not floating.
3. Place water-immersed objective of the multiphoton microscope directly in contact with the tissue (**Fig.1C**).
4. Obtain images with an excitation wavelength of 800 nm and collect emitted light between 371-425 nm (SHG, collagen) and 474-532 nm (autofluorescence, elastin) (**Fig.3C**). Perform two-photon microscopy in an upright confocal microscope that is equipped with a femtosecond laser using a 20X/ 1.0 NA water-immersion objective. Process confocal stacks with manufacturer's software.

Note: Excitation with a near infrared laser of collagen molecules creates high contrast imaging of native collagen structures in different depths.

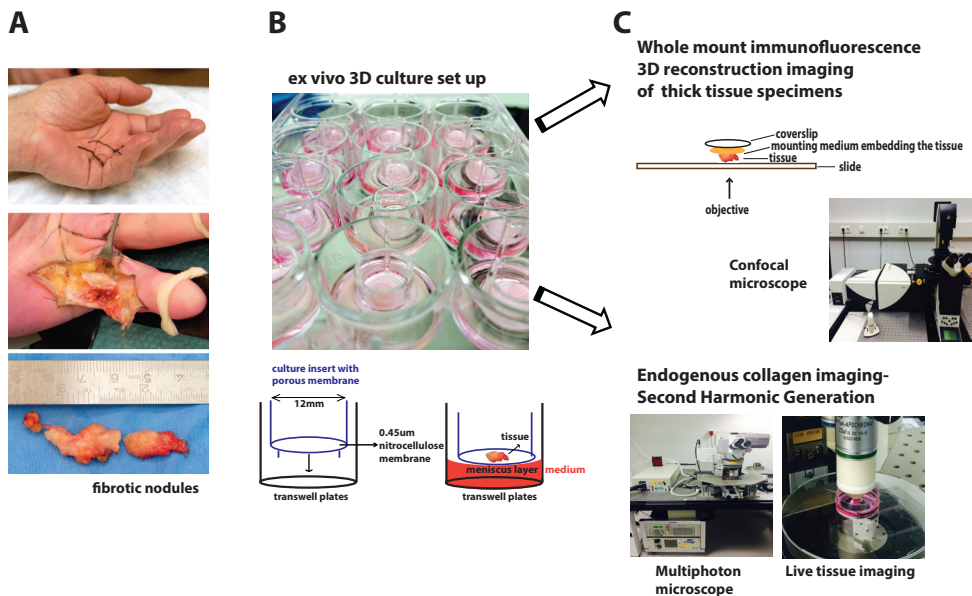


**Fig.1. Scheme of ex vivo 3D tissue culture system**

(A). DD permanent flexion contracture in the hand of a patient prior to surgical removal. This figure has been modified from previous study<sup>5</sup>. (B). Example of ex vivo culture set up. (C). Examples of experimental approaches that can be used for analysis of ECM deposition.



### Representative Results

The method of *ex vivo*, 3D culture of connective tissue is an easy and robust set up system to understand the relation between ECM and other cell components constituting the DD tissue and potentially other types of fibrosis as well. Moreover this system provides a reliable method to test the effects of compounds on different cell types and their effects on the fibrotic load <sup>20</sup>.

The steps from collection of surgical waste material derived from Dupuytren's fibrosis, the assembly of the culture chamber and examples of analysis tools are presented in **Fig.1**. As illustrated in **Fig.1**, this method provides an experimental tool for large screens drug screens, e.g., antifibrotic drug compounds as well as the study of ECM modelling in a real-time and reproducible manner. Nodular parts of the fibrotic cord are equally sliced and placed in transwell plates; each tissue part (100-200  $\mu\text{m}$ ) is cultured on top of the membrane of a culture insert (0.45  $\mu\text{m}$  pore size, 12 mm diameter). Culture medium is added at the bottom chamber, allowing contact with the tissue through the membrane. On average 30-40 tissue parts can be derived from a single resection specimen, which allows large-scale screening of drugs; compounds, small molecules or growth factors. Experiments addressing the concentration and/or time-dependent effect of drugs are feasible.

As shown in **Fig.2**, gene expression can be manipulated (overexpression/ knock down) by the use of adeno/ lentiviruses directly injected into the tissue. Fluorescently tagged viral transduction is performed in fresh thick tissue specimens by injection. Tissue remains in culture for 24- 48 hours post-injection and is subsequently fixed, embedded and sectioned in 0.7  $\mu\text{m}$  cryosections.

Moreover, to analyze the effect of different compounds or culture conditions the tissue parts are fixed and subjected to whole mount immunofluorescence as shown in **Fig.3**. 3D imaging of thick tissues is done by confocal microscopy (**Fig.3A-B**). Another method is the live 3D imaging on tissues maintained in culture; endogenous collagen remodeling is studied real-time in freshly dissected, non-fixed tissue parts by second harmonic generation (SHG) (**Fig.3C**). The effect of potential anti-fibrotic drugs is also followed in parts of the same tissue at different time points. Collagen structures of thick tissue are imaged using SHG in an upright multiphoton microscope. During imaging, tissue specimens are placed in medium and are imaged with a water-immersion objective. After imaging, the tissues can be transferred back to the culture system. Effects can be studied at the level of cellular and extracellular environment providing an advantage over *in vitro* cell-based assays. There are multiple possibilities for analysis of biological effects such as histology of fixed tissue sections, whole mount immunofluorescence and 3D reconstruction imaging by confocal microscopy, SHG and two-photon excited fluorescence imaging of endogenous collagen and elastin. Some of the advantages of the SHG imaging are the use of fresh, non-fixed tissue, that no antibody staining preparation is required and that the same tissue can be imaged multiple times (time course during culture conditions). SHG and two-photon excited fluorescence imaging has been described previously for muscle and connective tissue<sup>21-23</sup> and unstained arterial wall structure<sup>24</sup>, however, here we report an alternative application for the study of Dupuytren's fibrosis.

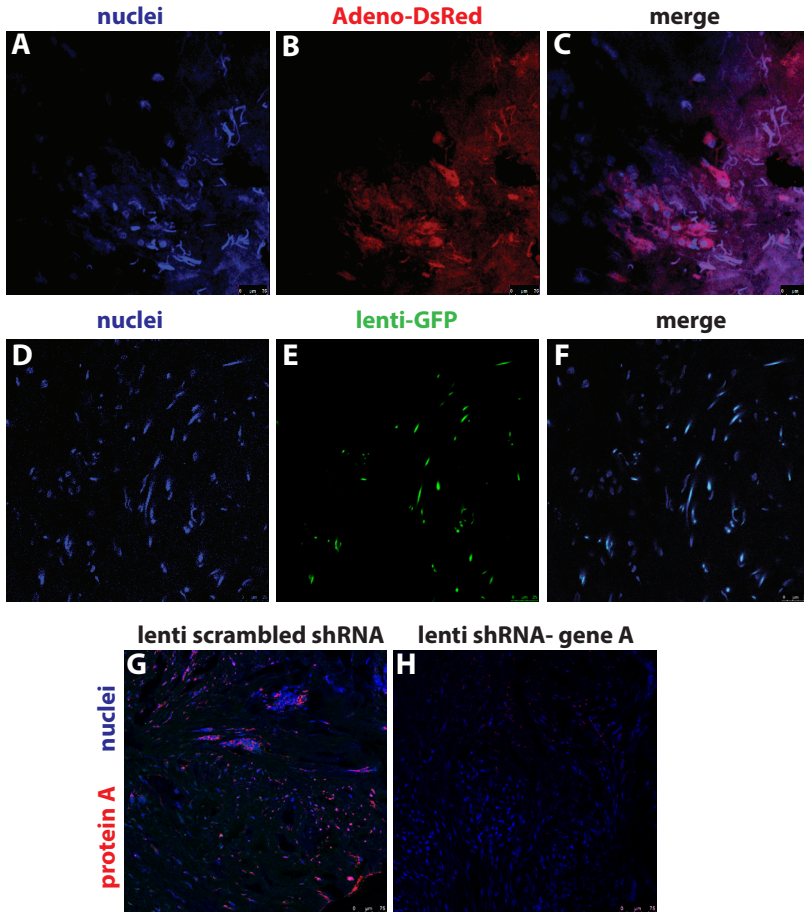


**Fig.2. Proof-of-principle *ex vivo* viral-mediated gene expression modulation in whole mount tissue**

(A-C). Adenoviral transduction; (A). Nuclei are visualized with TO-PRO-3 dye (blue). Bars 75  $\mu\text{m}$ . (B). Direct visualization of the fluorescent dye DsRed (red), post-injection with Adenovirus expressing-DsRed. Bars 75  $\mu\text{m}$ . (C). Merged image (nuclear staining in blue, DsRed in red). Cytoplasmic localization of DsRed indicating adenoviral delivery in the cells within 24 hours. Bars 75  $\mu\text{m}$ . (D-F). Lentiviral transduction; (D). Nuclei are visualized with TO-PRO-3 dye (blue). Bars 25  $\mu\text{m}$ . (E). Direct visualization of GFP in tissue sections (green), post-injection with lenti-GFP particles. Bars 25  $\mu\text{m}$ . (F). Merged image of D and E indicating intracellular localization of lenti-GFP. Bars 25  $\mu\text{m}$ . (G-H). Example of lentivirus-mediated knockdown against gene of interest (designated as "A"); (G). Lentivirus carrying scrambled shRNA sequence was injected *ex vivo* into the tissue. Immunofluorescence staining for protein of interest (designated as "A") shown in red. Bars 75  $\mu\text{m}$ . (H). Lentivirus carrying gene A-shRNA sequence was injected *ex vivo* into the tissue. Immunofluorescence staining for protein "A". Nuclei are stained with TO-PRO-3 dye. Bars 75  $\mu\text{m}$ .

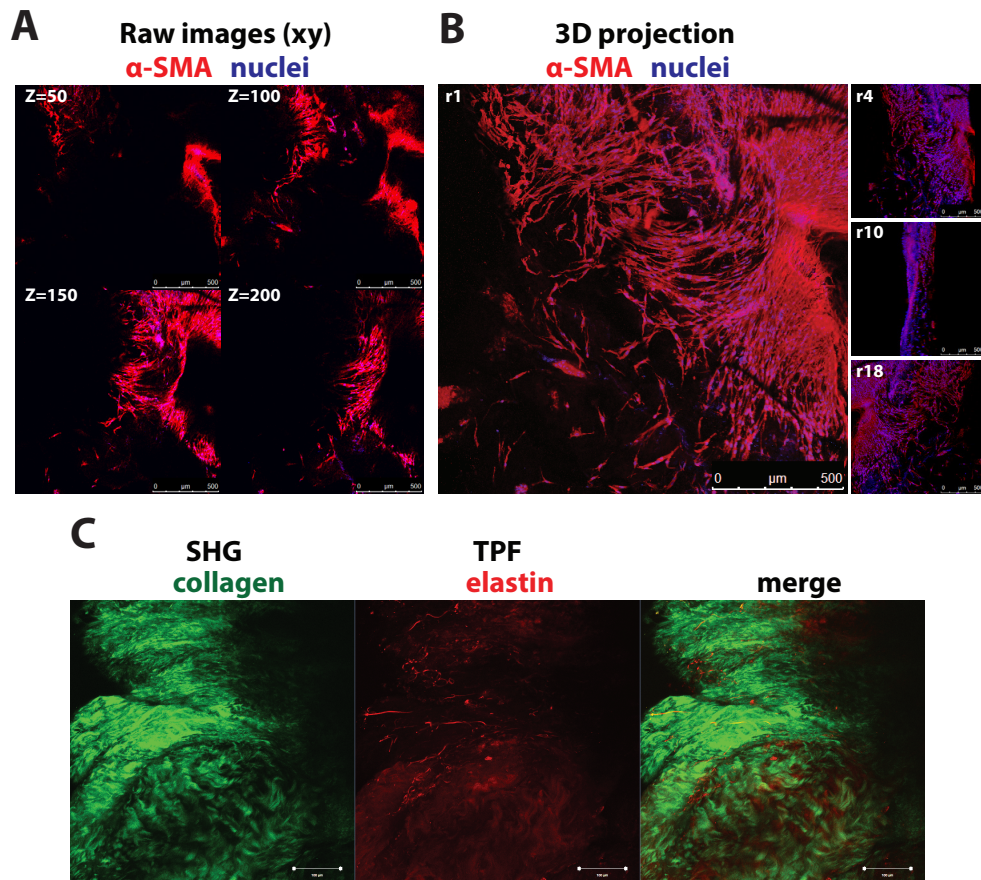


**Fig.3.3D reconstruction imaging, second harmonic generation and two-photon excited fluorescence imaging** (A). 3D imaging by confocal microscopy. Single (xy) images in focal planes along different tissue depths ( $z = 50\text{--}200\ \mu\text{m}$ ). Whole mount immunofluorescence staining; myofibroblast marker  $\alpha$ -smooth muscle actin ( $\alpha$ SMA, red), nuclear staining (TO-PRO-3, blue). Bars:  $500\ \mu\text{m}$ . (B). 3D reconstructed image (Z stack  $389\ \mu\text{m}$ ) of raw images as indicated in panel A at different 3D rotations indicated as “r1”, “r4”, “r10”, “r18”. Bars  $500\ \mu\text{m}$ . (C). Endogenous collagen content modeling by second harmonic generation (SHG) imaging in fresh, thick tissue parts (left panel, green). Two-photon excited fluorescence (TPF) of elastin structures of the ECM was captured by multiphoton microscopy (middle panel, red). Merged image of collagen (green) and elastin (red) (right panel). Bars:  $100\ \mu\text{m}$ .

**Supplementary Movie 1. Representative 3D reconstruction movie of Dupuytren’s whole mount tissue**

Confocal imaging of DD tissue was performed after seven-day *ex vivo* culture and processing for whole mount immunofluorescence staining; myofibroblast marker  $\alpha$ -smooth muscle actin ( $\alpha$ SMA, red), nuclear staining (TO-PRO-3, blue). Scale bar =  $500\ \mu\text{m}$ . Frames= 20. Z=  $389\ \mu\text{m}$ .

([http://www.jove.com/files/ftp\\_upload/52534/Movie%201.avi](http://www.jove.com/files/ftp_upload/52534/Movie%201.avi))

## Discussion

The most critical steps of culturing *ex vivo* human connective tissue are the immediate use of the tissue after surgical removal to ensure viability; the tissue should remain in medium or saline solution at all times; maintain a sterile culture; transverse sections of tissue should have maximum 200  $\mu\text{m}$  thickness; set up of the *ex vivo* culture system is optimal when tissue is in contact with the medium but not fully submerged. Medium should be added only on the outside chamber of the transwell in a small volume (e.g. 500- 600  $\mu\text{l}$  per 12-well plate surface area).

Connective tissue derived from Dupuytren's is entangled in a tough structure with high content of ECM proteins such as collagen, proteoglycans, and elastin; due to these properties and additionally due to myofibroblast contracture it can be challenging to cut through the tissue. It is important to use appropriate surgical tools; curved bladed Mayo scissors for cutting larger parts in equal thickness and smaller surgical scissors for cutting smaller tissue parts (e.g., if more tissue parts are required use 24- well plates).

Methods for the study of DD are histopathological analyses of the excised fibrotic specimen, or derivation of primary fibroblasts. Cell derivation from the patient material is done in two ways; in one of the methods, tissue parts are cultured in plastic culture plates for a number of weeks until there is outgrowth of fibroblasts. The second method is enzymatic treatment of tissue with collagenase and trypsin. The first method is time consuming, fibroblast properties are altered due to culture conditions and there is passage-dependent variability among passages of the same cell line. The enzymatic method is faster and it can be used for cell sorting assays, however, *in vitro* maintenance of these cells out of the innate ECM does not reflect the *in vivo* properties. The model presented here is suitable for cell and ECM morphology studies and several techniques have been successfully utilized such as immunofluorescence, flow cytometry, RNA analyses, whole mount 3D imaging, and collagen deposition measurements (secreted in the culture media). However, total protein isolation from the tissue parts, cell signaling experiments and protein immunoblotting require optimization and are not as robust as the monolayer fibroblast cultures. Another drawback of the method is lack of mechanical tension engineered to the culture system. Most connective tissues exist under a constant or basal mechanical force, even during resting conditions, which not only provides mechanical support but also influences cell behavior and signaling<sup>25</sup> (namely mechanoregulation and mechanotransduction). Loss of tension results in disassembly of  $\alpha\text{SMA}$  fibers in MFBs in short period of time<sup>26</sup>. The abundance of  $\alpha\text{SMA}$  in the *ex vivo* cultured tissues indicates MFB contractility. Nevertheless, our model could benefit from incorporation of an isometric force transducer<sup>27,28</sup>. Regarding technical and biological variability, our method is reproducible (viability, ECM network) and less prone to tissue alteration due to short time of culture. For instance, the method of fibroblast outgrowth requires several weeks which may cause biochemical changes (e.g. accumulation of genetic mutations, replicative senescence). However, patient- specific genetic characteristics and biological variability are *per se* challenges in the DD research field and cannot be tackled with any of the current methods.

As shown in this protocol, fibrotic DD specimens after surgical removal are directly cultured in the *ex vivo* 3D system and/or snap frozen. Depending on the scientific question, modification of the tissue is possible by addition of growth factors, chemical compounds, virus- mediated gene delivery, antisense oligonucleotides and miRNAs. Compounds can be delivered in the media or with local microinjections of the tissue in the 3D culture chamber. After 3 (up to

## Chapter 4

---

7) days of culture the tissue can either be homogenized for cell isolation and FACS analysis or isolation of total RNA and proteins for expression profile analysis, as well as processed for histological analysis. The expression status of fibrous proteins ( $\alpha$ SMA, collagen type I and II, fibronectin), tissue architecture of the nodule part of the cord and the consistency of the fibrous network is assessed before and after the treatments. In order to monitor the ECM rearrangements during the culture we combined the SHG (collagen) and two-photon excited fluorescence (elastin) imaging.

The extracellular rearrangements can then be quantified or modeled using an image quantification software. These parameters give an indication of the drug effects on fibrosis or the molecular alterations that have been induced during the culture. Moreover ECM arrays can also be performed on single slices to generate a better overview of the effects. Overall we have established a robust system that allows the study of fibrosis *ex vivo*.

### Disclosures

The authors have filed a Patent Application for Dupuytren's disease: 3D organ culture (# GB1307200).

### Acknowledgements

The authors are thankful to the nurses at the AMC that have facilitated the collection of tissue. We would also like to acknowledge A.M.A. van der Laan for excellent technical support with the SHG and the two-photon imaging.

## References

1. Shih, B. and A. Bayat, Scientific understanding and clinical management of Dupuytren disease. *Nat Rev Rheumatol*, 2010. 6(12): p. 715-726.
2. Bisson, M.A., et al., The different characteristics of Dupuytren's disease fibroblasts derived from either nodule or cord: expression of  $\alpha$ -smooth muscle actin and the response to stimulation by TGF- $\beta$ 1. *J Hand Surg Br*, 2003. 28(4): p. 351-356.
3. Brickley-Parsons, D., et al., Biochemical changes in the collagen of the palmar fascia in patients with Dupuytren's disease. *J Bone Joint Surg Am*, 1981. 63(5): p. 787-797.
4. Berndt, A., et al., Appearance of the myofibroblastic phenotype in Dupuytren's disease is associated with a fibronectin, laminin, collagen type IV and tenascin extracellular matrix. *Pathobiology*, 1994. 62(2): p. 55-8.
5. Karkampouna, S., et al., Novel ex vivo culture method for the study of Dupuytren's disease: effects of TGF $\beta$  type 1 receptor modulation by antisense oligonucleotides. *Mol Ther Nucleic Acids*, 2014. 3: p. e142.
6. Kruithof-de Julio, M., et al., Canonical Wnt signaling regulates Nkx3.1 expression and luminal epithelial differentiation during prostate organogenesis. *Dev Dyn*, 2013. 242(10): p. 1160-1171.
7. Krause, C., P. Kloen, and P. ten Dijke, Elevated transforming growth factor  $\beta$  and mitogen-activated protein kinase pathways mediate fibrotic traits of Dupuytren's disease fibroblasts. *Fibrogenesis Tissue Repair*, 2011. 4(1): p. 14.
8. O'Gorman, D.B., et al., Wnt expression is not correlated with  $\beta$ -catenin dysregulation in Dupuytren's disease. *J Negat Results Biomed*, 2006. 5: p. 13.
9. Streuli, C.H., et al., Extracellular matrix regulates expression of the TGF- $\beta$  1 gene. *J Cell Biol*, 1993. 120(1): p. 253-260.
10. Vogel, V. and M. Sheetz, Local force and geometry sensing regulate cell functions. *Nat Rev Mol Cell Biol*, 2006. 7(4): p. 265-275.
11. Gottrup, F., M.S. Ågren, and T. Karlsmark, Models for use in wound healing research: A survey focusing on in vitro and in vivo adult soft tissue. *Wound Repair Regen*, 2000. 8(2): p. 83-96.
12. Gudjonsson, T., et al., Normal and tumor-derived myoepithelial cells differ in their ability to interact with luminal breast epithelial cells for polarity and basement membrane deposition. *J Cell Sci*, 2002. 115(1): p. 39-50.
13. Xu, R., A. Boudreau, and M. Bissell, Tissue architecture and function: dynamic reciprocity via extra- and intra-cellular matrices. *Cancer Metastasis Rev*, 2009. 28(1-2): p. 167-176.
14. Jokinen, J., et al., Integrin-mediated cell adhesion to type I collagen fibrils. *J Biol Chem*, 2004. 279(30): p. 31956-31963.
15. Au-Yong, I.T.H., et al., A review of common practice in Dupuytren surgery. *Tech Hand Up Extrem Surg*, 2005. 9(4): p. 178-187.
16. Deries, M., J.J.P. Collins, and M.J. Duxson, The mammalian myotome: a muscle with no innervation. *Evol Dev*, 2008. 10(6): p. 746-755.
17. Deries, M., et al., Extracellular matrix remodeling accompanies axial muscle development and morphogenesis in the mouse. *Dev Dyn*, 2012. 241(2): p. 350-364.
18. Martins, G.G., et al., Dynamic 3D cell rearrangements guided by a fibronectin matrix underlie somitogenesis. *PLoS One*, 2009. 4(10): p. e7429.
19. Yokomizo, T., et al., Whole-mount three-dimensional imaging of internally localized immunostained cells within mouse embryos. *Nat. Prot*, 2012. 7(3): p. 421-431.
20. Karkampouna, S. and M. Kruithof-de Julio, Fibrosis: a novel approach for an old problem. *Receptors Clin Investig*, 2014. 1(5).
21. Wolf, K., et al., Collagen-based cell migration models in vitro and in vivo. *Semin Cell Dev Biol*, 2009. 20(8): p. 931-941.
22. Freund, I., M. Deutsch, and A. Sprecher, Connective tissue polarity. Optical second-harmonic microscopy, crossed-beam summation, and small-angle scattering in rat-tail tendon. *Biophys J*, 1986. 50(4): p. 693-712.
23. Mohler, W., A.C. Millard, and P.J. Campagnola, Second harmonic generation imaging of endogenous structural proteins. *Methods*, 2003. 29(1): p. 97-109.
24. Boulesteix, T., et al., Micrometer scale ex vivo multiphoton imaging of unstained arterial wall structure. *Cytometry Part A*, 2006. 69A(1): p. 20-26.
25. Tomasek, J.J., et al., Myofibroblasts and mechano-regulation of connective tissue remodelling. *Nat Rev Mol Cell Biol*, 2002. 3(5): p. 349-363.

## Chapter 4

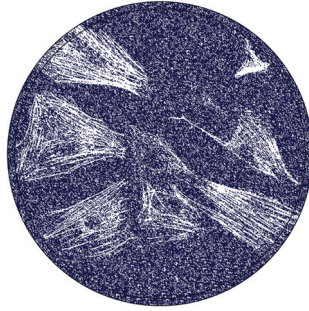
---

26. Hinz, B., et al., Mechanical tension controls granulation tissue contractile activity and myofibroblast differentiation. *Am J Pathol*, 2001. 159(3): p. 1009-1020.
27. Eastwood, M., D.A. McGrouther, and R.A. Brown, A culture force monitor for measurement of contraction forces generated in human dermal fibroblast cultures: evidence for cell-matrix mechanical signaling. *Biochim Biophys Acta*, 1994. 1201(2): p. 186-192.
28. Verjee, L.S., et al., Post-transcriptional regulation of  $\alpha$ -smooth muscle actin determines the contractile phenotype of Dupuytren's nodular cells. *J Cell Physiol*, 2010. 224(3): p. 681-690.









## Chapter 5

# Novel *ex vivo* culture method for the study of Dupuytren's disease: effects of TGF $\beta$ type I receptor modulation by antisense oligonucleotides

**Sofia Karkampouna<sup>1</sup>, Boudewijn P.T. Kruithof<sup>1</sup>, Peter Kloen<sup>2</sup>, Miryam C. Obdeijn<sup>3</sup>, Annelies M.A. van der Laan<sup>1</sup>, Hans J. Tanke<sup>1</sup>, Dwi U. Kemaladewi<sup>4</sup>, Willem M. H. Hoogaars<sup>4</sup>, Peter A.C. 't Hoen<sup>4</sup>, Annemieke Aartsma-Rus<sup>4</sup>, Ian M. Clark<sup>5</sup>, Peter ten Dijke<sup>1</sup>, Marie-José Goumans<sup>1</sup>, Marianna Kruithof-de Julio<sup>1,\*</sup>**

<sup>1</sup>Department of Molecular Cell Biology, Leiden University Medical Center, Leiden, The Netherlands.

<sup>2</sup>Department of Orthopedic Surgery, Academic Medical Center, Amsterdam, The Netherlands.

<sup>3</sup>Department of Plastic, Reconstructive and Handsurgery, Academic Medical Center, Amsterdam, The Netherlands.

<sup>4</sup>Department of Human Genetics, Leiden University Medical Center, Leiden, The Netherlands.

<sup>5</sup>School of Biological Sciences, University of East Anglia, Norwich Research Park, UK.

\* Corresponding author

***Molecular Therapy Nucleic Acids, 2014 Jan 21;3:e142***



## **Abstract**

Dupuytren's disease is a benign fibro-proliferative disease of the hand. It is characterized by the excessive production of extracellular matrix proteins, which form a strong fibrous tissue between the handpalm and fingers, permanently disrupting the fine movement ability. The major contractile element in Dupuytren's disease is the myofibroblast. This cell has both fibroblast and smooth muscle cell-type characteristics and causes pathological collagen deposition. Myofibroblasts generate contractile forces that are transmitted to the surrounding collagen matrix. Major pro-fibrotic factors are members of the Transforming growth factor-β pathway which directly regulate the expression levels of several fibrous proteins such as collagen type I, collagen type III and alpha-smooth muscle actin. Molecular modulation of this signaling pathway could serve as a therapeutic approach. We, therefore, have developed an *ex vivo* "clinical trial" system to study the properties of intact, patient-derived resection specimens. In these culture conditions, Dupuytren's tissue retains its three-dimensional structure and viability. As a novel antifibrotic therapeutic approach, we targeted Transforming growth factor-β type I receptor (also termed Activin receptor-like kinase 5) expression in cultured Dupuytren's specimens by antisense oligonucleotide-mediated exon skipping. Antisense oligonucleotides targeting Activin receptor-like kinase 5 showed specific reduction of extracellular matrix and potential for clinical application.

## **Introduction**

Dupuytren's disease (DD) is a common fibrotic disorder of the hand, found with high prevalence among Caucasians of Northern European descent<sup>1</sup>. This enigmatic benign fibro-proliferative disease affecting the connective tissue (**Fig.1A**) results from a complex interplay of genetic, anatomic and environmental factors<sup>2</sup> with main clinical manifestation being the excessive collagen deposition. A disturbance of the heterogeneous mix of static and dynamic contractile elements located throughout the fascia of the palm and digits can lead to the development of flexion deformities (contracture). Although not associated with high morbidity, the impact on movement ability and quality of life of the patients affected by DD is major. Currently, the common therapy for DD is palmar fasciectomy, which consists of surgical removal of fibrotic tissue and results in immediate improvement of disease. However, due to the high recurrence rate and re-manifestation of fibrotic bands, surgery is not a permanent solution.

Several studies have elucidated the aetiopathology of DD which is crucial for the design of novel therapies. Uncontrolled wound healing response leads to permanent extracellular matrix (ECM) deposition e.g. collagen. The cell responsible for ECM production in normal as well as in pathologic conditions is the myofibroblast (MFB), containing both fibroblast and smooth muscle cell-type characteristics<sup>3</sup>. MFBs generate contractile forces that are transmitted to the surrounding collagen matrix<sup>4</sup> and are distinguished by alpha-smooth muscle actin (ACTA2) expression. In pathological conditions ACTA2 expression is persistent. Major pro-fibrotic factors are members of the transforming growth factor-β (TGFβ) pathway which directly regulate the expression levels of several intracellular and extracellular fibrous proteins such as COL1A1, COL3A1 and ACTA2<sup>3,5-7</sup>, fibronectin, matrix metalloproteases, integrins, all of which are aberrantly deregulated in DD<sup>8,9</sup>. TGFβ ligands interact with TGFβ type I receptor (also termed Activin receptor-like kinase 5 (ALK5)/TGFβRI and type II (TGFβRII) receptor complexes which subsequently activate by phosphorylation the SMAD2/3 effectors,

which form heteromeric complexes with SMAD4 and act as downstream transcriptional effectors of the pathway. Activation and transdifferentiation of DD fibroblasts towards MFBs is mainly controlled by TGF $\beta$  signaling<sup>10-13</sup>. Other cytokines, such as platelet-derived growth factor (PDGF), are induced by TGF $\beta$ <sup>14</sup> and also enhance MFB differentiation. TGF $\beta$  and PDGF factors are aberrantly activated in DD<sup>10,15,16</sup>. In particular, in DD patient-derived MFB cultures, overactive TGF $\beta$  signaling causes spontaneous contraction and proliferation<sup>13,15</sup>. Contractility is attenuated by inhibiting TGF $\beta$  and TGF $\beta$  receptor (ALK5) function<sup>15,17,18</sup>. We have recently shown that the TGF $\beta$ /SMAD and PDGF/ERK1/2 MAP kinase pathways cooperate in mediating the enhanced proliferation and spontaneous contraction of DD fibroblasts<sup>15</sup>. Inhibiting the uncontrolled fibrotic mechanisms by directly targeting the overactivation of the TGF $\beta$  signaling, mediated via its ALK5 receptor, at the molecular level, could be an effective treatment.

A promising approach to deplete the cells from the function of key receptor of TGF $\beta$  signaling (ALK5) is by alternative splicing methodology. Particular exon(s) encoding protein domains crucial for protein function can become excluded from the mature messenger RNA (mRNA). Specific antisense oligonucleotides (AON) bind to sites involved in exon splicing to the splice sites of a targeted exon and interfere with the splice machinery; therefore the particular exon is not integrated as part of the mRNA<sup>19</sup>. The resulting mRNA has an intact open reading frame and is translated into a protein which lacks only the particular peptide sequence encoded by the skipped exon. The advantage of this system is that no genetic alterations are introduced, since interference is exclusive during pre-mRNA splicing process. AON methodology has broad therapeutic applicability in certain human diseases<sup>20</sup>, particularly in the field of muscular dystrophies<sup>20</sup> with very promising results reported for clinical trials<sup>21,22</sup>. Based on this principle, we employed the AON-mediated exon skipping technology for disrupting the protein function of the ALK5, targeting in particular the extracellular ligand binding domain. AONs targeting splice sites of exon encoding extracellular ligand binding domain (exon 2) of the ALK5<sup>23</sup> have been developed and tested *in vivo* (D.U. Kemaladewi et al., manuscript submitted). This strategy ensures no loss of other important domains of ALK5, such as the transmembrane domain (encoded by exon 3) or serine-threonine kinase activity domain (exon 4- 9). ALK5 AON was administered directly to the DD patient-derived specimens by microinjecting it in the center of the tissue, and the effects on fibrosis and ECM deposition were assessed with various imaging and biochemical methods. In this study we show that DD resected specimens, which are discarded as waste material after surgery, can be maintained viable in defined culture conditions in our novel *ex vivo* model. Their study can provide us with useful information about the underlying patient-specific pathology and drug response.

## Materials and Methods

### Generation of 3D culture system

Specimens from DD surgeries are equally sliced and placed in transwell plates onto 0.4  $\mu$ m nitrocellulose membranes (Greiner Bio One) in defined culture conditions (Dulbecco's Modified Eagle's Medium (DMEM, with 1% fetal calf serum (FCS), 1% penicillin-streptomycin) and allowed to grow (seven days). Nutrient exchange occurs by diffusion from the medium through the membrane while DD tissue remains continuously in contact with the liquid but is not immersed. Tissue resection specimens (N=9 DD and N=4 normal fascia palmaris)

were treated with a combination of activators and inhibitors of the TGF $\beta$  signaling pathway (e.g. TGF $\beta$ , 5ng/ml; SB-431542, 10ng/ml, Tocris). After culture, tissues were processed for RNA isolation or were fixed in 4% paraformaldehyde, incubated in 30% sucrose buffer, embedded in Tissue Tek- O.C.T. compound and stored at -80°C.

### Human tissue specimens

DD tissue was collected during a standard partial fasciectomy procedure. Indications for surgery were contracture(s) of the digit(s) with an inability to put the hand flat on the table (table top test). Only patients with first time occurrence of DD were included in this study. The range of age of patients was between 63- 88 years old, with 91% being males. Macroscopic identification (with surgical loupe magnification) of a nodule (representing most active disease) was done by the operating surgeon. Only nodules were used in our study. The nodules were defined as being the hard thick parts of the cord, mostly situated in the palm of the hand. This part was taken out of the cord after resection of the entire DD cord. The normal fascia palmaris tissue of the control group was collected during carpal tunnel release procedures. The included control patients did not suffer from DD. The operations were performed under local anaesthesia and under tourniquet control. After opening the skin through a longitudinal incision the fascia was identified and a small piece of fascia was harvested before incising the transverse carpal ligament. The tissue specimen was divided in two equal pieces, one of each was immediately processed for 3D culture and the other one was snap-frozen in liquid nitrogen and stored at -80°C. Oral consent for removal of the tissue for research purposes was obtained from the patients. Confirmation that the Medical Research Involving Human Subjects Act (WMO) does not apply to the present study was obtained by the local ethics committee (reference number W12\_245 #12.17.0279) since the research was performed on "waste" material.

### Antisense Oligonucleotides

The antisense oligonucleotides (AONs) used to target ALK5 were developed and recently described in another study, in which *in vitro* and *in vivo* efficiency of the different AONs was extensively tested in the context of muscular dystrophies (D.U. Kemaladewi et al., manuscript submitted). In short, the AONs targeting ALK5 specifically bind to and induce exon skipping of exon 2 of the ALK5 precursor mRNA transcript. Exon 2 encodes for the ligand binding domain, which is, together with the type II receptor, essential in capturing the ligand to initiate signaling. Exclusion of exon 2 generate a transcript with intact open reading frame, while the resulting protein will lack the ligand binding domain and is therefore functionally impaired. Vivo-morpholino AONs with a morpholino backbone and an octaguanidine moiety to enhance cellular uptake were used in this study since they have been shown to increase exon skipping efficiency in animal models<sup>24</sup>. ViM AONs (0.5 nmol and 1 nmol, Genetools) were diluted in 1% FBS-DMEM or PBS and were microinjected in the tissue. The sequences (5'-3') of the ViM AONs are the following: ALK5ViM: GCAGTGGTCTCTGATTGCAGCAATAT, ScrViM: CCTCTTACCTCAGTTACAATTTATA. The 2'-O-methyl ribose AONs with phosphorothioate modifications (2'-O-Me) were obtained by Eurogentec.

ALK5 2'-O-Me: UGUACAGAGGUGGCAGAAACA, Scr 2'-O-Me: GCAAGAUGCCAGCAGA

### RNA isolation, RT-PCR and Quantitative PCR

See Supplementary Materials and Methods for details.

### Microscopy and Image analysis

See Supplementary Materials and Methods for details.

### Immunofluorescence

See Supplementary Materials and Methods for details.

## Results

### Human derived DD tissue can be maintained under *ex vivo* culture conditions

Fibroblast derivation from DD specimens requires a long culture period during which cells adapt to culture conditions (plastic surface, high oxygen, removal of ECM). Such changes of the native microenvironment may result in partial recapitulation of the disease state or fibro-proliferative characteristics of the tissue in fibroblast two- dimensional cultures<sup>25,26</sup>. We have developed a three- dimensional (3D) culture system (**Fig.1A-B**), which allows human resection specimens to be grown *ex vivo* (up to seven days) in defined conditions. Longer culture periods (up to 12 days, data not shown) lead to increased cell death (cleaved caspase 3 positive cells) and absence of proliferation, suggesting non viability of tissue after a certain time point (day 7). We show that DD resection specimens in the *ex vivo* “clinical trial” system maintain viability, proliferation (phosphohistone-3, pH3) and apoptosis levels (TUNEL) (**Fig.1G**). As control tissue we have used normal fascia palmaris from carpal tunnel surgeries, which is not affected by DD. Control tissue was successfully maintained in culture for up to seven days and is characterized by low levels of proliferation (pH3) and apoptosis (TUNEL) (**Fig.S1**, upper panel). Histological characterization of the cultured DD biopsies showed that the high expression of fibrotic proteins: ACTA2, COL1A1 and COL3A1 is preserved (**Fig.1G**, representative images), therefore they recapitulate the *in vivo* properties. Similar data were obtained from a number of biopsies (normal fascia palmaris, N=7, DD non cultured tissue, N=4, and DD tissue after seven days 3D culture, N=9) indicating the reproducibility of the method. Quantification of immunofluorescence signal for COL1A1, COL3A1 and ACTA2 (**Fig.1D-F**), in multiple patient-derived specimens showed that biopsies cultured *ex vivo* retain the expression characteristics with regards to fibrosis.

Basal expression of ACTA2, COL1A1 and COL3A1 (**Fig.1C-G**), as well as *TGFβ1* and *PAI-1* mRNA levels (*TGFβ* target genes) (**Fig.1C**), are elevated in both cultured and non-cultured DD resection specimens compared to fascia palmaris (control, non- affected tissue). Moreover, the snap-frozen and the 3D cultured DD (matching) resection specimens similarly show areas of proliferating MFBs and low apoptosis (**Fig.1G**). All together, the above data indicate that DD tissue under culture conditions remains representative of the disease.

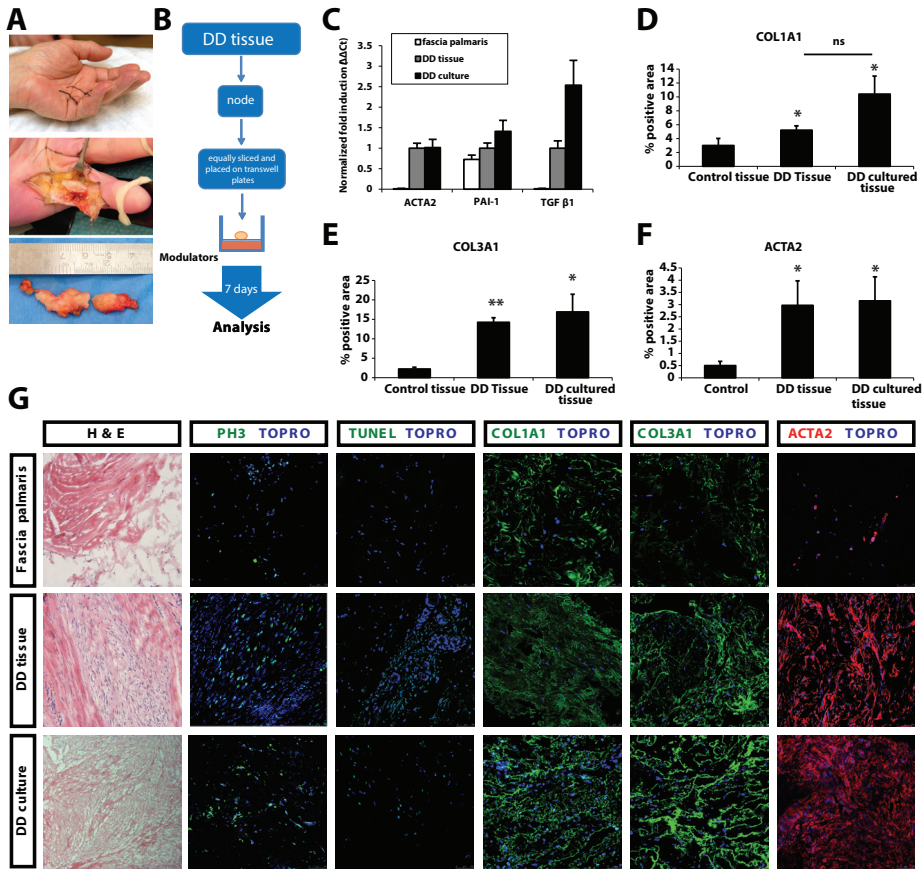


**Fig.1. Characterization of DD contracture tissue in the 3D *ex vivo* “clinical trial” system**

(A). DD contracture in the hand of a patient; example of DD tissue prior and after resection. (B). Cartoon describing 3D culture method: DD tissues are equally sliced (about 1 mm), placed on a nitrocellulose membrane and cultured up to seven days. (C). Q-PCR on control normal fascia palmaris (N=7), DD non-cultured tissue (see DD tissue, N=4) and DD cultured tissue (see DD culture, N=9). Error bars represent  $\pm$ S.E.M. *ACTA2*, *TGFβ1* and *PAI-1* mRNA levels have been quantified and normalized to *ACTRT1*. Fold induction values compared to DD non-cultured tissue are shown. (D-F). Quantification (described in methods) of immunofluorescence signal of COL1A1, COL3A1 and ACTA2 in normal fascia palmaris (N=7), DD non cultured tissue (see DD tissue, N=4) and DD tissue after seven days 3D culture (see DD culture, N=9). Multiple focal planes were quantified per sample, error bars represent  $\pm$ S.E.M. Statistical significance was calculated by one-tailed paired t-test. \* $p < 0.05$ , \*\* $p < 0.01$ . (G). Immunohistochemical and immunofluorescent analysis of normal fascia palmaris, DD non-cultured tissue and DD cultured tissue. Hematoxylin and Eosin (H&E), proliferation marker phosphohistone 3 (PH3, green), apoptosis terminal deoxynucleotidyl transferase dUTP nick end labeling (TUNEL) assay (green), Collagen type I (COL1A1, green), Collagen type III (COL3A1, green) and smooth muscle actin, alpha 2 (ACTA2, red). Nuclei were visualized with TO-PRO3 (TOPRO, blue). Scale bars, 25  $\mu$ m.



### Small molecule inhibitor of TGF $\beta$ type I receptor kinase (SB-431542) decreases expression of fibrotic proteins in DD specimens

Our novel *ex vivo* culture method was further used to test the response of the DD tissue to stimulation with different factors directly after fasciectomy procedure. Main profibrogenic stimulus in DD is the TGF $\beta$  signaling; consequently we decided to interfere with the activation status of this particular pathway. Resection specimens (both control (**Fig.S1**) and DD (**Fig.2A**)) were treated with TGF $\beta$  ligand as well as a pharmacological TGF $\beta$  type I receptor (ALK4, ALK5, ALK7) kinase activity inhibitor (SB-431542). Addition of TGF $\beta$  to cultured DD specimens resulted in increased expression of target genes ACTA2, COL1A1 and COL3A1 in the majority of individual human samples tested or sustained the high levels (**Fig.2B-D**). This observation suggests high sensitivity of DD MFB cells to TGF $\beta$ , also confirmed by high expression of phosphorylated SMAD2 protein (pSMAD2) (**Fig.2A**). As expected, treatment with the SB-431542 inhibitor compound in our model suppressed the profibrogenic action of TGF $\beta$  and resulted in a trend reduction of the expression of fibrous proteins ACTA2, COL1A1 and COL3A1 (**Fig.2**). Differential expression levels among individual samples after TGF $\beta$  and/or SB-431542 treatments were observed. Proliferation (pH3) and apoptosis (Caspase 3) were not significantly affected by the addition of either TGF $\beta$  or SB-431542 (**Fig.2A**). Treatment of control tissue with TGF $\beta$  cytokine caused an upregulation of ACTA2, COL1A1, COL3A1 expression (**Fig.S1**, middle panel), suggesting a responsiveness of the tissue to the treatment and underlining the profibrotic effect of TGF $\beta$ . The above observations may suggest that the 3D *ex vivo* culture system is suitable for chemical compound screening. Differences in the response of human specimens to growth factor or inhibitor SB-431542 most probably derives from variation among different individuals which can be effectively observed and represented using our *ex vivo* culture system.

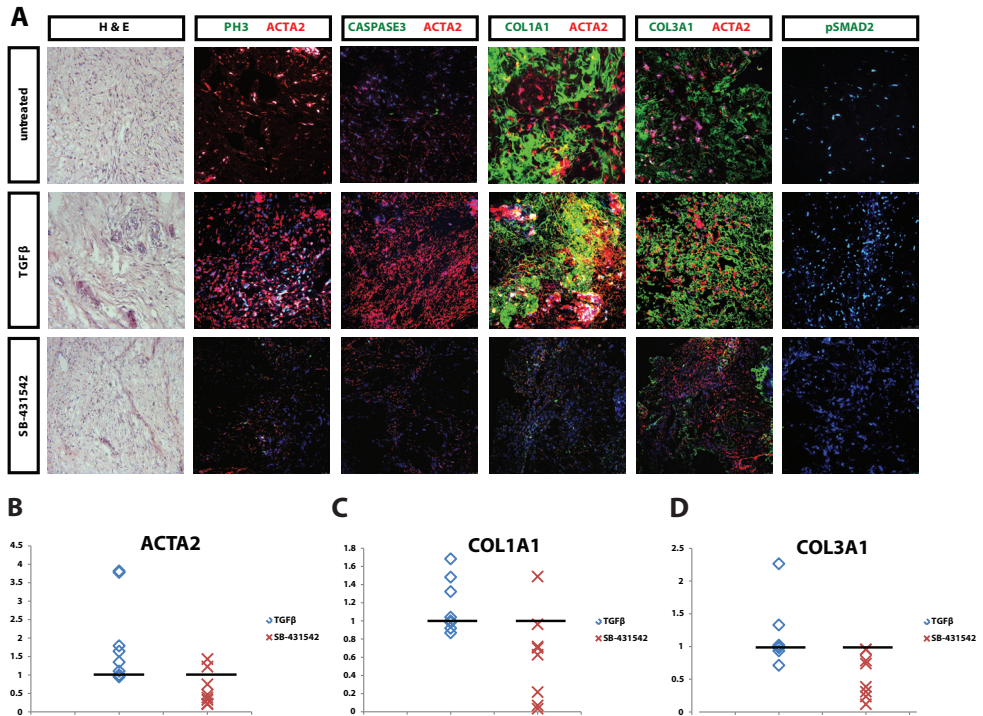


**Fig.2. Inhibition and stimulation of TGFβ pathway in DD resection specimens cultured in 3D *ex vivo* “clinical trial” system**

(A). Immunohistochemical and immunofluorescent analysis of 3D cultured DD resection specimens before treatment (untreated) and after seven-day treatment with TGFβ or ALK4/5/7 kinase inhibitor SB-431542. Hematoxylin and Eosin (H&E), proliferation marker phosphohistone 3 (PH3, green), apoptosis marker cleaved caspase 3 (CASPASE3, green), Collagen type I (COL1A1, green), Collagen type III (COL3A1, green), smooth muscle actin, alpha 2 (ACTA2, red) and phosphorylated SMAD2 (pSMAD2) (green). Nuclei were visualized with TO-PRO-3 (TOPRO, blue). Representative data from eight patient derived specimens (N=8). Scale bars, 25 μm. (B-D) Distribution of fold quantitative values of ACTA2 (B), COL1A1 (C), and COL3A1 (D) among 8 patient-derived specimens after *ex vivo* culture. Quantification of fluorescent signal within certain area fraction was calculated in Image J software for every specimen in three different conditions; untreated (control, no exogenous factors), TGFβ cytokine and ALK4/5/7 kinase inhibitor SB-431542 compounds. Graph represents the values of positive signal of ACTA2, COL1A1, COL3A1, after treatment with TGFβ or SB-431542 compounds as a fold induction over the value of the control “untreated” sample (indicated by black line).

### AON- mediated exon skipping of ALK5

While treatment with SB-431542 resulted in a promising downregulation of fibrotic pathways, this chemical inhibitor blocks the kinase activity of ALK4, ALK5 and ALK7 in a dose dependent way<sup>27</sup>. Thus, in order to ensure higher specificity and less interference with other signaling pathways we have tested a novel strategy to selectively inhibit the function of the ALK5. We used *vivo*-morpholinos (ViM) based on previously developed AON sequence (D.U. Kemaladewi et al., manuscript submitted) that selectively target and disrupt the ligand binding domain of ALK5 by inducing exon skipping of mRNA transcripts. Microinjection (**Fig.3A**) of resection specimens with fluorescently labelled AON demonstrated efficient uptake (>90%) and transport to the nucleus throughout the tissue (**Fig.3B-C**). Similarly, the AON targeting ALK5 (ALK5ViM) was microinjected in the centre of the tissues after placing them on the nitrocellular membrane of the transwell culture plates (**Fig.3A**). At day 3 we validated the skipping of exon 2 by PCR (**Fig.3D-E**) and verified reduction of full length ALK5 mRNA expression (**Fig.4B**) compared to tissues injected with control scrambled ViM (ScrViM). No effect on the proliferation rate and apoptosis was observed by the use of ALK5ViM (**Fig.4A**). We performed a time course experiment to monitor the levels of full length ALK5 mRNA expression versus the exon skipped mRNA. Full length ALK5 mRNA is decreased by 70-75% during the first 48 hours after AON administration (**Fig.S2A**). These data indicate that high rate of exon skipping is achieved at early time points and maintained in the tissue explant cultures. We also determined the collagen expression in different time points and observed a gradual decrease of COL1A1 expression (**Fig.S2B**).

### ALK5 AON causes a reversal of fibrotic phenotype *ex vivo*

Constant collagen deposition is the main feature of DD, thus, clinical attempts have been focused on direct induction of collagen degradation *in vivo*, such as by injectable collagenase treatment<sup>28</sup>. Although very promising, this therapeutic approach is associated with several limitations (high morbidity), and cannot completely replace the surgical treatment<sup>29</sup>. Our objective was to interfere with the fibrogenic role of TGF $\beta$  in a clinically relevant manner. However, TGF $\beta$  is a regulator of many crucial processes such as inflammation and wound healing in many organs and is secreted by many cell types including macrophages, endothelial cells, lymphocytes, epithelial cells. Thus, TGF $\beta$  should be tightly regulated and complete abolishment may lead to adverse effects. The process of exon skipping by AONs is advantageous because it results in partial and not complete blockage of the ALK5 receptor activity. Administration of the ALK5ViM directly to DD tissues (N=3) remarkably reduced the overall protein expression of ACTA2, COL1A1 and COL3A1 (**Fig.4A**) and activation of downstream pSMAD2 (**Fig.4A, S3**), rendering the tissue more similar to the control, normal fascia palmaris (**Fig.S1**). Quantification of the expression patterns among different specimens (N=3) confirmed a reproducible decrease observed after ALK5ViM treatment (**Fig.4C-E**). The spatiotemporal imaging of the endogenous extracellular distribution of collagen structure was determined by Second Harmonic Generation (SHG) on DD specimens during 3D culture, prior and after ALK5ViM application (**Fig.4F**). Reorganization/ degradation of collagen fibres, specifically at the site of injection with the ALK5ViM was observed with SHG (**Fig.4F**, white arrow) similarly to immunofluorescence signal (**Fig.4A**). In contrast, tissue injected with ScrViM retained the highly anisotropic collagen structures and did not exhibit signs of reorganization/degradation (**Fig.4F**). A partial reduction of available ALK5 molecules

appears already sufficient to reduce the fibro-proliferative effect mediated by TGFβ in fibroblasts/ MFBs. Importantly; mRNA molecules that escape exon skipping do produce functional ALK5 protein able for ligand binding (TGFβ) and protein complex formation with type II receptors. Thus, application of AONs does not cause complete abolishment of the TGFβ signaling, which is required at a basal level for tissue/ ECM maintenance.

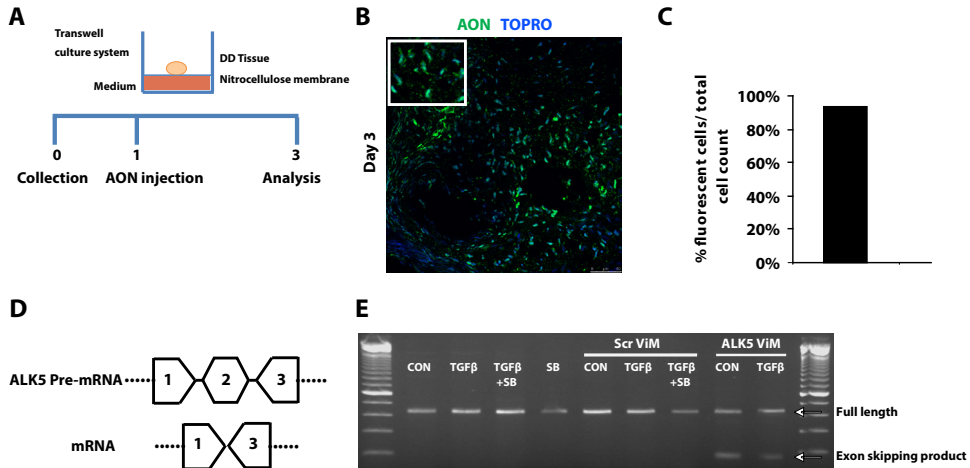


**Fig.3. Microinjection of AONs in DD resection specimen maintained in 3D culture and ALK5 exon skipping** (A). AONs coupled to a fluorochrome (AON-fluorescent) were delivered by microinjecting the center of the tissue on the nitrocellulose membrane as described in the cartoon. The tissue was then cultured for three days and sectioned in order to determine the presence of nuclei, which had taken up the AON. (B). Direct visualization of the AON-fluorescent (green) and nuclei (TOPRO, blue) in a DD tissue section. (C). Quantification of the percentage of fluorescent cells (AON) relative to total cell count. Scale bars, 50 μm. (D). Description of exon skipping (exon 2) of the ALK5 pre-mRNA. Primer position (exon 1 and exon 3) of primers used for detecting the full length ALK5 and the exon skipped mRNA product are depicted here. (E). DD tissues were cultured and injected with either scrambled (ScrViM) or ALK5ViM. For comparison, treatment with TGFβ or SB-431542 compound was also combined with ViM administration. After three days of treatments, tissues were homogenized and used for RNA isolation and cDNA synthesis. Touchdown PCR was performed to validate the exon skipping and products were visualized by agarose gel electrophoresis. Full length ALK5 mRNA transcripts were detected in all conditions while exon2-skipped ALK5 mRNA transcripts were only detected in tissues injected with ALK5ViM. CON: untreated condition; TGFβ: treatment with TGFβ cytokine, SB: treatment with SB-431542 compound; TGFβ+SB: treatment with both TGFβ and SB-431542 compound.

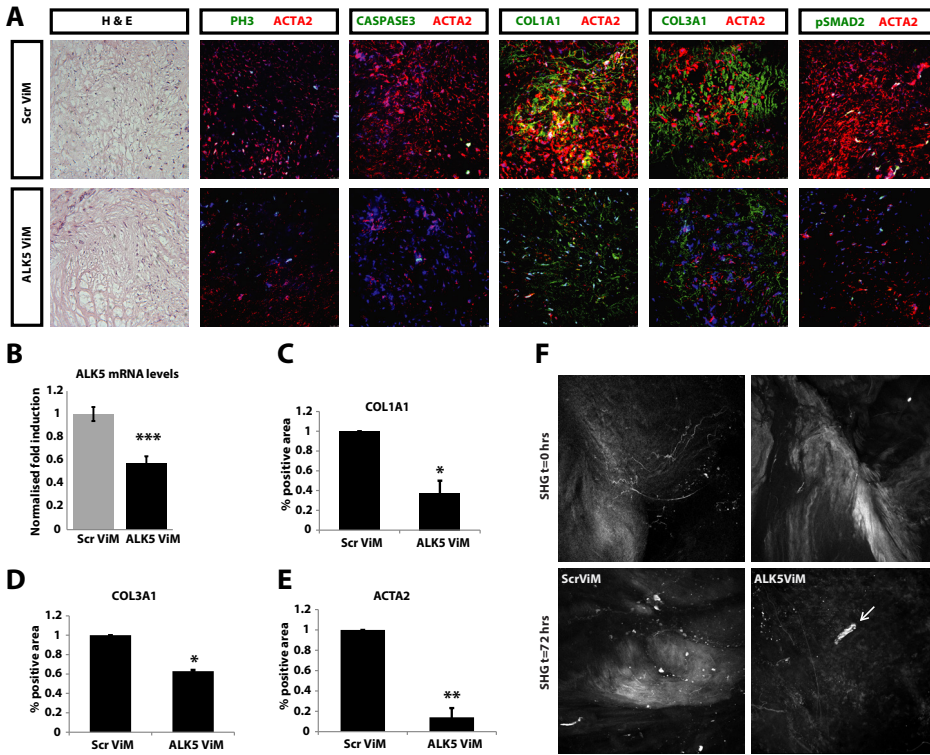


**Fig.4. ALK5ViM treatment of DD resection specimens cultured in the 3D *ex vivo* “clinical trial” system**

(A). Immunohistochemical and immunofluorescent analysis of 3D cultured DD resection specimens after three-day treatment with scrambled ViM (ScrViM) and ALK5ViM. Hematoxylin and Eosin (H&E), proliferation marker phosphohistone 3 (PH3, green), apoptosis marker cleaved caspase 3 (CASPASE3, green), Collagen type I (COL1A1, green), Collagen type III (COL3A1, green), phosphorylated SMAD2 (pSMAD2) (green) and smooth muscle actin, alpha 2 (ACTA2, red). Nuclei were visualized with TOPRO-3 (TOPRO, blue). (B). QPCR to detect expression levels of full length *ALK5* mRNA was performed on tissues injected with ScrViM and ALK5ViM (N=3). Values were normalized to *CAPNS1*. Fold induction values compared to ScrViM condition are shown. Statistical significance was calculated by one-tailed paired t-test. \*\*\*p<0.001. (C-E). Quantification (described in methods) of immunofluorescence signal of COL1A1, COL3A1, ACTA2 from different patient-derived specimens (N=3) after three-day treatment with scrambled ViM (ScrViM) and ALK5ViM. Fold induction values compared to ScrViM condition are shown. Multiple areas were quantified per sample, error bars represent  $\pm$ S.E.M. Statistical significance was calculated by one-tailed paired t-test. \*p<0.05, \*\*p<0.01. Scale bars, 25  $\mu$ m. (F). SHG images of endogenous DD tissue in the 3D culture system. Collagen distribution was imaged at control time point (SHG, t=0, upper panel) in adjacent parts of the specimen. The exact tissue parts were imaged at 72 hrs (SHG, t=72 hrs, bottom panel) after injection of ScrViM or ALK5ViM. Arrow indicates site of injection.

## Discussion

In the present study, we have developed a novel method for *ex vivo* analysis of human DD disease and we provide evidence of its suitability for molecular modulation by AONs. AONs were designed to target and inhibit a key profibrotic signaling pathway, which results in significant antifibrotic effects. Given the high risk of recurrence of DD, it would be therapeutically beneficial to reduce local collagen content in order to extend the symptom-free period after surgery, needle fasciotomy and/or collagenase injection. Our *ex vivo* "clinical trial" system allows the culture of DD specimens after surgical removal, without the need of fibroblast derivation, or grafting experiments<sup>30</sup>, while preserving the pathological status of the disease by maintaining the complex organization of the ECM and the 3D tissue structure. The main challenges in *ex vivo* culture methods are viability and preservation of the *in vivo* normal or pathological traits of the tissue to be studied. Several organ culture and precision cut tissue slice methods have been developed such as the submerged system<sup>31,34</sup>, the dynamic organ culture<sup>32</sup> and the gas exchange method<sup>31</sup>. Organ viability, functionality, metabolism and toxicity can be well studied in all these systems for complex organs such as liver, kidney, intestine, and lungs<sup>33,34</sup>. A limitation of these methods is the relatively short incubation time possible (approximately 24- 72 hours), depending on the tissue origin, as well as the challenge of organ/disease recapitulation. Our methodology is based on an enhanced setup where tissue parts are placed continuously and statically in contact with nutrients but are not fully immersed into medium, thus maintaining proper oxygenation and avoiding necrosis in the center of the tissue. Such setup appears suitable for culture of dense tissue such as DD fibrotic parts and facilitates viability for longer periods (up to seven days tested). Exposure of one side of the tissue to the medium is sufficient for diffusion and absorbance of nutrients throughout the tissue. Small tissue parts (<200um) are preferable in order to allow cell proliferation and longer viability<sup>35</sup>. Static incubation was performed, in contrast to most dynamic culture conditions, in order to maintain positional information and cellular sensing<sup>36,37</sup>.

In addition, this particular setup allows for manipulation (e.g. AON injection) and direct visualisation of the effects on the ECM (SHG). Since DD tissue shows rapid production of ECM proteins, all tissues were cultured in absence of any exogenous matrix substrates. This is advantageous for the maintenance of native ECM turnover. Moreover, this culture setup is optimal for DD fibrotic tissue due to the content of highly proliferative MFBs and because the nodules and cords are *in vivo* quite isolated structures with autonomous characteristics (such as cell/ tissue growth and fibrosis). Due to these innate properties, it is likely that the tissues can be maintained *ex vivo* efficiently.

In this study, we have exclusively utilized the nodule parts, which are the firm thickenings and are considered pathologically very active due to the high content of MFBs. Cord parts are mainly fibrotic flexions and contain few fibroblasts, which are in a dormant state<sup>38</sup>. It has been proposed that active nodules may progress into cord structures at more advanced stage of the disease<sup>39</sup> therefore it is more clinically relevant to target the fibrotic characteristics of the node parts. TGF $\beta$  has been found to be expressed in both parts, as well as in the surrounding tissue<sup>4</sup> (appearing not affected by the disease), which may play a role in promoting recurrence of fibrosis as part of wound healing response due to tissue damage from the primary surgery. The majority of the resection specimens we have analysed using this system respond to TGF $\beta$  stimulation by upregulation or maintenance of the expression levels of fibrotic proteins (**Fig.2B-D**). Decrease in COL1A1 and COL3A1 but not of ACTA2 has

been detected in two biopsies after TGF $\beta$  stimulation which may suggest the function of a negative feedback loop due to high levels of TGF $\beta$ <sup>40,41</sup>. Upon treatment of DD biopsies with the SB-431542 inhibitor, expression of collagen and ACTA2 were decreased in the majority of biopsies or sustained the same levels as if untreated (**Fig.2B-D**).

Previous studies have attempted manipulation of TGF $\beta$  by neutralizing antibodies<sup>30</sup> and kinase inhibitors<sup>15</sup>. TGF $\beta$  has been also targeted in indirect ways such as by cyclic AMP<sup>42</sup>, angiotensin inhibitors<sup>43</sup>, tamoxifen<sup>44</sup>, administration of Bone morphogenetic protein-6<sup>15</sup>. Given the pleiotropic effect of TGF $\beta$  signaling, the aim is to normalize and not completely abolish its function. Therefore, in order to restore the balance of pathway activation without fully disrupting its function, we have selectively inhibited the ALK5- mediated profibrotic pathway by exon skipping technology. It is worth noting that AON approach provides the advantage of high specificity exclusively for ALK5 mRNA (exon 2 encoding ligand binding domain), while the SB-431542 compound targets activity of three kinase receptors (ALK4, ALK5, ALK7), all implicated in the activin/ TGF $\beta$  pathway. Moreover, SB-431542 may not block TGF $\beta$ / ALK5 induced non-SMAD signaling<sup>45,46</sup> whereas ALK5 AON will inhibit both pathways. TGF $\beta$ / p38 and ERK MAP kinases have been shown to be involved in fibro-proliferative response in Dupuytren's disease<sup>15</sup>. Delivery of ALK5 AON by affecting SMAD and non-SMAD TGF $\beta$  signaling may thus achieve better inhibition than ALK5 kinase inhibitors by interfering with multiple pathways downstream of ALK5. Compared to regular oligonucleotides, small molecule inhibitors have better pharmacokinetic properties, due to the short half-life and inability to efficiently cross tissue membranes. However, currently there are many oligonucleotide modifications available that ensure improved stability, serum half-life and uptake of oligonucleotides. Our studies here use ViMs, which are antisense phosphorodiamidate morpholino oligomers covalently linked to a molecular scaffold that carries a guanidinium group at each of its eight tips to enhance delivery, to show proof-of-concept for this approach. Efficacy of ViMs has also been shown by others in animal models<sup>47</sup>. However, further clinical development of this particular compound is hampered by toxic effects. Nevertheless, there is a plethora of chemical modifications available that can be studied further for clinical development<sup>48</sup>. In light of this, it is encouraging that we were able to obtain similar results with ALK5 AONs of the 2'-O-methyl phosphorothioate AON chemistry (**Fig.S4**, which is very similar to the chemistry approved by FDA (mipomersen<sup>49</sup>) and identical to drisapersen, which is in phase III clinical trials for Duchenne muscular dystrophy). TGF $\beta$  secretion might also play a significant role in the recurrence of fibrosis after surgical removal. In this context, a hypothetical therapeutic setting would be the administration of AONs prior to or instead of the surgical intervention to counteract the TGF $\beta$  signaling in the remaining MFBs.

A challenge in the field of Dupuytren's is the lack of *in vivo* modelling of the disease. Here, we have developed a very robust and reproducible *ex vivo* 3D culture method with a simple setup (no growth factors or matrix protein support required). By using the ALK5ViM AON in this system, we have showed significant decrease in collagen protein expression and degradation/reorganisation of collagen structures. Excessive collagen production is the main clinical symptom in this disease and here we provide proof of decrease in collagen deposition *ex vivo*. The average reduction of full length ALK5 mRNA achieved was 70-75% within the first 48 hours (**Fig.S2A**) and about of 30-60% by day 3 (**Fig.4B, S2A**). Our data indicate the potential of MFBs to reverse into a less fibrotic phenotype and to respond to growth factor inhibition even after advanced disease progression. In addition, we show the feasibility of a well-established *ex vivo* imaging approach, such as the SHG<sup>41,50</sup>, for the

study of ECM structure in native unstained tissue which to our knowledge has not been previously used for DD. The above observations may change the view of therapeutic approaches currently used for DD. Ultimately, the *ex vivo* “clinical trial” system can be applied for individualized therapy research after tissue resection as a drug screening method to test for specific responsiveness of DD tissues to a panel of growth factors and inhibitors and eventually lead to targeted therapy in case of recurrence.

## Acknowledgements

This study was supported by Netherlands Organization for Scientific Research (NWO-MW), Netherlands Institute for Regenerative Medicine (NIRM), Cancer Genomics Centre and Netherlands Centre for Biomedical Genetics.

## Conflict of interest

The authors declare no conflict of interest.

## Supplementary Material

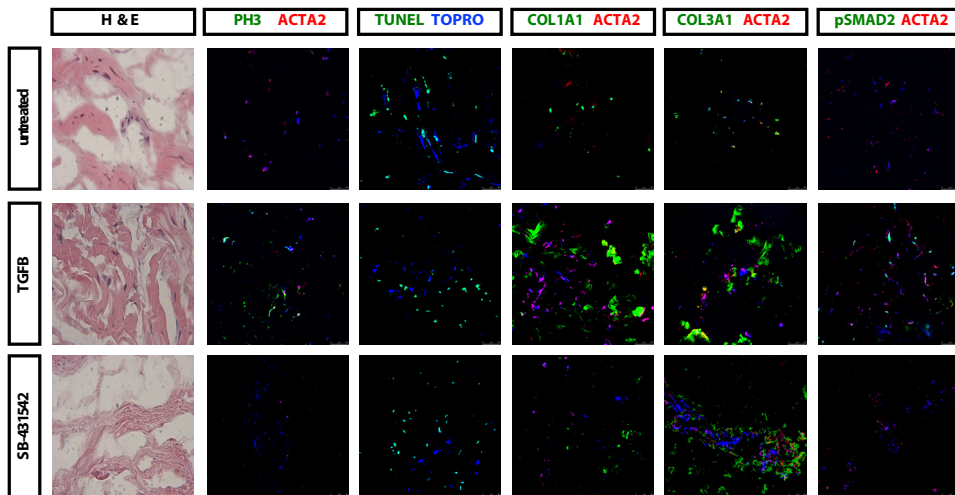


**Fig.S1. Normal fascia palmaris tissue cultures in the 3D *ex vivo* “clinical trial” system**

Representative immunohistochemical and immunofluorescent analysis of 3D cultured normal fascia palmaris specimens (N=4). Hematoxylin and Eosin (H&E), proliferation marker phosphohistone 3 (PH3, green), apoptosis terminal deoxynucleotidyl transferase dUTP nick end labeling assay (TUNEL, green) in control normal fascia palmaris without any additional factors (untreated), after treatment with TGFβ and after treatment with ALK4/5/7 kinase inhibitor SB-431542. Collagen type I (COL1A1, green), Collagen type III (COL3A1, green), phosphorylated SMAD2 (pSMAD2, green) and smooth muscle actin, alpha 2 (ACTA2, red) protein expression in control normal fascia palmaris without any additional factors (untreated), after treatment with TGFβ and after treatment with ALK4/5/7 inhibitor (SB-431542). Nuclei were visualized with TO-PRO-3 (TOPRO, blue). Scale bars, 25 μm.



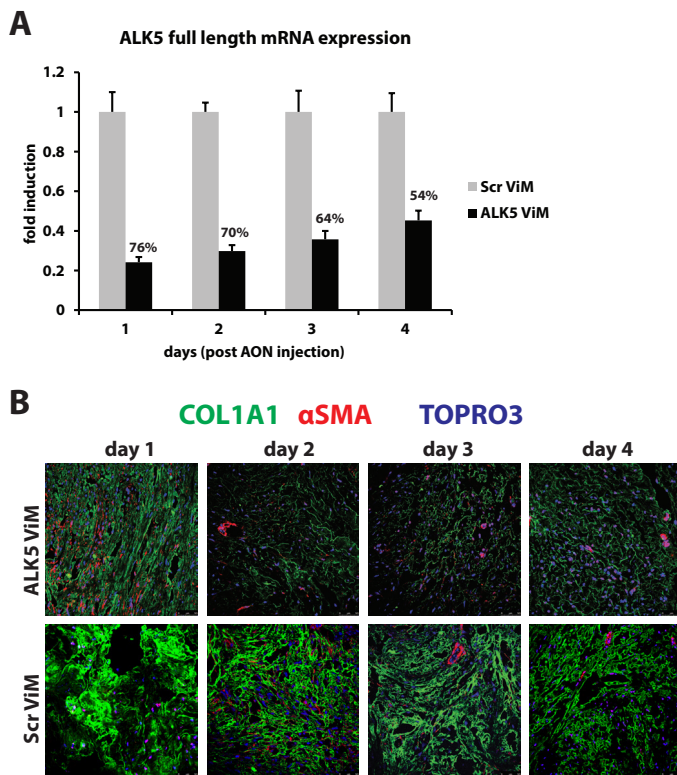


**Fig.S2. Time course of ex vivo delivery of ALK5 ViM AON**

Tissues were injected with ScrViM AON (scrambled sequence) or ALK5ViM AON and cultured for 1- 4 days. (A). Expression of full length ALK5 mRNA as measured by Q-PCR at different time points (day 1- day 4 after AON injection). Values were calculated as fold induction over the ScrViM (control) values for each time point. Error bars represent  $\pm$ S.D. Percentages indicate the decrease of ALK5 full length mRNA expression. (B). Immunofluorescent analysis of DD tissue specimens cultured in the 3D ex vivo system. Expression of Collagen type I (COL1A1, green), smooth muscle actin, alpha 2 (ACTA2, red) is shown. Nuclei were visualized with TO-PRO-3 (TOPRO, blue). Scale bars, 50  $\mu$ m.

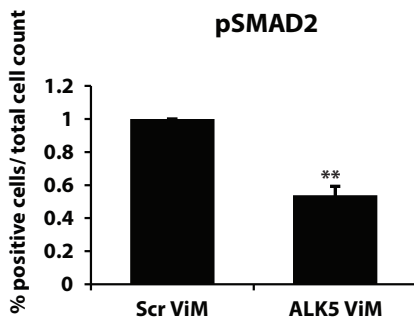


**Fig.S3. Quantification of pSMAD2 immunofluorescence by image analysis.**

Number of pSMAD2 positive nuclei over total cell count (TO-PRO-3) after three-day treatment with scrambled ViM (ScrViM) and ALK5ViM. Fold induction values compared to ScrViM condition are shown. Multiple areas were quantified per sample (N=3), error bars represent  $\pm$ S.E.M. Statistical significance was calculated by one-tailed paired t-test. \*\* $p < 0.01$ .

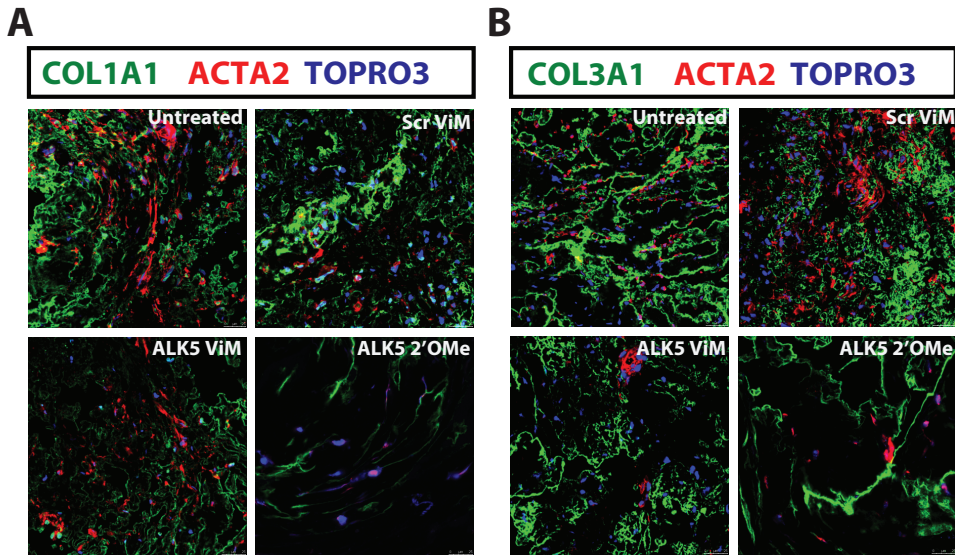


**Figure S4. Ex vivo delivery of ALK5 AON with ViM and 2'OMe chemical backbones**

Immunofluorescent analysis of DD tissue specimens cultured in the 3D *ex vivo* system. Tissues were injected with ScrViM AON (scrambled sequence), ALK5ViM AON or ALK5 2'OMe AON and cultured for 72 hours. (A). Expression of Collagen type I (COL1A1, green), smooth muscle actin, alpha 2 (ACTA2, red). (B). Collagen type III (COL3A1, green) and smooth muscle actin, alpha 2 (ACTA2, red) protein expression. Nuclei were visualized with TO-PRO-3 (TOPRO, blue). Scale bars, 25  $\mu$ m.

## Supplementary Materials and Methods

### Generation of 3D culture system

In order to bypass the need for exogenous ECM and the derivation of fibroblasts, we have developed a patient- derived specimen culture system. This is the first tissue resection culture system that allows human tissue from DD patients to be grown *ex vivo* and functionally tested, recapitulating the *in vivo* situation. The system is based on a nitrocellulose membrane that allows contact of the tissue with the medium but not with the plastic, thus preventing the alteration of the tissue upon attachment, as previously observed when culturing DD fibroblasts. No collagen gel or other ECM protein substrate is required, since the DD tissue itself produces large amounts of these proteins. In brief: specimens from DD surgeries are equally sliced and placed in transwell plates onto nitrocellulose filters. Tissues remain continuously and statically in contact with defined culture conditions (Dulbecco's Modified Eagle's Medium (DMEM, with 1% fetal calf serum (FCS), 1% penicillin-streptomycin) but without being entirely submerged and are allowed to grow (seven days). Tissue resection specimens (N=9 DD and N=4 normal fascia palmaris) were treated with a combination of activators and inhibitors of the TGF $\beta$  signaling pathway (e.g. TGF $\beta$ , 5ng/ml; SB-431542, 10ng/ml, Tocris). After culture, tissues were processed for RNA isolation or they were fixed in 4% paraformaldehyde, incubated in 30% sucrose buffer, embedded in Tissue Tek- O.C.T. compound and stored at -80°C.

### Immunofluorescence

Hematoxylin and Eosin (H&E) staining were performed using standard protocols on 10- $\mu$ m cryosections. Immunofluorescence staining was performed on 10- $\mu$ m cryosections. For antigen retrieval sections were boiled in antigen unmasking solution (Vector Labs) and were incubated in 3% H<sub>2</sub>O<sub>2</sub> for endogenous peroxidase sequestering. Primary antibodies and dilutions used: anti-ACTA2 1:500 (Sigma), anti-COL1A1 1:500 (Southern Biotech), anti-COL3A1 1:500 (Southern Biotech), and anti-phospho-SMAD2 1:1000 (Cell Signaling). Sections were blocked with 1% bovine serum albumin (BSA)- PBS-0.1% v/v Tween 20) and incubated with primary antibodies diluted in the blocking solution, overnight at 4°C or room temperature. Sections then were incubated with secondary antibodies labeled with Alexa Fluor 488, 555, or 647 (Invitrogen/Molecular Probes, 1:250 in PBS-0.1% Tween 20). Detection of pSMAD2, was enhanced using tyramide amplification (Invitrogen/Molecular Probes) by incubation of slides with horseradish peroxidase (HRP)-conjugated secondary antibody (1:100 dilution) (Invitrogen/Molecular Probes), followed by incubation with tyramide-488 for 10 minutes. Sections were counterstained with TO-PRO3 (Invitrogen/Molecular Probes) at 1:1000 dilution in PBS-0.1% Tween-20 for nuclei visualization, and mounted with Prolong G mounting medium (Invitrogen/Molecular Probes), which contains DAPI.

### RNA isolation, RT-PCR and Quantitative PCR

Nodule parts (100  $\mu$ m) were homogenized using an Ultra Turrax homogenizer (T25 basic, IKA) in TRIpure reagent (Roche) and directly processed for total RNA isolation according to the TRIpure RNA extraction protocol. Total RNA (0.5  $\mu$ g) was used for first strand cDNA synthesis using RevertAid H Minus first strand cDNA synthesis kit (Fermentas). For quantitative PCR (Q-PCR) ten- fold diluted cDNA was amplified in a CFX Real Time Detection system (Bio-rad) using SYBR Green Supermix reagent (Bio-rad). To detect full length ALK5 mRNA levels, primers flanking exon 2 and exon 3 were used. Expression levels were normalized to housekeeping gene (*ACTRT1* or *CAPNS1*) and analyzed using the linear regression method. For exon skipping test, cDNA was amplified by touchdown PCR using ALK5 specific primers, which are designed to amplify both the full length and exon 2-skipped mRNA transcripts (forward primer in exon 1, reverse primer in exon 3). Primer sequences and detailed PCR protocol are available upon request.

### Microscopy and Image analysis

Confocal microscopy of labelled specimens was performed on a Leica TC-SP5 microscope with a 40X 1.4 NA oil-immersion objective Z series were collected and reassembled in Image J software ([rsbweb.nih.gov/ij](http://rsbweb.nih.gov/ij)). Mean area fraction fluorescence was calculated in Image J software using threshold to select the root boundary and measuring the percentage of positive surface inside the intensity defined by the threshold. Experiments were repeated three times and stained specimens in a given experiment were imaged using identical microscopic exposure and recording settings. Second-harmonic generation (SHG) was performed for imaging the organization of collagen fibers in native tissue. This type of two-photon microscopy was performed on a Zeiss 710 NLO upright confocal microscope (Jena, Germany) equipped with a femtosecond Spectra-Physics Deep See MP laser (Santa Clara, United States) using a Plan-Apochromat 20x/1.0 NA water-immersion objective. The images

were obtained with an excitation wavelength of 750 nm and emitted light was collected between 371–467 nm. Confocal stacks were processed with the Zeiss ZEN2009 software.

## References

1. Shih, B. and A. Bayat, Scientific understanding and clinical management of Dupuytren disease. *Nat Rev Rheumatol*, 2010. 6(12): p. 715-726.
2. Hindocha, S., et al., Dupuytren's diathesis revisited: evaluation of prognostic indicators for risk of disease recurrence. *J Hand Surg Am*, 2006. 31(10): p. 1626-1634.
3. Brickley-Parsons, D., et al., Biochemical changes in the collagen of the palmar fascia in patients with Dupuytren's disease. *J Bone Joint Surg Am*, 1981. 63(5): p. 787-797.
4. Berndt, A., et al., Appearance of the myofibroblastic phenotype in Dupuytren's disease is associated with a fibronectin, laminin, collagen type IV and tenascin extracellular matrix. *Pathobiology*, 1994. 62(2): p. 55-8.
5. Chen, S.-J., et al., Stimulation of type I collagen transcription in human skin fibroblasts by TGF- $\beta$ : involvement of Smad 3. *J Invest Dermatol*, 1999. 112(1): p. 49-57.
6. Varga, J., J. Rosenbloom, and S.A. Jimenez, Transforming growth factor  $\beta$  (TGF $\beta$ ) causes a persistent increase in steady-state amounts of type I and type III collagen and fibronectin mRNAs in normal human dermal fibroblasts. *Biochem J*, 1987. 247(3): p. 597-604.
7. Vaughan, M.B., E.W. Howard, and J.J. Tomasek, Transforming growth factor- $\beta$ 1 promotes the morphological and functional differentiation of the myofibroblast. *Exp Cell Res*, 2000. 257(1): p. 180-189.
8. Tomasek, J.J., Schultz, R.J, Haakma, C.J Extracellular matrix-cytoskeletal connections at the surface of the specialized contractile fibroblast (myofibroblast) in Dupuytren disease. *J Bone Joint Surg Am*, 1987. 69(9): p. 1400-1407.
9. Ratajczak-Wielgomas, K., et al., Expression of MMP-2, TIMP-2, TGF- $\beta$ 1, and decorin in Dupuytren's contracture. *Connect Tissue Res*, 2012. 53(6): p. 469-477.
10. Rehman, S., et al., Molecular phenotypic descriptors of Dupuytren's disease defined using Informatics analysis of the transcriptome. *J Hand Surg Am*, 2008. 33(3): p. 359-372.
11. Kloen, P., et al., Transforming growth factor- $\beta$ : possible roles in Dupuytren's contracture. *J Hand Surg Am*, 1995. 20(1): p. 101-108.
12. Dugina, V., et al., Focal adhesion features during myofibroblastic differentiation are controlled by intracellular and extracellular factors. *J Cell Sci*, 2001. 114(18): p. 3285-3296.
13. Malmström, J., et al., Transforming growth factor- $\beta$ 1 specifically induce proteins involved in the myofibroblast contractile apparatus. *Mol Cell Proteomics*, 2004. 3(5): p. 466-477.
14. Battice, E.J., et al., TGF- $\beta$  induces bimodal proliferation of connective tissue cells via complex control of an autocrine PDGF loop. *Cell*, 1990. 63(3): p. 515-524.
15. Krause, C., P. Kloen, and P. ten Dijke, Elevated transforming growth factor  $\beta$  and mitogen-activated protein kinase pathways mediate fibrotic traits of Dupuytren's disease fibroblasts. *Fibrogenesis Tissue Repair*, 2011. 4(1): p. 14.
16. Bayat, A., et al., Genetic susceptibility to Dupuytren's disease: transforming growth factor  $\beta$  receptor (TGF $\beta$ R) gene polymorphisms and Dupuytren's disease. *Br J Plast Surg*, 2003. 56(4): p. 328-333.
17. Tse, R., et al., Enhanced Dupuytren's disease fibroblast populated collagen lattice contraction is independent of endogenous active TGF- $\beta$ 2. *BMC Musculoskelet Disord*, 2004. 5(1): p. 41.
18. Verjee, L.S., et al., Unraveling the signaling pathways promoting fibrosis in Dupuytren's disease reveals TNF as a therapeutic target. *Proc Natl Acad Sci U S A*, 2013. 110(10): p. E928-E937.

19. Aartsma-Rus, A., et al., Guidelines for antisense oligonucleotide design and insight into splice-modulating mechanisms. *Mol Ther*, 2008. 17(3): p. 548-553.
20. Aartsma-Rus, A., et al., Targeted exon skipping as a potential gene correction therapy for Duchenne muscular dystrophy. *Neuromuscul Disord*, 2002. 12(0): p. S71-S77.
21. Goemans, N.M., et al., Systemic administration of PRO051 in Duchenne's muscular dystrophy. *N Engl J Med*, 2011. 364(16): p. 1513-1522.
22. Cirak, S., et al., Exon skipping and dystrophin restoration in patients with Duchenne muscular dystrophy after systemic phosphorodiamidate morpholino oligomer treatment: an open-label, phase 2, dose-escalation study. *The Lancet*, 2011. 378(9791): p. 595-605.
23. Vellucci, V.F. and M. Reiss, Cloning and genomic organization of the human Transforming growth factor- $\beta$  type I receptor gene. *Genomics*, 1997. 46(2): p. 278-283.
24. Wu, B., et al., Octa-guanidine morpholino restores dystrophin expression in cardiac and skeletal muscles and ameliorates pathology in dystrophic mdx mice. *Mol Ther*, 2009. 17(5): p. 864-871.
25. Guillouzo, A., et al., Long-term culture of functional hepatocytes. *Toxicol In Vitro*, 1990. 4(4-5): p. 415-427.
26. O'Gorman, D.B., et al., Wnt expression is not correlated with  $\beta$ -catenin dysregulation in Dupuytren's Disease. *J Negat Results Biomed*, 2006. 5: p. 13.
27. Vogt, J., R. Traynor, and G.P. Sapkota, The specificities of small molecule inhibitors of the TGF $\beta$  and BMP pathways. *Cell Signal*, 2011. 23(11): p. 1831-1842.
28. Gilpin, D., et al., Injectable collagenase *Clostridium Histolyticum*: a new nonsurgical treatment for Dupuytren's disease. *J Hand Surg Am*, 2010. 35(12): p. 2027-2038.e1.
29. Witthaut, J., et al., Efficacy and safety of Collagenase *Clostridium Histolyticum* injection for Dupuytren contracture: short-term results from 2 open-label studies. *J Hand Surg Am*, 2013. 38(1): p. 2-11.
30. Kuhn, M.A., et al., Cytokine manipulation of explanted Dupuytren's affected human palmar fascia. *Int J Surg Investig*, 2001. 2(6): p. 443-56.
31. Olinga, P., et al., Comparison of five incubation systems for rat liver slices using functional and viability parameters. *J Pharmacol Toxicol Methods*, 1997. 38(2): p. 59-69.
32. van de Bovenkamp, M., et al., Precision-cut liver slices as a new model to study toxicity-induced hepatic stellate cell activation in a physiologic milieu. *Toxicol Sci*, 2005. 85(1): p. 632-638.
33. de Graaf, I.A.M., et al., Preparation and incubation of precision-cut liver and intestinal slices for application in drug metabolism and toxicity studies. *Nat. Protocols*, 2010. 5(9): p. 1540-1551.
34. van de Bovenkamp, M., et al., Liver slices as a model to study fibrogenesis and test the effects of anti-fibrotic drugs on fibrogenic cells in human liver. *Toxicol In Vitro*, 2008. 22(3): p. 771-778.
35. Fisher, R., Ulreich, JB, Nazakato, PZ, Brendel, K., Histological and biochemical evaluation of precision-cut liver slices *Toxicol Mech Methods*, 2001. 11(2): p. 59-79.
36. Vogel, V. and M. Sheetz, Local force and geometry sensing regulate cell functions. *Nat Rev Mol Cell Biol*, 2006. 7(4): p. 265-275.
37. Gottrup, F., M.S. Ågren, and T. Karlsmark, Models for use in wound healing research: A survey focusing on in vitro and in vivo adult soft tissue. *Wound Repair Regen*, 2000. 8(2): p. 83-96.
38. Bisson, M.A., et al., The different characteristics of Dupuytren's disease fibroblasts derived from either nodule or cord: expression of  $\alpha$ -smooth muscle actin and the response to stimulation by TGF- $\beta$ 1. *J Hand Surg Am*, 2003. 28(4): p. 351-356.
39. Townley, W.A., et al., Dupuytren's contracture unfolded. *BMJ*, 2006. 332(7538): p. 397-400.
40. Wong, M. and V. Mudera, Feedback inhibition of high TGF- $\beta$ 1 concentrations on myofibroblast induction and contraction by Dupuytren's fibroblasts. *J Hand Surg Am*, 2006. 31(5): p. 473-483.
41. Bayat, A., et al., Genetic susceptibility to Dupuytren disease: association of Zf9 transcription factor gene. *Plast Reconstr Surg*, 2003. 111(7).

42. Satish, L., et al., Reversal of TGF-β1 stimulation of alpha-smooth muscle actin and extracellular matrix components by cyclic AMP in Dupuytren's - derived fibroblasts. *BMC Musculoskelet Disord*, 2011. 12(1): p. 113.
43. Kopp, J., et al., N-Acetyl-L-Cysteine abrogates fibrogenic properties of fibroblasts isolated from Dupuytren's disease by blunting TGF-β signaling. *J Cell Mol Med*, 2006. 10(1): p. 157-165.
44. Kuhn, M.A., et al., Tamoxifen decreases fibroblast function and downregulates TGF(β2) in dupuytren's affected palmar fascia. *J Surg Res*, 2002. 103(2): p. 146-52.
45. Sorrentino, A., et al., The type I TGF-β receptor engages TRAF6 to activate TAK1 in a receptor kinase-independent manner. *Nat Cell Biol*, 2008. 10(10): p. 1199-1207.
46. Kim, S.I., et al., Transforming growth factor-β (TGF-β1) activates TAK1 via TAB1-mediated autophosphorylation, independent of TGF-β receptor kinase activity in mesangial Cells. *J Biol Chem*, 2009. 284(33): p. 22285-22296.
47. Morcos, P.A., Y. Li, and S. Jiang, Vivo-Morpholinos: a non-peptide transporter delivers morpholinos into a wide array of mouse tissues. *Biotechniques*, 2008. 45(6): p. 613-4, 616, 618.
48. Saleh AF, A.A., Gait MJ, Overview of alternative oligonucleotide chemistries for exon skipping. *Methods Mol Biol*, 2012. 867: p. 365-78.
49. Stein, E.A., et al., Apolipoprotein B synthesis inhibition with mipomersen in heterozygous familial hypercholesterolemia: Results of a randomized, double-blind, placebo-controlled trial to assess efficacy and safety as add-on therapy in patients with coronary artery disease. *Circulation*, 2012. 126(19): p. 2283-2292.
50. Wolf, K., et al., Collagen-based cell migration models in vitro and in vivo. *Semin Cell Dev Biol*, 2009. 20(8): p. 931-941.





## Chapter 6

# **ALK1Fc suppresses tumor growth by impairing angiogenesis and affects cell proliferation of human prostate cancer cells *in vivo***

**Eugenio Zoni<sup>1,\*</sup>, Sofia Karkampouna<sup>2,\*</sup>, Peter C. Gray<sup>3</sup>, Marie Jose Goumans<sup>2</sup>,  
Lukas J.A.C. Hawinkels<sup>2</sup>, Gabri van der Pluijm<sup>1</sup>,  
Peter ten Dijke<sup>2</sup> and Marianna Kruthof-de Julio<sup>1,2,#</sup>.**

<sup>1</sup>Dept. of Urology, Leiden University Medical Centre, Leiden, The Netherlands

<sup>2</sup>Dept. of Molecular Cell Biology, Leiden University Medical Centre,  
Leiden, The Netherlands

<sup>3</sup>Clayton Foundation Laboratories for Peptide Biology, The Salk Institute for  
Biological Studies, La Jolla CA, USA.

\* Equally contributed, # Corresponding author

***Manuscript submitted***





## Abstract

Prostate cancer is the second most common cancer in men worldwide and lethality is almost inevitable due to the consequences of metastasis. Therefore, targeting the molecular pathways that underlie primary tumor growth and spread of metastases is of great clinical value. Bone morphogenetic proteins (BMPs) play a critical role in prostate cancer. BMP9 and the closely related BMP10 signal via the transmembrane serine kinase receptors Activin receptor-Like Kinase 1 (ALK1) and ALK2 and the cytoplasmic proteins SMAD1 and SMAD5. The human ALK1 extracellular domain (ECD) binds BMP9 and BMP10 with high affinity and we show that a soluble chimeric protein consisting of the ALK1 ECD fused to human Fc (ALK1Fc) prevents activation of endogenous signaling via ALK1 and ALK2. We also show for the first time in prostate cancer that ALK1Fc reduces BMP9-mediated signaling and decreases tumor cell proliferation *in vitro*. In line with these observations, we demonstrate that ALK1Fc impairs angiogenesis and reduces tumor growth *in vivo*. Our data identify BMP9 as a putative therapeutic target and ALK1Fc as a potential therapy capable of targeting tumor cells and the supportive tumor angiogenesis. Together these findings justify the continued clinical development of drugs blocking ALK1 and ALK2 receptor activity.

## Introduction

Prostate cancer is the second most common cancer in men worldwide<sup>1</sup>. The survival rate of prostate cancer patients is mostly determined by the extent of the tumor. If the cancer is restricted to the prostatic gland the median survival is estimated up to 5 years<sup>2</sup>. If prostate cancer has metastasized to distant organs, the current therapies are not curative and the median survival drops to 1 to 3 years<sup>3</sup>. Currently prostate cancer, when still in its first phase of androgen dependency, can be successfully treated surgically. Follow up with androgen deprivation therapy will then contain the cancer and reduce the possibility of metastasis<sup>4,5</sup>. However, once the cancer develops in an androgen-independent state, therapy is no longer useful or successful<sup>5</sup>. Risk of lethality rate is high due to the consequences of prostate cancer metastasis<sup>6</sup>. Indeed, the prognosis for patients diagnosed with metastatic disease has not markedly improved in recent decades, and metastases remain the direct cause of approximately 90% of cancer deaths<sup>7</sup>. Therefore, understanding the molecular pathways that underlie the emergence and spread of metastases from primary tumors are of great biological and clinical value.

Different lines of research have highlighted the role of the type I activin receptor-like kinase-1 (ALK1) of the transforming growth factor- $\beta$  (TGF $\beta$ ) pathway as key regulator of normal as well as tumor angiogenesis<sup>8,9</sup>. Bone morphogenetic protein-9 (BMP9) and BMP10 are high affinity ligands for ALK1, which is predominantly expressed by endothelial cells<sup>10</sup>. Alternatively, BMP9 signals through the BMP type I receptor ALK2<sup>11-13</sup>. Binding of BMP9/BMP10 to ALK1/ ALK2 results in phosphorylation and activation of downstream effectors SMAD1 and/ or SMAD5<sup>12-14</sup>. BMP9 is produced in the liver, secreted in circulation<sup>15</sup> and it promotes liver cell proliferation of primary hepatocytes and human hepatoma HepG2 cells<sup>16</sup>. In ovarian cancer, BMP9 can act as proliferative factor, promoting human epithelial ovarian cancer and human immortalized ovarian surface epithelial cell proliferation through ALK2/ SMAD1/ SMAD4 pathway<sup>13</sup>. Similarly, BMP9 stimulates cell proliferation of liver cancer cells<sup>17</sup> and osteosarcoma growth<sup>18</sup>. Among the BMPs, BMP9 is the most recently identified<sup>15</sup> and least studied ligand. Current research has not only attributed a tumor promoter role to

BMP9<sup>13,17,18</sup> but also tumor suppressing properties<sup>19-21</sup> in different types of cancer, including prostate cancer.

Several studies have highlighted the role of BMP9/ ALK1 in the genetics and development of blood vessel formation, outlining its critical involvement in pathological and tumor angiogenesis<sup>22,23</sup>. Interestingly, alterations of signal transduction pathways that are important for blood vessel formation, such as the NOTCH pathway, have also been associated with arterio-venous malformations<sup>24,25</sup>. Recently, BMP9 and BMP10 signaling have been linked to NOTCH signaling, one of the major pathways involved in prostate cancer development, progression and bone metastasis<sup>26</sup>. Expression profiling studies have shown that members of NOTCH pathway are characteristic of high grade (Gleason 4+4=8) micro-dissected prostate cancer cells compared to low grade (Gleason 3+3=6)<sup>27</sup>. Moreover, inhibition of NOTCH1 reduces prostate cancer cell growth, migration and invasion<sup>28</sup>. Interestingly, NOTCH signaling pathway activates ALDH1A1, a well-known marker of prostate cancer stem cells<sup>29-32</sup>.

In order to understand the role of BMP9 in prostate cancer tumor progression, we have employed here the soluble chimeric protein (ALK1Fc/ ACE-041)<sup>33</sup> containing the human ALK1 extracellular domain that binds with high affinity the ligands BMP9 and BMP10<sup>34</sup>, thus, reducing activation of endogenous ALK1, ALK2 and downstream signaling<sup>35</sup>. BMP9 induces endothelial cell proliferation and vessel formation<sup>36</sup> while ALK1Fc has previously been shown to inhibit vascularization and tumor growth of breast cancer *in vivo* in an orthotopic transplantation model<sup>34</sup>. ALK1Fc binds and neutralizes only BMP9 and BMP10 ligands and not TGFβ<sup>34,35</sup>, which plays an important role in angiogenic processes. Phase I clinical trials have been completed using ALK1Fc as anti-angiogenesis therapy in myeloma (clinicaltrials.gov identifier NCT00996957).

Here we show, for the first time in prostate cancer, that ALK1Fc reduces BMP9 signaling and decreases cell proliferation of highly metastatic and tumor initiating human prostate cancer cells *in vitro*. We further demonstrate that ALK1Fc reduces tumor growth by impairing angiogenesis and affecting cell proliferation of human prostate cancer cells *in vivo*. Taken together these data suggest BMP9 as a possible therapeutic target and thus justifies the continued clinical development of drugs blocking ALK1 and ALK2.

## Materials and Methods

### Cell line and culture conditions

Human osteotropic prostate cancer cell lines PC-3M-Pro4luc2 cells<sup>37</sup> were maintained in Dulbecco's Modified Eagle Medium (DMEM) supplemented with 10% FetalClone II (FCII) serum (Thermo Fisher, Waltham MA, USA), 0.8 mg/ml Neomycin (Santacruz, Dallas, USA) and 1% Penicillin-Streptomycin (Life Technologies, Carlsbad, USA). C4-2B cells were maintained in T-medium DMEM (Sigma-Aldrich, the Netherlands) supplemented with 20% F-12K nutrient mixture Kaighn's modification (GibcoBRL, the Netherlands), 10% fetal calf serum (FCS) 0.125 mg/ml biotin, 1% Insulin-Transferin-Selenium, 6.825 ng/ml T3, 12.5 mg/ml adenine and 1% penicillin/streptomycin (all from (Life Technologies, Carlsbad, USA). Cells were maintained at 37°C with 5% CO<sub>2</sub>.

### **Luciferase reporter gene constructs**

PC-3M-Pro4Luc2 cells were seeded at a density of 50,000 cells in 500  $\mu$ L medium in a 24-wells plate. Transient transfection of reporter constructs was performed with Lipofectamine2000 (Life Technologies, Carlsbad, USA) according manufacturer's protocol. For each well, 100 ng of NOTCH reporter RBP-Jk-luc, 10 ng CAGGS-Renilla luciferase, 100 ng BRE renilla and 100 ng BRE-luc38 per well were transfected. After 24 hours, medium was replaced and cells were treated with BMP9 for 24 hours. The Firefly luciferase and Renilla luciferase levels in the lysates were measured using Dual Luciferase Assay (Promega, Madison, USA).

### **RNA isolation and Real-time qPCR**

Total RNA was isolated with Trizol Reagent (Invitrogen, Waltham, USA) and cDNA was synthesized by reverse transcription (Promega, Madison, USA) according to manufacturer's protocol. qRT-PCR was performed with Biorad CFX96 system (Biorad, The Netherlands). Gene expression was normalized to *GAPDH* or  *$\beta$ -actin*. (For primer sequences see Supplementary Table I). Total RNA from frozen section (5 $\mu$ m) was isolated with Qiagen Mini Isolation kit (Qiagen, the Netherlands) according to manufacturer protocol. Primer sequences are listed in Table 1.

### **MTS assay**

Cells were seeded at density of 2.000 cells/ well, in 96- well plates and treated with ALK1Fc or control-Fc (CFc) (10ug/ml, Acceleron, USA) allowed growing for 24, 48, 72 and 96 hours. After incubation, 20  $\mu$ l of 3-(4,5 dimethylthiazol- 2- yl)- 5 -(3 -carboxymethoxyphenyl)- 2 -(4 -sulfophenyl)- 2 H-tetrazolium was added and metabolic activity (absorbance of formazan product at 490nm) was measured after 2 hours incubation at 37°C. MTS absorbance values are positively proportional to total number of metabolically active cells providing an indirect correlation with cell proliferation rate<sup>39</sup> (CellTiter96 Aqueous Non-radioactive Cell proliferation assay, Promega).

### **Animals**

Male, 6-8 week-old, athymic nude mice (Balb/c nu/nu), purchased from Charles River (L'Arbresle, France), were used in all *in vivo* experiments (n=15 per group). Mice were housed in individual ventilated cages under sterile condition, and sterile food and water were provided ad libitum. Animal experiments were approved by the local committee for animal health ethics and research of Leiden University (DEC #11246), and carried out in accordance with European Communities Council Directive 86/609/EEC. After the experimental periods, mice were injected with hypoxia probe (6mg/kg, Burlington, Massachusetts, USA) and lectin-Tomato (1mg/kg, Vector Laboratories, USA) intravenously prior to perfusion and sacrificed according to our mouse protocol. Tumors were dissected and processed for further histomorphological analysis as described below.

### **Orthotopic prostate transplantation and ALK1Fc treatment**

A total of 25.000 PC-3M-Pro4luc2 cells (10ul final volume) were injected in the dorsal lobe

of nude mice. In brief: after anesthetizing the mice with isoflurane, each mouse was placed on its back and a small incision was made along the lower midline of the peritoneum for about 1 cm. The prostate dorsal lobes were exteriorized and stabilized gently. A 30-gauge needle attached to a 1-cc syringe was inserted into the right dorsal lobe of the prostate and 10  $\mu$ l of the material were slowly injected. A well-localized bleb indicates a successful injection. After retracting the needle a Q-tip was placed over the injection site for about 1 min to prevent bleeding and spillage of material. The prostate was then returned to the peritoneum and the abdominal wall and skin layer was sutured. After establishment of the primary tumor, at 10 days after the orthotopic transplantation, mice were intraperitoneally injected with Control-Fc (CFc) or ALK1Fc compounds (1 mg/kg) twice per week.

Administration of compounds was performed for four weeks. ALK1-Fc is a fusion protein comprised of the extracellular domain of human ALK1 fused to the Fc region of IgG and was obtained from Acceleron Pharma, Cambridge, USA. The Fc domain of IgG1 was used as a control (MOPC-21; Bio Express, West Lebanon NH).

### Whole body bioluminescent imaging (BLI)

Tumor growth was monitored weekly by whole body bioluminescent imaging (BLI) using an intensified-charge-coupled device (I-CCD) video camera of the *in vivo* Imaging System (IVIS100, Xenogen/Perkin Elmer, Alameda, CA, USA) as described previously<sup>40</sup>. Mice were anesthetized using isoflurane and injected intraperitoneally with 2mg D-luciferin (Perbio Science, the Netherlands). Analyses for each metastatic site were performed after definition of the region of interest and quantified with Living Image 4.2 (Caliper Life Sciences, Belgium). Values are expressed as relative light units (RLU) in photons/sec.

### Immunofluorescence

Immunofluorescence staining was performed as described previously<sup>41</sup>. In brief, 5- $\mu$ m paraffin embedded sections were used. For antigen retrieval, sections were boiled in antigen unmasking solution (Vector Labs, Peterborough, UK) and stained with following antibodies, CD31 (Sigma), ALDH1A1 (Abcam), phosphoHistone 3 (Millipore) and cleaved Caspase 3 (Cell Signaling). Sections were blocked with 1% bovine serum albumin (BSA)- PBS-0.1% v/v Tween-20 and incubated with primary antibodies diluted in the blocking solution, overnight at 4°C or room temperature. Sections then were incubated with secondary antibodies labelled with Alexa Fluor 488, 555, or 647 (Invitrogen/Molecular Probes, Waltham, MA, USA) at 1:250 in PBS-0.1% Tween-20. Nuclei were visualized by TO-PRO-3 (Invitrogen/Molecular Probes, 1:1000 diluted in PBS-0.1% Tween-20) or DAPI which was included in the mounting medium (Prolong G, Invitrogen/Molecular Probes).

### Western immunoblotting

Proteins were extracted by using RIPA buffer (Thermo Scientific) and protein concentrations were quantified according to manufacturer's protocol (Thermo Scientific). Proteins samples (20  $\mu$ g per sample) were separated by 15% SDS- PAGE followed by transfer to a blotting membrane. The membrane was blocked with 5% Milk, dissolved in PBS-Tween-20 for 1 hour at room temperature. The membrane was incubated with 1:1000 primary antibody (anti-NOTCH1, Cell Signaling, catalogue number 3608) at 4°C overnight. Subsequently, the

membrane was incubated with 1:10000 secondary horseradish peroxidase (HRP) antibody. All antibodies were dissolved in PBS-Tween-20. Chemi-luminescence was used to visualize the bands.

### Statistical analysis

Statistical analysis was performed with GraphPad Prism 6.0 (GraphPad software) using t-test or ANOVA for comparison between more groups. Data is presented as mean  $\pm$  SEM. P-values  $\leq 0.05$  were considered to be statistically significant (\*  $P < 0.05$ , \*\*  $P < 0.01$ , \*\*\*  $P < 0.001$ ).

## Results

### ALK1Fc reduces primary prostate tumor burden *in vivo*

To investigate the role of BMP9 in prostate cancer progression, the BMP9- ligand trap, ALK1Fc, was administered in a mouse model of orthotopic prostate cancer. Orthotopic prostate tumor growth was induced by intra-prostatic inoculation of human prostate cancer PC-3M-Pro4Luc2 cells in Balb/c nude mice and tumor progression was followed by bioluminescence imaging (BLI)37 (**Fig.1A**). Based on the BLI signal the mice were distributed between two treatment groups; ALK1Fc or CFc (n=15 per group). The compounds were injected twice weekly and tumor imaging and body weights were monitored weekly for 5 weeks (**Fig.S1**). Tumor burden was quantitatively assessed for each animal during the course of treatment. The group of animals that received ALK1Fc exhibit smaller tumor size compared to the animals that received CFc based on the size after resection (**Fig.1B**) and bioluminescence quantification (**Fig.1C**,  $p < 0.05$ ).

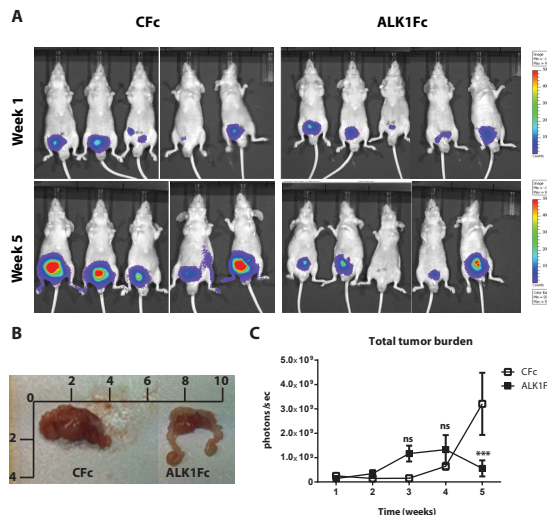


**Fig.1. Effect of ALK1Fc *in vivo***

(A). PC-3M-Pro4Luc2 cells were orthotopically injected in the anterior lobe of prostate gland of nude mice (n=15 per group). Detection of primary tumor burden was observed at 2 weeks after injection, time point designated as “week 1” at the start of treatment with ALK1Fc or CFc. Representative examples of bioluminescent images of tumor burden at the start of treatment with ALK1Fc/ CFc (week 1) and at the end point (week 5). (B). Representative images of primary tumor size from a recipient of CFc versus ALK1Fc treatment after 5 weeks. (C). Quantification of bioluminescent signal (photons/sec) in mice treated with either CFc (n=14) or ALK1Fc (n=15) for 5 weeks. P value <0.001 (\*\*\*).

### Effect of ALK1Fc in vascular density, hypoxia and cell proliferation of the primary prostate tumor

The acquisition of tumor angiogenesis promotes tumor growth beyond a few mm<sup>3</sup> sizes. Intravital lectin perfusion was used to map the perfused elements of the tumor vasculature in mice. Fluorescent-conjugated lectin (lectin-Tomato) was visualized in tumor tissue sections and quantified. Vascular density, indicated by the overall lectin presence, was overall decreased in the tumors treated with ALK1Fc compared to the CFc group (**Fig. 2A-B**; p value= 0.058 statistically not significant). We evaluated the presence of endothelial cells in tumor sections by CD31 immunofluorescence. CD31 expression in tumors showed decreased trend after treatment with ALK1Fc which could indicate fewer endothelial cells and vessels (**Fig. 2C-D**; p value= 0.052, statistically not significant). Hypoxia is an important component of angiogenesis and critical for tumor formation. A hypoxia-induced fluorescent probe was injected in tumor bearing mice prior to sacrifice and the hypoxic areas within the tumors were visualized after tumor resection (**Fig. 2E-F**). Hypoxic areas are found in both treatment groups; however, the overall amount of hypoxia seems higher in ALK1Fc-treated, tumor-bearing mice over the CFc-treated groups (**Fig. 2E-F**; p=0.05, non-significant). We assessed the presence of total cell proliferation and cell death in these tumors by immunofluorescence for mitosis marker, phosphorylated histone 3 (PH3), and apoptosis marker, cleaved caspase 3 (CASP3). Dividing PH3 positive cells are predominantly located in normoxic areas (**Fig. 2E**, left panel). Quantification of immunofluorescence signal shows that the number of dividing cells is significantly lower in the ALK1Fc-treated animals (**Fig. 2G**; p<0.05). Total amount of apoptotic cells (Caspase-3 positive) is significantly higher in the ALK1Fc-treated tumors (**Fig. 2H**; p<0.05). Histological analysis indicates localization of apoptotic cells mostly, however not exclusively, in the hypoxic areas (**Fig. 2E**), suggesting a correlation between hypoxia and tumor cell death.

### ALK1Fc decreases proliferation of human prostate cancer cells

To investigate the effect of ALK1Fc on prostate cancer cells we first measured the mRNA levels of BMP9 type I receptors ALK1 and ALK2 in PC-3M-Pro4Luc<sup>237</sup> human prostate cancer cell line and tested their response to BMP9. As previously reported in highly metastatic PC-3 and PC-3M prostate cancer cells<sup>42</sup>, qRT-PCR analysis in osteotropic PC-3M-Pro4Luc2 cells revealed undetectable levels of ALK1 mRNA and mRNA expression of ALK2 (**Fig. S2A**). Treatment with BMP9 showed a dose-dependent induction of BRE-Renilla luciferase activity (p <0.01 and p<0.05 with 0.5nM and 1 nM BMP9, respectively) indicative of conserved and active signaling machinery (**Fig. S2B**). Using the 1nM BMP9 dose for subsequent experiments, we tested the individual effect of CFc and ALK1Fc or the combined effect of BMP9 with either ALK1Fc or CFc on BRE reporter assay (**Fig. S2C**). Treatment with ALK1Fc (10ug/ml) completely abolished the BMP9-mediated BRE luciferase (luc) activity (**Fig. S2C**; BMP9+ALK1Fc) to levels similar to the non-stimulated control (Untreated). Treatment with BMP9+CFc (10ug/ml) led to induction of BRE-luc activity of similar level as the BMP9 treatment (**Fig. S2C**; p-value <0.05). Taken together, these results indicate that ALK1Fc blocks ALK2-mediated BMP9 signaling in PC-3M-Pro4Luc2 cells. The functional effect of ALK1Fc on human prostate cancer cells was investigated by measuring metabolic activity by accumulation of MTS substrate, indicative of cell growth rate (proliferation). BMP9 stimulation *in vitro* led to increase of MTS absorbance indicating higher cell number (**Fig. 3A**). Treatment with 10ug/ml ALK1Fc, but not

with control Fc (CfC), reduced BMP9-induced PC-3M-Pro4Luc2 cell proliferation ( $p < 0.001$  at day 4 comparing vehicle versus BMP9 or ALK1Fc treatment, respectively) (**Fig.3A**). Effect of only ALK1Fc or CfC on MTS assay was also assessed in absence of exogenously-added BMP9 and showed no influence of these compounds on the basal cell growth levels (**Fig. S2D**). The BMP9 effect was also tested in the C4-2B prostate cancer cell line; however no significant difference in MTS assay was measured (**Fig.S2E**). Additionally, BMP9 treatment in PC-3M-Pro4Luc2 cells combined with ALK2 functional inhibition by small molecule BMP type I receptor inhibitor LDN193189 (LDN)<sup>43,44</sup> showed abolishment of BMP9-induced proliferation (**Fig.3B**). LDN effectively blocked the activity of the BRE-luc reporter after BMP9 stimulation of PC-3M-Pro4 cells (**Fig.S2F**) and the effect of LDN showed minimal impact on basal cell proliferation levels in absence of exogenously added BMP9 (**Fig.S2G**). Finally, we evaluated the clonogenic ability of PC-3M-Pro4Luc2 cells after BMP9 treatment alone (**Fig.S3A**) and confirmed that BMP9 affects cell growth, strongly increasing the size of the colonies (**Fig.S3B**,  $p < 0.05$ ). However, BMP9 showed no effect on colony formation/self-renewal ability of PC-3M-Pro4Luc2 since the total number of colonies formed is similar (**Fig.S3C**). Together, these data indicate that ALK1Fc strongly reduces BMP9-induced cell proliferation of human prostate cancer cells.



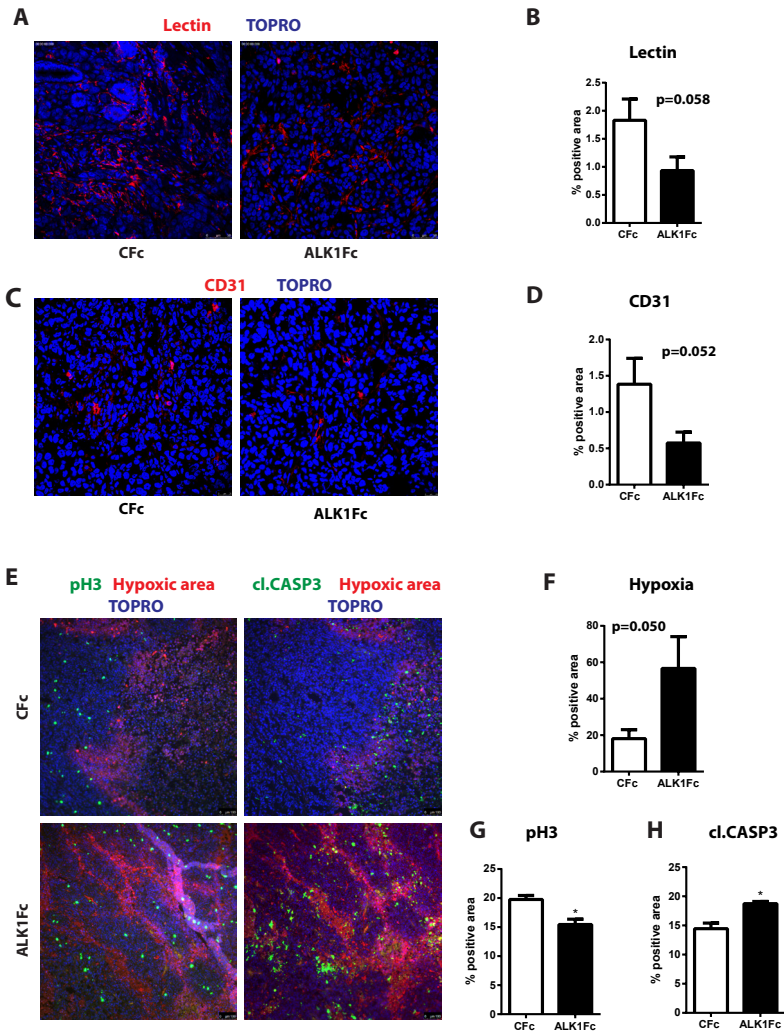


**Fig.2. Effect of ALK1Fc on vascular density, cell proliferation and apoptosis *in vivo***

(A). Representative images of lectin detection in primary prostate tumor samples after perfusion with lectin-DsRed (red). TOPRO (blue) marks the nuclei. Treatment groups: ALK1Fc or CFc. (B). Quantification of lectin positive surface area in all tumor samples of each group (n=14 CFc group, n=15 ALK1Fc group) (C). Representative images of CD31 (green) immunofluorescence staining in primary prostate tumor samples after 5 weeks of treatment with either ALK1Fc or CFc. (D). Quantification of CD31 positive surface area in all tumor samples of each group (n=14 CFc group, n=15 ALK1Fc group). (E). Representative images of hypoxia immunofluorescence staining (red) in primary prostate tumor samples after 5 weeks of treatment with either ALK1Fc or CFc. Hypoxia probe was injected prior to sacrifice and was detected by a specific fluorescent antibody. White lines are used to arbitrarily distinguish the hypoxic (red) area from the non-hypoxic one. Immunofluorescence images for colocalization of apoptotic or proliferating cells in hypoxic/ normoxic area within the prostate tumor area in ALK1Fc and CFc treated animals. pH3: Phosphorylated Histone 3 cell proliferation marker (green); cleaved caspase 3 apoptosis marker (green); Hypoxic probe-antibody; hypoxic area (red). (F). Quantification of hypoxia positive area in all tumor samples of each group (n=15 per group). (G). Quantification of total pH3 positive area in all tumor samples of each group (n=14 CFc group, n=15 ALK1Fc group). (H). Quantification of total cleaved caspase 3 positive (apoptotic cells) in all tumor samples of each group (n=14 CFc group, n=15 ALK1Fc group).

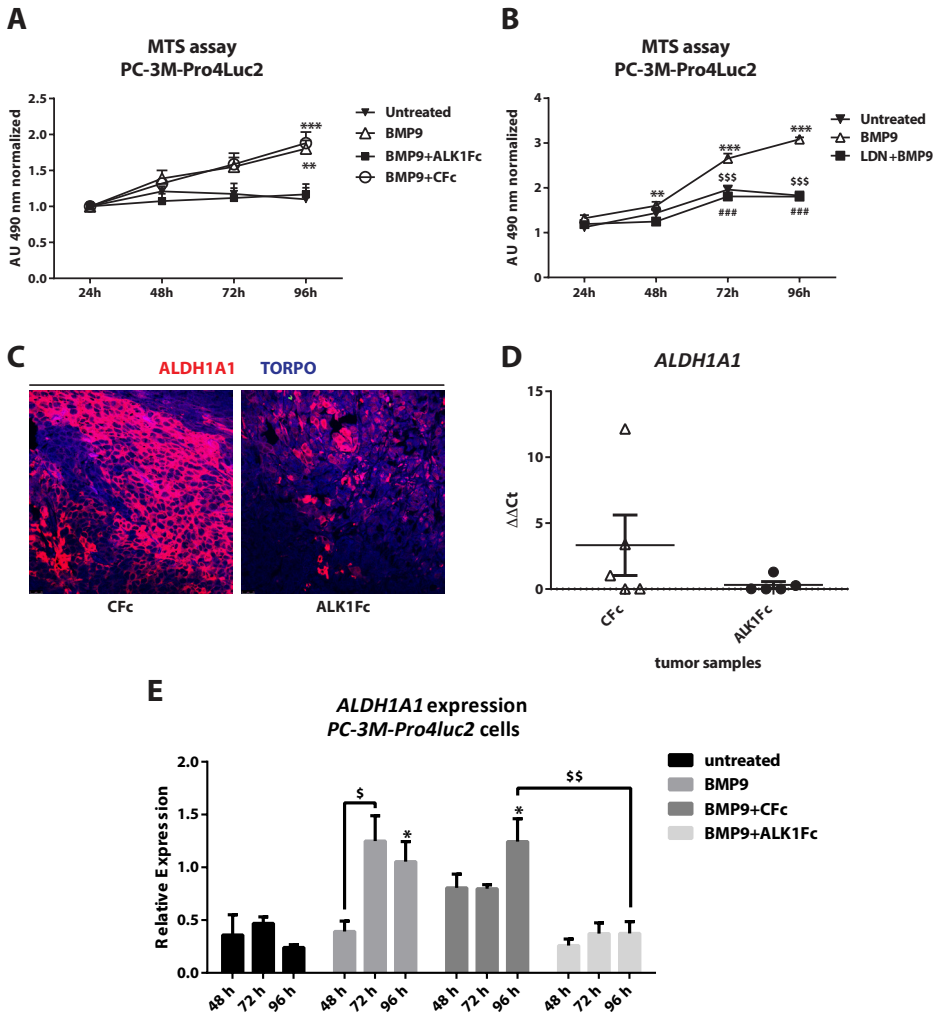


**Fig.3. Effect of BMP9 and ALK1Fc on proliferation and ALDH1A1 expression**

(A). Cell proliferation MTS assay (24, 48, 72, 96 hours) in PC-3M-Pro4Luc2 cells stimulated with recombinant BMP9 (1nM), BMP9 (1nM)+ALK1Fc (10ug/ml) or BMP9 (1nM)+CFc (10ug/ml). Accumulation of MTS was measured based on absorbance at 490 nm. Values are normalized to the basal measurements at 24 hours after cell seeding and treatments. Graph represents values for three independent experiments (n=3). Error bars indicate  $\pm$  SEM. P value < 0.01 (\*\*) BMP9 versus Untreated and P-value < 0.001 (\*\*\*) BMP9+CFc versus Untreated. (B). Cell proliferation assessed by MTS assay (24, 48, 72, 96 hours). PC-3M-Pro4Luc2 cells were seeded at low density in 96-well plates and treated with BMP9 (1nM) and in combination with LDN (BMP type I receptor inhibitor LDN193189, 120nM) (LDN+BMP9). (n=2). Error bars indicate SEM. (C). Representative images of ALDH1A1 immunofluorescence in prostate tumor samples from ALK1Fc and CFc treated animals. ALDH1A1: red; TOPRO: blue nuclear dye. (D). Quantification of ALDH1A1 mRNA by Q-PCR in tumor samples of each group (n=5 for CFc, n=5 for ALK1Fc). (E). Expression of ALDH1A1 in PC-3M-Pro4Luc2 cells. Relative mRNA expression was measured by Q-PCR from cDNA obtained from PC-3M-Pro4Luc2 cells treated with BMP9, BMP9+ALK1Fc, BMP9+CFc, for 48, 72 and 96 hours. Values are normalized to  $\beta$ -actin expression. Error bars are  $\pm$ SEM (n=3).

### Expression of BMP9, ALK1 and ALK2 in human and murine prostate tumor tissues

To investigate the *BMP9*, *ALK1* and *ALK2* expression in human prostate cancer samples we performed bioinformatics analysis using data mining platforms (R2: microarray analysis and visualization platform <http://r2.amc.nl>, source: GEO ID: gse29079) of mRNA expression of *ALK1*, *ALK2* receptor and *BMP9* ligand (**Fig.S3D-F**) in 48 benign tumors versus 47 malignant prostate tumors<sup>45</sup>. Levels of *ALK1* transcripts are decreased in the malignant tumor group compared to the benign group ( $p < 0.001$ ). Interestingly, levels of *ALK2* transcripts are significantly increased ( $p < 0.01$ ) in the malignant tumor group compared to the benign group, thus correlating with disease progression, while *BMP9* mRNA expression is similar in both groups ( $p = 0.28$ ). Previously, cDNA microarray analysis was performed in the study of Bacac *et al.*,<sup>46</sup> using laser-microdissected stromal cells from murine prostate intraepithelial neoplasia (PIN) and invasive prostate tumors. Analysis of *ALK1*, *ALK2* and *BMP9* expression (**Fig.S3G-I**) in this dataset indicated elevated mRNA expression of *ALK1* and similarly increased expression of both *ALK2* and *BMP9* during the invasive stage of murine prostate cancer.

### ALK1Fc inhibits ALDH1A1 expression *in vivo* and interferes with NOTCH signaling

Finally, given the reduction of primary tumor burden and the *in vitro* effects of the ALK1Fc on cell proliferation we assessed the relative expression of the *ALDH1A1* marker that is associated with cancer stem-like cells and poor patient prognosis<sup>31,32</sup>. Treatment with ALK1Fc affected the number of proliferative ALDH1A1 positive cells in the prostate tumor tissues both at protein (**Fig.3C**) and mRNA levels (**Fig.3D**). *In vitro* stimulation with BMP9 of the same cell line used to induce tumors in xenograft mouse model, confirmed that BMP9 and BMP9+Cfc upregulates *ALDH1A1* expression, while BMP9+ALK1Fc treatment abolishes this effect (**Fig.3E**). Interestingly, ALDH1A1 is known to be regulated by NOTCH signaling<sup>29-31</sup>. The role of NOTCH1 in prostate cancer cell proliferation and migration has been extensively studied<sup>28,47-50</sup>. Larrivée *et al.*, have shown that ALK1 and NOTCH converge on common downstream pathways and that BMP9 treatment alone upregulates *JAG1* levels in human umbilical vein endothelial (HUVEC) non-transformed cells<sup>51</sup>. To verify the effect of BMP9 on NOTCH signaling activation in our cancer model, we quantified by qRT-PCR the expression of *JAG1* after BMP9 stimulation in presence of ALK1Fc or Cfc. Our transcriptional analysis showed that BMP9 and BMP9+Cfc induce mRNA expression of *JAG1* and that ALK1Fc is able to reduce the BMP9-mediated induction of *JAG1* (**Fig.4A**). To assess the clinical relevance of BMP9/ALK2-mediated NOTCH pathway activation in human prostate cancer we performed bioinformatics analysis using data mining platforms (R2: microarray analysis and visualization platform <http://r2.amc.nl>, source: GEO ID: gse29079). Levels of NOTCH ligand *JAG1* transcript show statistically significant enrichment in the malignant tumor group compared to the benign group (**Fig.4B**) and positively correlates with *ALK2* expression and disease progression (**Fig.4D**). In addition, expression levels of *NOTCH1* receptor in human prostate tumor microarray data indicate a positive correlation with progression to malignancy (**Fig.4C**) and with *ALK2* expression (**Fig.4E**). Overexpression of *JAG1* in PC-3M-Pro4Luc2 human prostate cancer cells seems to increase metabolic activity and total cell number as assessed by MTS assay (**Fig.4F**).

Knockdown of the NOTCH1 receptor in PC-3M-Pro4Luc2 (shNOTCH1), validated by western immunoblotting for NOTCH1 protein detection (**Fig.S4A**) and NOTCH reporter (RBP-JK-

luc) assay (Fig.S4B), showed reduced mRNA levels of *JAG1* (Fig.S4C) and decreased cell proliferation, as compared to cells transduced with non-targeting shRNA lentivirus ( $p < 0.05$  at 48 hrs) (Fig.4G). Stimulation of shNOTCH1-knockdown cell line with BMP9 increases their cell growth rate (Fig.4H) overcoming the knockdown of NOTCH1. Our data therefore suggest that BMP9/ ALK2 directly induces activation of NOTCH downstream target genes (*JAG1*) likely in a NOTCH1-independent way<sup>45,52,53</sup> which leads to higher cell proliferation and is associated with tumor progression in PCa.

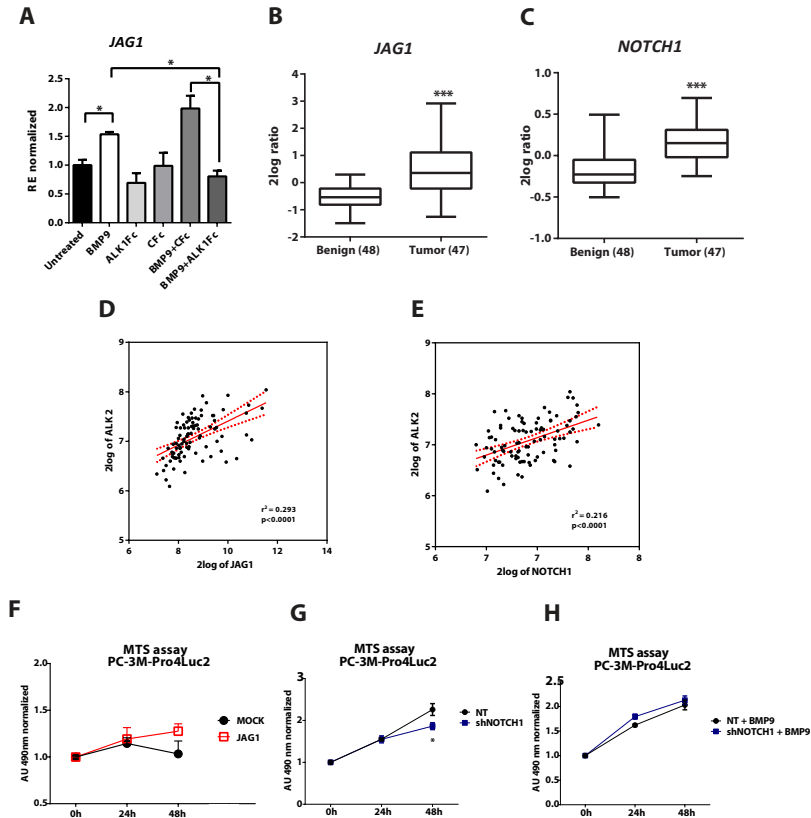


**Fig.4. Effect of BMP9 and ALK1Fc on NOTCH signaling pathway and correlation study**

(A). Expression of *JAG1* in PC-3M-Pro4Luc2 cells. Relative mRNA expression was measured by Q-PCR from cDNA obtained from PC-3M-Pro4Luc2 cells treated with BMP9, ALK1Fc, CfC, BMP9+ALK1Fc or BMP9+CfC for 96 hours. Values are normalized to  $\beta$ -actin expression. Error bars are  $\pm$ SEM (n=3). (B-C). Bioinformatics analysis of AMC OncoGenomics database (Suelman transcript comparison) showing mRNA expression of *JAG1* (B) and *NOTCH1* (C) and in prostate tissues among benign prostate tissues (n=48) versus tumor tissues (n=47). Values are expressed as 2log ratio tumor/ benign. ns: non-significant. P value < 0.001 (\*\*\*). (D). Correlation analysis of *JAG1* and *ALK2* expression ( $p < 0.0001$ ) and (E). correlation analysis of *NOTCH1* and *ALK2* expression ( $p < 0.0001$ ) in prostate tissues among benign prostate tissues (n=48) versus tumor tissues (n=47). Bioinformatic analysis was performed using the AMC OncoGenomics database (Suelman transcript comparison), values are expressed as 2log ratio tumor/ benign. ns: non-significant. (F). Cell numbers were assessed by MTS assay (0, 24 and 48 hours) in PC-3M-Pro4Luc2 cells transfected with 1ug *JAG1* or Mock expression vector (n=2). (G-H). Cell numbers were assessed by MTS assay (0, 24 and 48 hours). PC-3M-Pro4Luc2 cells were transduced with short hairpin RNA against NOTCH1 (shNOTCH1) lentiviral vector or non-targeting (NT) shRNA vector (mock) and plated at low density. Treatment with BMP9 (1nM) was done once at cell seeding (t=0) MTS absorbance was measured. Values are normalized to the basal measurements t=0 after cell seeding and treatments. Graph represents values from four independent experiments (n=4). Error bars indicate SEM. P value < 0.05 (\*).

### Discussion

In this study, BMP9 was found to have a tumor-promoting effect on human prostate cancer cell *in vitro* and *in vivo*. We demonstrated here that blocking of BMP9 with ALK1Fc ligand trap efficiently diminished BMP9-driven cell proliferation in human prostate cancer cells and significantly reduced tumor growth in orthotopic model of human prostate cancer. BMP9 was first identified in the liver<sup>15</sup> and active forms are present in serum<sup>13</sup>. BMP9 is a ligand for the ALK1 receptor in endothelial cells<sup>10</sup> and has been shown to exert both stimulatory and inhibitory effects on endothelial cell type growth and migration<sup>36,54</sup>. Aberrant regulation of the TGF $\beta$  and BMP signaling pathway members often results in cancer progression<sup>55,56</sup>. In particular, BMP ligands, such as BMP9 as well as BMP type I receptors (e.g. ALK1 and ALK2) have been associated with tumor angiogenesis and cancer progression. In non-endothelial cells, BMP9 signals through ALK2 receptor such as in ovarian epithelium, where it has been shown to promote ovarian cancer cell proliferation<sup>13</sup>. Similarly, in hepatocellular carcinoma BMP9 has been reported to act as proliferative and survival factor<sup>17</sup>. In breast cancer few studies have highlighted the role of BMP9 in reducing breast cancer cells growth and metastasis<sup>57-59</sup>. However, the role of BMP9 and ALKs, in promoting or suppressing different cancer types, remains controversial. Collectively, these indicate that the effect of BMP9 on tumor promotion versus tumor suppression might be cancer-type specific, thus providing the rationale to elucidate the role of BMP9 in prostate cancer, for which little information is available to our knowledge.

Using publicly available databases of human prostate cancer specimens, we found that ALK2 is significantly upregulated in malignant versus benign tumor tissue samples, whereas ALK1 is significant downregulated, supporting the notion that the tumor-promoting effect of BMP9 is mediated by ALK2 as in our model<sup>45</sup>. Additionally, microarray analysis of data from mouse prostate intraepithelial neoplasia (PIN) versus invasive cancer in a multistage model of prostate carcinogenesis showed upregulation of ALK2 and BMP9 at the invasive stage in the stromal compartment<sup>60</sup>. Taken together, these data suggest a tumor-promoting role of BMP9 produced by the supportive stroma during prostate cancer progression. The fact that the BMP9 transcript levels registered in the selected dataset are similar in benign versus tumor stage in human prostate tumor samples, suggest a paracrine effect of BMP9 in human prostate cancer<sup>45</sup>. The significant increased expression of ALK2 in human prostate tumor tissue samples suggest that the BMP9 produced by the stromal compartment might be responsible for the tumor promoting effect that we documented here.

Our *in vitro* findings strengthen the afore-mentioned expression data and suggest that BMP9 exerts a proliferative effect in human prostate cancer cells. Moreover, functional blocking of ALK2 activity by LDN193189 supports the notion that ALK2 is critically involved in mediating this BMP9 effect. As depicted in the supplementary data, ALK1Fc and LDN193189 alone did not affect cell proliferation of human prostate cancer cells, thus, suggesting a paracrine effect of stroma-derived BMP9 on tumor cells. BMP9 does not influence clonogenic ability of human prostate cancer cells but a significant stimulatory effect on the colony size was observed, suggesting an influence on colony expansion rather than on colony formation. In the orthotopic model of human prostate cancer used in this study, ALK1Fc significantly reduced the prostate tumor burden compared to control group. Strikingly, ALK1Fc treatment of tumor-bearing animals resulted in highly hypoxic tumors and a trend for decreased number of CD31+ tumor capillaries, thus supporting the notion that ALK1Fc could possibly block BMP9-induced neovascularization. Additionally, vascular density manifested by

lectin may suggest an overall reduced trend in lectin- positive area in animals treated with ALK1Fc versus CFc. Lectin distribution appeared to be less diffused, suggesting that ALK1Fc treatment contributes to vessel integrity and maintenance rather than angiogenesis.

As expected, areas of tumor cell proliferation and apoptosis were found to be mutually exclusive distribution, with apoptotic regions highly, but not completely, overlapping with the hypoxic areas, suggesting that blocking of BMP9 by ALK1Fc might have an effect on cell proliferation and apoptosis of human prostate cancer cells besides targeting vessel maintenance<sup>34</sup>.

SMAD1 and SMAD5 (effectors of BMP9 signaling) can directly interact with JAG1 promoter, following BMP9 treatment<sup>61</sup>. BMP9 stimulation of SMAD signaling induces transcription of NOTCH ligand JAG1<sup>51</sup>. Transcriptional analysis revealed that ALK1Fc systemically blocked the induction of *JAG1* mRNA in presence of BMP9<sup>61</sup> at latest time point. We hypothesized that the crosstalk between BMP9 and NOTCH has translational implications in prostate cancer. *In silico* analysis of previously published dataset of human prostate cancer specimens, confirmed upregulation of *NOTCH1* and *JAG1* at the tumor stage<sup>45</sup>. Database analysis in a multistage model of prostate carcinogenesis on mouse prostate intraepithelial neoplasia (PIN) versus invasive cancer also indicated that *Jag1* is significantly upregulated in the stroma of invasive cancer stage<sup>60</sup>.

Interestingly, NOTCH activates aldehyde dehydrogenase 1A1 (ALDH1A1), which is a well-known marker of highly tumorigenic prostate cancer stem-like cells<sup>29-31</sup>. This subpopulation contributes to both initiation and progression of the cancer and when highly expressed in advanced-stage correlates with poor survival in hormone-naïve patients<sup>37</sup>. ALK1Fc treated tumours showed significant reduction of ALDH1A1, which in combination with the data described above, suggest that ALK1Fc might potentially interfere with NOTCH signaling in the regulation of ALDH1A1. In conclusion, our findings provide novel information on the role of BMP9 in human prostate cancer and suggest the promising use of BMP9 targeting molecules for the treatment of tumor and supportive microenvironment in prostate cancer patients.

## Supplementary Material

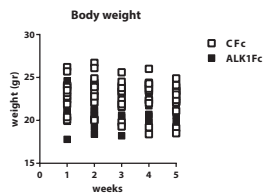


**Fig.S1. Body weight of animals used in the *in vivo* experiment**

Body weight (grams) of all the animals of treatment groups measured weekly during the course of treatment with either CFc (n=6) (A) or ALK1Fc (n=7).

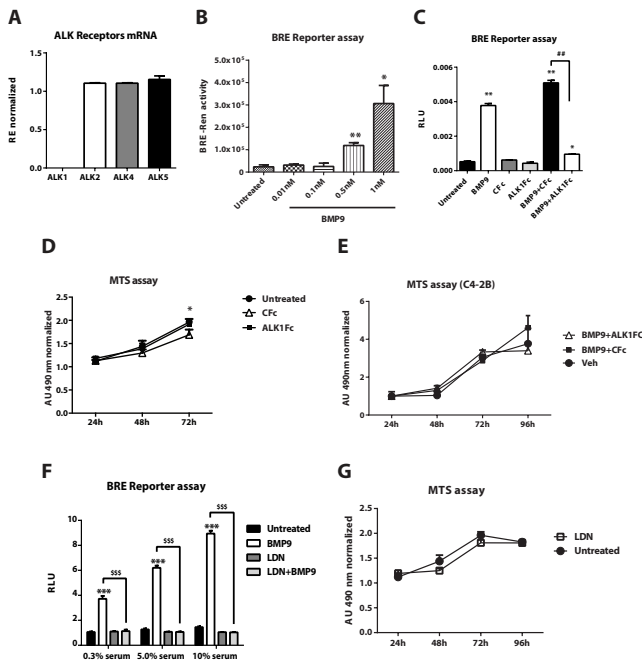


**Fig.S2. Characterization of BMP9 response *in vitro***

(A). Endogenous expression of *ALK1*, *ALK2*, *ALK4* and *ALK5* receptors in PC-3M-Pro4Luc2cells (mRNA level). Relative expression levels normalized to  $\beta$ -actin are shown. Error bars indicate  $\pm$ -SD. (B). Dose dependent response of PC-3M-Pro4Luc2 cells to recombinant BMP9 (0.01, 0.1, 0.5, 1 nM). Downstream activation of BMP signaling was tested by transfection of BRE-renilla construct and measured by reporter activity assay. Graph represents values from three independent experiments; error bars indicate  $\pm$  SEM (n=3). P value < 0.05 (\*) and P value < 0.01 (\*\*). (C). BRE reporter luciferase (BRELuc) assay; Inhibitory concentration of ALK1Fc or CFc (10ug/ml) was determined in cells stimulated with 1nM BMP9. Graph represents values from two independent experiments; error bars indicate  $\pm$  SEM (n=2). P value < 0.05 (\*) and P value < 0.01 (\*\*) compared to “untreated” control. P value < 0.01 (##). (D). MTS assay (24, 48, 72 hours) was performed in PC-3M-Pro4-luc2 human prostate cancer cell line treated with recombinant ALK1Fc (10ug/ml), CFc (10ug/ml). Accumulation of MTS was measured based on absorbance at 490 nm. Values are normalized to the basal measurements at 24 hours after cell seeding and treatments. Graph represents values from two independent experiments (n=2). Error bars indicate  $\pm$ SEM. (E). MTS assay (24, 48, 72, 96 hours) was performed in C4-2B human prostate cancer cell lines stimulated with recombinant BMP9 (1nM), BMP9 (1nM)+ALK1Fc (10ug/ml) or BMP9 (1nM)+CFc (10ug/ml). (n=3). (F). BMP transcriptional reporter assay (BRE-luciferase). PC-3M-Pro4 were seeded and, transfected with BRE-luc and renilla plasmid DNA. After 24 hours the medium was replaced with 0.3%, 5%, 10% FCII serum containing media and treated with BMP9 (1nM), LDN193189 (LDN, 120nM) and BMP9+LDN. Luc and Ren values were measured 24 hrs after treatment. RLU ratio values are shown (Luc/Ren). Error bars indicate  $\pm$ SD. (G). MTS assay (24, 48, 72 hours) was performed in PC-3M-Pro4-luc2 human prostate cancer cell line treated with LDN inhibitor (LDN193189, 120nM). (n=2). Error bars indicate  $\pm$ -SEM.

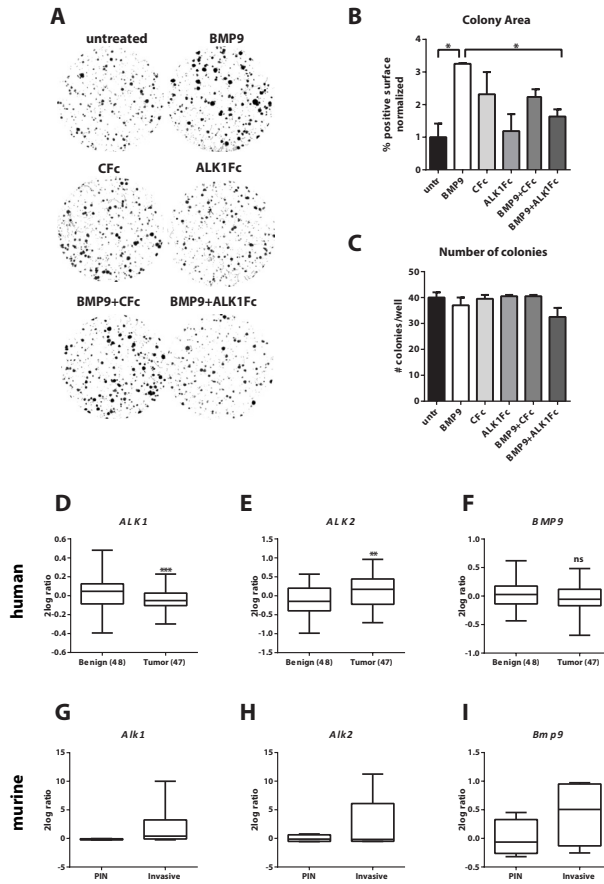


**Fig. S3. Effect of BMP9 and ALK1Fc on clonogenicity and ALK expression in human samples**

(A). Clonogenic assay of PC-3M-Pro4Luc2 cells. Low-density cultures (100 cells per well of 6well plate) were stimulated with BMP9, CFc, ALK1Fc, BMP9+CFc, BMP9+ALK1Fc. Colony formation was assessed after 10 days by crystal violet staining. Representative images are shown. (B-C). Quantification of surface covered by crystal violet positive colonies (colony area) and colony number. Graph shows percentage of positive surface normalized per condition (average of three independent experiments). P value < 0.05 (\*), ns; non-significant. Error bars indicate SEM. (D-F). Bioinformatics analysis of AMC OncoGenomics database (Sueltman transcript comparison) showing mRNA expression of *ALK1*, *ALK2* and *BMP9* in prostate tissues among benign prostate tissues (n=48) versus tumor tissues (n=47). Values are expressed as 2log ratio tumor/ benign. ns: non-significant. P value < 0.01 (\*\*). (G-I). Microarray cDNA analysis (adapted from Bacac *et al.*,<sup>46</sup>) of *Alk1*, *Alk2* and *Bmp9* expression in microdissected murine stroma derived from two tumor stages; prostate intraepithelial neoplasia (PIN, n=4), and invasive tumors (n=6).



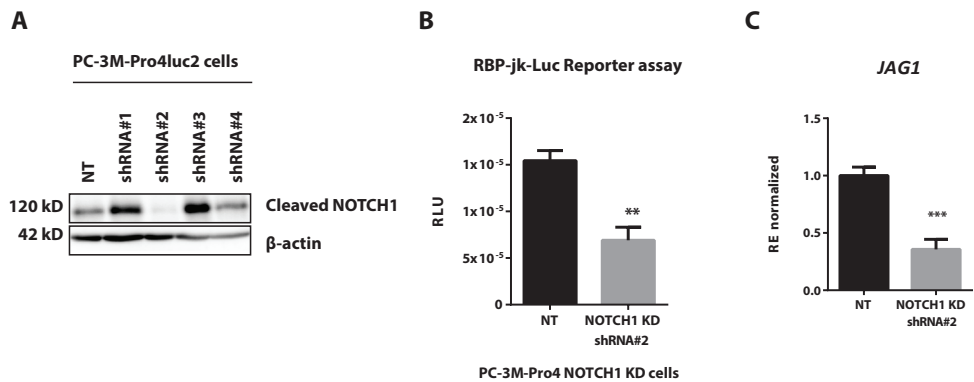


#### Fig.S4.Characterization of NOTCH1 knock-down

(A). Western immunoblotting for NOTCH1 protein as validation of lentiviral shRNA-mediated knockdown of NOTCH1 intracellular domain (cleaved) in PC-3M-Pro4Luc2 PCa cell line using five shRNA constructs. Based on the downregulation of cleaved NOTCH1 observed after lentiviral transduction and puromycin selection, the stable line expressing the shRNA #2 construct was selected for further experiments. NT; non-targeting shRNA lentiviral mediated transduction. β-actin was used as loading control. (B). NOTCH transcription factor RBP-Jk-luciferase reporter assay in non-targeting (NT) and NOTCH1 (shRNA#2) knockdown (KD) PC-3M-Pro4Luc2 cells. RLU: relative luciferase units (signal of luciferase normalised to renilla values). n=3, P value < 0.01 (\*\*)

(C). QPCR for *JAG1* mRNA levels in non-targeting (NT) and NOTCH1 (shRNA#2) knockdown (KD) PC-3M-Pro4Luc2 cells. Fold over the value of NT is represented. Error bars indicate ±SD. P value < 0.001 (\*\*\*)

#### Acknowledgements

The research leading to these results has received funding from the FP7 Marie Curie ITN under grant agreement No. 264817- BONE-NET (EZ) and from the Netherlands Initiative of Regenerative Medicine (NIRM, grant No. FES0908). We would also like to thank Marjan van de Merbel.

## References

1. Jemal, A., et al., Global patterns of cancer incidence and mortality rates and trends. *Cancer Epidemiol Biomarkers Prevent*, 2010. 19(8): p. 1893-907.
2. Chang, A.J., et al., High-risk prostate cancer classification and therapy. *Nat Rev Clin Oncol*, 2014. 11(6): p. 308-323.
3. [http://www.cancer.gov/types/prostate/hp/prostate-treatment-pdq#section/\\_1](http://www.cancer.gov/types/prostate/hp/prostate-treatment-pdq#section/_1).
4. Barlow, L.J. and M.M. Shen, Snapshot: prostate cancer. *Cancer Cell*, 2013. 24(3): p. 400-401.
5. Chen, Y., N.J. Clegg, and H.I. Scher, Anti-androgens and androgen-depleting therapies in prostate cancer: new agents for an established target. *Lancet Oncol*, 2009. 10(10): p. 981-991.
6. Nelson, W.G., A.M. De Marzo, and W.B. Isaacs, Prostate cancer. *N Engl J Med*, 2003. 349(4): p. 366-381.
7. Redig, A.J. and S.S. McAllister, Breast cancer as a systemic disease: a view of metastasis. *J Intern Med*, 2013. 274(2): p. 113-126.
8. Bendell, J.C., et al., Safety, pharmacokinetics, pharmacodynamics, and antitumor activity of dalantercept, an activin receptor-like kinase-1 ligand trap, in patients with advanced cancer. *Clin Cancer Res*, 2014. 20(2): p. 480-9.
9. Hawinkels, L.J., A. Garcia de Vinuesa, and P. Ten Dijke, Activin receptor-like kinase 1 as a target for anti-angiogenesis therapy. *Expert Opin Investig Drugs*, 2013. 22(11): p. 1371-83.
10. van Meeteren, L.A., et al., Anti-human Activin receptor-like kinase 1 (ALK1) antibody attenuates Bone morphogenetic protein 9 (BMP9)-induced ALK1 signaling and interferes with endothelial cell sprouting. *J Biol Chem*, 2012. 287(22): p. 18551-18561.
11. Bragdon, B., et al., Bone morphogenetic proteins: a critical review. *Cell Signal*, 2011. 23(4): p. 609-620.
12. David, L., et al., Identification of BMP9 and BMP10 as functional activators of the orphan activin receptor-like kinase 1 (ALK1) in endothelial cells. *Blood*, 2007. 109(5): p. 1953-61.
13. Herrera, B., et al., Autocrine bone morphogenetic protein-9 signals through activin receptor-like kinase-2/Smad1/Smad4 to promote ovarian cancer cell proliferation. *Cancer Res*, 2009. 69(24): p. 9254-62.
14. Scharpfenecker, M., et al., BMP-9 signals via ALK1 and inhibits bFGF-induced endothelial cell proliferation and VEGF-stimulated angiogenesis. *J Cell Sci*, 2007. 120(Pt 6): p. 964-72.
15. Celeste AJ, S.J., Cox K, Rosen V, Wozney JM, Bone morphogenetic protein-9, a new member of the TGF- $\beta$  superfamily. *J Bone Min Res*, 1994. 1(136).
16. Song, J.J., et al., Bone morphogenetic protein-9 binds to liver cells and stimulates proliferation. *Endocrinology*, 1995. 136(10): p. 4293-4297.
17. Herrera, B., et al., BMP9 is a proliferative and survival factor for human hepatocellular carcinoma cells. *PLoS One*, 2013. 8(7): p. e69535.
18. Li, R., et al., Targeting BMP9-promoted human osteosarcoma growth by inactivation of notch signaling. *Curr Cancer Drug Targets*, 2014. 14(3): p. 274-85.
19. Wang, K., et al., BMP9 inhibits the proliferation and invasiveness of breast cancer cells MDA-MB-231. *J Cancer Res Clin Oncol*, 2011. 137(11): p. 1687-1696.
20. Ye, L., H. Kynaston, and W.G. Jiang, Bone morphogenetic protein-9 induces apoptosis in prostate cancer cells, the role of prostate apoptosis response-4. *Mol Cancer Res*, 2008. 6(10): p. 1594-1606.
21. Olsen, O.E., et al., Bone morphogenetic protein-9 suppresses growth of myeloma cells by signaling through ALK2 but is inhibited by endoglin. *Blood Cancer J*, 2014. 4: p. e196.
22. Cunha, S.I. and K. Pietras, ALK1 as an emerging target for antiangiogenic therapy of cancer. *Blood*, 2011. 117(26): p. 6999-7006.
23. Urness, L.D., L.K. Sorensen, and D.Y. Li, Arteriovenous malformations in mice lacking activin receptor-like kinase-1. *Nat Genet*, 2000. 26(3): p. 328-31.
24. Gale, N.W., et al., Haploinsufficiency of delta-like 4 ligand results in embryonic lethality due to major defects in arterial and vascular development. *Proc Natl Acad Sci U S A*, 2004. 101(45): p. 15949-54.
25. Krebs, L.T., et al., Haploinsufficient lethality and formation of arteriovenous malformations in Notch pathway mutants. *Genes Dev*, 2004. 18(20): p. 2469-73.
26. Carvalho, F.L., et al., Notch signaling in prostate cancer: a moving target. *Prostate*, 2014. 74(9): p. 933-45.
27. Ross, A.E., et al., Gene expression pathways of high grade localized prostate cancer. *Prostate*, 2011.
28. Wang, Z., et al., Down-regulation of Notch-1 and Jagged-1 inhibits prostate cancer cell growth, migration and invasion, and induces apoptosis via inactivation of Akt, mTOR, and NF-kappaB

- signaling pathways. *J Cell Biochem*, 2010. 109(4): p. 726-36.
29. Zhao, D., et al., NOTCH-induced aldehyde dehydrogenase 1A1 deacetylation promotes breast cancer stem cells. *J Clin Invest*, 2014. 124(12): p. 5453-65.
  30. Ginestier, C., et al., ALDH1 is a marker of normal and malignant human mammary stem cells and a predictor of poor clinical outcome. *Cell Stem Cell*, 2007. 1(5): p. 555-67.
  31. Le Magnen, C., et al., Characterization and clinical relevance of ALDH bright populations in prostate cancer. *Clin Cancer Res*, 2013. 19(19): p. 5361-71.
  32. Li, T., et al., ALDH1A1 is a marker for malignant prostate stem cells and predictor of prostate cancer patients' outcome. *Lab Invest*, 2010. 90(2): p. 234-44.
  33. Seehra, J., et al., Antagonists of Bmp9, Bmp10, Alk1 and other Alk1 ligands, and uses thereof (International Patent WO2009139891). 2009.
  34. Mitchell, D., et al., ALK1-Fc inhibits multiple mediators of angiogenesis and suppresses tumor growth. *Mol Cancer Ther*, 2010. 9(2): p. 379-88.
  35. Cunha, S.I., et al., Genetic and pharmacological targeting of activin receptor-like kinase 1 impairs tumor growth and angiogenesis. *J Exp Med*, 2010. 207(1): p. 85-100.
  36. Suzuki, Y., et al., BMP-9 induces proliferation of multiple types of endothelial cells in vitro and in vivo. *J Cell Sci*, 2010. 123(10): p. 1684-1692.
  37. Kroon, J., et al., Glycogen synthase kinase-3 $\beta$  inhibition depletes the population of prostate cancer stem/progenitor-like cells and attenuates metastatic growth. *Oncotarget*, 2014. 5(19): p. 8986-94.
  38. Korchynskiy, O. and P. ten Dijke, Identification and functional characterization of distinct critically important Bone morphogenetic protein-specific response elements in the Id1 promoter. *J Biol Chem*, 2002. 277(7): p. 4883-4891.
  39. Berridge, M.V., P.M. Herst, and A.S. Tan, Tetrazolium dyes as tools in cell biology: new insights into their cellular reduction, in *Biotechnology Annual Review*. 2005, Elsevier. p. 127-152.
  40. van der Pluijm, G., et al., Interference with the microenvironmental support impairs the de novo formation of bone metastases in vivo. *Cancer Res*, 2005. 65(17): p. 7682-90.
  41. Karkampouna, S., et al., Novel ex vivo culture method for the study of Dupuytren's Disease: effects of TGF $\beta$  type 1 receptor modulation by antisense oligonucleotides. *Mol Ther Nucleic Acids*, 2014. 3: p. e142.
  42. Craft, C.S., et al., Endoglin inhibits prostate cancer motility via activation of the ALK2-Smad1 pathway. *Oncogene*, 2007. 26(51): p. 7240-50.
  43. Shi, S., et al., BMP antagonists enhance myogenic differentiation and ameliorate the dystrophic phenotype in a DMD mouse model. *Neurobiol Dis*, 2011. 41(2): p. 353-60.
  44. Cuny, G.D., et al., Structure-activity relationship study of bone morphogenetic protein (BMP) signaling inhibitors. *Bioorg Med Chem Lett*, 2008. 18(15): p. 4388-92.
  45. Borno, S.T., et al., Genome-wide DNA methylation events in TMPRSS2-ERG fusion-negative prostate cancers implicate an EZH2-dependent mechanism with miR-26a hypermethylation. *Cancer Discov*, 2012. 2(11): p. 1024-35.
  46. Bacac, M., et al., A mouse stromal response to tumor invasion predicts prostate and breast cancer patient survival. *PLoS One*, 2006. 1(1): p. e32.
  47. Shou, J., et al., Dynamics of notch expression during murine prostate development and tumorigenesis. *Cancer Res*, 2001. 61(19): p. 7291-7.
  48. Zhang, Y., et al., Down-regulation of Jagged-1 induces cell growth inhibition and S phase arrest in prostate cancer cells. *Int J Cancer*, 2006. 119(9): p. 2071-7.
  49. Leong, K.G. and W.Q. Gao, The Notch pathway in prostate development and cancer. *Differentiation*, 2008. 76(6): p. 699-716.
  50. Bin Hafeez, B., et al., Targeted knockdown of Notch1 inhibits invasion of human prostate cancer cells concomitant with inhibition of matrix metalloproteinase-9 and urokinase plasminogen activator. *Clin Cancer Res*, 2009. 15(2): p. 452-9.
  51. Larrivee, B., et al., ALK1 signaling inhibits angiogenesis by cooperating with the Notch pathway. *Dev Cell*, 2012. 22(3): p. 489-500.
  52. Ricard, N., et al., BMP9 and BMP10 are critical for postnatal retinal vascular remodeling. 2012. 119(25): p. 6162-6171.
  53. Kerr, G., et al., A small molecule targeting ALK1 prevents Notch cooperativity and inhibits functional angiogenesis. *Angiogenesis*, 2015.
  54. David, L., et al., Identification of BMP9 and BMP10 as functional activators of the orphan activin

- receptor-like kinase 1 (ALK1) in endothelial cells. *Blood* 2007. 109(5): p. 1953-1961.
55. Siegel, P.M. and J. Massague, Cytostatic and apoptotic actions of TGF $\beta$  in homeostasis and cancer. *Nat Rev Cancer*, 2003. 3(11): p. 807-820.
56. Massagué, J., TGF $\beta$  in Cancer. *Cell*, 2008. 134(2): p. 215-230.
57. Wang, K., et al., BMP9 inhibits the proliferation and invasiveness of breast cancer cells MDA-MB-231. *J Cancer Res Clin Oncol*, 2011. 137(11): p. 1687-96.
58. Ren, W., et al., BMP9 inhibits the bone metastasis of breast cancer cells by downregulating CCN2 (connective tissue growth factor, CTGF) expression. *Mol Biol Rep*, 2014. 41(3): p. 1373-83.
59. Ren, W., et al., BMP9 inhibits proliferation and metastasis of HER2-positive SK-BR-3 breast cancer cells through ERK1/2 and PI3K/AKT pathways. *PLoS One*, 2014. 9(5): p. e96816.
60. Bacac, M., et al., A mouse stromal response to tumor invasion predicts prostate and breast cancer patient survival. *PLoS One*, 2006. 1: p. e32.
61. Morikawa, M., et al., ChIP-seq reveals cell type-specific binding patterns of BMP-specific Smads and a novel binding motif. *Nucleic Acids Res*, 2011. 39(20): p. 8712-27.





## Chapter 7

# General Discussion & Future Perspectives



---

## Discussion and Future Directions

### TGF $\beta$ - the “Many-Faced God”

Cell signaling from members of the TGF $\beta$  pathway regulate homeostasis of many organ systems during embryonic development and adult life. TGF $\beta$  suppresses the proliferation of epithelial, endothelial and immune cells (tumor suppressor activity) and its action is under constant regulation. When the levels of TGF $\beta$  ligands or receptors are abnormally increased or decreased, due to occurrence of genetic mutations that affect gene expression, the cell homeostasis is disturbed; increased apoptosis/ proliferation, immune suppression/ hyperactivation, insufficient wound healing upon injury or excess ECM remodeling. In fact, in human pathological conditions, such as organ fibrosis and cancer, the circulating levels of TGF $\beta$  and BMP ligands are often found increased<sup>7</sup>. In particular, in many types of human cancer, TGF $\beta$  plays multiple roles<sup>2</sup>; at the initial stages of cancer formation it has tumor suppressing role. Upon establishment of a carcinoma TGF $\beta$  is considered to be a tumor promoter factor (mediated via linker phosphorylation of SMAD2/3<sup>3</sup> or non-SMAD pathways); tumor cells deactivate the cytostatic branch of TGF $\beta$  and maintain responsiveness to TGF $\beta$ -mediated EMT transition, cell motility, migration, differentiation to MFB phenotype and ECM remodeling<sup>2,4,5</sup>. These processes facilitate the spread of tumor cells and metastasis to other organs. Given the increased lethality of cancer patients associated with occurrence of metastasis and the lack of therapeutic treatments for organ fibrosis, several drugs inhibiting the function of TGF $\beta$  pathway members have been developed as promising cancer and fibrosis targeted therapies<sup>6</sup>.

### Summary of Findings

Our studies focused on modulation of TGF $\beta$  pathway in homeostasis, human fibrosis and cancer by *in vivo* and *ex vivo* approaches in different organs (liver, prostate, connective tissue). Inhibition of TGF $\beta$ / BMP pathway was performed using an antisense oligonucleotide, a ligand trap and a small molecule kinase inhibitor. Main goal of these different lines of research was to investigate the basic regulatory mechanisms during tissue regeneration (liver), fibrosis (Dupuytren's disease), tumor angiogenesis and cancer (prostate) and potential therapeutic benefits of TGF $\beta$ / BMP inhibition.

The main findings of this thesis are summarized in **Fig.1**.

1. Dynamics in TGF $\beta$  signaling activation regulates liver regeneration. Downstream effector SMAD2 mediates cell cycle arrest in hepatocytes and pro-fibrotic effects in HSCs (liver myofibroblasts). Systemic administration of small molecule TGF $\beta$  type I receptor kinase inhibitor LY-364947, selective for ALK5 inhibition, reduces basal SMAD2 signaling in hepatocytes, which leads to escape from cell cycle arrest (low p21, high PCNA and phosphorylated histone 3 levels). Hepatocyte proliferation due to ALK5 inhibition leads to improved cell replenishment during acute liver injury in mice and enhanced liver function (Chapter 3).



## Chapter 7

2. Systemic administration of TGF $\beta$  type I receptor kinase inhibitor, LY-364947, is not sufficient to abrogate the fibrogenic response of HSCs in acute, reversible liver injury model (Chapter 3).
3. Human connective tissue from Dupuytren's fibrosis is maintained in *ex vivo* culture for seven-day time period allowing real time study of fibrotic mechanisms by second harmonic generation imaging and three-dimensional reconstruction (Chapter 4).
4. *Ex vivo* delivery of ALK5 inhibitors SB-431542 and ALK5-AON have anti-fibrotic effects in human Dupuytren's fibrosis (Chapter 5).
5. Inhibition of BMP9 by ALK1Fc ligand trap has potential tumor anti-angiogenic effects on human prostate cancer in mouse xenograft model (Chapter 6).
6. ALK1Fc diminishes primary prostate tumor size by inhibiting BMP9 pro-proliferative role directly on tumor cells. BMP9 mediates tumor growth via binding to ALK2 and inducing NOTCH signaling (Chapter 6).

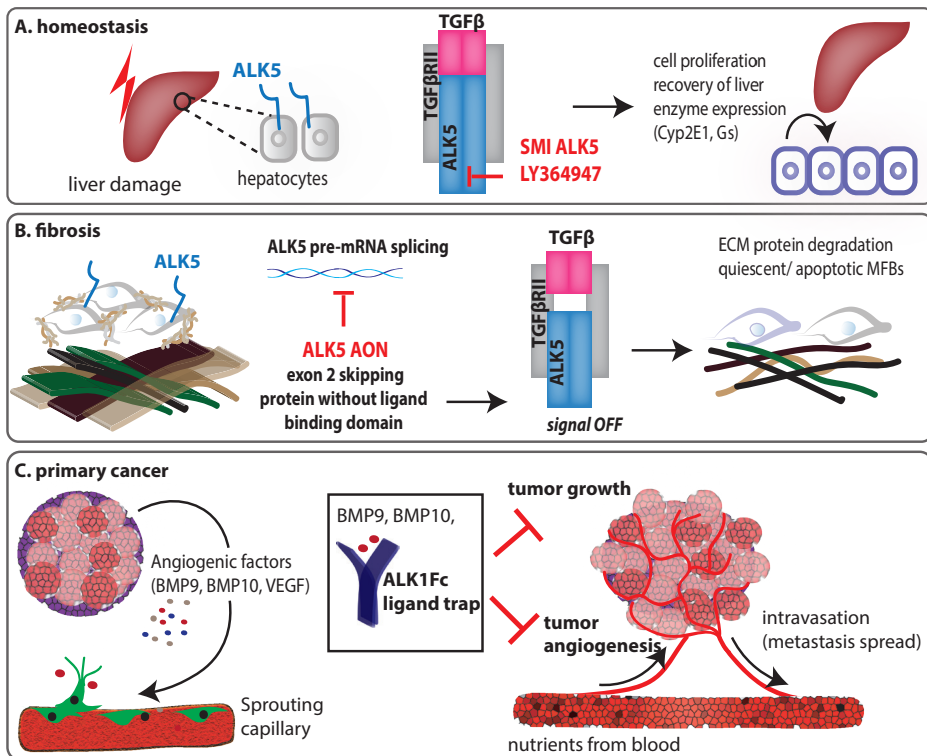


**Fig.1. Summary of key findings of this thesis**

(A). Liver homeostasis and the effects of *in vivo* administration of small molecule kinase inhibitor LY364947 to inhibit ALK5 signaling (Chapter 3). (B). Connective tissue fibrosis (Dupuytren's disease) and *ex vivo* tissue culture of human specimens (Chapter 4). *Ex vivo* inhibition of ALK5 using antisense oligonucleotide-mediated exon skipping showed anti-fibrotic effects on extracellular matrix protein deposition (Chapter 5). (C). *In vivo* inhibition of tumor angiogenesis and primary prostate tumor growth using the ALK1Fc ligand trap of BMP9/BMP10 in order to interfere with ALK1 and ALK2 downstream signaling.

## Modulation of TGF $\beta$ - Insight from *In Vivo* Liver Regeneration

Several studies have thoroughly investigated the contribution of hepatic progenitor cells on liver regeneration (reviewed in Chapter 2). These normally quiescent cells (oval cells), reside in the bile duct area and upon chronic injury become activated (ductular reaction) and differentiate to replenish hepatocytes and biliary epithelial cells (cholangiocytes). Various cytokines and cell types (resident and recruited immune or bone marrow cells) play a dynamic role during liver regeneration. Recent studies have increased our understanding of how regeneration is regulated, for instance by transcription factor gene expression alterations<sup>7</sup>, contribution of hepatic stellate cells as either source of oval cells<sup>8</sup> or collagen producing MFBs<sup>9</sup>, and bile duct (ductular) reaction and its role was studied by *in vivo* lineage tracing<sup>10</sup>. Preliminary data from this thesis (Appendix I) suggest a potential role for TGF $\beta$  type III auxiliary receptor CRIPTO in ductular reaction of oval cells during liver regeneration. However, the origin of these cells requires further characterization, considering that there are various other sources for MFBs<sup>11</sup> during liver injury such as recruited bone marrow derived cells<sup>12</sup>, pericytes and endothelial cells<sup>13</sup>. Furthermore, CRIPTO-expressing cells are found in the microenvironment of hematopoietic stem cells<sup>14,15</sup> while CRIPTO can function not only as membranous protein but also in a paracrine or systemic way as a soluble factor<sup>16</sup>. Thus, the origin and identity of CRIPTO-positive cells and their circulating or local role in the liver remain to be elucidated.

Tissue injury causes changes in tissue architecture, different mechanical tension between the connective tissue, pH, altered levels of oxygen and nutrients delivered to cells<sup>17</sup>; all these factors trigger release of latent TGF $\beta$  from the matrix proteins and upon activation TGF $\beta$  dimer is then able to bind to its receptors on the cell surface and activate the pathway<sup>18</sup>. In Chapter 3, we studied different aspects liver regeneration after experimental injury *in vivo*; response of epithelial cells (hepatocytes), hepatic stellate cells (HSCs, MFBs) and liver functionality. We show that the levels and duration of TGF $\beta$  pathway activation are determinants of the regenerative response and that TGF $\beta$  has pleiotropic effects in different cell types. *In vivo* systemic administration of small molecule kinase inhibitor (SMI) LY-364947 indicated that decrease of TGF $\beta$ /ALK5 pathway in the liver is applicable and has cell-type specific effects. Delivery of SMI and pathway inhibition is more efficient in the hepatocytes and less potent in targeting activated MFBs. It is known that TGF $\beta$  has a cytostatic role on hepatocytes (SMAD2-mediated) and a profibrotic and mitogenic role on the MFBs (SMAD3)<sup>19</sup>. In our study, inhibition of ALK5 activity induced proliferation of hepatocytes consistent with the TGF $\beta$ -mediated cytostasis. Regarding previous studies showing that soluble TGF $\beta$ RII delivered *in vivo* reduces fibrosis<sup>20</sup> we expected similar effects with the SMI LY-364947. Our data indicated that deposition of fibrous proteins by MFBs is not inhibited by SMI targeting ALK5. A variety of reasons may account for this response; (1) Kinetics and cell type specific delivery of the SMI<sup>21</sup>. (2) The acute liver injury model used is suitable for the study of regeneration and scar tissue formation (fibrogenesis) but not of pathological fibrosis<sup>22</sup>. Thus, to delineate the antifibrotic effects of LY-364947 different experimental models should be used such as chronic CCl<sub>4</sub> fibrosis model. (3) Alternative non SMAD signaling mechanisms may become activated to compensate for ALK5/SMAD2/3 inhibition<sup>23</sup>. Imatinib, a SMI of c-Abelson (c-ABL) kinase, is an FDA approved drug for chronic myeloid leukemia and also decreases lung fibrosis by inhibiting PDGF and TGF $\beta$ -non-SMAD mediated activation of c-ABL<sup>24</sup>.

Recent studies using similar SMI for ALK5, such as EW-7197, show reduction of TGF $\beta$ -induced reactive oxygen species production and promising anti-fibrotic outcome in liver fibrosis both *in vivo* and *in vitro*<sup>25</sup>. Another inhibitor of ALK5, LY-2157299, has shown safety and efficacy in advanced human cancer such as glioma<sup>26</sup> and in *ex vivo* studies of hepatocellular carcinoma<sup>27,28</sup>.

Clinically approved kinase inhibitors are Imatinib (Gleevec), Eftinib (Iressa) and Erlotinib (Tarceva) for cancer treatment have paved the “translational” way of SMIs<sup>29</sup>. The main advantages of SMIs are the high cell permeability due to small molecular weight and decreased toxicity due to rapid metabolism and removal by the renal system. However, *in vivo* evaluation of SMIs requires frequent or periodic administration, since dosage-related and cell type-specific effects are difficult to monitor<sup>30</sup> because the majority of these inhibitors bind to the ATP site of kinases. Cross-inhibition of multiple kinases is a consideration when using ATP inhibitors; however, experimental advances, such as high-throughput screening, have improved the specificity properties for a particular kinase<sup>30-33</sup>. Novel methodologies, in particular in Proteomics and Nanotechnology are needed to further improve the substrate specificity and delivery of SMIs to a particular tissue or cell type that is most likely to benefit from the drug and circumventing toxic effects to other tissues.

### **Insight on TGF $\beta$ -mediated Fibrotic Mechanisms from an *Ex Vivo* Human Model**

Fibrosis is a pathological state characterized by the excessive deposition of connective tissue commonly occurring during wound healing and tissue regeneration<sup>34</sup>. It can affect most organ systems and lead to a variety of diseases including liver cirrhosis, pulmonary hypertension, systemic sclerosis and congestive heart failure, representing one of the major medical challenges of our time. To treat fibrotic disease, it is necessary to control the improper wound mechanism process and redirect it towards a pure regenerative/repair process<sup>35</sup>. Design of novel anti-fibrotic therapies can only be achieved after thorough characterization of the disease profile. Our aim was to improve the current methodology available for DD fibrosis in order to better study the molecular pathogenesis. In Chapter 4, we present the development of an *ex vivo* culture method for the maintenance of human fibrotic tissue from Dupuytren's connective tissue disease. This model combines the near-*in vivo*, physiological microenvironment as equivalent to the *in vitro* method where culture conditions and gene expression can be modulated. Given the high rate of recurrence and surgical resection of fibrotic nodules being the main treatment to restore hand functionality, our model provides a patient-specific, preclinical platform for screening of anti-fibrotic compounds using surgical waste material. Fibroblast cell derivation remains the main method to study fibrosis; however it can only provide one-sided information excluding the influence of the microenvironment on cell behavior<sup>36,37</sup>. The advantage of this system is that we circumvent the need for fibroblast cell derivation and instead we study the three-dimensional context of cells and surrounding extracellular matrix<sup>35,38</sup>.

## Novel *Ex Vivo* Culture Method of Dupuytren's Fibrosis: Preclinical Translation for Human Anti-Fibrotic Drug Screening

DD tissue composition consists mainly of fibroblasts, MFBs, with fewer subset of endothelial, smooth muscle cells and immune cells<sup>39</sup> (**Fig.2**). ALK5 is expressed mainly in MFBs in DD, and not in endothelial cells, which express ALK1<sup>40</sup>. In Chapter 5, using the *ex vivo* model of human fibrotic tissue we demonstrated how interference with the mRNA processing of ALK5 by AON exhibits altered gene expression in favor of fibrosis reversal. We have showed that AONs with two different chemical modifications, Vivo morpholinos and 2'-O-methyl (2'-O-Me), are effectively delivered in tissue and do not cause cell death or toxicity. In our system, the fibroproliferative properties of the disease have been hampered by ALK5 AON treatment, suggesting that partial reduction of the TGF $\beta$  signaling is sufficient to "decrease" the fibrotic content of the disease. One possible explanation of the strong anti-fibrotic effect of ALK5 AON observed in DD tissue may be attributed to the occurrence of "flywheel effect" upon downstream proteins. Although, the initial stimulus is removed (ALK5 exon skipping) there seems to be a continuous oscillation of downstream effects, such as protein expression of target genes (collagens,  $\alpha$ SMA). Another consideration is that full skipping is not the goal for the treatment of DD especially since partial skipping already has beneficial effects of collagen deposition. Complete abrogation of ALK5 receptor activity might elicit compensatory mechanisms by other signaling pathways with no therapeutic benefit. Therefore, a more subtle and titrable regulation is required, which is one of the major advantages of the AON approach.

In addition, ALK5 kinase activity was effectively inhibited *ex vivo* by kinase inhibitor SMI SB-431542, which is an ATP antagonist and blocks ALK4, -5, -7 kinase activity. In both strategies (SB-431542 and ALK5 AON) expression of fibrous proteins collagens type I and type III was decreased and the number of  $\alpha$ -smooth muscle actin ( $\alpha$ SMA)-positive MFBs was reduced. Since there was no increase in cell death events in our model, perhaps the existing MFBs were modulated in order to secrete fewer amounts of fibrous proteins. Moreover, degradation of collagen is induced by specialized enzymes MMP1, MMP8, MMP13 and MMP14. MMP13 and MMP14 may indirectly also activate TGF $\beta$  (via MMP2 and MMP9) exacerbating fibrosis<sup>41</sup>. MFBs produce high levels of tissue inhibitor of matrix metalloproteases (TIMPs) to promote ECM deposition instead of degradation. Fibrosis resolution is associated with disappearance of MFBs and decrease in TIMP expression<sup>42</sup>. Reduction of fibrotic burden and MFBs in our model may be induced from the inhibition of TGF $\beta$ -mediated EMT process<sup>13</sup>. Quiescent fibroblasts are distinguished from activated MFBs by  $\alpha$ SMA expression, thus, reduction of  $\alpha$ SMA observed in real time due to TGF $\beta$  inhibition *ex vivo* (Chapter 5) may indicate reversal of MFBs to a quiescent state.

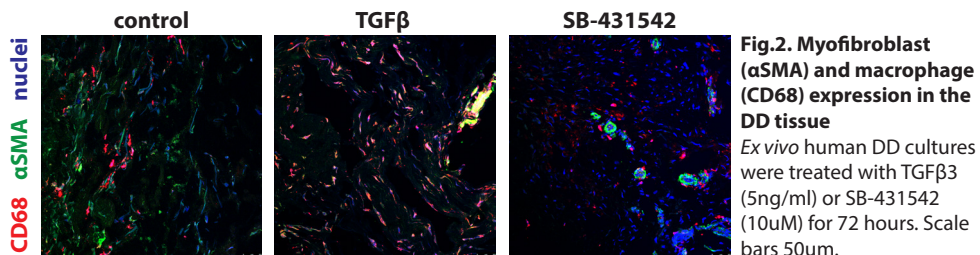


**Fig.2. Myofibroblast ( $\alpha$ SMA) and macrophage (CD68) expression in the DD tissue**

*Ex vivo* human DD cultures were treated with TGF $\beta$ 3 (5ng/ml) or SB-431542 (10uM) for 72 hours. Scale bars 50um.

The current opinion is that MFBs once activated and their function is no longer required, they undergo senescence<sup>43</sup> or apoptosis<sup>44</sup>. Another hypothesis is that MFBs may reverse back to a quiescent fibroblast phenotype, which requires further experimental evidence<sup>11,45</sup>. Lineage tracing experiments are required to address whether this hypothesis is valid for DD, with genetic tools applied for tracing MFBs in liver and lung fibrosis *in vivo* (glial fibrillary acidic protein- Cre recombinase (GFAP-Cre)<sup>8</sup>, collagen 1 type I (Col-GFP)<sup>11</sup>, and PDGF receptor  $\beta$  (PDGFR  $\beta$ - Cre)<sup>46</sup>. MFBs in several organs are marked by PDGFR $\beta$  expression and deletion of  $\alpha\beta 6$  integrin in those cells caused a reduction of TGF $\beta$  activation and subsequently of fibrosis<sup>46</sup>. Similar effects were observed by small molecule inhibitor targeting  $\alpha\beta 6$  integrin<sup>46</sup>. Given the recurrent properties of DD fibrosis the role of stem/ progenitor cells (for instance mesenchymal stem cells) that constantly differentiate towards MFBs might be a valid hypothesis for the origin of fibrosis. Thus, we need to identify the key regulatory proteins that trigger the start of fibrosis in DD and test whether their inhibition provides resolution of fibrosis. Performing drug screens on surgical waste, patient-derived tissue, instead of e.g. rodent models, could be an effective and quick way of drug categorization for further experimentation or dismiss, and thus it could reduce the number of animal studies<sup>35</sup>. Future research will focus on understanding the role of the immune system in DD contracture and ways of altering the immune response to trigger matrix degradation. (Pre) clinical studies using the *ex vivo* culture method could potentially reveal immunological response triggered by candidate substances, and could be further used to delineate the exact mechanism of action of anti-fibrotic drugs.

### Tumor Angiogenesis and Cancer

Cellular and extracellular context (microenvironment) has a great influence on tumor growth and development of drug resistance<sup>47,48</sup>. Tumor microenvironment consists of tumor cells, and abnormally functioning, non-malignant stromal cells such as fibroblasts, endothelial cells and infiltrating immune cells. Initial experiments with viral oncogene Src showed induction of transformation *in vitro* but not when overexpressed in embryos<sup>49,50</sup>. Moreover, mutated stromal fibroblasts have the potential to oncogenically transform normal epithelial cells<sup>51</sup>. Thus, the extracellular matrix and cellular context exert powerful influence on the behavior of cancer cells despite the presence of mutated oncogenic proteins. From this prospective, properties of the microenvironment and its impact on both normal and tumor cells is highly similar during fibrosis (as discussed previously) and cancer, which should be considered in the study of both human diseases. A hallmark in the progression of solid tumors is the formation of blood vessels (angiogenesis) within the primary tumor, which paradoxically requires the contribution of non-malignant cells<sup>48</sup>. Tumors perform neovascularization to sustain their growth utilizing non-malignant cells from their niche. In contrast to the wound healing angiogenesis where new vessels integrate within the existing network, in tumors there is destruction of the vasculature and formation of immature, leaky vessels. Several factors induce angiogenesis such vascular endothelial growth factor, platelet derived growth factor, hypoxia, BMPs along with matrix degrading enzymes that disrupt existing vasculature in order to recruit pericytes, endothelial and smooth muscle cells. In our studies we investigated the contribution of a BMP ligand, BMP9, in ALK1-mediated angiogenesis and tumor growth of human prostate cancer.

Sequestering of BMP9 by ALK1Fc ligand trap reduced tumor angiogenesis in primary prostate cancer xenografts and led to decreased tumor growth. Along with the anti-angiogenic effects, a direct effect of BMP9 inhibition on tumor cells was observed. Thus, BMP9 levels from the circulation, stroma and possibly secreted also from tumor cells, have a dual role in prostate cancer; pro-angiogenic effects on ALK1 expressing endothelial cells and pro-proliferative role on tumor cells via ALK2.

BMPs plays role in prostate tissue homeostasis as well as in tumor formation and metastasis to the bone, which is the predominant metastasis site for prostate cancer (PCa)<sup>52</sup>. Most BMP ligands and receptors are regulated by androgens and are expressed in the normal prostate tissue while up/downregulation is associated with primary or metastatic tumor<sup>53</sup>. BMP2, 4, 6, 7 and GDF15 have been extensively studied in this context and have tumor suppressing role on the proliferation of androgen-sensitive cancer cells<sup>54</sup>. Loss of function of many BMP ligands, SMAD4, SMAD8 and type II receptors (ACVR2A, ACVR2B, BMPRII) is associated with hormone insensitive stage of PCa and bone metastases<sup>53-55</sup>. BMP9 seems to have dual effects in PCa; proangiogenic mediated via ALK1 in endothelial cells and tumor promoting role in ALK2-expressing PCa cells, similar to pro-proliferative role on ovarian cancer<sup>56</sup> and hepatocellular carcinoma cells<sup>57</sup>. An explanation for the different PCa tumor effects between BMP9 and other BMP ligands, such as BMP7<sup>58,59</sup>, may be the preference of BMP9 for ALK1 and ALK2 binding in different cell types, as opposed to BMP7 that utilizes ALK2, ALK3 and ALK6. Given the high affinity of BMPs to type I receptors this first binding step determines which type II receptor will be recruited to the complex causing different biological responses. Also, BMP9 binds to all three type II BMP receptors while BMP7 binds to BMPRII and ACVR2A<sup>53</sup>. Autocrine or paracrine BMP9 exert proliferative effect on PC3 tumor cells via ALK2 supported by microarray data indicating elevated ALK2 levels in PCa versus normal or benign prostate tissues (Chapter 6). Constitutively active ALK2 phosphorylates ENDOGLIN and promotes cell migration of PC3 cells<sup>60</sup>. Another potential mechanism is the synergy between BMPs and NOTCH signaling pathway; several studies prove that SMAD binding to transcription factors of NOTCH-intracellular domain class (NICDs) regulates myogenic differentiation and the balance between endothelial cell migration and quiescence<sup>61</sup>. In Chapter 6, we provide evidence of synergy between BMP9 and NOTCH ligand JAGGED that enhances the proliferation of PC3 cells and positively correlates with tumor progression in human microarray data.

Treatment with BMP9 ligand trap, ALK1Fc, showed promising anti-angiogenic and anti-tumorigenic effects in xenograft model of human PCa cells in mice (Chapter 6) and is currently being used in clinical trials for recurrent solid cancers (head and neck, ovarian, endometrial)<sup>62</sup>. ALK1 is an effective target for angiogenesis given its expression in endothelial cells and the complex formation with other pro-angiogenic factors such as BMP9, BMP10, TGF $\beta$ , ENDOGLIN<sup>63-65</sup>. However, the outcome on vessel quiescence or activation is often contradictory due to TGF $\beta$ -functioning via both ALK5 and ALK1 in endothelial cells leading to codependence or between SMAD1/5/8 and SMAD2/3 pathways<sup>64</sup>. Activation of both ALK1 and ALK5 by BMP9 and TGF $\beta$ , induce expression of proangiogenic factor VEGF<sup>66</sup>. BMP9/ALK1 signaling may inhibit and promote endothelial cell growth depending highly on the cell context<sup>67</sup>. ENDOGLIN, the type III auxiliary receptor of TGF $\beta$  signaling favours signaling via ALK1 by binding to BMP9, BMP10 as well as to TGF $\beta$ 1, 3 and preventing their interaction with ALK5<sup>67-69</sup>.

However, ENDOGLIN associates with other type I receptors such as ALK2, ALK3 and ALK6, thereby influencing TGF $\beta$  and BMP signaling in various ways<sup>70</sup>. Inhibitors of ENDOGLIN have been developed as anti-angiogenic treatment (TRC-105<sup>71</sup>, ENDOGLIN-Fc<sup>72</sup>) based on the ability of soluble ENDOGLIN to bind to BMP9 and BMP10 and inhibit vessel formation and tumor growth<sup>73</sup>. Several other anti-angiogenic drugs are investigated in clinical trials for cancer therapy<sup>74</sup>; thalidomide (ClinicalTrials.gov identifier; NCT00083551), AG-013736 (NCT00094107), Axitinib (NCT01321437), VEGF inhibitor SU5416 (NCT00006155), endostatin (NCT00518557).

### Clinical Applications and Future Prospective

Deregulated TGF $\beta$  signaling is associated with disease progression, for instance, chronic inflammation, cardiovascular disorders, organ fibrosis and malignancies, thus inhibition of this pathway is a promising therapeutic approach. Given the pleiotropic role of TGF $\beta$  signaling and its critical function in maintaining homeostasis of various tissues, therapies should tackle the pathogenic aspects of the signaling without interfering with homeostatic mechanisms.

As evidenced in Chapter 3, short term TGF $\beta$  inhibition may be beneficial in enhancing cell proliferation after acute liver injury; however, it may eventually delay or exacerbate the fibrogenic response needed for appropriate regeneration. Thus, from a translational perspective TGF $\beta$  inhibition must be spatiotemporally controlled in particular cell type(s), during specific stages of during disease progression. Such approach comes from liver fibrosis studies where decrease of collagen chaperone expression was performed *in vivo* using siRNA delivered via liposomes that were coated with retinol protein<sup>75</sup>. Based on the retinol-storing properties of collagen producing HSCs<sup>71</sup> the liposome-mediated drug delivery is beneficial in decreasing ECM protein secretion and limiting fibrosis<sup>76</sup>. Other studies performed HSC-specific drug targeting of ALK5 inhibitor LY-364947 utilizing the specific binding of mannose 6 phosphate human serum albumin (M6PHSA) on the insulin-like growth factor II receptor, which is expressed in HSCs<sup>77</sup>.

A hypothetical therapeutic setting for Dupuytren's disease could be the administration of AONs (Chapter 4 and 5) prior to the surgical intervention or postoperatively, in order to counteract the TGF $\beta$  activity in the remaining MFBs. Early application of ALK5 AON could prevent destructive TGF $\beta$  action which is triggered by tissue damage during surgery, with consideration of the long term fibrotic effect that results from exposure to TGF $\beta$ <sup>78</sup>. Combination treatments targeting both the ECM and MFBs could be a promising approach; for instance treatment with matrix degrading enzymes, such as the FDA approved Clostridium Collagenase Xiflex compound, would enhance the ability of TGF $\beta$  inhibitors (AONs or SMIs) to pass through the extracellular space and enter the MFBs. (Pre)clinical studies involving DD *ex vivo* culture method could potentially reveal anti-fibrotic candidate substances, that could be studied within a therapeutic context focused on patient-specific gene expression, drug and immune responses. Therefore, stratification of patients participating in clinical trials could be better monitored.

Systemic administration of TGF $\beta$  inhibitors in humans might have detrimental effects due to inhibition of the cytostatic and immune suppressive role of TGF $\beta$  in many organs leading

to formation of carcinomas and inflammation. However, studies in transgenic mice (soluble TGF $\beta$ RII fused to Fc is under the control of mammary specific promoter MMTV-LTR) showed that lifelong exposure to TGF $\beta$ RIIFc does not induce toxic effects or have negative impact on homeostasis<sup>79</sup> that is observed in mice with TGF $\beta$  gene deletion<sup>80</sup>. Most importantly, experimental induction of tumors in this mouse model showed that they are resistant to metastasis development<sup>79</sup>. A similar study showed beneficial effects in tumor apoptosis and migration in breast cancer after systemic administration of TGF $\beta$ RIIFc, however no effect was observed on tumor angiogenesis<sup>81</sup>. Given the impact of the vasculature and surrounding stroma, combination treatment of TGF $\beta$  inhibitors with chemotherapeutics, immune modulatory agents or anti-angiogenesis factors<sup>6</sup> have gained scientific and clinical interest as an approach for cancer treatment<sup>82-84</sup>. Monotherapy in cancer treatment often results in drug resistance, while combinations of drugs that target tumor cell proliferation but also the microenvironment are more likely to slow progression to metastasis. A major limitation and growing concern in cancer field is multidrug resistance (MDR), a process via which tumor cells acquire mutations that provide them synchronous resistance to different drugs when given in combination<sup>85</sup>. To stop this vicious cycle of drug resistance and cancer progression to metastasis, several chemosensitising compounds have been developed to interfere with MDR, such as steroids, channel blockers or stealth liposomes<sup>86</sup>. Moreover, drug resistance to anti-angiogenic compounds is less prevalent because of the genome stability of endothelial cells compared to tumor cells<sup>87</sup>.

One of the drawbacks of chemotherapy or radiation is the induction of apoptosis of normal cells which are not replenished but rather replaced by fibrotic scar tissue. In this case long term inhibition of TGF $\beta$  might be beneficial to block the progression of fibrosis in cancer survivors<sup>88</sup>. ECM deposition in the tumor stroma and MFB contraction affect the influx and outflux of fluid from the interstitial space causing high interstitial fluid pressure (IFP)<sup>89</sup>; a property found in tumors which hampers the delivery of drug compounds into the tumor cells<sup>90</sup>. This is another aspect where TGF $\beta$  inhibition in the tumor microenvironment may enhance the delivery and benefits of chemotherapy<sup>91</sup>.

Collectively, the studies in this thesis aimed to improve insight on the molecular mechanisms exerted by TGF $\beta$  in various tissues and in different disease stages. Inhibition of the TGF $\beta$  shows pleiotropic effects consistent with the plethora of biological processes regulated by TGF $\beta$ . Modulation of the gene expression or protein activity of key components of the TGF $\beta$ /BMP pathway was performed using clinically relevant drug compounds. Our studies in homeostasis, fibrosis, tumor angiogenesis and cancer highlight the importance of a holistic view when interpreting the effects of TGF $\beta$  although therapeutic inhibitory approaches need to be cell type/tissue specific, administered at a specific stage of disease, in a controlled dosing scheme and taking into consideration the genetic variability of individual patients.



### References

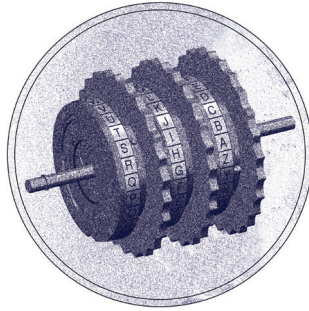
1. Akhurst, R.J., TGF $\beta$  signaling in health and disease. *Nat Genet*, 2004. 36(8): p. 790-792.
2. Massagué, J., TGF $\beta$  in Cancer. *Cell*, 2008. 134(2): p. 215-230.
3. Yamaguchi, T., et al., Phosphorylated Smad2 and Smad3 signaling: Shifting between tumor suppression and fibro-carcinogenesis in chronic hepatitis C. *Hepato Res*, 2013. 43(12): p. 1327-1342.
4. Levy, L. and C.S. Hill, Alterations in components of the TGF- $\beta$  superfamily signaling pathways in human cancer. *Cytokine Growth Factor Rev*, 2006. 17(1-2): p. 41-58.
5. Roberts, A.B. and L.M. Wakefield, The two faces of transforming growth factor  $\beta$  in carcinogenesis. *Proc Natl Acad Sci U S A*, 2003. 100(15): p. 8621-8623.
6. Akhurst, R.J. and A. Hata, Targeting the TGF $\beta$  signaling pathway in disease. *Nat Rev Drug Discov*, 2012. 11(10): p. 790-811.
7. Nishikawa, T., et al., Resetting the transcription factor network reverses terminal chronic hepatic failure. *J Clin Invest*, 2015. 125(4): p. 1533-1544.
8. Yang, L., et al., Fate-mapping evidence that hepatic stellate cells are epithelial progenitors in adult mouse livers. *Stem Cells*, 2008. 26(8): p. 2104-2113.
9. Kim, K.-H., et al., CCN1 induces hepatic ductular reaction through integrin  $\alpha$ v $\beta$ 5-mediated activation of NF- $\kappa$ B. *J Clin Invest*, 2015. 125(5): p. 1886-1900.
10. Jörs, S., et al., Lineage fate of ductular reactions in liver injury and carcinogenesis. *J Clin Invest*, 2015. 125(6): p. 2445-2457.
11. Iwaisako, K., et al., Origin of myofibroblasts in the fibrotic liver in mice. *Proc Natl Acad Sci U S A*, 2014. 111(32): p. E3297-E3305.
12. Gressner, O.A. and C. Gao, Monitoring fibrogenic progression in the liver. *Clin Chim Acta*, 2014. 433(0): p. 111-122.
13. Zeisberg, M. and R. Kalluri, Cellular mechanisms of tissue fibrosis: Common and organ-specific mechanisms associated with tissue fibrosis. *Am J Physiol Cell Physiol*, 2013. 304(3): p. C216-C225.
14. Miharada, K., et al., Cripto regulates hematopoietic stem cells as a hypoxic-niche-related factor through cell surface receptor GRP78. *Cell Stem Cell*, 2011. 9(4): p. 330-344.
15. Miharada, K., et al., Hematopoietic stem cells are regulated by Cripto, as an intermediary of HIF-1 $\alpha$  in the hypoxic bone marrow niche. *Ann NY Acad Sci*, 2012. 1266(1): p. 55-62.
16. Klauzinska, M., et al., The multifaceted role of the embryonic gene Cripto-1 in cancer, stem cells and epithelial-mesenchymal transition. *Semin Cancer Biol*, 2014. 29(0): p. 51-58.
17. Taub, R., Liver regeneration: from myth to mechanism. *Nat Rev Mol Cell Biol*, 2004. 5(10): p. 836-847.
18. Shi, M., et al., Latent TGF $\beta$  structure and activation. *Nature*, 2011. 474(7351): p. 343-349.
19. Zhang, L., et al., Smad2 protects against TGF- $\beta$ 1/Smad3-mediated collagen synthesis in human hepatic stellate cells during hepatic fibrosis. *Mol Cell Biochem*, 2015. 400(1-2): p. 17-28.
20. George, J., et al., In vivo inhibition of rat stellate cell activation by soluble transforming growth factor  $\beta$  type II receptor: A potential new therapy for hepatic fibrosis. *Proc Natl Acad Sci U S A*, 1999. 96(22): p. 12719-12724.
21. Vogt, J., R. Traynor, and G.P. Sapkota, The specificities of small molecule inhibitors of the TGF $\beta$  and BMP pathways. *Cell Signal*, 2011. 23(11): p. 1831-1842.
22. Liedtke, C., et al., Experimental liver fibrosis research: update on animal models, legal issues and translational aspects. *Fibrogenesis Tissue Repair*, 2013. 6: p. 19-19.
23. Connolly, E.C., J. Freimuth, and R.J. Akhurst, Complexities of TGF $\beta$  targeted cancer therapy. *Int J Biol Sci*, 2012. 8(7): p. 964-978.
24. Daniels, C.E., et al., Imatinib mesylate inhibits the profibrogenic activity of TGF $\beta$  and prevents bleomycin-mediated lung fibrosis. *J Clin Invest*, 2004. 114(9): p. 1308-1316.

25. Park, S.-A., et al., EW-7197 inhibits hepatic, renal, and pulmonary fibrosis by blocking TGF- $\beta$ /Smad and ROS signaling. *Cell Mol Life Sci*, 2015. 72(10): p. 2023-2039.
26. Rodon, J., et al., First-in-human dose study of the novel Transforming growth factor  $\beta$  receptor I kinase inhibitor LY2157299 monohydrate in patients with advanced cancer and glioma. *Clin Cancer Res*, 2015. 21(3): p. 553-560.
27. Serova, M., et al., Effects of TGF- $\beta$  signaling inhibition with galunisertib (LY2157299) in hepatocellular carcinoma models and in ex vivo whole tumor tissue samples from patients. *Oncotarget*, 2015.
28. Dituri, F., et al., Differential inhibition of the TGF $\beta$  signaling pathway in HCC cells using the small molecule inhibitor LY2157299 and the D10 monoclonal antibody against TGF- $\beta$  receptor type II. *PLoS One*, 2013. 8(6): p. e67109.
29. Arora, A. and E.M. Scholar, Role of tyrosine kinase inhibitors in cancer therapy. *J Pharmacol Exp Ther*, 2005. 315(3): p. 971-979.
30. Hong, C.C. and P.B. Yu, Applications of small molecule BMP inhibitors in physiology and disease. *Cytokine Growth Factor Rev*, 2009. 20(5-6): p. 409-418.
31. Fabian, M.A., et al., A small molecule-kinase interaction map for clinical kinase inhibitors. *Nat Biotech*, 2005. 23(3): p. 329-336.
32. Arkin, M.R. and J.A. Wells, Small-molecule inhibitors of protein-protein interactions: progressing towards the dream. *Nat Rev Drug Discov*, 2004. 3(4): p. 301-317.
33. Alsamarah, A., et al., Uncovering molecular bases underlying Bone morphogenetic protein receptor inhibitor selectivity. *PLoS One*, 2015. 10(7): p. e0132221.
34. Karkampouna, S. and M. Kruthof-de Julio, Fibrosis: a novel approach for an old problem. *Receptors Clin Investig*, 2014. 1(5).
35. Shih, B. and A. Bayat, Scientific understanding and clinical management of Dupuytren disease. *Nat Rev Rheumatol*, 2010. 6(12): p. 715-726.
36. Casalone, R., et al., Cytogenetic and interphase cytogenetic analyses reveal chromosome instability but no clonal trisomy 8 in dupuytren contracture. *Cancer Genet Cytogenet*, 1997. 99(1): p. 73-76.
37. Wynn, T.A., Cellular and molecular mechanisms of fibrosis. *J Pathol*, 2008. 214(2): p. 199-210.
38. Vogel, V. and M. Sheetz, Local force and geometry sensing regulate cell functions. *Nat Rev Mol Cell Biol*, 2006. 7(4): p. 265-275.
39. Verjee, L.S., et al., Unraveling the signaling pathways promoting fibrosis in Dupuytren's disease reveals TNF as a therapeutic target. *Proc Natl Acad Sci U S A*, 2013. 110(10): p. E928-E937.
40. Pardali, E., M.J. Goumans, and P. ten Dijke, Signaling by members of the TGF- $\beta$  family in vascular morphogenesis and disease. *Trends Cell Biol*, 2010. 20(9): p. 556-567.
41. Wilkinson, J.M., et al., MMP-14 and MMP-2 are key metalloproteases in Dupuytren's disease fibroblast-mediated contraction. *Biochim Biophys Acta*, 2012. 1822(6): p. 897-905.
42. Parks, W.C., C.L. Wilson, and Y.S. Lopez-Boado, Matrix metalloproteinases as modulators of inflammation and innate immunity. *Nat Rev Immunol*, 2004. 4(8): p. 617-629.
43. Krizhanovsky, V., et al., Senescence of activated stellate cells limits liver fibrosis. *Cell*, 2008. 134(4): p. 657-67.
44. Phan, S.H., The myofibroblast in pulmonary fibrosis. *Chest*, 2002. 122(6 Suppl): p. 286S-289S.
45. Friedman, S.L. and M.B. Bansal, Reversal of hepatic fibrosis -- fact or fantasy? *Hepatology*, 2006. 43(2 Suppl 1): p. S82-8.
46. Henderson, N.C., et al., Targeting of  $\alpha$ v integrin identifies a core molecular pathway that regulates fibrosis in several organs. *Nat Med*, 2013. 19(12): p. 1617-1624.
47. Nakasone, E.S., et al., Imaging tumor-stroma interactions during chemotherapy reveals contributions of the microenvironment to resistance. *Cancer Cell*, 2012. 21(4): p. 488-503.
48. Folkman, J., Tumor angiogenesis: therapeutic implications. *N Engl J Med*, 1971. 285(21): p. 1182-1186.

49. Mintz, B. and K. Illmensee, Normal genetically mosaic mice produced from malignant teratocarcinoma cells. *Proc Natl Acad Sci U S A*, 1975. 72(9): p. 3585-3589.
50. Dolberg, D.S. and M.J. Bissell, Inability of Rous sarcoma virus to cause sarcomas in the avian embryo. *Nature*, 1984. 309(5968): p. 552-6.
51. Olumi, A.F., et al., Carcinoma-associated fibroblasts direct tumor progression of initiated human prostatic epithelium. *Cancer Res*, 1999. 59(19): p. 5002-5011.
52. Ehata, S., et al., Bi-directional roles of bone morphogenetic proteins in cancer: Another molecular Jekyll and Hyde? *Pathol Int*, 2013. 63(6): p. 287-296.
53. Ye, L., et al., Bone morphogenetic proteins and their receptor signaling in prostate cancer. *Histol Histopathol*, 2007. 22(10): p. 1129-47.
54. Kim, I.Y., et al., Expression of Bone morphogenetic protein receptors type-IA, -IB, and -II correlates with tumor grade in human prostate cancer tissues. *Cancer Res*, 2000. 60(11): p. 2840-2844.
55. Horvath, L.G., et al., Loss of BMP2, Smad8, and Smad4 expression in prostate cancer progression. *Prostate*, 2004. 59(3): p. 234-242.
56. Herrera, B., et al., Autocrine Bone morphogenetic protein-9 signals via Activin receptor like kinase-2/Smad1/Smad4 to promote ovarian cancer cell proliferation. *Cancer Res*, 2009. 69(24): p. 9254-9262.
57. Herrera, B., et al., BMP9 is a proliferative and survival factor for human hepatocellular carcinoma cells. *PLoS One*, 2013. 8(7): p. e69535.
58. Morrissey, C., et al., Bone morphogenetic protein 7 is expressed in prostate cancer metastases and its effects on prostate tumor cells depend on cell phenotype and the tumor microenvironment. *Neoplasia*, 2010. 12(2): p. 192-205.
59. Buijs, J.T., et al., BMP7, a putative regulator of epithelial homeostasis in the human prostate, is a potent inhibitor of prostate cancer bone metastasis in vivo. *Am J Pathol*, 2007. 171(3): p. 1047-1057.
60. Romero, D., et al., Endoglin phosphorylation by ALK2 contributes to the regulation of prostate cancer cell migration. *Carcinogenesis*, 2010. 31(3): p. 359-366.
61. Klüppel, M. and J.L. Wrana, Turning it up a Notch: cross-talk between TGF $\beta$  and Notch signaling. *Bioessays*, 2005. 27(2): p. 115-118.
62. Bendell, J.C., et al., Safety, pharmacokinetics, pharmacodynamics, and antitumor activity of dalantercept, an activin receptor-like kinase-1 ligand trap, in patients with advanced cancer. *Clin Cancer Res*, 2014. 20(2): p. 480-9.
63. Goumans, M.J., et al., Balancing the activation state of the endothelium via two distinct TGF- $\beta$  type I receptors. *EMBO J*, 2002. 21(7): p. 1743-53.
64. Cunha, S.I. and K. Pietras, ALK1 as an emerging target for antiangiogenic therapy of cancer. *Blood*, 2011. 117(26): p. 6999-7006.
65. Cunha, S.I., et al., Genetic and pharmacological targeting of activin receptor-like kinase 1 impairs tumor growth and angiogenesis. *J Exp Med*, 2010. 207(1): p. 85-100.
66. van Meeteren, L.A., et al., Anti-human activin receptor-like kinase 1 (ALK1) antibody attenuates bone morphogenetic protein 9 (BMP9)-induced ALK1 signaling and interferes with endothelial cell sprouting. *J Biol Chem*, 2012. 287(22): p. 18551-18561.
67. Pardali, E., M.-J. Goumans, and P. ten Dijke, Signaling by members of the TGF $\beta$  family in vascular morphogenesis and disease. *Trends Cell Biol*, 2010. 20(9): p. 556-567.
68. ten Dijke, P., M.J. Goumans, and E. Pardali, Endoglin in angiogenesis and vascular diseases. *Angiogenesis*, 2008. 11(1): p. 79-89.
69. Lebrin, F., et al., Endoglin promotes endothelial cell proliferation and TGF $\beta$ /ALK1 signal transduction. *EMBO J*, 2004. 23(20): p. 4018-28.
70. Barbara, N.P., J.L. Wrana, and M. Letarte, Endoglin is an accessory protein that interacts with the signaling receptor complex of multiple members of the Transforming growth factor- $\beta$  superfamily. *J*

- Biol Chem, 1999. 274(2): p. 584-594.
71. Karzai, F.H., et al., A phase I study of TRC105 anti-endoglin (CD105) antibody in metastatic castration-resistant prostate cancer. *BJU Int*, 2014.
  72. Rosen, L., et al., Endoglin for targeted cancer treatment. *Curr Oncol Rep.*, 2014. 16(2): p. 1-9.
  73. Castonguay, R., et al., Soluble endoglin specifically binds bone morphogenetic proteins 9 and 10 via its orphan domain, inhibits blood vessel formation, and suppresses tumor growth. *J Biol Chem*, 2011. 286(34): p. 30034-46.
  74. Bhatt, R.S. and M.B. Atkins, Molecular pathways: can Activin-like kinase pathway inhibition enhance the limited efficacy of VEGF inhibitors? *Clin Cancer Res*, 2014. 20(11): p. 2838-2845.
  75. Sato, Y., et al., Resolution of liver cirrhosis using vitamin A-coupled liposomes to deliver siRNA against a collagen-specific chaperone. *Nat Biotechnol*, 2008. 26(4): p. 431-42.
  76. Ishiwatari, H., et al., Treatment of pancreatic fibrosis with siRNA against a collagen-specific chaperone in vitamin A-coupled liposomes. *Gut*, 2013. 62(9): p. 1328-39.
  77. van Beuge, M.M., et al., Enhanced effectivity of an ALK5-inhibitor after cell-specific delivery to hepatic stellate cells in mice with liver injury. *PLoS One*, 2013. 8(2): p. e56442.
  78. Michael Wormstone, I., et al., Short-term exposure to transforming growth factor  $\beta$  induces long-term fibrotic responses. *Exp Eye Res*, 2006. 83(5): p. 1238-1245.
  79. Yang, Y.-a., et al., Lifetime exposure to a soluble TGF $\beta$  antagonist protects mice against metastasis without adverse side effects. *J Clin Invest*, 2002. 109(12): p. 1607-1615.
  80. Bottinger, E.P., J.J. Letterio, and A.B. Roberts, Biology of TGF $\beta$  in knockout and transgenic mouse models. *Kidney Int*, 1997. 51(5): p. 1355-1360.
  81. Muraoka, R.S., et al., Blockade of TGF $\beta$  inhibits mammary tumor cell viability, migration, and metastases. *J Clin Invest*, 2002. 109(12): p. 1551-1559.
  82. Bhola, N.E., et al., TGF $\beta$  inhibition enhances chemotherapy action against triple-negative breast cancer. *J Clin Invest*, 2013. 123(3): p. 1348-1358.
  83. Biswas, S., et al., Inhibition of TGF $\beta$  with neutralizing antibodies prevents radiation-induced acceleration of metastatic cancer progression. *J Clin Invest*, 2007. 117(5): p. 1305-1313.
  84. Park, J., et al., Combination delivery of TGF $\beta$  inhibitor and IL-2 by nanoscale liposomal polymeric gels enhances tumour immunotherapy. *Nat Mater*, 2012. 11(10): p. 895-905.
  85. Gottesman, M.M., T. Fojo, and S.E. Bates, Multidrug resistance in cancer: role of ATP-dependent transporters. *Nat Rev Cancer*, 2002. 2(1): p. 48-58.
  86. Krishna, R. and L.D. Mayer, Multidrug resistance (MDR) in cancer: Mechanisms, reversal using modulators of MDR and the role of MDR modulators in influencing the pharmacokinetics of anticancer drugs. *Eur J Pharm Sci*, 2000. 11(4): p. 265-283.
  87. Eikesdal, H.P. and R. Kalluri, Drug resistance associated with antiangiogenesis therapy. *Semin Cancer Biol*, 2009. 19(5): p. 310-317.
  88. Anscher, M.S., The irreversibility of radiation-induced fibrosis: fact or folklore? *J Clin Oncol*, 2005. 23(34): p. 8551-8552.
  89. Wiig, H., D. Keskin, and R. Kalluri, Interaction between the extracellular matrix and lymphatics - consequences for lymphangiogenesis and lymphatic function. *Matrix Biol*, 2010. 29(8): p. 645-656.
  90. Heldin, C.H., et al., High interstitial fluid pressure: an obstacle in cancer therapy. *Nat Rev Cancer*, 2004. 4(10): p. 806-813.
  91. Lammerts, E., et al., Interference with TGF $\beta$ 1 and  $\beta$ 3 in tumor stroma lowers tumor interstitial fluid pressure independently of growth in experimental carcinoma. *Int J Cancer*, 2002. 102(5): p. 453-462.





**THE CRIPTO ENIGMA**

## **Appendix I**

# **Role of type III receptor, CRIPTO, in injury-induced liver regeneration and hepatocellular carcinoma**

**Sofia Karkampouna<sup>1\*</sup>, Danny van der Helm<sup>2\*</sup>, Peter ten Dijke<sup>1</sup>, Hein Verspaget<sup>2</sup>, Minneke Coenraad<sup>2</sup>, Marianna Kruithof-de Julio<sup>1,3,#</sup>**

<sup>1</sup>Department of Molecular and Cell Biology, Leiden University Medical Center, Leiden, the Netherlands,

<sup>2</sup>Department of Gastroenterology and Hepatology, Leiden University Medical Center, Leiden, the Netherlands,

<sup>3</sup>Department of Urology, Leiden University Medical Center, Leiden, the Netherlands

\* Equally contributed, # Corresponding author

***Manuscript in preparation***



## **Abstract**

Hepatocellular carcinoma (HCC) is the third cause of cancer-related death with a growing incidence worldwide. A comprehensive view of the mechanism initiating the switch from liver regeneration to liver failure and tumor formation is needed. Here we report on studies regarding the potential role of a Transforming growth factor  $\beta$  (TGF $\beta$ ) family member, the type III receptor for NODAL ligand, CRIPTO, in adult liver disease progression. We investigated the expression status of CRIPTO and its interaction partners *in vivo* in an acute liver injury mouse model and examined the *in vivo* effects on liver regeneration of adenoviral-mediated CRIPTO overexpression. Liver tissue specimens from HCC patients were evaluated for CRIPTO protein expression. Induction of CRIPTO was observed after experimental liver injury in mice and induction of CRIPTO overexpression caused bile duct reaction and hepatic progenitor cell activation. Both transient and stable CRIPTO overexpression in human hepatoma HepG2 cells led to upregulation of liver progenitor cell activity, epithelial-to-mesenchymal transition (EMT), increased expression of EMT and cancer stem cell markers along with enhancement of cell proliferation and migration. The majority of human HCC tumor samples exhibit high levels of CRIPTO as compared to the non-tumorous counterpart tissue from the same patients. Overall, our preliminary data suggest CRIPTO as potential driver of liver progenitor activation during liver injury and possibly of human HCC progression.



**Introduction**

Hepatocellular carcinoma (HCC) accounts for the majority of primary liver cancer cases and is the sixth common type of cancer<sup>1</sup>. HCC arises in the majority of cases on a background of cirrhosis, which may be caused by chronic exposure to damaging factors, such as alcohol, or viral hepatitis (HBV, HCV)<sup>2</sup>. Systemic treatment available is the tyrosine kinase RAF inhibitor, sorafenib, which delays HCC progression and metastasis and is indicated for advanced tumors or tumors progressing upon loco-regional therapies<sup>3,4</sup>. There are no clinical or biochemical biomarkers available to identify responders to sorafenib<sup>4</sup>. Many other compounds have been tested in recent years, but none of them has proven to be superior to sorafenib yet<sup>5</sup>. Circulating TGF $\beta$  and  $\alpha$ -fetoprotein (AFP) levels have been explored as biomarkers in HCC<sup>6</sup>. AFP is reactivated in pathological conditions and is considered a marker of liver progenitor cells (oval cells)<sup>7</sup>. However, detection of high levels of AFP cannot be used for diagnosis or prognosis as it does not predict tumor size, stage and HCC progression and is absent in 30% of HCC cases<sup>6</sup>. Signaling from Transforming growth factor  $\beta$  (TGF $\beta$ ) pathway is an established regulator of liver homeostasis with tumor suppressor role during early tumor development<sup>8</sup>. As with other types of cancer, TGF $\beta$  exerts tumor promoter effects on established primary tumors and enhances epithelial-to-mesenchymal transition (EMT), cell motility and invasion contributing to metastases formation<sup>9</sup>.

High levels of circulating TGF $\beta$  have been detected in HCC patients with a small HCC<sup>10</sup> although mutations in TGF $\beta$  pathway members have low prevalence in HCC. High levels of SMAD7<sup>11</sup>, downregulation of TGF $\beta$  receptor type I and II expression<sup>12,13</sup> and high levels of SMAD4 have been associated with poor prognosis in HCC patients<sup>14</sup>. SMAD3-mediated NODAL signaling has been linked to increased EMT and HCC cell invasion via a mechanism involving pluripotency transcription factor NANOG<sup>15</sup>. NANOG induces NODAL/CRIPTO expression and correlates with HCC metastasis and poor survival. NODAL and CRIPTO are involved in plasticity of tumor cells, cancer-stem cell maintenance and metastasis<sup>16,17</sup>. CRIPTO is an oncofetal protein suggested to partially promote tumorigenesis by inhibiting TGF $\beta$  signaling<sup>18-20</sup> and is involved in the crosstalk of TGF $\beta$ / NODAL pathways with p38/ c-Jun N-terminal kinase (JNK), sarcoma viral oncogene (c-SRC)/ Mitogen-activated protein kinase (MAPK)/ protein kinase B thymoma oncogene (AKT) and Wntless type (WNT) signaling pathways<sup>21-23</sup>. CRIPTO is silenced postnatally and re-expression is often associated with pathological conditions such as neoplasias of breast, lung, prostate, ovarian, bladder, colon, skin, lung and brain<sup>15,24-32</sup>. NODAL-independent CRIPTO signaling is mediated through the heat shock glucose-regulated protein (GRP78), which promotes c-SRC/MAPK/AKT activation. This pathway is oncogenically mutated in liver cancer<sup>33</sup>. Moreover, liver-specific deletion of GRP78 indicated a homeostatic and protective role during endoplasmic reticulum-stress response while elevated GRP78 levels are associated with HCC progression<sup>34-36</sup>. In the present study we investigated the role of CRIPTO-associated pathways NODAL and GRP78 aiming to identify novel TGF $\beta$ -related regulators of liver regeneration and HCC progression.

## **Materials and Methods**

### **Human specimens**

Liver tissue was obtained from resected livers during orthotopic liver transplantation. Paraffin embedded HCC and non-tumor tissue of anonymous patients transplanted for HCC in the setting of alcoholic liver disease (ALD) or viral hepatitis C (HCV) etiology were randomly selected. Selection of tissues was performed in agreement with the "code of good practice".

### **Acute liver damage model and administration of adenovirus**

Animal protocols were in full compliance with the guidelines for animal care and were approved by the Leiden University Medical Center Animal Care Committee. Acute liver injury was induced in 5-6 weeks old male C57Bl6 mice weighing 20- 25 g by intraperitoneal injection of a single dose of 1 ml/kg body weight carbon tetrachloride (CCl<sub>4</sub>) (Sigma, from a 50% solution mixed in mineral oil) or mineral oil (control). Mice were sacrificed at 3, 6, 24, 48, 72 hours and day 6 (n=2- 3 per time point).

Adenoviral constructs expressing β-galactosidase (lacZ) or Cripto were prepared using the Gateway adenoviral expression vectors pAd/CMV/V5-lacZ or pAd/CMV/V5-DEST, mouse Cripto expression plasmid was a gift from from Dr. Peter Gray<sup>18</sup>. AdlacZ (AdCon) or AdCripto (1x10E+9 viral particles/ mouse) was injected intravenously via the tail vein to enhance delivery to the liver<sup>37</sup>. After 24 hours, CCl<sub>4</sub> was intraperitoneally injected (day 0). Treatment groups were as follows: AdlacZ, CCl<sub>4</sub>+AdlacZ, AdCripto, CCl<sub>4</sub>+AdCripto. At day 1, day 2 and day 3 after CCl<sub>4</sub> administration mice were sacrificed and liver tissues were collected for histology preparation, RNA/ protein isolation and analysis.

### **Immunofluorescence**

Liver tissues were fixed in 4% paraformaldehyde solution overnight, washed in phosphate buffer saline (PBS) and processed for paraffin embedding. For every mouse, one of the liver lobules was embedded in a paraffin block and multiple serial sections (6 μm) were prepared. From the human tissue, serial sections of 4 μm were prepared. For antigen retrieval, sections were boiled 10-30 min in antigen unmasking solution (Vector Labs) and were incubated in 3% H<sub>2</sub>O<sub>2</sub> for endogenous peroxidases sequestering. Sections were blocked with 1% bovine serum albumin in PBS-0.1% v/v Tween 20 and subsequently incubated with primary antibodies diluted in the blocking solution, overnight at 4°C or room temperature. Primary antibodies and dilutions used are as follows: anti-CRIPTO 1:2000 and anti-GRP78 1:1000 (kindly provided by Dr. Peter Gray), anti-αSMA 1:500 (Sigma). Next day, sections were incubated with secondary antibodies labeled with Alexa Fluor 488, 555, or 647 (Invitrogen/Molecular Probes, 1:250 in PBS-0.1% Tween-20). Detection of CRIPTO and GRP78 was enhanced using tyramide amplification (Invitrogen/ Molecular Probes) as described previously<sup>38</sup>. All sections were counterstained with TO-PRO-3 (Invitrogen/Molecular Probes) at 1:1000 dilution in PBS-0.1% Tween-20 for nuclei visualization, and mounted with Prolong G mounting medium (Invitrogen/ Molecular Probes). All immunofluorescence experiments were repeated multiple times using different sections from the same lobule of every mouse.

### RNA isolation, RT-PCR and Quantitative PCR

During liver tissue collection, one of the liver lobules of each individual mouse was snapfrozen in liquid nitrogen and stored at -80°C for RNA analyses. Tissue (100 mg) was homogenized using an UltraTurrax homogenizer (T25 basic, IKA) in TRIpure reagent (Roche) and directly processed for total RNA isolation according to the TRIpure RNA extraction protocol. Total RNA (0.5 µg) was used for first strand cDNA synthesis using RevertAid H Minus first strand cDNA synthesis kit (Fermentas). For quantitative PCR (Q-PCR) ten-fold diluted cDNA was amplified in a CFX Real Time Detection system (Bio-rad) using SYBR Green Supermix reagent (Bio-rad). Expression levels were normalized to housekeeping gene  $\beta$ -actin.

Primer sequences:

*$\beta$ -actin (human): for-* AATGTCGCGGAGGACTTTGATTGC,  
*rev-* GGATGGCAAGGGACTTCCTGTAAA  
 *$\beta$ -actin (mouse): for-* GGGGTGTTGAAGGTCTCAAA, *rev-* AGAAAATCTGGCACCCC  
*Ck19 (mouse): for-* CCGGACCCTCCCGAGATTA, *rev-* CTCCACGCTCAGACGCAAG  
*Afp (mouse): for-* CGATGTGTTGGCTGCAATGA, *rev-* GTGCCAGCAGACACTGATG  
*Cripto (mouse): for-* CGCCAGCTAGCATAAAAGTG, *rev-* CCAAGAAGTGTTCCTGTG  
*GRP78 (human): for-* GAACGTCTGATTGGCGATGC, *rev-* TCAACCACCTTGAACGGCAA  
*NODAL (human): for-* CTTCTCCTCCTGAGCCAACAAGAGG,  
*rev-*GGTGACCTGGGACAAAAGTGACAGTG  
*N-CADHERIN (human): for-* CAGACCGACCCAAACAGCAAC,  
*rev-* GCAGCAACAGTAAGGACAAACATC  
*E-CADHERIN (human): for-* TTGACGCCGAGAGCTACAC, *rev-* GACCGGTGCAATCTTCAAA  
*VIMENTIN (human): for-* CCAAACCTTTCTCCCTGAACC, *rev-* CGTGATGCTGAGAAGTTTCGTTGA  
*OCT4 (human): for-* GAGAACCGAGTGAGAGGCAACC, *rev-* CATAGTCGCTGCTTGATCGCTTG  
*NANOG (human): for-* AATACCTCAGCCTCCAGCAGATG, *rev-* TGCGTCACACCATTGCTATTCTTC  
*BMI-1 (human): for-* TCATCCTCTGCTGATGCTG, *rev-* CCGATCCAATCTGTTCTGGT  
*CD44 (human): for-* TGGCACCCGCTATGTCCAG, *rev-* GTAGCAGGGATTCTGTCTG  
*ALK4 (human): for-* GCTCGAAGATGCAATTCTGG, *rev-* TTGGCATAACCAACTCTCG  
*LEFTY (human): for-*CGAGTGCTGCGCGTCCGCGA, *rev-* CGAGGCACAGCTGCACTTCTGCACC  
*ZEB-1 (human): for-* CCATATTGAGCTGTTGCCG, *rev-* GCCCTTCCTTCTGTGTCA  
*ZEB-2 (human): for-* GACCTGGCAGTGAAGGAAAA, *rev-* GGCACCTGCAGAAACACAGA  
*TWIST (human): for-* GCCGGAGACCTAGATGTCATT, *rev-* TTTTAAAAGTGCGCCCCACG  
*SNAIL-2 (human): for-* TGTGTGGACTACCGCTGC, *rev-* TCCGGAAAGAGGAGAGAGG  
*EPCAM (mouse): for-* AGGGGCGATCCAGAACAACG, *rev-* ATGGTCGTAGGGGCTTTCTC

### Cell lines

The HCC cell line, HepG2, were maintained in Dulbecco's Modified Eagle Media (DMEM) supplemented with 10% fetal calf serum and 1% penicillin/streptomycin. For adenovirus transduction, 200 multiplicity of infection (MOI) of high titer virus was incubated with the media for 24 hours. Migration, proliferation assays and mRNA analysis were performed at 48 hours after transduction.

### **Migration, measurement of metabolic rate MTS assay and wound healing assay**

Transwell cell migration and aqueous soluble tetrazolium/ formazan (MTS) metabolic activity/ proliferation assay were performed as described in previous studies<sup>39</sup>.

For the wound-healing assay 500.000 cells/ well of a 24- well plate were seeded. After 24 hours, the wound was made and culture medium was refreshed. Subsequently pictures were taken (4x magnification) at at 0, 24, 48 and 76- hour time points. Size of wound was measured with ImageJ software.

### **Microscopy and Image analysis**

Confocal microscopy of labeled specimens was performed on a Leica TC-SP5 microscope with a 40X 1.4 NA oil-immersion objective. Series of Z stacks were collected and reassembled in Image J software ([rsbweb.nih.gov/ij](http://rsbweb.nih.gov/ij)). Mean area fraction fluorescence was calculated in Image J software using threshold to select the root boundary and measuring the percentage of positive surface inside the intensity defined by the threshold. For quantifications of immunofluorescence signal, staining experiments were performed on all the samples simultaneously to reduce technical variation and imaged using identical exposure and recording settings.

### **Statistical analysis**

Statistical analysis was performed using GraphPad Prism 5.0 software (San Diego, CA) and two-way ANOVA tests. Data are presented as mean±SEM. Statistically significant differences are indicated with asterisks (\* P<0.05, \*\* P<0.01, \*\*\* P<0.001, \*\*\*\*P<0.0001). For quantitative PCR analysis experiments were repeated at least three times as technical replicates for every sample (different cDNA preparations using the RNA of one liver lobule per mouse or HepG2) and the average value was calculated. The mean values obtained from individual animals for every group (n=2-3) were used for ANOVA statistical analysis. For quantifications of immunofluorescence signal every stained section (representing one mouse liver sample) multiple fields of view were imaged and quantified (see section Microscopy and Image analysis). The average of these values was calculated for every mouse sample. Statistical analyses were performed on the values of all the mouse samples per treatment group (n=2-3 in total).

## **Results**

### **Short term re-expression of Cripto after CCl<sub>4</sub>-induced liver damage**

To assess whether Cripto is involved in liver homeostasis we analysed its expression in normal and injury-induced regenerating liver tissues from wild type C57Bl6 male mice. As previously reported for other tissues<sup>40</sup>, Cripto is not expressed postnatally in the liver under physiological conditions (**Fig.1A**). Cripto expression is induced during acute liver damage. A single CCl<sub>4</sub> injection leads to acute liver damage and fibrogenesis within the first 72 hours but is completely reversible within 6-7 days. In this model, a series of time points was analysed and Cripto protein expression was observed at 24 hours (**Fig.1A**). mRNA expression was induced within the first 3 hours after CCl<sub>4</sub> administration, with a peak of expression at 24

hours and a gradual downregulation from 48 hours onwards (**Fig.1B**).

### ***In vivo* overexpression of Cripto indicates progenitor cell activation**

Early induction of Cripto in response to tissue damage and localised expression around the damaged central vein area (**Fig.1A**) suggests a functional requirement. To further assess the function of Cripto we utilised the CCl<sub>4</sub>-induced acute liver injury model in combination with adenoviral-mediated overexpression of mouse Cripto. At 24 hours prior to CCl<sub>4</sub> injection, the control adenovirus-lacZ (AdlacZ) or Cripto-adenovirus (Ad-Cripto) was administered to the 4 treatment groups AdlacZ, CCl<sub>4</sub>+AdlacZ, AdCripto, CCl<sub>4</sub>+AdCripto. Liver tissues were analysed at 24, 48 and 72 hours after CCl<sub>4</sub> administration. Histological analysis after Cripto overexpression indicated an aberrant number of bile ducts in the portal triad area (**Fig.1C**). This area is not directly affected by CCl<sub>4</sub> (due to lack of metabolising enzymes) and is the site of residence of hepatic stem/progenitor, also termed as oval cells<sup>47</sup>. Each portal triad normally consists of the portal vein, the hepatic artery and one bile duct. The newly formed bile ducts indicate bile duct proliferation, and a process termed bile duct reaction due to liver progenitor (oval cell) activation<sup>42</sup>. In particular, the additional bile ducts (basal number is one bile duct; only the additional ducts are indicated) are positive for  $\alpha$ -smooth muscle actin ( $\alpha$ SMA) and were exclusively observed in liver tissues of the AdCripto and CCl<sub>4</sub>+AdCripto groups (**Fig.1D**).

Cripto upregulation was detected at 24 hours in AdCripto or CCl<sub>4</sub>+AdCripto mice (**Fig.1E**), exponentially upregulated at 48 hours (**Fig.1F**) and normalised back to the basal levels in all treatment groups (**Fig.1G**). Next, we evaluated the expression of oval cell markers (AFP, cytokeratin 19 (CK19)) to test whether bile duct proliferation may be attributed to presence of oval cells. AFP expression (**Fig.1H-J**), measured in whole liver mRNA extracts, showed a pattern of transient upregulation similar to Cripto expression (**Fig.1E-G**), i.e., upregulated at 24 hours following AdCripto administration (**Fig.1H**), overall induced at 48 hours in all the treatment groups (**Fig.1I**) and reduced again after 72 hours. At this time point (72 hours), AFP levels remain elevated only in the CCl<sub>4</sub>+AdCripto group (**Fig.1J**). CK19 expression was induced transiently early after CCl<sub>4</sub> administration at 24 hours (**Fig.1K-M**), preceding, but not after, the Cripto expression.

Further, transient overexpression by AdCripto was also validated *in vitro* in the HCC cell line HepG2. Upregulation of Cripto (**Fig.2A**) in the HepG2 led to induction of both interaction partners NODAL (**Fig.2B**) and GRP78 (**Fig.2C**), mesenchymal markers N-CADHERIN and VIMENTIN (**Fig.2D-E**) as well as pluripotency/cancer stem cell (CSC) markers, Octamer binding transcription factor 4 (OCT4), homeobox transcription factor (NANOG), polycomb ring finger protein (BMI-1) and cell surface glycoprotein (CD44) (**Fig.2F-I**), were increased upon transient Cripto overexpression.

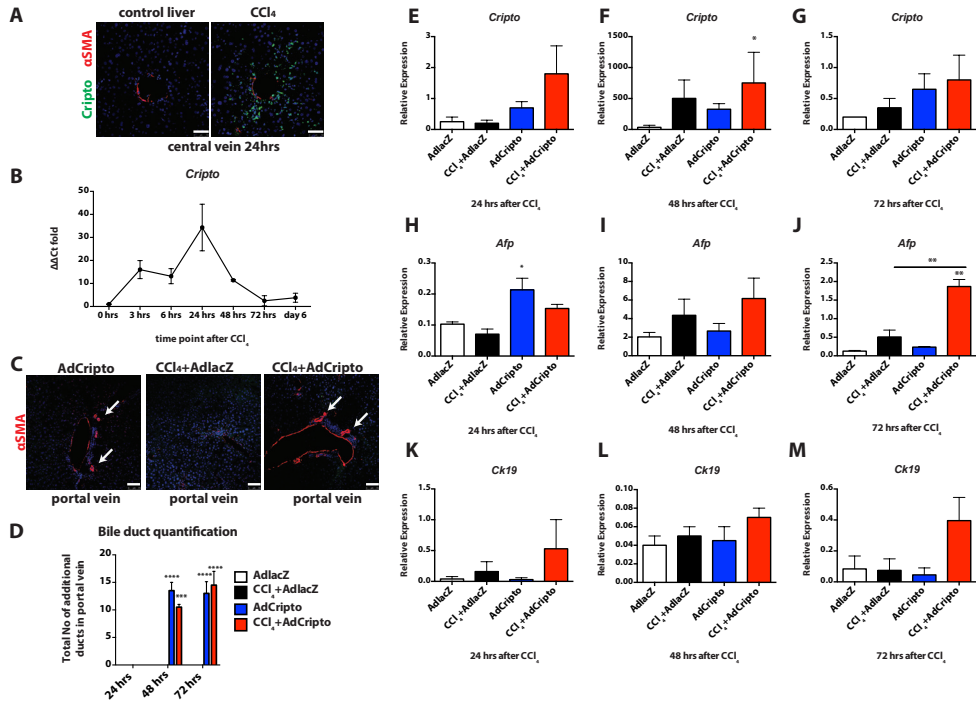


**Fig.1. Cripto is re-expressed during early response of CCl<sub>4</sub>-induced regeneration in mouse liver and may stimulate oval cell (progenitor) activation**

(A). Immunofluorescence staining for Cripto (green) and  $\alpha$ SMA (red) in liver tissue at 24 hours after vehicle or CCl<sub>4</sub> injection. Central vein area of the liver is depicted. Nuclei are stained with TO-PRO-3 (blue). Scale bars 50  $\mu$ m. (B). *Cripto* mRNA expression in liver homogenates at different time points after CCl<sub>4</sub> treatment; 3 hours, 6 hours, 24 hours, 48 hours, 72 hours, 6 days. Values are normalized to  $\beta$ -actin and time point 0 hours ( $\Delta\Delta$ Ct fold). Error bars indicate SEM (n=3). (C). *In vivo* overexpression of Cripto was induced by adenovirus transduction in the acute CCl<sub>4</sub> liver injury model. Bile duct (oval progenitor cell-driven) reaction in the periportal area after overexpression of Cripto in the liver is depicted using immunofluorescence for  $\alpha$ SMA (red) in livers administered with CCl<sub>4</sub>+AdlacZ, CCl<sub>4</sub>+AdCripto or AdCripto. Nuclei are stained with TO-PRO-3 (blue). Scale bars 75  $\mu$ m. (D). Quantification of the additional bile ducts observed in the periportal vein area. Total number of additional bile ducts in 5 areas per section was averaged. Error bars indicate  $\pm$ SEM (n=2). (E). *Cripto* mRNA expression in liver homogenates at 24 hours, 48 hours (F), 72 hours (G) after CCl<sub>4</sub> injection. Treatment groups: AdlacZ, CCl<sub>4</sub>+AdlacZ, AdCripto, CCl<sub>4</sub>+AdCripto. Values are normalized to  $\beta$ -actin. Error bars indicate SEM (n=3). (H). *A-fetoprotein (Afp)* (oval cell marker) mRNA expression in liver homogenates at 24 hours, (I). 48 hours and (J). 72 hours after CCl<sub>4</sub>. (K). *Cytokeratin-19 (Ck-19)* (oval cell marker) mRNA expression in liver homogenates at 24 hours, (L). 48 hours and (M). 72 hours after CCl<sub>4</sub>. Treatment groups: AdlacZ, CCl<sub>4</sub>+AdlacZ, AdCripto, CCl<sub>4</sub>+AdCripto. Values are normalized to  $\beta$ -actin. Error bars indicate  $\pm$ SEM (n=3).

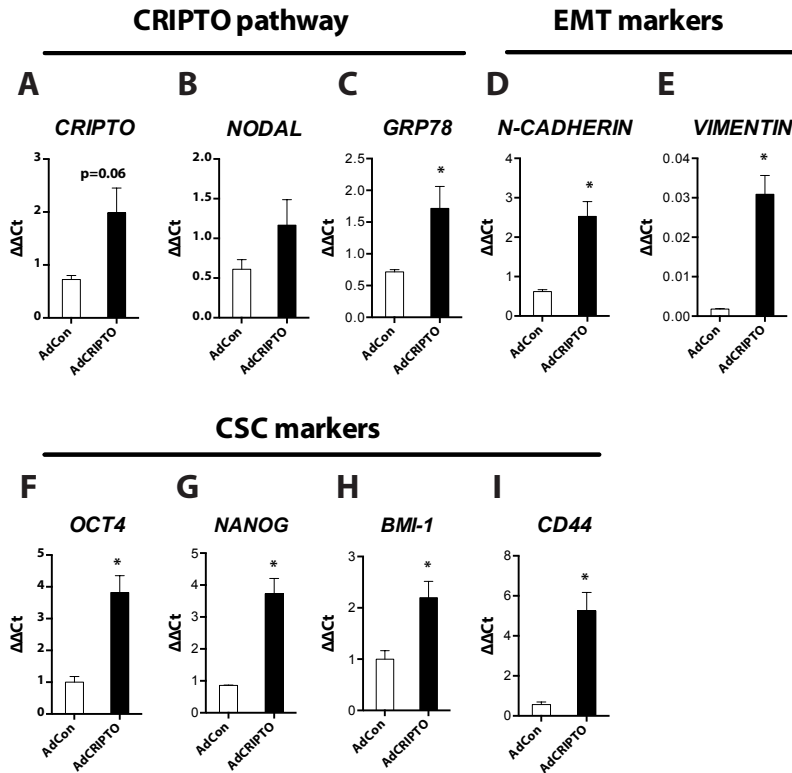


**Fig.2. Effects of transient CRIPTO overexpression in EMT and stem cell marker induction**

(A). Confirmation of expression of the CRIPTO adenoviral construct used previously *in vivo* and transient overexpression of CRIPTO in HepG2 cells; quantitative mRNA expression of *CRIPTO* and its interaction partners *NODAL* (B) and *GRP78* (C) in HepG2 cells 48 hours (hours) after transduction with control Adenovirus (AdCon) or CRIPTO expressing Adenovirus (AdCRIPTO). Error bars indicate  $\pm$ SD (n=3). (D-E). mRNA expression levels of mesenchymal markers *NCADHERIN* and *VIMENTIN*. (F-I). mRNA expression levels of cancer stem cell (CSC) markers *OCT4* (F), *NANOG* (G), *BMI-1* (H), *CD44* (I) and in HepG2 cells 48 hours after transduction with control Adenovirus (AdCon) or CRIPTO expressing Adenovirus (AdCRIPTO). Error bars indicate  $\pm$ SD (n=3).

### CRIPTO and GRP78 expression in human HCC

Based on the induction of CSC and EMT markers *in vivo* and *in vitro*, the expression levels of CRIPTO and GRP78 in human HCC liver specimens were evaluated. Aetiopathological heterogeneity in HCC was taken into account during the selection of HCC patient material; in this study we assessed specimens from HCV infection-driven HCC (HCV-HCC) or alcoholic liver disease-driven HCC (ALD-HCC). Adjacent tissue to the resected tumor, derived from the same patient, was used for comparison (control). We found that CRIPTO protein levels are lower in the adjacent non-tumor tissue compared to the tumor area in 50% of the patients with HCV-related and in all ALD-related HCC patients (n=4 per group) (Fig.3A-B, 3D-E). In tumor tissue areas, higher CRIPTO expression levels were observed at the vicinity of the stroma (Fig.3A, 3D). For comparison, samples from patients with only HCV infection and without detected signs of cirrhosis or HCC were also analysed and revealed low to none CRIPTO and GRP78 expression (Fig.3B-C). GRP78 is upregulated in HCC tissue areas in 25%

of the analysed HCV-related HCC patient samples (**Fig.3A,C**) and in 50% of the analysed ALD-related HCC tissues compared to adjacent non-tumorous tissue (**Fig.3D,F**).

To assess functional effects exerted by CRIPTO in HCC, we generated a stable HepG2- CRIPTO cell line by lentiviral transduction (LV-MOCK, LV-CRIPTO). The overexpression of CRIPTO was confirmed at the mRNA level by quantitative PCR (**Fig.4A**). Associated NODAL pathway members (NODAL, ALK4, LEFTY) and GRP78 were also upregulated in the LV-CRIPTO HepG2 (**Fig.4B-E**). Moreover, proliferation (MTS assay), migration (transwell assay) and wound closure assay showed that the HepG2-CRIPTO cells become more proliferative (**Fig.4F**) and motile (**Fig.4G-H**). Consistent with the acquisition of invasive and mesenchymal properties CRIPTO overexpressing cells show downregulation of E-CADHERIN (**Fig.5A**), upregulation of EMT markers (VIMENTIN, ZEB-1, ZEB-2, TWIST and SNAIL-2) (**Fig.5B-F**) and increased CSC marker (EpCAM, BMI-1 and CD44) expression (**Fig.5G-I**).

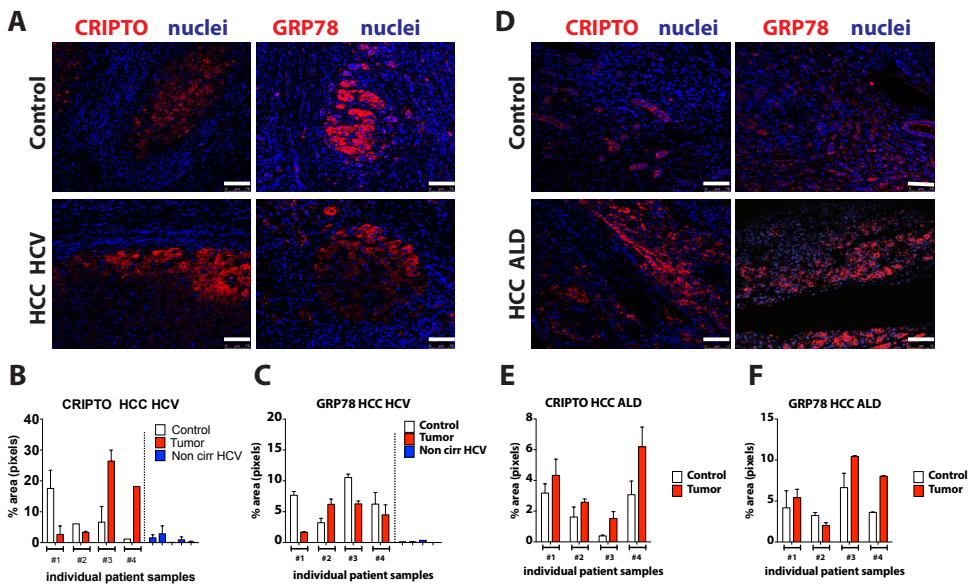


**Fig.3. Expression of CRIPTO and its interaction partner GRP78 in human HCC liver tissues**

(A). Representative immunofluorescence images of CRIPTO and its interaction partner GRP78 staining in human liver sections from HCV-derived HCC tissue (HCV infection-driven) and adjacent non-tumor control tissue from the same patient. Nuclei are stained with TO-PRO-3 (blue). Scale bars 75  $\mu$ m. (B). Quantification of CRIPTO and (C). GRP78 protein expression as assessed by immunofluorescence in tumor HCC HCV (Tumor) and in adjacent non-tumor tissue (Control) from the same patient (n=4). Liver tissue from patients with HCV infection but absence of cirrhosis (non-cirrhotic HCV, n=4) was used for comparison. The percentage of positive pixel area was an average from two-four focal areas per section. Each bar represents values from each patient. Error bars indicate  $\pm$ SD. (D). Representative immunofluorescence images of CRIPTO and its interaction partner GRP78 protein expression in human liver sections from alcoholic liver disease (ALD)-derived HCC tissue and adjacent non-tumor control tissue from the same patient. Nuclei are stained with TO-PRO-3 (blue). Scale bars 75  $\mu$ m. (E). Quantification of CRIPTO and (F) GRP78 protein expression as assessed by immunofluorescence in tumor HCC ALD (Tumor), adjacent non-tumor tissue (Control) from the same patient (n=4). The percentage of positive area (pixels) was the average from two-four focal areas per section. Each bar represents values from each patient. Error bars indicate  $\pm$ SD.



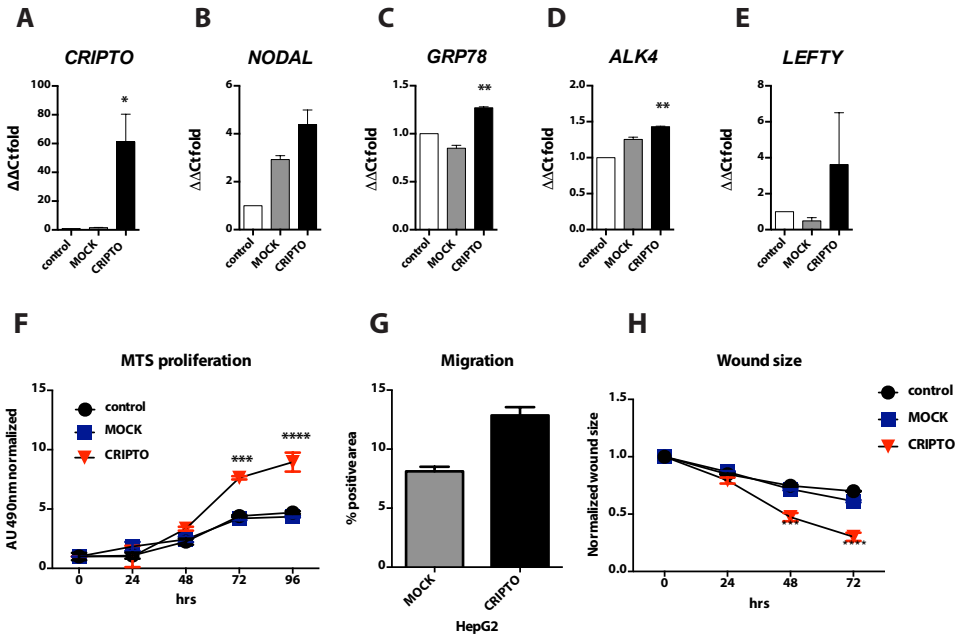


**Fig.4. In vitro effects of stable overexpression of CRIPTO in HepG2 cells**

(A-E). Quantitative PCR for mRNA expression of Cripto associated members of the NODAL and GRP78 pathways in wild type HepG2 cells; control, stably overexpressing Mock construct after lentivirus transduction (MOCK) and stably overexpressing CRIPTO (CRIPTO). (A). CRIPTO, (B). NODAL, (C). GRP78, (D). ALK4 and (E). LEFTY mRNA expression (n=3, ±SEM). Values are normalized to  $\beta$ -actin and to control sample ( $\Delta\Delta$ CT fold expression). (F). Metabolic activity MTS assay (24, 48, 72, 96 hours) was performed in control, MOCK and CRIPTO overexpressing HepG2 cells. Accumulation of MTS was measured based on absorbance at 490 nm. Values are normalized to the basal measurements at 0 hours after cell seeding. Graph represents values for three independent experiments (n=3). Error bars indicate SEM. p value < 0.001 (\*\*\*), < 0.0001 (\*\*\*\*). (G). Transwell migration assay of LV-MOCK and LV-CRIPTO overexpressing HepG2 cells; quantification of percentage (%) of positive area of migrated cells (Crystal violet cell dye) was performed in two independent experiments. Error bars indicate ±SEM. (H). Cell motility was assessed in wound healing (scratch) assay. Wound size was quantified in a time-dependent manner (0, 24, 48 and 72 hours) in two independent experiments. Error bars indicate ±SEM.

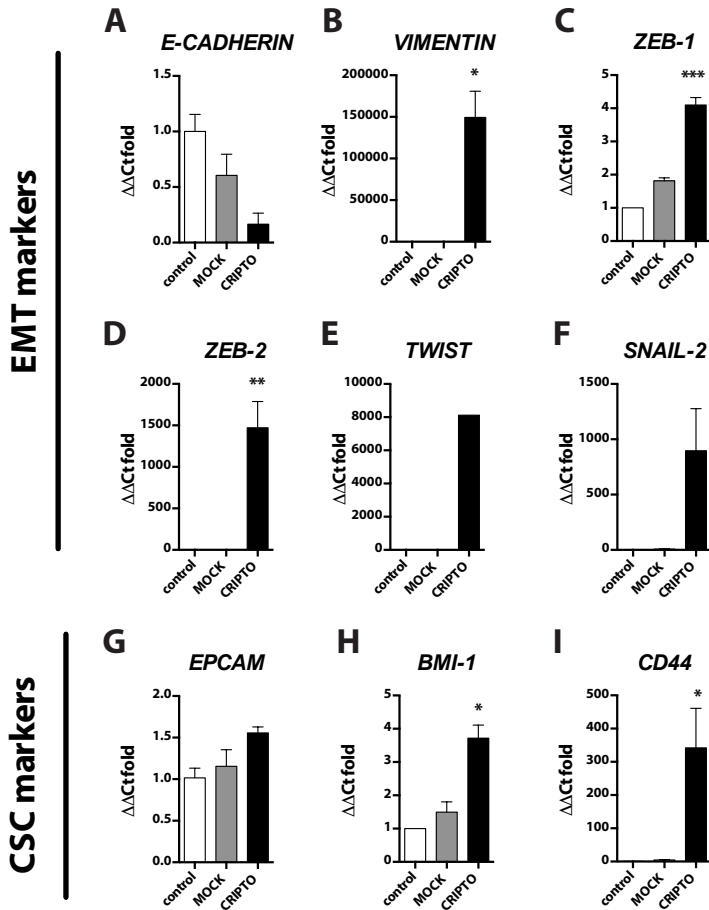


**Fig.5. Expression of EMT and CSC markers in HepG2 cells upon stable overexpression of CRIPTO**

(A-F). The levels of mRNA expression of epithelial-to-mesenchymal (EMT) markers in control, MOCK and CRIPTO-overexpressing HepG2 cells was assessed by quantitative PCR; (A). *E-CADHERIN*, (B). *VIMENTIN*, (C). *ZEB-1*, (D). *ZEB-2*, (E). *TWIST*, (F). *SNAIL2*. (G-I). mRNA expression levels of cancer stem cell (CSC) markers; (G). *EPCAM*, (H). *BMI-1*, (I). *CD44*. All values are normalized to  $\beta$ -actin and to control sample ( $\Delta\Delta$ Ct fold expression), n=3,  $\pm$ SEM.

## Discussion

The ability of quiescent hepatocytes to become proliferative and replace the damaged cells, both of the hepatocyte and cholangiocyte lineage, is at the foundation of liver regeneration<sup>47</sup>. In addition, hepatic stellate cells and Kupffer cells orchestrate wound healing response by the secretion of cytokines, removal of dead cells and extracellular matrix restoration. The general perception is that liver progenitor cells (oval cells) reside in the bile duct (at the portal triad) and their role is largely compensated by hepatocytes, bone marrow-derived fibrocytes and possibly hematopoietic stem cells. Oval cells typically are only detectable upon chronic liver injury or carcinogenesis and not upon acute CCl<sub>4</sub> damage<sup>43</sup>. However, in our model we observed reactivation of CK19 and AFP, markers of oval cells, followed by bile duct proliferation, a process associated with oval cell activation usually observed after partial hepatectomy or bile duct ligation<sup>42,44,45</sup>. Oval cell marker AFP has important functions during embryogenesis, it is postnatally silenced and re-expression often drives clonal expansion of oval cell-derived tumors<sup>43,46</sup>. AFP has been discarded from diagnostic schemes in recent guidelines due to the limited sensitivity<sup>4,47</sup>.

Here we report preliminary evidence that (1) pluripotency-associated protein CRIPTO is reactivated *in vivo* at early stages after acute liver injury, (2) CRIPTO overexpression induces bile duct reaction and AFP upregulation, (3) acute liver injury may also elicit the activation of oval cells. The rapid dynamics of CRIPTO and AFP expression and downregulation *in vivo* suggest that their expression levels are tightly regulated in order to induce a short-term cellular response; in this case perhaps a beneficial role in regenerative response. We speculate that due to the oncogenic role of high AFP levels in the liver and of CRIPTO in other tissues, both proteins are silenced in the adult organism to prevent abnormal activation of oval cells and tumor formation.

In the majority of human HCV-related HCC and ALD-related HCC tissue samples, the levels of CRIPTO were elevated in the tumor area compared to adjacent non-tumorous tissue from the same patient. CRIPTO- GRP78- mediated AKT signaling has been found to contribute to tumorigenesis<sup>24</sup>, thus, we assessed the expression levels of GRP78 in human HCC specimens. Indeed, higher levels of GRP78 were detected in 50% of the tumor tissues of the ALD-HCC group and in 25% of the HCV-HCC group, similar to CRIPTO. However, 75% of HCV-related HCC showed reduced GRP78 expression that coincides with previous findings showing that GRP78 has a protective role in the liver, against steatosis and cancer.

The location of CRIPTO in the hepatocytes, in particular those at the border between tumor nodule and stroma, has led us to the hypothesis that CRIPTO may promote invasiveness. Stable overexpression of CRIPTO in HepG2 cells induces their proliferative and migratory potential and is associated with an increase of EMT transcription factor and mesenchymal marker expression. Transient and stable overexpression of CRIPTO upregulates NODAL, LEFTY and GRP78, thus more aggressive, EMT-like phenotype of these cells may be attributed to either or both GRP78 and canonical NODAL signaling, however, further investigations are required.

In summary, this study provides supportive evidence for a novel role of developmental protein Cripto during progenitor cell activation during acute liver injury, suggesting that common developmental programs also regulate liver development and adult liver injury response. CRIPTO expression correlates with progression to human hepatic carcinogenesis in response to HCV hepatitis infection and alcoholic disease. The implication of fetal oncoprotein Cripto in the early response to acute liver injury and in advanced liver cancer may indicate

that CRIPTO is part of the missing link between acute and chronic liver injury, progression to cirrhosis and further to cancer formation.

### **Acknowledgements**

We thank Midory Thorikay for technical assistance with the adenovirus construct, Boudewijn Kruihof, Peter Gray and Eugenio Zoni for critical discussions.

### **References**

1. Attwa, M.H. and S.A. El-Etreby, Guide for diagnosis and treatment of hepatocellular carcinoma. *World J Hepatol*, 2015. 7(12): p. 1632-51.
2. El-Serag, H.B. and K.L. Rudolph, Hepatocellular carcinoma: epidemiology and molecular carcinogenesis. *Gastroenterology*, 2007. 132(7): p. 2557-2576.
3. Llovet, J.M., et al., Sorafenib in advanced hepatocellular carcinoma. *N Engl J Med*, 2008. 359(4): p. 378-390.
4. European Association for the Study of the L., R. European Organisation for, and C. Treatment of, EASL-EORTC Clinical practice guidelines: management of hepatocellular carcinoma. *J Hepatol.* . 56(4): p. 908-943.
5. Rahimi, R.S. and J.F. Trotter, Liver transplantation for hepatocellular carcinoma: outcomes and treatment options for recurrence. *Ann Gastroenterol.*, 2015. 28(3): p. 323-330.
6. Behne, T. and M.S. Copur, Biomarkers for hepatocellular carcinoma. *Int J Hepatol.*, 2012. 2012: p. 7.
7. Petersen, B.E., V.F. Zajac, and G.K. Michalopoulos, Hepatic oval cell activation in response to injury following chemically induced periportal or pericentral damage in rats. *Hepatology*, 1998. 27(4): p. 1030-1038.
8. Dooley, S. and P. ten Dijke, TGF- $\beta$  in progression of liver disease. *Cell Tissue Res*, 2012. 347(1): p. 245-56.
9. Battaglia, S., et al., Liver cancer-derived hepatitis C virus core proteins shift TGF $\beta$  responses from tumor suppression to epithelial-mesenchymal transition. *PLoS One*, 2009. 4(2): p. e4355.
10. Song, B.-C., et al., Transforming growth factor- $\beta$ 1 as a useful serologic marker of small hepatocellular carcinoma. *Cancer*, 2002. 94(1): p. 175-180.
11. Park, Y.N., et al., Expression of Smad7 in hepatocellular carcinoma and dysplastic nodules: resistance mechanism to transforming growth factor- $\beta$ . *Hepatogastroenterology*, 2004. 51(56): p. 396-400.
12. Serova, M., et al., Effects of TGF- $\beta$  signaling inhibition with galunisertib (LY2157299) in hepatocellular carcinoma models and in ex vivo whole tumor tissue samples from patients. *Oncotarget*2015(Epub ).
13. Paik, S.Y., et al., Expression of transforming growth factor- $\beta$ 1 and transforming growth factor- $\beta$  receptors in hepatocellular carcinoma and dysplastic nodules. *Mod Pathol*, 2003. 16(1): p. 86-96.
14. Torbenson, M., et al., Smad4 overexpression in hepatocellular carcinoma is strongly associated with transforming growth factor  $\beta$  II receptor immunolabeling. *Hum Pathol.*, 2002. 33(9): p. 871-876.
15. Sun, C., et al., NANOG promotes liver cancer cell invasion by inducing epithelial-mesenchymal transition through NODAL/SMAD3 signaling pathway. *Int J Biochem Cell Biol.*, 2013. 45(6): p. 1099-1108.
16. Lonardo, E., et al., Nodal/Activin signaling drives self-renewal and tumorigenicity of pancreatic cancer stem cells and provides a target for combined drug therapy. *Cell Stem Cell*, 2011. 9(5): p. 433-46.
17. Wakefield, L.M. and C.S. Hill, Beyond TGF $\beta$ : roles of other TGF $\beta$  superfamily members in cancer. *Nat Rev Cancer*, 2013. 13(5): p. 328-341.
18. Gray, P.C., et al., Cripto binds Transforming growth factor  $\beta$  (TGF- $\beta$ ) and inhibits TGF- $\beta$  signaling. *Mol Cell Biol.*, 2006. 26(24): p. 9268-9278.

## Appendix I

---

19. Gray, P.C., C.A. Harrison, and W. Vale, Cripto forms a complex with activin and type II activin receptors and can block activin signaling. *Proc Natl Acad Sci U S A.*, 2003. 100(9): p. 5193-5198.
20. Gray, P.C. and W. Vale, Cripto/GRP78 modulation of the TGF- $\beta$  pathway in development and oncogenesis. *FEBS Lett.*, 2012. 586(14): p. 1836-1845.
21. Klauzinska, M., et al., The multifaceted role of the embryonic gene Cripto-1 in cancer, stem cells and epithelial-mesenchymal transition. *Semin Cancer Biol.*, 2014. 29(0): p. 51-58.
22. Bianco, C., et al., A Nodal- and ALK4-independent signaling pathway activated by Cripto-1 through Glypican-1 and c-Src. *Cancer Res*, 2003. 63(6): p. 1192-1197.
23. Kruihof-de Julio, M., et al., Regulation of extra-embryonic endoderm stem cell differentiation by Nodal and Cripto signaling. *Development*, 2011. 138(18): p. 3885-3895.
24. Spike, Benjamin T., et al., CRIPTO/GRP78 signaling maintains fetal and adult mammary stem cells ex vivo. *Stem Cell Reports.*, 2014. 2(4): p. 427-439.
25. Xu, C.-H., et al., Elevated expression of Cripto-1 correlates with poor prognosis in non-small cell lung cancer. *Tumour Biol.*, 2014. 35(9): p. 8673-8678.
26. Cocciaferro, L., et al., Profiling cancer stem cells in androgen-responsive and refractory human prostate tumor cell lines. *Ann N Y Acad Sci.*, 2009. 1155(1): p. 257-262.
27. Terry, S., et al., CRIPTO overexpression promotes mesenchymal differentiation in prostate carcinoma cells through parallel regulation of AKT and FGFR activities. *Oncotarget*, 2015. 6(14): p. 11994-2008.
28. D'Antonio, A., et al., Transforming growth factor alpha, amphiregulin and cripto-1 are frequently expressed in advanced human ovarian carcinomas. *Int J Oncol*, 2002. 21(5): p. 941-8.
29. Fujii, K., et al., Expression of CRIPTO in human gall bladder lesions *J Pathol.*, 1996. 180(2): p. 166-168.
30. Giorgio, E., et al., Cripto haploinsufficiency affects in vivo colon tumor development. *Int J Oncol.*, 2014. 45(1): p. 31-40.
31. Strizzi, L., et al., The significance of a Cripto-1-positive subpopulation of human melanoma cells exhibiting stem cell-like characteristics. *Cell Cycle*, 2013. 12(9): p. 1450-1456.
32. Tysnes, B.B., et al., Age-dependent association between protein expression of the embryonic stem cell marker Cripto-1 and survival of glioblastoma patients. *Transl Oncol.*, 2013. 6(6): p. 732-741.
33. Steelman, L.S., et al., Roles of the Raf/MEK/ERK and PI3K/PTEN/Akt/mTOR pathways in controlling growth and sensitivity to therapy-implications for cancer and aging. *Aging (Albany NY)*, 2011. 3(3): p. 192-222.
34. Ji, C., et al., Liver-specific loss of GRP78 perturbs the global unfolded protein response and exacerbates a spectrum of acute and chronic liver diseases. *Hepatology* 2011. 54(1): p. 229-239.
35. Kuo, T.-C., et al., A unique P-glycoprotein interacting agent displays anticancer activity against hepatocellular carcinoma through inhibition of GRP78 and mTOR pathways. *Biochem Pharmacol.*, 2011. 81(9): p. 1136-1144.
36. Chen, W.-T., et al., GRP78 as a regulator of liver steatosis and cancer progression mediated by loss of the tumor suppressor PTEN. *Oncogene*, 2014. 33(42): p. 4997-5005.
37. Shayakhmetov, D.M., et al., Analysis of adenovirus sequestration in the liver, transduction of hepatic cells, and innate toxicity after injection of fiber-modified vectors. *J Virol.*, 2004. 78(10): p. 5368-5381.
38. Karkampouna, S., et al., Inhibition of TGF $\beta$  type I receptor activity facilitates liver regeneration upon acute CCl<sub>4</sub> intoxication in mice. *Arch Toxicol.*, 2015: p. 1-11.
39. Zoni, E., et al., miR-25 modulates invasiveness and dissemination of human prostate cancer cells via regulation of  $\alpha$ v- and  $\alpha$ 6-integrin expression. *Cancer Res*, 2015. 75(11): p. 2326-36.
40. Bianco, C., et al., Role of Cripto-1 in stem cell maintenance and malignant progression. *Am J Pathol.*, 2010. 177(2): p. 532-540.
41. Fausto, N. and J.S. Campbell, The role of hepatocytes and oval cells in liver regeneration and repopulation. *Mech Dev.*, 2003. 120(1): p. 117-130.

## ***Role of CRIPTO in liver regeneration and hepatocellular carcinoma***

---

42. Limaye, P.B., et al., Expression of hepatocytic- and biliary-specific transcription factors in regenerating bile ducts during hepatocyte-to-biliary epithelial cell transdifferentiation. *Comp Hepatol*, 2010. 9: p. 9-9.
43. Dabeva, M.D., et al., Models for hepatic progenitor cell activation. *Proc Soc Exp Biol Med*, 1993. 204(3): p. 242-52.
44. Liu, Z., et al., Interleukin-6, hepatocyte growth factor, and their receptors in biliary epithelial cells during a type i ductular reaction in mice: Interactions between the periductal inflammatory and stromal cells and the biliary epithelium. *Hepatology*, 1998. 28(5): p. 1260-1268.
45. Yoshioka, K., et al., Cell proliferation activity of proliferating bile duct after bile duct ligation in rats. *Vet Pathol*, 2005. 42(3): p. 382-385.
46. Kuhlmann, W.D. and P. Peschke, Hepatic progenitor cells, stem cells, and AFP expression in models of liver injury. *Int J Exp Pathol*, 2006. 87(5): p. 343-59.
47. Bruix, J. and M. Sherman, Management of hepatocellular carcinoma. *Hepatology*, 2005. 42(5): p. 1208-1236.



## **Appendix II**

Summary

Samenvatting

List of abbreviations

Curriculum Vitae

List of publications

Acknowledgements





---

## Summary

Cancer and chronic fibrosis are devastating diseases of high mortality rate with limited curative therapies available. Both of these diseases may influence the function of one or multiple organs while the extracellular microenvironment is a contributing factor in the pathogenesis of both disorders. Considering the increasing number of cases per year, a better understanding of the biological drivers of these diseases is fundamental in order to develop effective therapeutics. At the molecular level, signaling pathways control cell growth, differentiation or apoptosis during development and adult life of the organism ensuring homeostasis. In a paradox, the same signals are often implicated or even drive disease progression. Environmental or genetic factors have impact on gene functions by direct gene alterations or indirect epigenetic factors that change the function of signaling members. One of the signaling pathways with key regulatory functions in homeostasis, tissue fibrosis and cancer in many organs is the TGF $\beta$ / BMP pathway.

In this thesis we have addressed the role and therapeutic potential of TGF $\beta$ / BMP pathway inhibition using different drug compounds that are currently towards the clinic or being tested in clinical trials. Three distinct types of inhibitors were used; small molecule inhibitors of the ALK4, 5 and 7 TGF $\beta$  receptor kinases, an antisense oligonucleotide interfering with ALK5 mRNA splicing and an ALK1 ligand trap; a peptide that contains the extracellular domain of ALK1 fused to Fc and sequesters BMP9 and BMP10. These inhibitors were used in an *ex vivo* human fibrosis model or *in vivo* mouse models of various human diseases (acute liver failure/ liver regeneration, Dupuytren's fibrosis) and cancer (prostate, liver).

Chapter 1 introduces the basic aspects of the TGF $\beta$ / SMAD signaling pathway, including its regulation, crosstalk with other pathways and the role during homeostasis of liver, prostate and connective tissue. Moreover, the impact of TGF $\beta$  and BMP deregulation is introduced in relation to common abnormalities; liver wound healing, Dupuytren's fibrosis and prostate tissue malignancies. Advances in drug development have provided researchers with therapeutic strategies with potential clinical application. In this Chapter we address the properties of individual classes of drugs targeting (mainly inhibiting) the TGF $\beta$  pathway and their status on ongoing or completed clinical trials.

In Chapter 2 the current knowledge on TGF $\beta$  signaling in relation to its contribution in liver regeneration is reviewed. Different aspects are addressed such as embryonic development, the molecular mechanisms regulating hepatocyte and oval cell regeneration, plasticity of hepatic lineages, and induced reprogramming of hepatocytes as cell based therapies for human liver diseases. Repeated tissue injury leads to unrepairable cell regeneration and a shift towards scar tissue formation (fibrosis). The end stage of excess fibrosis in the liver (cirrhosis) is a risk factor for hepatocellular carcinoma development. In order to understand the progression of liver disease further investigation of the mechanisms that balance cell replenishment and fibrosis is needed. Excess activation of TGF $\beta$  leads to epithelial cell apoptosis (acute liver failure), epithelial-to-mesenchymal transition, liver cirrhosis and eventually cancer. Thus, *in vivo* inhibition of TGF $\beta$  may prove a beneficial therapeutic strategy in liver diseases.

## Appendix II

---

In Chapter 3 we investigated the *in vivo* applicability of a drug compound, the small molecule inhibitor (LY364947) targeting the kinase activity of TGF $\beta$  type I receptor (ALK5), in a mouse model of acute injury-induced liver regeneration. Administration of LY364947 in mice that received hepatotoxin carbon tetrachloride (CCl<sub>4</sub>) enhanced the proliferation of hepatocytes and recovery of the liver enzyme expression pattern, showing overall improved wound healing compared to mice that did not receive the ALK5 inhibitor. The possible mechanism of this effect is inhibition of the cytostatic effect of TGF $\beta$  by downregulation of p21, and/or upregulation of proliferating nuclear antigen and phosphorylation of histone 3.

In Chapter 4 and 5 we addressed the limitations to study the effects of TGF $\beta$  inhibition using the current methods available in the field of fibrosis (primary fibroblast cultures). For this we developed novel *ex vivo* culture methodology that allows us to maintain human fibrotic connective tissue from palmar fascia (Dupuytren's fibrosis). The proof-of-principle for this *ex vivo* method is introduced in detail in Chapter 4 along with further applications, such as biochemical and imaging techniques to be used for studying patient-specific pathogenesis and responses to candidate antifibrotic drugs. In Chapter 5, we have used the *ex vivo* culture system to assess the anti-fibrotic potential of TGF $\beta$  inhibitors. Antisense oligonucleotide and small molecule kinase inhibitor-mediated ALK5 inhibition diminished the number of collagen-producing myofibroblasts and decreased the expression of extracellular matrix proteins indicating an amelioration of fibrosis *ex vivo*. Such preclinical studies highlight the importance of TGF $\beta$  inhibition as monotherapy or in combination with other substances, such as anti-inflammatory agents, for the treatment of fibrosis.

In Chapter 6 we explored the effect of the anti-angiogenesis compound ALK1Fc (ACE-041, Acceleron), which acts on different fronts; tumor microenvironment (matrix and vasculature) and tumor cells. Administration of ALK1Fc exhibited *in vivo* anti-angiogenic and tumor suppressive effects in a primary prostate cancer mouse model established by orthotopic transplantation of human prostate cancer cells. ALK1Fc ligand trap is currently being tested in clinical trials for solid tumor treatment as tumor angiogenesis inhibitor. ALK1Fc reduced the tumor volume of primary prostate cancer (formed by aggressive prostate cancer cell line PC3-M-Pro4) possibly due to reduced tumor vasculature. *In vivo* administration of ALK1Fc acted as anti-angiogenic factor by inhibiting BMP9 binding to its receptor ALK1 on endothelial cells. However, ALK1Fc also indicated a direct effect of BMP9 on tumor cells; BMP9 was found to mediate upregulation of the NOTCH ligand JAGGED, the cancer stem cell marker Aldehyde dehydrogenase 1 (ALDH1A1) and to enhance the proliferation of prostate cancer cells.

In Chapter 7 the findings of this thesis presented in the different chapters are discussed under a common denominator; the inhibition of TGF $\beta$ / BMP signaling in human diseases. Furthermore, the implications of TGF $\beta$  inhibitory strategies in basic and clinical research along with future perspectives are discussed. Molecular signatures characteristic of tissue injury often reminisce the expression status of human malignancies. Preliminary data indicate a role for the TGF $\beta$  type III receptor CRIPTO in liver regeneration and human hepatocellular carcinoma (Appendix I). Normally, CRIPTO is expressed only during embryonic development. We show that reactivation of CRIPTO takes place in the mouse liver after toxin-induced acute injury. CRIPTO has the potential to reduce SMAD2/3 signaling by directly binding to TGF $\beta$  and has been suggested as a mediator of the TGF $\beta$ - tumor promoting effect by deactivating the

cytostatic role of TGF $\beta$  and activating other cell survival signals. Moreover, elevated protein levels of CRIPTO in liver tissue specimens of human hepatocellular carcinoma suggest a tumor-promoting role of CRIPTO in the liver, which may be of potential diagnostic value as biomarker for human hepatocellular carcinoma.

Collectively, after the discovery of the TGF $\beta$  numerous studies have contributed to a holistic and comprehensive view of the molecular properties of all the proteins assembling the pathway and the biological processes that TGF $\beta$  is involved in. Given the disease-promoting role of deregulated TGF $\beta$ / BMP signaling the key aspect of current research is therapeutic intervention by targeting pathway activation in a clinical relevant way. Based on our observations, inhibition of TGF $\beta$  is promising in many diseases and has additive beneficial effects in combination with other drug compounds, for instance chemotherapeutic, anti-inflammatory, immune modulatory agents depending on the disease setting.

However, TGF $\beta$  inhibition is not panacea mainly because of the TGF $\beta$  homeostatic role in many organs. Successful modulation of TGF $\beta$  requires careful patient stratification and disease staging by using prognostic tools such as biomarkers and patient-specific genetic variation. Current and future development in drug delivery will hopefully enhance the tissue-specific or cell type-specific targeting of drugs against TGF $\beta$  pathway members along with precise dosing and timing in a personalized scheme of treatment.

### Samenvatting

Kanker en chronische fibrose zijn verwoestende ziekten met een hoog sterftecijfer en een beperkt aantal therapieën die tot genezing kunnen leiden. Beide ziekten beïnvloeden het functioneren van en/of beschadigen meerdere organen, waarbij het extracellulaire micromilieu een essentiële rol speelt. Gezien de toename van het aantal gevallen per jaar is het verkrijgen van een beter inzicht in de biologische drijvers van deze ziekten van fundamenteel belang om effectieve therapieën te kunnen ontwikkelen.

Tijdens de embryonale ontwikkeling en het volwassen leven van een organisme wordt homeostase gereguleerd via diverse signaaltransductie routes die op moleculair niveau processen als celgroei, differentiatie of apoptose aansturen. Dezelfde signalen en signaal routes zijn vaak betrokken bij ziekten en ziekteprogressie, of zelfs de directe oorzaak ervan. Omgevingsfactoren en genetische factoren kunnen namelijk de werking van signaleringsmoleculen negatief beïnvloeden via mutaties in het DNA of via epigenetische mechanismen.

Een van de signaalroutes die in vele organen een belangrijke regulerende functie heeft, is de TGF $\beta$ / BMP route, betrokken bij onder andere homeostase, weefselfibrose en kanker. In dit proefschrift is de rol van de TGF $\beta$ / BMP route bij deze processen nader onderzocht, en is tevens gekeken naar het therapeutisch potentieel van het remmen van specifieke componenten van de route, daarbij gebruik makend van drugs die momenteel gebruikt worden in de kliniek, of nog getest worden in klinische studies.

Drie verschillende klassen van inhibitoren zijn gebruikt: remmers van de kinase activiteit van een subklasse TGF $\beta$  membraan receptoren (ALK4, 5 en 7); een antisense oligonucleotide dat ALK5 mRNA splicing remt; en een zogenaamde ALK1 ligand trap: een peptide waarin het extracellulaire domein van ALK1 gefuseerd is met het Fc domein van antilichamen, wat daardoor BMP9 en BMP10 kan wegvangen. Deze remmers zijn gebruikt in een *ex vivo* humaan fibrose model en in (*in vivo*) muismodellen voor acuut leverfalen/ leverregeneratie, Dupuytren fibrose, en prostaat en lever kanker.

Hoofdstuk 1 beschrijft de basis aspecten van de TGF $\beta$ / SMAD signaleringsroute, de regulering ervan, de interactie met andere signaalroutes en de rol bij homeostase van de lever, prostaat en bindweefsel. Bovendien wordt het effect van TGF $\beta$  en BMP deregulering geïntroduceerd in de context van een aantal daaraan gerelateerde processen en ziekten: lever regeneratie, Dupuytren fibrose en prostaatweefsel maligniteiten. Vooruitgang in de ontwikkeling van geneesmiddelen heeft onderzoekers voorzien van therapeutische strategieën met potentiële klinische toepassing. In dit hoofdstuk worden de eigenschappen van de verschillende klassen van medicijnen die de TGF $\beta$  route beïnvloeden beschreven, en hun status in lopende of afgeronde klinische studies.

In hoofdstuk 2 wordt een overzicht gegeven van de huidige kennis over de TGF $\beta$  signaleringsroute in relatie tot de rol van de route bij leverregeneratie. Verschillende aspecten worden behandeld, zoals de embryonale ontwikkeling, de moleculaire mechanismen betrokken bij de regeneratie van hepatocyten en ovaal cellen, de plasticiteit van leverceltypen, en geïnduceerde herprogrammering van hepatocyten als celtherapie voor menselijke leverziekten. Herhaalde weefselbeschadiging leidt tot onherstelbare celregeneratie en een verschuiving naar de vorming van littekenweefsel (fibrose). Het eindstadium van overmatige fibrose in de lever (cirrose) is tevens een risicofactor voor de ontwikkeling van hepatocellulair

carcinoom. Om de progressie van leverziekte te begrijpen is nader onderzoek nodig naar de mechanismen die de balans tussen normale cel vervanging en fibrose bepalen. Overmatig activeren van de TGF $\beta$  route leidt tot apoptose van epitheel cellen (acuut leverfalen), epitheliale-mesenchymale transitie, levercirrose en uiteindelijk kanker. *In vivo* remming van TGF $\beta$  zou daarom gunstige effecten op leverziekten kunnen hebben.

In hoofdstuk 3 onderzochten we in een muizenmodel voor leverregeneratie na acute verwonding de *in vivo* toepasbaarheid van LY364947, een kleine chemische remmer van de kinase activiteit van de TGF $\beta$  type I receptor ALK5. Toediening van LY364947 aan muizen behandeld met het hepatotoxine koolstoftetrachloride (CCl<sub>4</sub>), versterkte zowel proliferatie van levercellen als herstel van het normale lever enzym expressie patroon, wat duidt op verbeterde genezing in vergelijking met muizen die de ALK5 remmer niet ontvingen. Het mogelijke mechanisme van dit effect is de remming van het cytostatische effect van TGF $\beta$  door onderdrukking van de celcyclus remmer p21, opregulatie van prolifererend nucleair antigeen (PCNA) en fosforylering van histon 3.

In hoofdstuk 4 en 5 richtten, we ons op de beperkingen van de bestaande methoden in het fibrose onderzoek, om de effecten van TGF $\beta$  remming te bestuderen (primaire fibroblast kweken). Hiervoor ontwikkelden we nieuwe *ex vivo* methodiek voor onderzoek naar fibrotisch menselijk bindweefsel van de palmaire fascia (Dupuytren fibrose, een primair door TGF $\beta$ -aangestuurde ziekte). Deze *ex vivo* methode wordt geïntroduceerd in hoofdstuk 4, samen met mogelijke toepassingen, zoals biochemische en beeldvormingstechnieken voor het bestuderen van de patiënt-specifieke pathogenese en de respons op potentiële antifibrotische geneesmiddelen. In hoofdstuk 5 hebben we dit nieuwe *ex vivo* kweekstelsel gebruikt om het anti-fibrotische potentieel van TGF $\beta$  inhibitoren te analyseren. Remming van de ALK5 functie m.b.v. het antisense oligonucleotide of de kleine chemisch kinase-remmer verminderde het aantal collageen producerende myofibroblasten en verlaagde de expressie van extracellulaire matrixeiwitten, wat wijst op een verbetering van fibrose *ex vivo*. Zulke preklinische studies benadrukken het belang van TGF $\beta$  remming voor de behandeling van fibrose, als monotherapie of in combinatie met andere stoffen, zoals anti-inflammatoire middelen.

In hoofdstuk 6 is het effect onderzocht van de anti-angiogene verbinding ALK1Fc (ACE-041, Acceleron), een stof die zowel aangrijpt op de tumor microomgeving (matrix en vasculatuur) als op de tumorcellen zelf. Toediening van ALK1Fc had *in vivo* anti-angiogene en tumor onderdrukkende effecten in een muizenmodel voor primaire prostaatkanker (geïnduceerd door orthotope transplantatie van menselijke prostaatkankercellen).

ALK1Fc is, zoals hierboven vermeld, een peptide dat BMP9 en BMP10, de TGF $\beta$  familieleden die binden aan de TGF $\beta$  type I receptor ALK1, kan binden en neutraliseren; de stof wordt momenteel getest als tumor angiogenese inhibitor in klinische studies voor de behandeling van vaste tumoren.

ALK1Fc verminderde het volume van primaire prostaattumoren (gevormd door de agressieve prostaatkanker cellijn PC3-M-Pro4), mogelijk door verminderde tumorvasculatuur. *In vivo* toediening van ALK1Fc werkte anti-angiogeen door op endotheel cellen de binding van BMP9 aan ALK1 te remmen. Echter, gebruik van ALK1Fc duidde ook op een direct effect van BMP9 op tumorcellen; BMP9 veroorzaakte opregulatie van de NOTCH ligand JAGGED en de kanker stamcel marker aldehyde dehydrogenase 1 (ALDH1A1) en versterkte de proliferatie

van prostaat tumorcellen.

In hoofdstuk 7 worden de bevindingen van dit proefschrift die gepresenteerd zijn in de eerdere hoofdstukken besproken onder een gemeenschappelijke noemer; de remming van TGF $\beta$ / BMP signaaloverdracht in humane ziekten. Bovendien wordt de invloed van TGF $\beta$  remmende strategieën in fundamenteel en klinisch onderzoek besproken, ook in relatie tot de toekomstperspectieven. Moleculaire signaturen kenmerkend voor weefselschade lijken vaak op de expressie patronen in menselijke maligniteiten. Onze preliminaire data wijzen op een rol van de TGF $\beta$  type III receptor CRIPTO in leverregeneratie en humane hepatocellulaire carcinoomen (Appendix I). Normaliter komt CRIPTO alleen tot expressie tijdens de embryonale ontwikkeling. We laten echter zien dat in de muizenlever reactivering van CRIPTO plaatsvindt na acute schade door toxine. Door direct aan TGF $\beta$  te binden kan CRIPTO TGF $\beta$  signalering via SMAD2/ 3 verminderen; dit zou het cytostatische functie van TGF $\beta$  kunnen verminderen en celoverlevings signalen kunnen activeren. Daardoor zou CRIPTO een mediator van het tumor stimulerende effect van TGF $\beta$  kunnen zijn. De verhoogde eiwitniveaus van CRIPTO gevonden in biopten van menselijk hepatocellulair carcinoom duiden bovendien op een mogelijke kanker-bevorderende rol van CRIPTO in de lever, en geven aan dat CRIPTO gebruikt zou kunnen worden als een potentiële diagnostische biomarker voor humaan hepatocellulaire carcinoom.

Samengevat kan gezegd worden dat na de ontdekking van TGF $\beta$  zeer veel studies hebben bijgedragen aan het tot stand komen van een begrijpelijk overzicht van al de moleculaire eigenschappen van de eiwit componenten van de route, en de biologische processen waarbij TGF $\beta$  betrokken is. Vanwege het ziekte stimulerende effect van gedereguleerde TGF $\beta$ / BMP signaaloverdracht is het belangrijkste aspect van het huidige onderzoek de therapeutische interventie in de signalering, op een klinisch relevante wijze. Op basis van onze waarnemingen kan remming van TGF $\beta$  signalering veelbelovende effecten hebben bij vele ziekten en heeft het tevens additieve gunstige effecten in combinatie met andere geneesmiddelen, bijvoorbeeld - afhankelijk van de ziekte - in combinatie met chemotherapie, of anti-inflammatoire en immune modulerende middelen.

Echter, remming van TGF $\beta$  signalering kan niet altijd toegepast worden, voornamelijk vanwege de homeostatische functie van TGF $\beta$  in vele organen. Succesvolle modulatie van TGF $\beta$  signalering vereist daarom zorgvuldige patiënt stratificatie en ziektekaracterisering met behulp van prognostische middelen zoals biomarkers en analyse van de patiënt-specifieke genetische variatie. De huidige en de toekomstige ontwikkelingen in drug toediening zullen hopelijk leiden tot verbetering van de weefsel-specifieke of celttype-specifieke targeting van de geneesmiddelen die op de TGF $\beta$  route aangrijpen, samen met een precieze dosering en timing en een gepersonaliseerd behandelingschema.

We thank Dr. Hans van Dam for the Dutch translation of the Summary.

## List of abbreviations

3D	Three-dimensional
ACTA2, $\alpha$ SMA	Aorta smooth muscle actin $\alpha$ 2
ACVR2A	ACTIVIN A receptor type IIA
ACVR2B	ACTIVIN A receptor type IIB
ACVRL (ALK)	ACTIVIN A receptor-like kinase
Ad	Adenovirus
AFP	$\alpha$ -fetoprotein
AKT	V-akt murine thymoma viral oncogene homolog
ALD	Alcoholic liver disease
ALDH1A1	Aldehyde dehydrogenase 1 family, member A1
ALK1Fc/ ACE-041	Activin receptor-like kinase-1- fragment crystallised region
ALK5	Activin receptor-like kinase-5
AMH	Anti-Mullerian hormone
AMSH	SH3 domain of signal transducing adaptor molecule
AON	Antisense oligonucleotide
AP-1	Activator protein 1
ARKADIA	Ring finger protein 11
BAM (BCL-XL)	BCL-2 associated agonist of cell death
BAMBI	BMP and ACTIVIN membrane-bound inhibitors
bFGF	Basic fibroblast growth factor
BIM;	BCL-2-like 11
BMI-1	B cell-specific Moloney murine leukemia virus integration site 1
BMP	Bone morphogenetic protein
BMPR	BMP receptor
BRE	BMP-response-element
CAGA	Cytosine adenine guanine adenine
CASP3	Cleaved caspase 3
CBP (TRX)	cAMP response element-binding protein, Trithorax protein
CCl <sub>4</sub>	Carbon tetrachloride
CDC42	Cell division cycle 42
CDK	Cyclin-dependent kinases
CDK4	Cyclin-Dependent Kinase 4
CDKN1A (p21)	Cyclin-dependent kinase inhibitor 1A
CDKN1B (p27KIP1)	Cyclin-dependent kinase inhibitor 1B
CDKN2B (p15INK2B)	Cyclin-dependent kinase inhibitor 2B
cDNA	Complementary DNA
CfC	Control Fc
C-FOS	Cellular FBJ (Finkel-Biskis-Jenkins) Murine Osteosarcoma viral oncogene homolog
C-JUN	Cellular- ju-nana (Abbreviated from Japanese, the number 17); derived from the ASV 17 provirus.
Ck19	Cytokeratin 19
CMYC	V-myc avian myelocytomatosis viral oncogene homolog



## Appendix II

---

COL1A1	Collagen type 1 $\alpha$ 1
COL1A2	Collagen type 1 $\alpha$ 2
co-SMAD	Common mediator SMAD (SMAD4)
c-SRC	Avian sarcoma (Schmidt-Ruppin A2) viral oncogene
CTGF/CCN2	Connective tissue growth factor
CV	Central vein
DAPPER2	Dishevelled-binding antagonist of $\beta$ -catenin
DCN	Decorin
DD	Dupuytren's disease
DDCt	Delta-delta cycle threshold algorithm
DNA	Deoxyribonucleic acid
DNDM	DNA demethylating complex
E1A	Adenovirus early gene1
E2F	Elongation factor-2
ECM	Extracellular matrix
EGF	Epidermal growth factor
EGF-CFC	EGF-like, cysteine-rich CRIPTO-FRL1-CRYPTIC
EMT	epithelial-to-mesenchymal transition
ERG	v-ets avian erythroblastosis virus E26 oncogene homolog
ERK	Mitogen-activated protein kinase 1
ERK	Extracellular signal-regulated kinase
FKBP12	Inhibitor FK506-binding protein
FN	Fibronectin
FOX	Forkhead Box
FOXH1	Forkhead Box H1
GADD34	Growth arrest and DNA damage protein
GADD45B	Growth arrest and DNA-damage-inducible 45 beta
GATA3	GATA binding protein 3
GC	Guanine cytosine
GDF	Growth and differentiation factors
GPI	Glucophosphatidylinositol
GRP-78	Glucose-related protein-78
GS	Glycine-serine
GSK3	Glycogen Synthase Kinase 3
GTPase	Guanosinetriphosphatase
HBV/ HCV	Viral hepatitis B/ C
HCC	Hepatocellular carcinoma
HDACs	Histone Deacetylases
HHT	Hereditary telangiectasia
HMGA2	High motility group AT-hook 2 protein
HSCs	Hepatic stellate cells
ID	Inhibitor of differentiation
IKBa	Nuclear factor of kappa light polypeptide gene enhancer in B-cells inhibitor, alpha,

I-SMAD	Inhibitory SMAD
JAG1	Jagged 1
JNK	C-Jun N-terminal kinase
JUNB	Jun B proto-oncogene
LAP	Latency-associated peptide
LEF	Lymphoid enhancer-binding factor
LLC	Large latency complex
LRP5	Leucine-rich protein 5
LTBP	Latent TGF $\beta$ binding protein
luc	Firefly luciferase
MAPK	Mitogen-activated protein kinase
MEK	MAPK/ERK
MET	Mesenchymal-to-epithelial transition
MFBS	Myofibroblasts
MH1, 2	MAD homology 1, 2 domain
miRNA	Micro ribonucleic acid
MMP	Matrix metalloprotease
mRNA	Messenger RNA
mTOR	Mammalian target of rapamycin
MYO-D	Myogenic differentiation antigen
NICD	Notch intracellular domain
NKX2.5	NK 2 homeobox 5
NR4A1	Nuclear Receptor Subfamily 4, Group A, Member 1
NT	Non targeting
OCT4	Octamer-binding transcription factor 4
ODN	Oligodeoxynucleotide
OSX	Osterix (Sp7 transcription factor)
p38	Mitogen-activated protein kinase 14
p53	tumor protein p53
PACE-4	Paired basic amino acid cleaving enzyme-4
PAI-1	Plasminogen activator inhibitor 1
PAR6	Par-6 family cell polarity regulator
PCa	Prostate cancer
PCNA	Proliferating nuclear antigen
PDGFB	Platelet derived growth factor $\beta$ polypeptide
PH3	Phosphorylated histone 3
PI3K	Phosphoinositole-3 kinase
PP1,2	Protein phosphatase
PTEN	Phosphatase and tensin homolog
PTM	Post translational modification
PV	Portal vein
qRT-PCR	Quantitative real time polymerase chain reaction
RAC	Rho Family, small GTP binding protein

RAF	Virus-induced rapidly accelerated fibrosarcoma
RAS	Retrovirus-associated DNA sequences
RBP-Jk	Recombination signal binding protein for immunoglobulin kappa J region
Ren	Renilla luciferase
RGM	Repulsive guidance molecule
RHO	Rhodopsin
RLU	Relative light units (luc/ ren)
R-SMAD	Receptor-activated SMAD
RTK	Receptor tyrosine kinase
RUNX	Runt-related protein
Ser	Serine
SHG	Second harmonic generation
shRNA	Short hairpin RNA
SKI	Avian sarcoma viral (v-ski) oncogene
SLC	Small latency complex
SMAD	Small mothers against decapentaplegic
SMI	Small molecule inhibitor
SMURF	SMAD specific E3 ubiquitin protein ligase
SNAIL	Snail family zinc finger protein,
SNON	SKI-related oncogene
SOX2	Sry-related HMG box protein 2
SP1	Specificity protein-1
SRE	SMAD-response element
SWI/SNF	SWItch/Sucrose non-fermentable
TAK1	TGF $\beta$ -associated kinase 1
TDGF1	Teratocarcinoma-derived growth factor
TGF $\alpha$	Transforming growth factor alpha
TGF $\beta$	Transforming growth factor $\beta$
TGIF	TGF $\beta$ -induced homeobox factor
Thr	Threonine
TIMPs	Tissue inhibitor of metalloproteinase 1
TMPRSS2-ERG	transmembrane protease, serine 2
TOPRO	TO-PRO-3 nuclear dye
TP53	tumor protein p53
TPF	Two photon excited fluorescence
TRAF6	TNF $\alpha$ -associated factor 6
TSP-1	Thrombospondin-1
TWIST	Twist family BHLH transcription factor
Tyr	Tyrosine
T $\beta$ RI	Transforming growth factor $\beta$ receptor type I
T $\beta$ RII	Transforming growth factor $\beta$ receptor type II
VEGF	Vascular endothelial growth factor
ViM	Vivo-morpholino

<b>WNT</b>	<b>Wingless-Type factor</b>
<b>X</b>	<b>any aminoacid</b>
<b>ZEB</b>	<b>zinc finger E-box binding homeobox</b>
<b>ZO-1</b>	<b>Tight junction protein 1</b>

## **Curriculum Vitae**

Sofia Karkampouna was born on 3 December, 1986 in Ioannina, Greece. In 2009 she obtained her Bachelor's diploma in Molecular Biology and Genetics at Democritus University in Alexandroupoli, Greece. During 2009-2011 she followed the MSc program of Molecular Medicine in the Erasmus Medical Centre, Rotterdam, the Netherlands.

During her first research internship at the Cell Biology department she worked with Dr. Mihaela Crisan in Prof. Dr. Elaine Dzierzak's group focusing on embryonic hematopoietic stem cell regulation by BMP and Hedgehog signaling pathways. Her second internship (MSc thesis) was performed at the Cell Biology department in the group of Dr. Raymond Poot, focusing on the identification of interaction partners of neural transcription factors. In September 2011 she started her PhD studies at the department of Molecular Cell Biology in Leiden University Medical Centre, in the group of Prof. Dr. Peter ten Dijke and under the supervision of Dr. Marianna Kruithof-de Julio. Since September 2015 she is appointed at the department of Urology in Leiden University Medical Centre working on preclinical *ex vivo* models of fibrosis.

## List of publications

1. ALK1Fc suppresses tumor growth by impairing angiogenesis and proliferation of human prostate cancer cells *in vivo*.

Zoni E., \* **Karkampouna S.**,\* Gray P., Goumans MJTH., Hawinkels L., van der Pluijm G., ten Dijke P and Kruithof-de Julio M. \* equal contribution. *Submitted*

2. Human Dupuytren's *ex vivo* culture for the study of myofibroblasts and extracellular matrix interactions.

**Karkampouna S.**, Kloen P., Obdeijn MC., Riester SM., van Wijnen AJ., Kruithof-de Julio M. *J Vis Exp*. 2015 Apr 18;(98). PMID:25938583

3. Inhibition of TGF $\beta$  type I receptor activity facilitates liver regeneration upon acute CCl<sub>4</sub> intoxication in mice.

**Karkampouna S.**, Goumans MJTH., ten Dijke P., Dooley S., Kruithof-de Julio M. *Arch Toxicol*. 2015 Jan 8. PMID:25566828

4. Fibrosis: a novel approach for an old problem.

**Karkampouna S.**, Kruithof-de Julio M.

*Receptors & Clinical Investigation* 2014 June;1:e151. Editorial Review

5. Novel *ex vivo* culture method for the study of Dupuytren's disease: effects of TGF $\beta$  type I receptor modulation by antisense oligonucleotides.

**Karkampouna S.**, Kruithof BPT., Kloen P., Obdeijn MC., van der Laan AM., Tanke HJ., Kemaladewi DU., Hoogaars WM., 't Hoen PA., Aartsma-Rus A., Clark IM., ten Dijke P., Goumans MJTH., Kruithof-de Julio M.

*Mol Ther Nucleic Acids*. 2014 Jan 21;3:e142. PMID:24448195

6. BMP7 activates brown adipose tissue and reduces diet-induced obesity only at subthermoneutrality.

Boon MR., van den Berg SA., Wang Y., van den Bossche J., **Karkampouna S.**, Bauwens M., De Saint-Hubert M., van der Horst G., Vukicevic S., de Winther MP., Havekes LM., Jukema JW., Tamsma JT., van der Pluijm G., van Dijk KW., Rensen PC.

*PLoS One*. 2013 Sep 16;8(9):e74083. PMID: 24066098

7. TGF $\beta$  signaling in liver regeneration.

**Karkampouna S.**, ten Dijke P., Dooley S., Kruithof-de Julio M.

*Curr Pharm Des*. 2012;18(27):4103-13. PMID:2263008. Review.

8. KLF10 gene expression is associated with high fetal hemoglobin levels and with response to hydroxyurea treatment in  $\beta$ -hemoglobinopathy patients.

Borg J., Phylactides M., Bartsakoulia M., Tafrafi C., Lederer C., Felice AE., Papachatzopoulou A., Kourakli A., Stavrou EF., Christou S., Hou J., **Karkampouna S.**, Lappa-Manakou C., Ozgur Z., van Ijcken W., von Lindern M., Grosveld FG., Georgitsi M., Kleanthous M., Philipsen S., Patrinos GP.

*Pharmacogenomics*. 2012 Oct;13(13):1487-500. PMID:23057549

## **Appendix II**

---

9. Realities and expectations of pharmacogenomics and personalized medicine: impact of translating genetic knowledge into clinical practice.

Squassina A., Manchia M., Manolopoulos VG., Artac M., Lappa-Manakou C.,

**Karkampouna S.**, Mitropoulos K., Del Zompo M., Patrinos GP.

Pharmacogenomics. 2010 Aug;11(8):1149-67. PMID:20712531. Review

## **Patents**

Kruithof-de Julio M., **Karkampouna S.**, Kruithof BPT., Goumans MJTH. Method for culturing tissue. INV-12MC349. WO/2014/173832. Filed April 17, 2014.

Published October 30, 2014.

## **Acknowledgements**

The work described in this thesis would not have been completed without the support of several people whom I would like to personally thank. Firstly, I am thankful to Prof.Dr. Peter ten Dijke for giving me the opportunity to be a member of the “TGFβ family”, I appreciate all the time, advice and scientific discussions.

I would like to thank Dr. Marianna Kruihof-de Julio for her supervision throughout my PhD, for mentoring me to be critical and pragmatic and for transmitting her “out-of-the-box” way of thinking.

Many thanks to Midory, Maarten and all the former and current colleagues from the TGFβ group. To the fellow PhD students that I shared the office with, Yihao and Jie, special thanks and I am looking forward to both of your thesis.

I would like to thank all the people at the MCB department, in particular; Prof. Hans Tanke and the microscopy facility group; Annelies, Joop and Willem, Julia at the secretary office for all the help in the past months, all the members of Marie-Jose’s group. Special thanks to Boudewijn Kruihof for scientific discussions. Thanks to all the S2-20 lab mates from the Parasitology group; Bruno, Gerard, Noemi. Ozge and Zary thanks for always being so positive and I wish you all the best. Maria Panagiotou, a.k.a Maraki, thank you and Kostas for the support, happy vibes, laughs and for sharing my loannina addiction :)

Many thanks to the colleagues at the Urology department and the neighboring D4 group of Endocrinology. From the department of Gastroenterology I would like to thank Minneke Coenraad, Hein Verspaget and Danny van der Helm for our collaboration during the past two years.

To my paranymphs; thank you both for your help and friendship!

To my wonderful friends; John B, Eva, Annemiek and Sven, Elvira, Elena, Maria K., Vasiliki, Aleksandra, Pavlos, Polynikis, Aristeia and Stefanos, Nilhan, Irem, thank you all so much! Thanks to Cheryl and Nteleah, good luck with everything! To Stavros G. many thanks for the support, scientific discussions, the never-ending survival kits with superfood supplies and nerdy jokes. To my Argentinian niche Juan, Alejandro and Romina, thanks for the game nights and excruciating laughs. Romina thank you for all your help and great work with the artistic part and mostly your patience! Robert words are not enough; thank you for being there since day #1 and for your “do or do not, there is no try” attitude.

To my fantastic (nuclear and extended) big family; thank you all for your unconditional love and support !



*"Nothing behind me, everything ahead of me,  
as is always so on the road".*

*Jack Kerouac  
On the road, 1957*

